2-Element Horizontal Beams

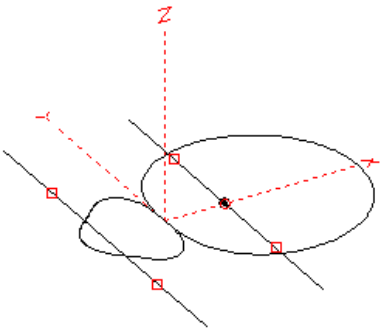

Volume 2

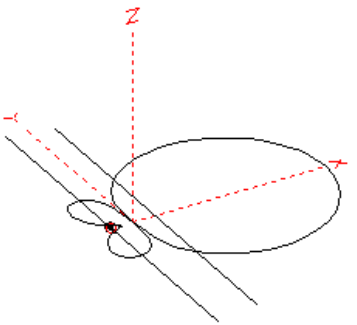

Parasitic Arrays

L. B. Cebik, W4RNL

Published by
antenneX Online Magazine
http://www.antennex.com/
POB 72022
Corpus Christi, Texas 78472 USA

ISBN: 1-877992-82-8

Table of Contents

Dedication

This volume of studies of 2-element beam antennas is dedicated to the memory of Jean, who was my wife, my friend, my supporter, and my colleague. Her patience, understanding, and assistance gave me the confidence to retire early from academic life to undertake full-time the continuing development of my personal web site (http://www.cebik.com). The site is devoted to providing, as best I can, information of use to radio amateurs and others–both beginning and experienced–on various antenna and related topics. This volume grew out of that work–and hence, shows Jean's help at every step.

Introduction to 2-Element Parasitic Beams

In Volume 1 of this set, we explored the nature and types of 2-element directional and bi-directional phased arrays. We call an array phased when we provide energy directly to each element in the array. We took a brief (chapter-length) look at arriving at the relative phasing between elements by feeding only one element and letting the antenna geometry (element length and spacing) set the relationships necessary for directional operation. However, we need to take a longer look at this situation for one simple reason: feeding a single element creates the most popular form of 2-element array. The longer look results in a completely new volume because there are so many variations on the basic 2-element parasitic scheme. Of course, we call an array parasitic when we feed one element (usually) and allow the other elements to arrive at the conditions for directional service solely by the mutual coupling between elements.

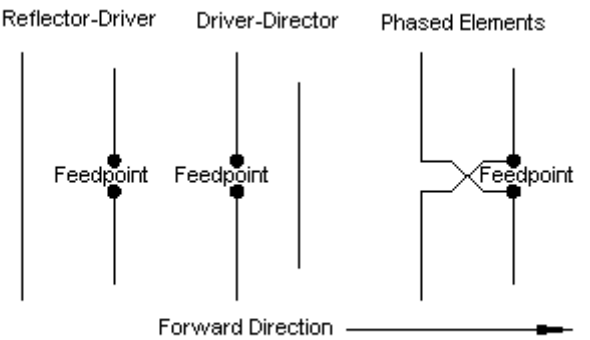

Fig. 0-1 3 Types of 2-Element Beams

Fig. 0-1 illustrates the difference between a phased array (on the right) and parasitic arrays or beams. The crossed feedline in the phased array indicates that we are providing energy from the source point, not only to the forward

element, but as well to the rear energy. In addition, the two elements interact or mutually couple so that the current magnitudes and phase angles at the center of each element result from complex factors.

Yagi and Uda introduced the parasitic beam in the late 1920s. Although Uda appears to be responsible for the fundamental ideas, Yagi was the senior academic. Not only does his name appear first, but the parasitic beam based on the use of ½-λ elements nowadays bears his name alone: the Yagi. Note that other parasitic beam forms do exists using other types of elements. I have looked at 2-element parasitic arrays using 1.25-λ elements, the so-called EDZ beam. The initial ideas for this type of array go back to the 1930s. As well, I have made parasitic arrays using half-squares and bobtail curtains, both of which provide vertical polarization, but with the narrower beamwidth we tend to expect from horizontal Yagis. Such beams may be useful in the VHF and UHF ranges for FM repeater use and—using wire—in the lower HF range.

We shall confine our attention to 2-element parasitic beams or Yagis, using elements that are close to ½-λ long. Even so, we find that they come in two varieties: the driver-reflector type and the driver-director type. The terms "reflector" and "director" are conventional only. For example, the reflector in a Yagi does not reflect like a mirror. There is a type of array that uses large screens to act as nearly optical-type reflector surfaces. When flat, we call them planar reflectors. However, they can take many shapes, of which the corner reflector may be the best known. (See my notes on *Planar and Corner Reflector Arrays*, available through *antenneX*.) Calling the single rearward element a reflector has bred much confusion, such as expecting a single wire laid on the ground to improve the performance of a NVIS dipole. Only a planar reflector will achieve that goal.

The Yagi reflector and the Yagi director in 2-element beams have the same goal: to establish the correct current magnitude and phase relationships between elements so that the elements—working together—have a directional radiation pattern. Since all that we have to work with is the element length and spacing, geometry sets limits as to what we may accomplish with only a single reflector or a single director.

Of the two types of 2-element Yagi, the driver-reflector version is the most popular. Amateur radio home workshops have produced more of these antennas than perhaps any other kind of directional beam. Therefore, we shall devote most of our time to this form, although not to the exclusion of the driver-director form. One potential offered by the driver-reflector Yagi is our ability to use various means to shrink the overall beam size—especially when we are working in the HF range—and still obtain some measure of directional performance. Our basic goal dictates that we look at these potentials as well as at standard linear elements.

The goal of this volume is not to provide a detailed mathematical treatment of parasitic relationships. Instead, the aim is to provide a realistic survey of the performance expectations that we may reasonably have of 2-element Yagis of various types and sub-types. Antenna modeling software provides a very accurate tool for achieving our goal. I shall use NEC-4 extensively—but not exclusively—as the tool of choice. In fact, attached to this volume are the models (in EZNEC format mostly) that are the source of most of the data. Therefore, you may easily verify the data and modify the designs to satisfy your own curiosity. The folder of models is divided by chapters to ease the process of finding a relevant model. I recommend that you copy the files onto your hard drive so that you can easily save your own modifications to them (under a separate but related model name, of course).

The Plan of Attack

I have divided our work into 3 major sections. Part 1 includes the first 5 chapters devoted specifically to 2-element Yagi expectations. Chapter 1 provides necessary background notes on the methods and units of measure that are applicable to evaluating beam performance. As well, we shall examine the simple ½-λ dipole, since that element serves as the foundation for all 2-element (and larger) Yagis. It is not only the element that we adjust to make a Yagi, but as well, it is the performance standard by which we gauge Yagi radiation patterns and other performance parameters.

Chapter 2 looks at the full-size driver-reflector Yagi. Our goal is to see what

we can achieve with these two elements—and what we cannot achieve. Unlike Volume 1, we shall select 29 MHz as our design frequency in order to survey a potential operating passband from 28 through 30 MHz. For most Yagis, this passband is wider than we can obtain either with radiation performance or with the feedpoint SWR. However, we shall be interested in how far short of this passband each design variation falls. All antenna models in Part 1 will use 3/8"-diameter aluminum elements. Hence, the models do not aim for replication. Instead, their purpose is to ensure that all comparisons are fair.

The third chapter introduces the idea of shortening the elements of a 2-element driver-reflector Yagi in order to discover what we can achieve and how far short of full-size performance the smaller Yagi falls. In this chapter, we shall introduce the so-called "capacity" hat as the method of element shortening that yields the highest level of performance. Chapter 4 provides an overview of other element-shortening methods, such as the use of center and mid-element inductive and linear loads.

The final chapter of Part 1 provides a potpourri of ideas used by various designers to improve the performance of the 2-element driver-reflector Yagi. We can improve performance in many ways: operating bandwidth, increased gain, and an improved front-to-back ratio, to mention just three. We shall look at the driver-director Yagi as a way to increase gain and the front-to-back ratio, but at the cost of operating bandwidth. Indeed, when we work with only 2 elements, virtually every improvement in one category involves a performance decline in at least one other category.

Most (but not all) of the beams that we shall examine do not have a 50-Ω feedpoint impedance. Indeed, standard-design Yagis of all lengths tend to have impedance values that fall below the ubiquitous 50-Ω coax that we use as the standard amateur radio feedline. Therefore, many Yagis require that we introduce a matching network to change the natural beam impedance to a 50Ω resistive impedance. Since the Yagi is essentially a narrow-band array, the most logical place to introduce the matching network is at the feedpoint terminals. Part 2 of these notes is devoted to the three most popular forms of matching Yagis to standard feedlines.

Chapter 6 provides information on three inter-related series matching systems that involve only the addition of transmission-line sections between the antenna and the main line. We shall look at the relatively straightforward math that lies behind the ¼-λ impedance transformer, the Bramham matching system, and the Regier system. The last of this set is the most general solution to series matching and includes the other two as special cases.

In Chapter 7, we shall review the beta or hairpin match. Although this system is one of the simplest, it scares most newcomers to death, as they somewhat naively view a beta hairpin as a short circuit rather than as an inductive reactive component formed from a section of shorted transmission line.

Perhaps the most confusing but also the most popular matching system is the gamma match. It is the only one that allows the builder to attach the driver element directly to the boom, effectively grounding the driver. It also employs the most complex set of calculations to estimate in advance of field adjustment the length of the gamma section and the required series capacitor. Therefore, we shall spend a considerable number of pages looking at both the thinking that underlies gamma-match design and why the result is at best a very general guide and not a precise calculation.

Part 3 of these notes takes us from the general to the practical level of Yagi design. Chapter 9 provides usable stepped-diameter aluminum Yagi designs for the upper HF bands from 20 through 10 meters. The available handbooks contain a myriad of such designs. The collection in this chapter therefore offers only special alternatives, not necessarily superior antennas. For the wider bands, the chapter offers wide-band driver-reflector Yagis, each of which covers the design band with a very low 50-Ω SWR without requiring any sort of matching network. Since 17 and 12 meters are so narrow, the designs for those bands use a driver-director arrangement set up for use with a simple beta match. Unlike like most commercial antenna offerings, the data collection for each sample provides performance information for the entire band.

One of the most effective small monoband beams for the upper HF range is

the Moxon rectangle. Chapter 10 provides customized designs using the same element-tapering schedule used by the linear elements in Chapter 9. The information on each model covers the same territory as the data for the beams with linear elements. Therefore, you may compare the performance information in the process of deciding what parasitic beam you should build.

Although these notes provide perhaps the most comprehensive coverage of 2-element beams currently available, they are by no means complete. Every time that I conclude an investigation, I discover new questions that I should have posed and one day will pose to a given subject. As well, the parasitic beams that we shall study have an indefinitely large number of variations. The variations cover both mechanical and electrical elements that go into producing a beam. For example, we shall not examine what happens when we try to bend our elements into some variation of a V. We shall also not look at wire Yagis that some operators use in the lower HF range and which are also usable in the upper HF domain. We shall not examine ideas for creating reversible beams to save ourselves the cost of a rotator.

However, let's not look just now at what remains uncovered in these notes. We shall have enough to do in this volume just mastering reasonable expectations of 2-element parasitic beams with "normal" properties and configurations. We can always do further work once we have gone that far.

Part 1: 2-Element Parasitic Beams

1. Methods, Units of Measure, and the Dipole Standard of Reference

Method

A 2-element Yagi can be configured either as a director and driven element or as a driven element and reflector. We shall concentrate on the latter, because it is the most common and perhaps the most versatile configuration used.

Developing a basic understanding of 2-element Yagis requires a consistent method. My method will be computer antenna modeling, using a variety of software: MININEC, NEC-2, and NEC-4. The advantage of the latter two engines is the availability of the Sommerfeld-Norton ground equations for more accurate modeling of antennas over real ground. However, some results will be crosschecked with MININEC in order to understand any differences that may arise. Models are convergence tested and use more than the minimum recommended number of segments per half-wavelength. Ground parameters will be average earth throughout.

Frequency: All models will be for 10-meters, with a design center of 29 MHz. Although this frequency is well up the band from the region of greatest activity, it allows an examination of performance curves that cover maximum gain, maximum front-to-back ratio, and feedpoint impedance while trying to stay within the ham band. However, what applies to 10 meters also applies to all other ham bands with suitable adjustments.

Element Diameter: The 10-meter models will employ single diameter aluminum elements. (Real elements may use stepped-diamet4er elements or a "tapered-diameter schedule." Such elements are a special topic all unto itself. In general, if we taper the diameter as we move away from the element center, then the element will be longer than an element using a uniform diameter, *even*

if the average tapered element diameter is somewhat larger than the uniform-diameter element. In fact, changing the taper schedule may call for a change in some element lengths to return a design to its original performance specifications.) I have chosen 0.375" (3/8") elements because they scale well to other bands. The equivalencies from band to band for element diameter appear in **Table 1-1**:

Approximate Scaled Diameters by Band		Table 1
Band m	Dia. "	Dia. "
10	0.375	3/8
15	0.5625	9/16
20	0.75	3/4
30	1.125	1-1/8
40	1.5	1-1/2

In fact, all antennas for 10 meters noted below have been scaled for each of the ham bands mentioned, and--as expected--give identical performance figures. When scaling an antenna, the diameter changes slowly within any ham band, so picking the closest real value to a calculated size usually does no harm to a design. However, picking a random value can create problems. In the table, each diameter is about the same fraction of a wavelength for each band.

Scaling. The idea of scaling an antenna from one band to another often creates a bit of confusion for newcomers. If we wish to scale the dimensions of an antenna for 10 meters to 20 meters, let's first take the ratio of the old frequency to the new frequency--and use some precision in the process. For example, if the 10-meter design is for 29.0 MHz and the new or scaled design is for 14.2 MHz, then the ratio of old to new is 29.5/14.2 or 2.077.

Next, lets multiply all dimensions by the scaling ratio. The dimensions include the length of each element, the spacing between elements, and the diameter of the element. Most casual builders forget this last factor. Indeed, it is common for newcomers to see a magazines article and think that they can build the antenna from whatever materials may be convenient. If we are dealing

with very thin wire (for example, AWG #12 wire is very thin as a function of a wavelength on 40 meters), then no great harm occurs. However, for fatter elements, such as the tubing used in beams, changing the element diameter will throw the design off frequency and out of its original design specifications.

The bottom line is simple: if you cannot scale all of the dimensions to a new frequency, then you will have to adjust the complete dimension set for the new frequency. That task is not a casual one.

Antenna Height above Ground: When we work with antennas and take the ground into consideration, we add another factor into the analysis. Antenna heights will be given in fractions of a wavelength as well as feet. This procedure will permit more ready scaling of results to antennas designed for other bands. As a reference, the **Table 1-2** lists the heights of an antenna at 29 MHz in terms of both feet and fractions of a wavelength. Heights in feet are rounded to the nearest tenth of a foot.

Height above		Table 2
Ground at 29 MHz		
Ht wl		Ht feet
1/8	0.125	4.2
1/4	0.25	8.5
3/8	0.375	12.7
1/2	0.5	17
5/8	0.625	21.2
3/4	0.75	25.4
7/8	0.875	29.7
1	1	33.9

Scaling for lower ham bands by up to a factor of 8 should introduce no significant errors in results. Note that although heights of antennas for 10 meters would rarely be placed at a 4' level, antenna heights for the lowest amateur bands are often forced to correspondingly low heights. An 80-meter dipole at 35' is very close to 1/8 λ above ground.

MININEC models of antennas at a height of 1/8 λ are not reliable, since the program only begins to approach reliability at antenna heights of 0.2 λ or greater. (One highly corrected MININEC program, Antenna Model, has grafted the NEC ground system to its MININEC core with very good results.) NEC with Sommerfeld-Norton (S-N) ground implemented is reliable at the lower heights.

None of the models will press any of the other internal modeling limitations. All elements will be of a single diameter and linear, thus assuring easy convergence of results. Indeed, NEC-2 and NEC-4 should provide identical results, +/-1 digit in the last decimal place of the output.

Models do have other limitations. Modeling programs assume level uniform terrain. Local variations can change some performance figures, such as the elevation angle of maximum radiation and feedpoint impedance. However, they do not change the basic expectation limits for any given design when related to other designs, since each design will be equally affected by the local terrain variations.

Units of Measure

One of the most confusing aspects of antenna performance figures lies in the units of measure. Therefore, let me explain the units used here, working from the least confusing to the most confusing.

SWR (standing wave ratio): SWR, wherever apt to produce a curve, will be given relative to the resonate impedance of the test model at the design frequency. Hence, all antennas modeled will show close to 1:1 SWR at or close to the design center frequency. Curves will assume that appropriate matching is employed, wherever applicable, to the user's desired feedline impedance, with no examination of matching circuit losses. For certain models, a 50-Ω reference may also be used, since some common designs can be developed specifically for 50-Ω cable use.

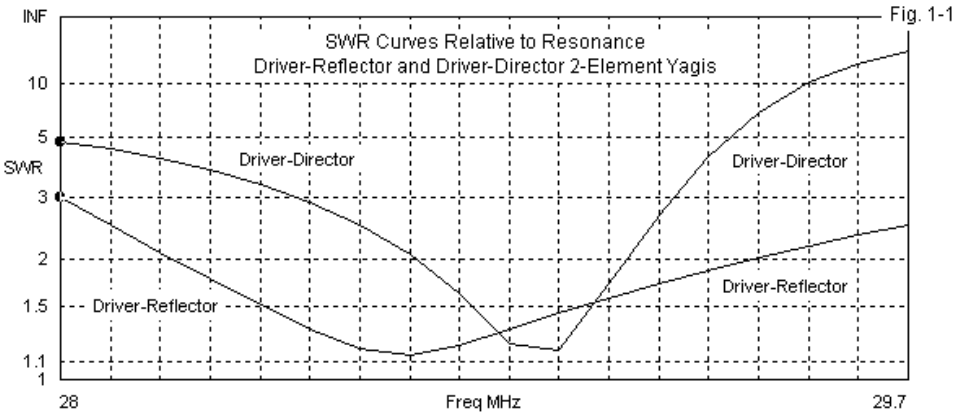

Fig. 1-1 compares sample SWR curves from 2 kinds of 2-element Yagis. Each curve is relative to the resonant feedpoint resistive impedance. The driver-reflector Yagi uses a 40-Ω reference, while the driver-director array uses a 17-Ω standard. The fact that the driver-reflector Yagi has a much wider frequency span between the points at which it crosses the 2:1 SWR line is one reason why this general design is more widely used than the driver-director version of the antenna. (See models 1-1.ez and 1-2.ez.)

Feedpoint Impedance (Z): Feed point impedance will always be given as a complex number involving resistance and reactance (R +/- jX) in Ohms (Ω). Resonance will be defined as a reactance less than +/-1 Ohm.

Both the resistance and the reactance of any antenna vary across any stretch of frequencies we might use for operation. **Fig. 1-2** shows a sample graph of the changes in both resistance and reactance on 10 meters for the driver-reflector Yagi used for the SWR curve in **Fig. 1-1**. Note that the reactance crosses the 0-line (right Y-axis) at about the point where the SWR curve shows its lowest value. Although the resistance is also changing with frequency, the reactance is changing faster, and so reactance is often (but not always) the limiting factor in SWR curves

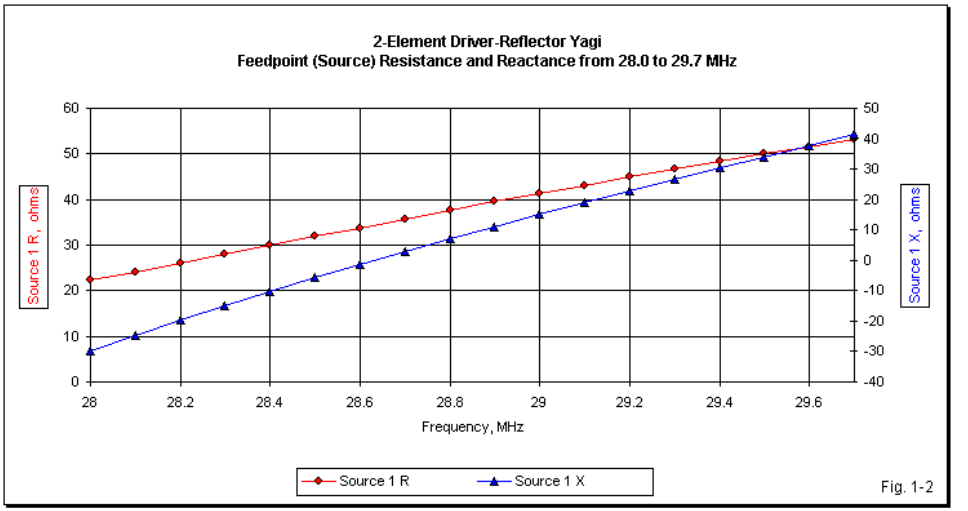

Fig. 1-2

Front-to-Back Ratio (F-B): Front-to-back ratio will be given in dB below the maximum gain of the forward lobe. Front-to-back ratio is taken at a 180° angle from the forward lobe. One may also employ a notion of front-to-rear ratio, using the simple or complex mean of values in the quadrant extending for 180 degrees (or some other number of degrees) to the rear of the forward lobe. For the present enterprise, this procedure is unnecessary, since the rear lobe of a 2-element beam is usually geometrically simple. Hence, front-to-back ratio is a sufficient performance indicator for these tests.

Special Note on Front-to-Back Ratios: **Fig. 1-3** uses the azimuth pattern of a driver-director Yagi to illustrate the variety of front-to-back ratio concepts that you may find in both articles and manufacturer specification sheets. The 180° ratio uses a straight line to the rear opposite the heading of maximum forward gain and compares the two gain readings. The worst-case ratio (sometimes called the front-to-rear ratio) compares the maximum forward gain to the gain of the strongest rearward lobe. The front-to-rear ratio (sometimes called the average front-to-back ratio) averages the gain across the entire rearward quadrants and compares that value to the maximum forward gain. When

reading about beams, always try to determine which front-to-back ratio calculation that the author is using.

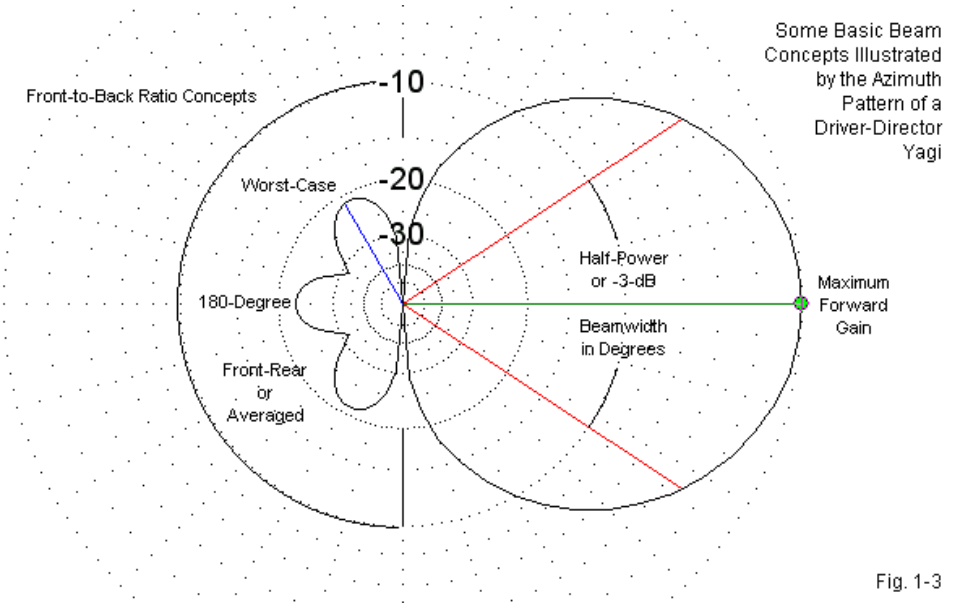

Fig. 1-3

Forward gain: The most complex question for the selection of units of measure is a proper characterization of gain. In **Fig. 1-3**, we can easily determine the direction of maximum forward gain, but the pattern does not tell us how to quantify that gain.

The most universal standard is gain in **dBi**, or dB over an isotropic source. An isotropic source is a hypothetical concept that one can approximate with various types of real antennas (but only in free space). It radiates equally well in any direction: up, down, left, right, etc. Hence, it is a universal comparator. Whenever two antennas require comparison, one simply subtracts one dBi-gain figure from the other to find the relative gain advantage or disadvantage.

A second common gain figure is **dBd**, dB relative to a dipole. The dipole standard arose in connection with horizontal antennas, since horizontal dipoles were in common use from the earliest days of radio. However, when gain is registered in dBd, at least 2 different measures may be indicated:

dBd(i): Gain in dBd(i) is gain relative to a free space dipole composed of lossless wire of infinitely thin diameter. This idea of a dipole is as hypothetical as a true isotropic source, and real dipoles only approximate the ideal. We may easily relate this notion of dBd to the notion of dBi by the following equation: Gain dBi = Gain dBd(i) + 2.15. This notion of dBd has limited utility, but appears in some tables.

dBd(r): Gain in dBd(r) is gain relative to a real dipole in the same defined situation as the test antenna. For modeling purposes, the dipole should be made from the same materials as the test antenna or from some predefined (and stated) set of materials. For these tests, the dipole will use the same material and element diameter as the test Yagi.

The notion of dBd(r) may also be used where gain figures result from range measurements. Whenever the notion is so employed, the complete set of test conditions for both the test antenna and the reference dipole should be explained. Otherwise, the figures cannot be meaningful, since replication of the test would not be possible. Range measurements will not be included in these notes. Therefore, dBd(r) will always refer to the gain of a full-length dipole of similar materials as the test antenna, and situated within the same parameters of height and ground specification.

However, a further complication arises in the use of dBd(r). Even 2-element Yagi antennas exhibit for the same antenna height, a (usually slightly) lower elevation angle of maximum radiation than a dipole, especially for antenna heights less than 1 λ. Therefore, simple gain figures must be accompanied by the elevation angle for those figures if a reasonable comparison is to be made.

Beamwidth: We think of a vertical antenna as omni-directional, radiating equally well in all azimuth or compass directions. By comparison, even a dipole

is directional, although it shows lobes that are identical in two directions. Hence, it falls in the group of antennas that we think of as bi-directional. When we use the term "directional" without a qualifier, we usually mean an antenna--like our sample Yagis--that shows very strong radiation in only one direction, with considerably weaker radiation in all other directions.

However, bi-directional and directional antennas do not radiate on a single compass heading. Rather, the gain slowly grows weaker as we move away from the heading of maximum forward gain. At a certain angular distance in either direction from the heading of maximum forward gain, we would find that the transmitted energy has half the power that it has in the direction of maximum power. These half-power points will show 3-dB less gain than in the maximum forward gain direction. We use these points as a convenient measure of an antenna's beamwidth, as measured in degrees between the two points. The pattern in **Fig. 1-3** shows a beamwidth of about 67° from one limit to the other.

These notes on basic beam specification concepts all presume that the antenna we are using is oriented horizontally relative to the ground. When we place beams above ground and orient them vertically, the azimuth pattern shape changes, and so too does the maximum forward gain at the heights we use in the HF range. However, the meanings of terms like forward gain, front-to-back ratio, and beamwidth will not change. Since we will normally use a 2-element beam horizontally on 80 through 10 meters, we shall bypass the vertical orientation in these notes. However, if you decide to build a VHF beam for repeater serve, remember that the horizontal patterns and numbers will not be applicable.

Where Does Beam Gain Come From?

A beam derives its gain from 3 main sources: ground reflection, directionality, and beamwidth. The total radiated energy from a beam can never be greater than from a dipole or an isotropic source (ignoring element resistances). Any directional antenna acquires gain by re-directing energy in a desired (or usable) direction.

Free space is equivalent to outer space with no population of particles or waves other than those produced by an antenna under study. In free space, there is no up or down to define azimuth and elevation. So we generally (but not always) consider radiation in the plane of a wire to be the E-plane or electrical plane. At right angles to the plane of the linear elements in the antenna, we have the H-plane or the magnetic plane. If we place the same array of linear element over ground with the elements parallel to the ground, this plane becomes the elevation pattern. (For convenience, modeling software will call any pattern taken in the +/-Z-plane an elevation pattern. Any plot taken in the X-Y-plane becomes an azimuth pattern.)

Antennas in free space show a maximum gain that is less than the value we find when we place the antenna over a ground surface. In free space, the radiation can equally go "up" and "down." However, the moment that we introduce the ground, we ultimately have only the "up" direction. What initially starts downward reflects (with some loss) back upward. Compare in **Fig. 1-4** the free-space and over-ground patterns for a simple dipole, looking along the length of the element.

The energy the goes "downward" in free space becomes reflected upward by the ground. However, the angle of the downward energy, once reflected, determines whether the waves will mutually add, mutually subtract, or something in between the two. Hence, the elevation pattern of an antenna over ground may show both lobes and nulls. The test antenna is 1 λ above ground. In general and subject to some modification for long-boom antennas, we can estimate the angle of any lobe (or null) from a horizontal (but not a vertical) antenna by using a simple equation.

$$A_{LN} = \arcsin(N / 4h)$$

A_{LN} is the angle of the lobe or null above the horizon. The term h is the height of the antenna above ground measured in wavelengths or fractions thereof. N is the lobe or null number. We give lobes odd numbers, so that the first lobe is 1, the second lobe is 3, etc. Nulls receive even numbers. Most often, we are concerned with the first lobe. In this case, for N=1, and h=1, we want the arcsin

(or $\sin^{-1}$) of 0.25. On any calculator, we take the inverse sine function of .25 and get a little over 14° for the value of A_{LN}.

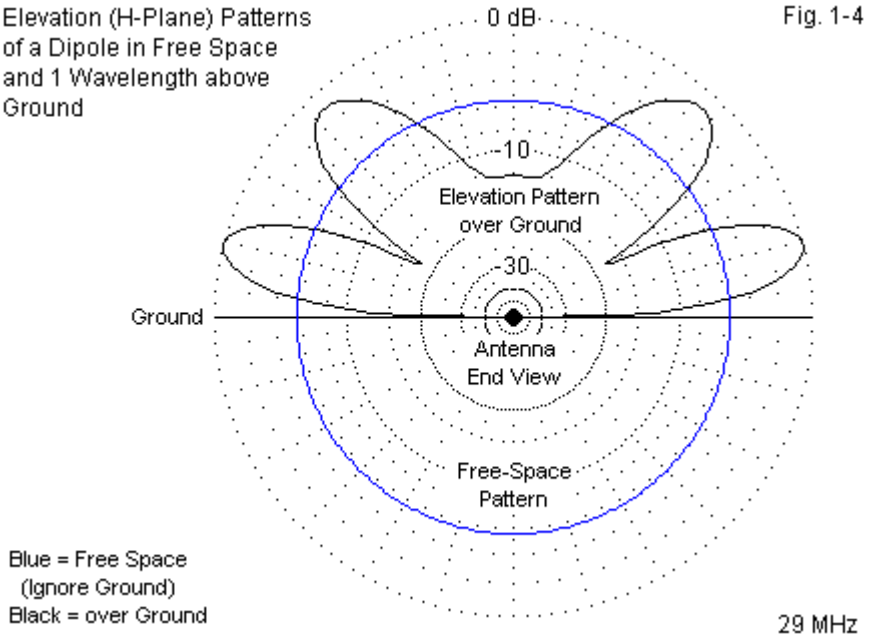

The peak gain at 14° elevation for the sample dipole is about 7.6 dBi, compared to a gain value of 2.1 dBi in free space. If the ground did not have any losses, we would see a 6-dB difference. However, over real ground, we find a 5.5-dB gain differential. (See models 1-3.ez and 1-4.ez)

The second way in which a beam acquires gain is in developing a pattern that favors a single direction. The dipole is already directional, but in two directions. We can further increase gain in a single favored direction by arranging the elements so that we have one large main (forward) lobe with only

one or more minor lobes in other directions. Compare the overlaid azimuth patterns for a dipole and a 2-element driver-reflector Yagi in **Fig. 1-5**. (Compare model 1-5.ez with model 1-4.ez.)

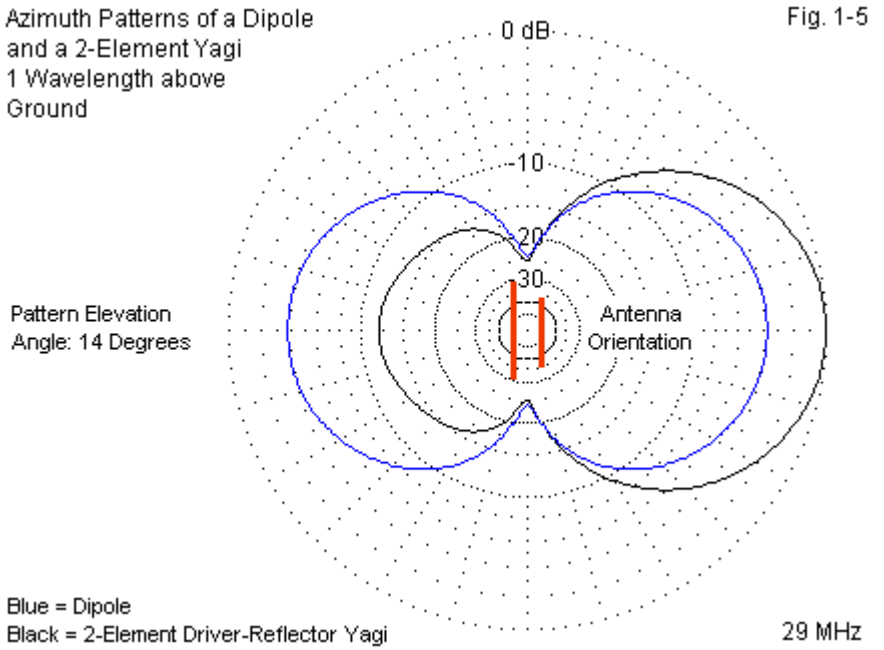

Note that, relative to the dipole, the 2-element Yagi shifts energy to the right in the pattern and removes energy toward the left. In free space, this particular sample beam has a maximum forward gain of about 6.0 dBi. Over ground, the maximum gain at 14° elevation is about 11.4 dBi. The ground provides 5.4 dB of gain relative to free space. The gain of this beam is about 3.8 to 3.9 dB higher than the gain of a dipole--in the favored direction only.

The beamwidth of the beam is about 69°. Although we shall not examine them closely, we may want to ask here how longer Yagis with more elements

obtain higher gain levels in the favored direction. The answer is both simple and complex at once. The simple part is the general statement that the longer Yagis reduce their beamwidth in order to produce a higher gain in the favored direction. **Fig. 1-6** shows both independent and overlaid patterns for our sample 2-element Yagi and for a sample 6-element Yagi.

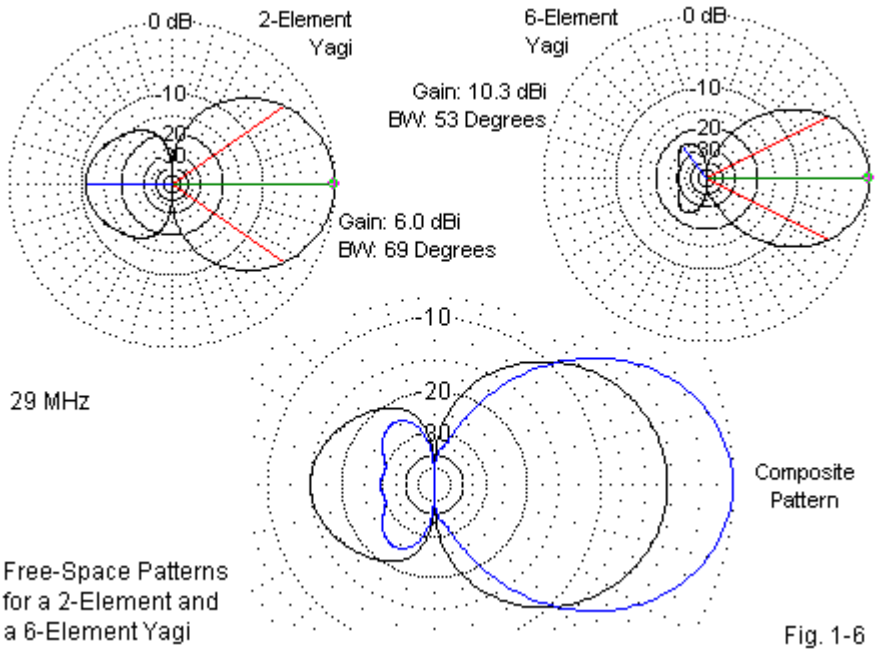

Fig. 1-6

The 6-element Yagi has somewhat less rearward radiation, and so it acquires a bit of gain from that source—but only a little. The main source of the increased forward energy and gain comes from the narrowing of the beamwidth--from 69° down to 53◦ in this example.

The picture given by these plots is incomplete, which is why the answer is more complex than it may initially seem. Not only does the longer Yagi

decrease the horizontal beamwidth, it also decreases the vertical beamwidth. This 3-dimensional beamwidth reduction shows up well when we start with free-space patterns, but for now we can simply use the azimuth patterns as an indicator of how beamwidth reduction becomes a source of additional gain in long Yagis and certain other kinds of horizontal beam antennas. However, **Fig. 1-7** shows the relationship between E-plane and H-plane patterns in free space and between elevation and azimuth patterns over ground for our sample 2-element driver-reflector Yagi.

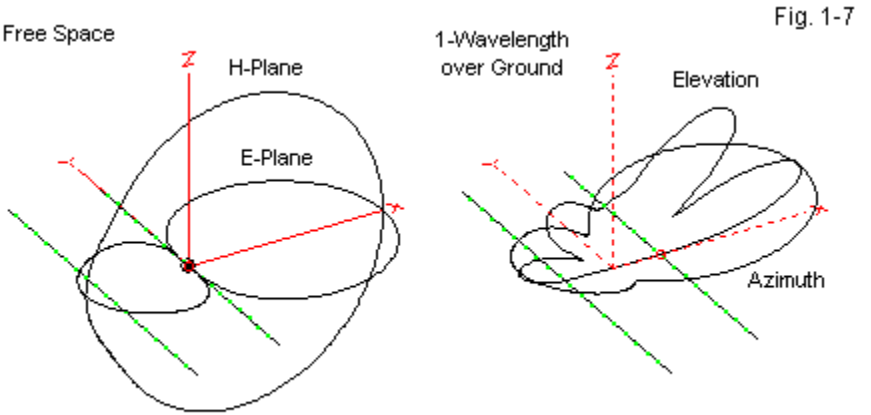

Fig. 1-7

Plot Orientations for Antennas in Free-Space and over Ground

Before we grow too attached to the 2-element Yagi, we need to understand a bit more about the behavior of a simple dipole over ground.

The Dipole Standard of Reference

All Yagis ultimately rest on the linear dipole. The elements relate to a resonant 1/2-λ dipole, with reflectors being slightly longer and directors slightly shorter. Therefore, understanding the behavior of a dipole over ground is a crucial factor in appreciating the behavior of 2-element beams.

29-MHz Dipole at Various Heights above Average Ground						Table 3
Height wl	Len feet	Feed R	Feed X	Gain dBi	Gain dBd	El Angle
0.0625	16.14	59	0.2	0.49	-1.66	90
0.125	16.01	55.2	0	4.64	2.49	88
0.1875	15.94	65.8	-0.3	5.78	3.63	87
0.25	16.02	77.9	0.3	5.73	3.58	62
0.3125	16.17	85	0.1	5.75	3.6	46
0.375	16.32	84.7	0	6.07	3.92	37
0.4375	16.4	78.4	0.3	6.62	4.47	32
0.5	16.38	70.2	0.2	7.23	5.08	28
0.5625	16.29	64.5	-0.1	7.66	5.51	25
0.625	16.18	63.8	-0.2	7.75	5.6	22
0.6875	16.13	67.4	0.3	7.56	5.41	20
0.75	16.13	72.8	0.1	7.28	5.13	18
0.8125	16.18	77.1	0	7.12	4.97	17
0.875	16.26	78.1	0.1	7.15	5	16
0.9375	16.31	75.7	-0.1	7.34	5.19	15
1	16.31	71.6	-0.2	7.63	5.48	14
1.0625	16.27	68.2	0.2	7.85	5.7	13
1.125	16.21	67.2	0	7.9	5.75	12
1.1875	16.17	69	0.1	7.81	5.66	12
1.25	16.17	72.3	0.3	7.63	5.48	11
See text for explanation of column labels.						

Table 1-3 present some interesting data for a full-size 3/8" aluminum dipole for various heights from 1/8 λ to 1-1/4 λ using 1/16-λ increments. Gain values use both dBi and dBd to familiarize you with the differences in the gain recording systems. El. Angle refers to the elevation angle of maximum radiation at which the gain figure is taken. Feed R and Feed X refer to the resistance and reactance at the feedpoint. (See and revise model 1-6.ez.)

Fig. 1-8 shows the gain values and the elevation angle of maximum radiation (also called the take-off or TO angle) for the sequence of models. The gain values are significant in several respects. First, note the very low gain at very low antenna heights. MININEC users may see very different results below

about 0.2-λ heights, because the ground system used by that program is very unreliable at low antenna heights. Next, note that the gain of a dipole does not rise and level off smoothly. Although the differences are not operationally significant, they do undulate as we raise the antenna, change its length to arrive at resonance, and then check the gain. We find small gain peaks at heights of 3/16 λ, 5/8 λ, and 1-1/8 λ. We also find dips at ¼ λ, and 13/16 λ, with the curve headed toward another dip at the end of the model sequence. (In a future episode, we shall show you a handy marketing trick that you can play if you should ever desire.) Perhaps the only consistent curve is the one for the elevation angle of maximum radiation. It decreases as we increase height, and the progression is very orderly.

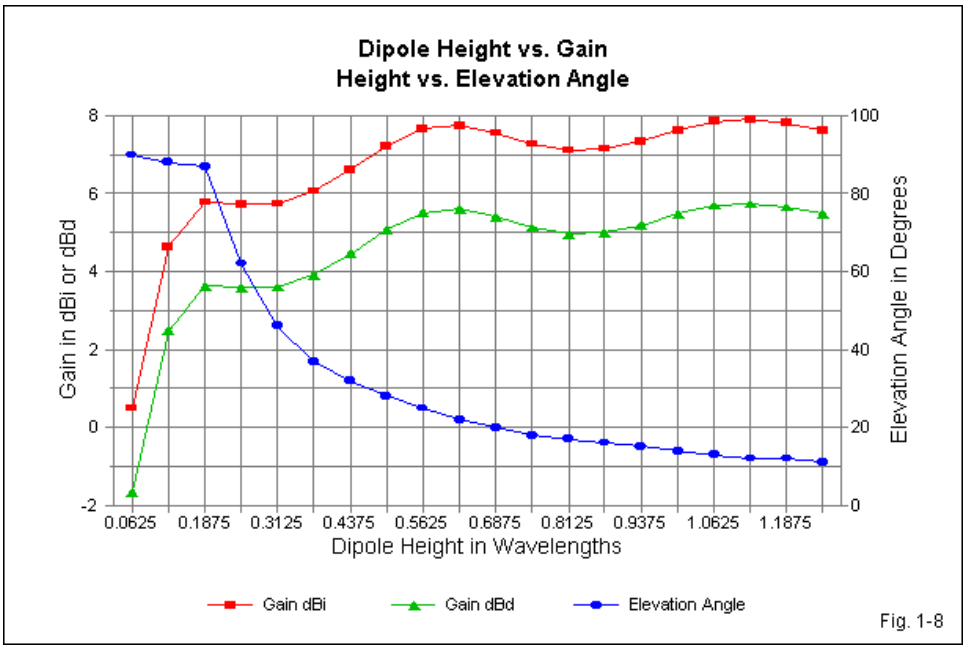

Fig. 1-8

It should be clear from the table that, except in the most unusual circumstance, the concept of dBd adds nothing to the analysis not already

contained in the notion of dBi. For purposes of determining gain relative to a dipole with respect to test antennas, we shall simply subtract the appropriate value of gain in dBi for the dipole from the value of gain in dBi for the test antenna at the same height. However, it is wise to keep the 2 notions of dBd (that is, dBd(i) and dBd(r)) in the back of your mind because some antenna manufacturers use one or the other to portray the performance of their offerings. The dBd measure remains popular among European antenna builders.

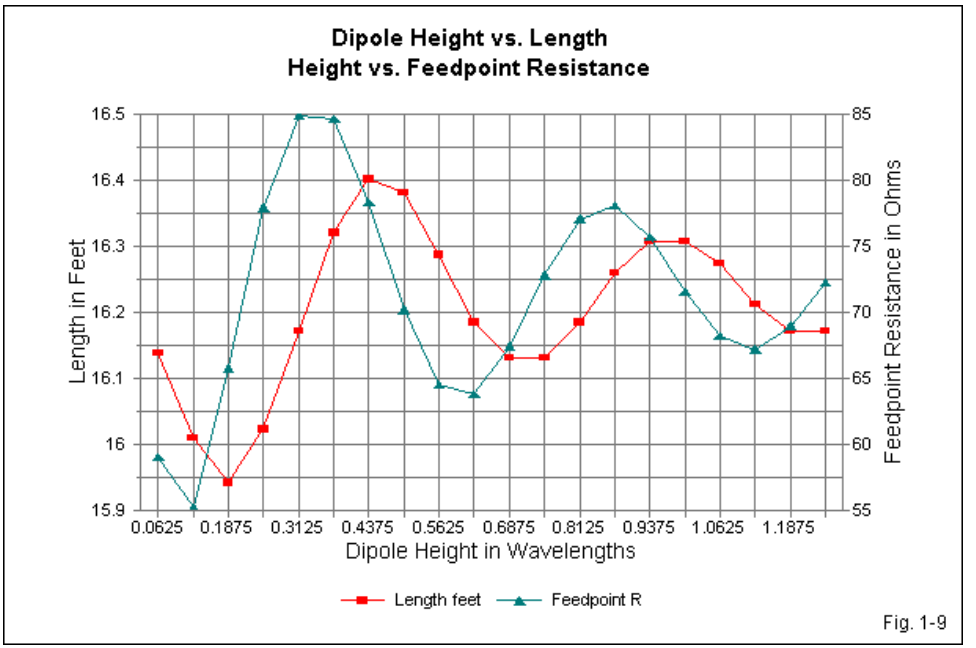

Fig. 1-9

As shown in the table and in **Fig. 1-9**, the required length of the dipole to achieve resonance varied from 15.9' to 16.4' but not in a linear progression. Short lengths appear at heights of 3/16 λ, ¾ λ, and 1-1/4 λ, a progression that does not quite correspond to the peaks or dips in gain. Likewise, long lengths appear at heights of 7/16 λ and 1 λ, again without coincidence with the gain curve.

The feedpoint impedance also varies with height, but not in a pattern that corresponds to the variance in length. However, the feedpoint resistance values tend to coincide with the changes in gain. Low feedpoint resistance values appear at 1/8 λ, 5/8 λ, and 1-1/8 λ heights, roughly corresponding to the gain peaks. High feedpoint values occur at heights of 5/16 λ and 7/8 λ, roughly corresponding to the gain dips.

One factor, but not the only factor, that plays a role in the undulations of gain is the changing spread of elevation lobes as we raise the antenna higher. **Fig. 1-10** provides only a few elevation patterns to illustrate how lobes emerge and change with changing antenna height.

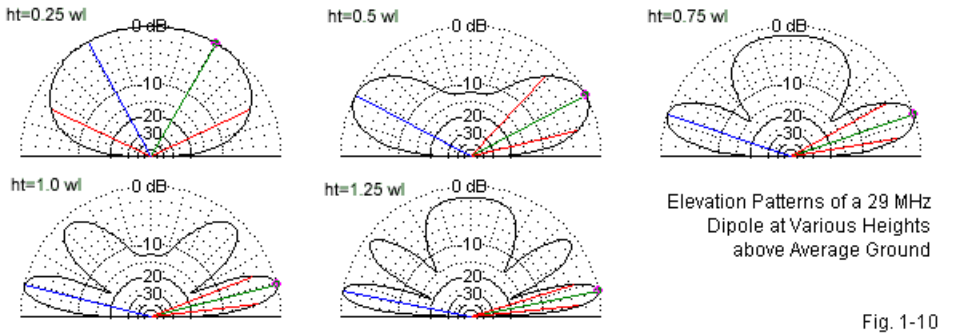

Elevation Patterns of a 29 MHz Dipole at Various Heights above Average Ground

Fig. 1-10

As we increase the height of an antenna, new lobes do not simply appear. Rather, they make their first appearance as vertical or near-vertical lobes. (The pattern for a height of 1/4-λ makes it clear why those who pursue Near-Vertical Incidence Skywave (NVIS) operations favor a relatively low horizontal antenna.) As we raise the antenna, the nearly vertical lobe splits and gradually lowers its angle of maximum radiation. At certain heights, we find almost no radiation straight up, and the lower lobes contain all of the radiated energy. Further increases in height show the emergence of a new upward lobe, which then undergoes the same transformation as we continue the upward trend in antenna height. In general, we acquire a new lobe with each 1/2-λ addition to the antenna height. For most purposes, we are only concerned with the lowest and

strongest elevation lobe, since it usually comes closest to matching the favored radiation angles for long-distance HF communications.

A Final Question about Gain

Not everyone who reads these notes will actually build his or her own beam. Instead, many individuals will choose to purchase one of the many fine antennas available on the amateur market. If any of us have examined the literature available on most commercially made antennas, we shall instantly recognize a significant difference between the scope of the data that I have presented and the scope of the information supplied in either advertisements or assembly manuals.

Even though we have assessed only some of the information relevant to antenna performance, we should note that in all cases, I shall try to present data that covers with reasonable thoroughness the entire possible operating span of the antenna. That span in some cases is the operating passband for the antenna. In other cases, it might be the variations of performance with the height above ground. The key data that we need to cover comprehensively include the gain, the front-to-back ratio and the feedpoint information.

Unfortunately, many antenna makers provide only “spot” information. Sometimes the data is for the design frequency. At other times, the data may be for the peak performance or for a minimal level of performance. Such information gives us no idea of the rates of change in the performance categories as we move across an operating passband. Moreover, sometimes the data can be ambiguous.

So, before we leave the subject of antenna gain, let's look at an all-too-typical claim. Suppose someone says that a certain antenna at a height of 7/8 λ has a gain of 5 dBd. How are we to understand this claim without further and full specification of what the idea of dBd means in this context? If we interpret the claim to mean dBd(i), then the assertion is that the antenna has only the gain of a dipole, since a dipole at 7/8 λ has a gain of 5.00 dBd(i) (assuming similar materials). If the antenna is an array, that would be a disappointing result.

If the claim is that the antenna has a gain of 5 dBd(r) (as applicable to modeling), then we would expect the antenna to have a gain of 12.15 dBi, since the gain of a dipole in dBi at 7/8 λ (assuming similar materials) is 7.15 dBi. Our next question is whether this claim is reasonable. To make such a judgment, we need to have some clear expectations of 2-element Yagi performance capabilities and limitations. That is the next stop on this road toward understanding 2-element beams.

2. The Full-Size 2-Element Yagi

In this episode, we shall develop some basic ideas about driver-reflector 2-element Yagis. The relatively broadband characteristics of the driver-reflector Yagi open it to relatively easy reproduction by the newcomer. As well, as we shall discover in the following 2 episodes, it is amenable to certain kinds of compacting. Therefore, we shall set aside the director in favor of the configuration shown in **Fig. 2-1**.

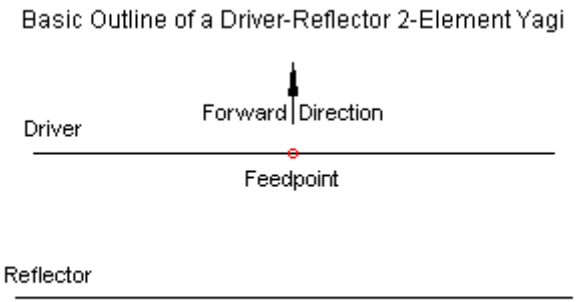

Fig. 2-1

By working with a full-size 2-element Yagi, we simplify construction. Besides a mast and boom, all that we need are linear elements, usually made from aluminum tubing. As in the first episode, we shall use 3/8"-diameter elements. In practice, a builder would usually use elements with a tapered-diameter schedule. Typical element tubing ranges are 3/4-5/8-1/2-inch for very high wind loads or 5/8-1/2-3/8-inch for moderate wind loads.

The Full-Size 2-Element Yagi

Two-element Yagis have several variables around which the design revolves.

1. Spacing between elements;
2. Length of reflector; and
3. Length of driven element.

We can also handle these variables in a number of ways. For example, we can

1. Optimize gain at the design frequency;
2. Optimize front-to-back ratio at the design frequency;
3. Strive for resonance;
4. Strive for maximum operating bandwidth (perhaps as defined by a 2:1 SWR); and/or
5. Strive for a 50-Ω match.

The mix and match of design goals leads to an almost indefinitely large number of antenna designs, according to what compromises the designer reaches. A maximum gain design may yield a combination of elements leaving considerable reactance at the feedpoint. Altering the driven element toward resonance may yield an element combination, even when the reflector is re-maximized for gain, which is slightly off peak. Similar compromises apply to any other combination of ingredients in the design goals.

Designing for Maximum Front-to-Back Ratio

We shall look at several models in free space using different spacing values. We shall optimize the design for maximum front-to-back ratio and resonance for each spacing value. The degree of element lengthening needed for a gamma or Tee match, or the degree of shortening needed for a beta match, is too small to make a significant difference in performance. To see why designers lean toward the maximum front-to-back ratio frequency as the design center (or near-center), we shall later examine some beams designed for maximum gain at the design center frequency. We shall also look at some models over real ground using one or two spacing values and optimized for front-to-back ratio at antenna resonance to determine the operating bandwidth characteristics of the array.

In general, 2-element Yagis optimized for maximum front-to-back ratio have

resonant feedpoint impedances in the mid-30-Ω range with spacing values of about 1/8 λ and in the 50-Ω range with spacing values in the vicinity of 0.16 λ. These values represent a range of 4.1 to 5.4 feet at 29 MHz, which you can scale to any other frequency with an appropriate multiplier.

Let's take a more comprehensive look at this collection of antennas by specifying a sequence of spacing at 0.04 λ intervals from 0.08 λ through 0.24 λ (2.7' through 8.1'). The models will be in free space. The dimensions used for these models appear in **Table 2-1**. (See models 2-1.ez through 2-5.ez.)

Table 2-1. Dimensions of models used in evaluating performance vs. element spacing. All elements 3/8" aluminum.

Spacing		Driver Length		Reflector Length	
WL	Feet	WL	Feet	WL	Feet
0.08	2.71	0.472	16.01	0.502	17.02
0.12	4.07	0.466	15.82	0.503	17.06
0.16	5.43	0.464	15.74	0.503	17.05
0.20	6.78	0.464	15.75	0.503	17.05
0.24	8.14	0.466	15.82	0.502	17.03

Although there may not be very much difference between element lengths for each step, obtaining adequate performance over a desired bandwidth requires very careful building.

Table 2-2 provides data on the modeled performance of these beams using NEC (either -2 or -4). The gain values are for free space. To obtain an estimate of the gain at 1-λ above ground, add about 5.4 dB to the gain values in the tables. The driven element is resonant within +/-j1 Ω in each case. Gain figures will be for 29 MHz, although that is the frequency of maximum front-to-back ratio. Maximum gain occurs somewhat lower in frequency.

Table 2-2. Modeled NEC (-2 or -4) performance of the 2-element Yagis in Table 2-1. (Reference dipole gain in free space = 2.13 dBi)

Spacing	Gain (dBi)	Gain (dBdr)	F-B (dB)	Feed Z (R +/- jX)
0.08 wl	6.32	4.19	11.37	17.27 + j0.06
0.12	6.25	4.12	11.20	32.04 - j0.00
0.16	6.12	3.99	10.84	46.87 + j0.03
0.20	5.88	3.75	10.35	61.07 - j0.13
0.24	5.56	3.43	9.71	73.01 - j0.34

Let's make the same run with MININEC (**Table 2-3**). Typically, MININEC

yields dimensions that are about 0.04' (1/2") shorter than NEC at 29 MHz, although some versions of MININEC have a correction factor to bring them into alignment as frequency increases. (The MININEC program Antenna Model has been so thoroughly corrected that its results correlate almost perfectly with NEC.)

Table 2-3. Modeled MININEC performance of the 2-element Yagis in Table 2-1. (Reference dipole gain in free space = 2.12 dBi)

Spacing	Gain (dBi)	Gain (dBdr)	F-B (dB)	Feed Z (R +/- jX)
0.08 wl	6.31	4.19	11.40	17.09 - j0.59
0.12	6.25	4.13	11.19	32.33 + j0.17
0.16	6.09	3.97	10.86	46.84 - j0.56
0.20	5.87	3.75	10.34	61.12 + j0.07
0.24	5.56	3.44	9.72	72.42 - j0.59

The differences between the two modeling systems are not great enough to make a difference under any practical circumstance. If you create your own models using the dimensions in **Table 2-1**, you may find very small differences in the results that you obtain. Different implementations of both NEC and MININEC exhibit very small (and operationally insignificant) differences due to methods of compilation. As well, different CPUs may also show slight differences in results, even though using the same program. These differences would only matter if they reach the level of being operationally significant.

To understand why designers tend to select spacing values of 0.12 λ to 0.16 λ, we need one additional data table in hand: the SWR of the antennas across the band from 28 to 30 MHz (given here in 0.5-MHz increments, using the SWR sweep facility of EZNEC). Each sweep in **Table 2-4** is centered on the resistive component of the feedpoint impedance at the design center frequency. Values greater than 1.0 occur at that frequency because of the remnant reactance.

Table 2-4. SWR values relative to the resonant impedance for the test models.

Spacing	SWR at 28	28.5	29	29.5	30 MHz
0.08 wl	30.3	5.64	1.02	3.01	5.66
0.12	7.34	2.37	1.00	1.82	2.78
0.16	3.52	1.70	1.00	1.47	2.00
0.20	2.31	1.42	1.00	1.31	1.66
0.24	1.82	1.29	1.01	1.23	1.48

Fig. 2-2 provides a graphic view of the same data so that you may better see the rates of change of SWR both above and below the design frequency.

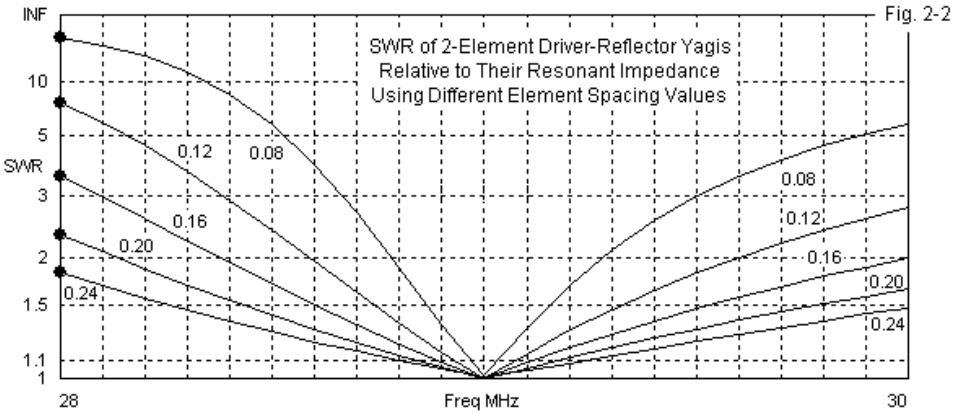

Obviously, the widest spacing offers the greatest operating bandwidth, but at the cost of reduced gain and front-to-back ratio. Consequently, a design tends to compromise among the highest gain, the highest front-to-back ratio, adequate operating bandwidth, and feedpoint impedance. 0.16 λ spacing offers the opportunity for a direct match to 50-Ω coax feedlines with a fairly useful bandwidth for most of the HF ham bands. (Remember to reduce the bandwidth by dividing the 10-meter figure by the ratio of 29 MHz to the frequency of interest for lower HF bands.) Spacing values closer to 0.12 λ yield higher gains and front-to-back ratios, but over a narrower bandwidth.

There are two other design problems one must consider. First, the frequency of maximum gain is well below the frequency of maximum front-to-back ratio. The gain tapers gradually as the frequency increases within the operating bandwidth. Second, SWR increases rapidly below the design frequency and more slowly above it. When this factor is combined with the gain situation, one can design an illusion: an antenna with decent SWR but very little gain or front-to-back ratio in the upper half of its operating range.

To illustrate this situation, let's look at the models in more detail, examining their gain and front-to-back patterns across 10 meters. **Table 2-5** presents sampled data in 0.5-MHz increments.

Table 2-5. Performance of the 2-element Yagis from 28 to 30 MHz.

Frequency	28	28.5	29	29.5	30 MHz
0.08 wl spacing					
Gain (dBi)	6.37	6.92	6.32	5.77	5.37
Gain (dBdr)	4.24	4.79	4.19	3.64	3.24
F-B (dB)	1.82	8.65	11.38	10.12	8.57
0.12 wl spacing					
Gain (dBi)	6.98	6.74	6.25	5.82	5.48
Gain (dBdr)	4.85	4.61	4.12	3.69	3.35
F-B (dB)	5.46	9.79	11.19	10.37	9.18
0.16 wl spacing					
Gain (dBi)	6.88	6.55	6.12	5.74	5.43
Gain (dBdr)	4.75	4.42	3.99	3.61	3.30
F-B (dB)	6.66	9.84	10.86	10.29	9.32
0.20 wl spacing					
Gain (dBi)	6.64	6.28	5.87	5.50	5.20
Gain (dBdr)	4.51	4.15	3.74	3.37	3.07
F-B (dB)	7.31	9.66	10.35	9.87	9.03
0.24 wl spacing					
Gain (dBi)	6.37	5.98	5.56	5.18	4.86
Gain (dBdr)	4.24	3.85	3.43	3.05	2.73
F-B (dB)	7.36	9.22	9.73	9.29	8.51

Fig. 2-3 provides a graph of the gain curves for three of the spacing values (0.08, 0.16, and 0.24 λ). Had I used only the 3 middle values from the table, the gain curve lines would not be clear. The increment used in the sweeps is 0.1 MHz.

The gain curves are generally parallel to each other. However, the display of the curve for the closest spacing shows what happens at some frequency below the design frequency. The gain rises slowly, but at a certain frequency, it begins to drop rapidly. The same phenomenon occurs with the curves for the wider spacing of elements, but the frequency at which the gain drops off falls below the limit of the sweep. The gain curve for the driver-reflector type of Yagi is unique. Any Yagi with at least one director will produce a curve with the

opposite characteristic; that is, the gain will rise as frequency increases.

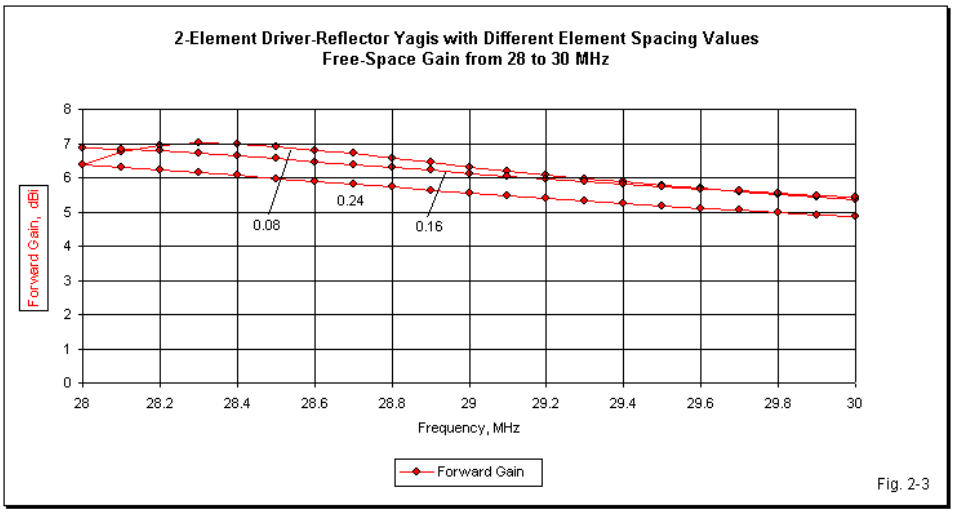

Fig. 2-3

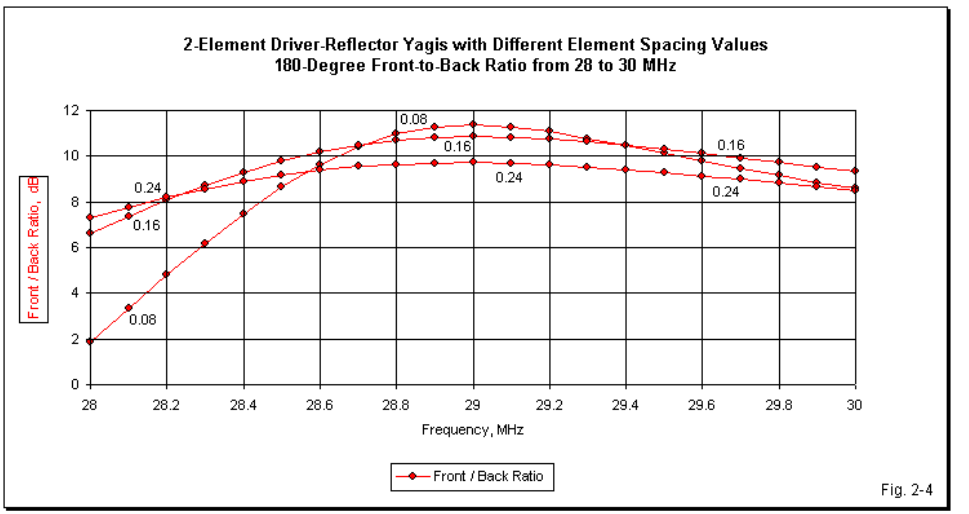

Fig. 2-4

Fig. 2-4 shows the 180° front-to-back ratios for the same three Yagi designs. At the design frequency, closer spacing yields a higher front-to-back ratio. However, closer spacing yields a smaller range over which the front-to-back ratio remains near its peak value. In contrast, wider spacing yields a lower value of peak front-to-back ratio, but the ratio remains near the peak value over a wider range of frequencies. Note that, like the SWR, the front-to-back ratio tends to decrease more rapidly below the design frequency than above it.

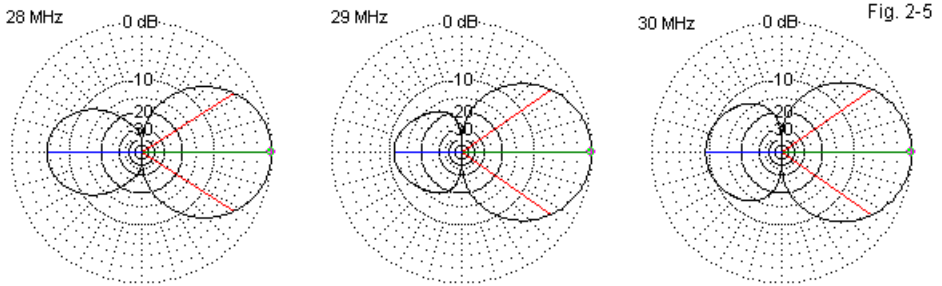

Free-Space E-Plane (Azimuth) Patterns: 2-Element Yagi with 0.12-Wavelength Spacing

Fig. 2-5 shows three free-space patterns for the Yagi with 0.16-λ element spacing. It illustrates typical patterns at 28, 29, and 30 MHz. Note that the rear lobe changes its size or strength, but it remains "well behaved." That is, it does not develop large multiple lobes, but remains a single rearward lobe. The patterns also illustrate why we may use the 180° front-to-back ratio as a marker of performance with this series of beams. The 180° ratio and the worst-case ratio are identical. As we saw in the first episode, this feature does not hold true for every possible 2-element Yagi design.

From tables and graphs we can draw several conclusions applicable to 2-element Yagis on any band.

1. Reading across the tables, it is clear that the maximum gain frequency is within the sweep for the closest spaced beam, but at or beyond the lower frequency limit for the other models. The closer the spacing, the closer together

are the frequencies of maximum gain and maximum front-to-back ratio.

2. The wider the spacing, the lower the overall values of gain for the entire sweep.

3. Gain falls off somewhat rapidly above the design center frequency. It rises even more rapidly below the design center frequency, although that curve is invisible in these tables.

4. If we compare SWR and gain data, it is clear that maximum gain occurs in a region of high SWR when the beam is designed for maximum front-to-back ratio.

5. Front-to-back ratio holds up best at spacing values between 0.12 λ and 0.20 λ, inclusive.

It is therefore possible to design a beam with a wide operating (2:1 SWR) bandwidth using spacing values of 0.20 or 0.24 λ, but accrue little more than 3 dB gain over a dipole and a front-to-back ratio under 10 dB for most of that bandwidth. Equally, achieving more than 4 dB gain over a dipole and a front-to-back ratio greater than 10 dB for a large portion of the operating bandwidth is not feasible with a full size 2-element driver-reflector Yagi.

As a result of these limiting conditions, when a 2-element Yagi is designed for maximum front-to-back ratio, design compromises are necessary. When the bandwidth requirements are narrow, as on 17 and 12 meters, a spacing in the vicinity of 0.12 λ is often chosen for the best combination of gain and front-to-back ratio, along with a sufficiently high feedpoint impedance to assure efficiency. For wider bands, a spacing around 0.16 λ is favored, trading some gain and front-to-back ratio for operating bandwidth and an easy match to 50-Ω coax.

Designing for Maximum Gain

The alternative design strategy that we might use is to design our beam so

that the array resonates at or close to the frequency of maximum gain. **Table 2-6** provides the dimensions for the new series of 2-element driver-reflector Yagis.

Table 2-6. Dimensions of maximum-gain models used in evaluating performance vs. element spacing. All elements 3/8" aluminum.

Spacing		Driver Length		Reflector Length	
WL	Feet	WL	Feet	WL	Feet
0.08	2.71	0.477	16.18	0.490	16.63
0.12	4.07	0.470	15.95	0.488	16.54
0.16	5.43	0.467	15.83	0.484	16.42
0.20	6.78	0.465	15.76	0.481	16.33
0.24	8.14	0.464	15.74	0.479	16.25

Compared to the Yagis designed for maximum front-to-back ratio at the design frequency, the maximum-gain versions have longer drivers and shorter reflectors, with the reflector length-differences being more radical. These differences yield a significant difference in performance at the design frequency (29.0 MHz), as shown in **Table 2-7**. (See models 2-6.ez through 2-10.ez.)

Table 2-7. Modeled free-space performance of 2-element driver-reflector Yagis designed for maximum gain at resonance.
NEC (-2 or -4) (Reference dipole gain in free space = 2.13 dBi)

Spacing	Gain (dBi)	Gain (dBdr)	F-B (dB)	Feed Z (R +/- jX)
0.08 wl	7.02	4.89	6.16	9.54 + j0.20
0.12	6.99	4.86	6.38	19.59 - j0.23
0.16	6.88	4.75	5.95	30.83 + j0.29
0.20	6.69	4.56	5.85	43.47 + j0.11
0.24	6.43	4.30	5.65	55.92 - j0.24

The gain figure for the 0.08 λ spaced Yagi optimized for gain approaches the absolute maximum gain obtainable from a 2-element parasitical array. However, this gain is obtained at a cost: a severe reduction in the front-to-back ratio and a very low feedpoint impedance. As spacing is increased, the maximum obtainable gain also decreases, along with the front-to-back ratio at that gain figure. Despite the severe reduction in the front-to-back ratio, which makes the beam almost a narrow-beamwidth dipole, the patterns remain well behaved with one exception. **Fig. 2-6** provides a sample pattern set at 28, 29, and 30 MHz to reveal the exception. The element spacing for the sample is 0.16-λ.

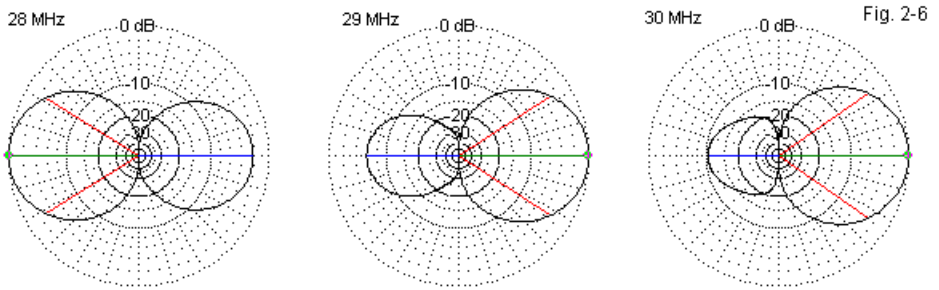

Fig. 2-6

Free-Space E-Plane (Azimuth) Patterns: 2-Element Maximum Gain Yagi with 0.16-Wavelength Spacing

At 30 MHz, the pattern almost replicates the maximum front-to-back ratio version pattern at its design frequency. However, at the other end of the swept range, we find that the pattern has reversed itself, with the major lobe in the formerly rearward direction. The illustration has some importance in thinking about Yagis. Just because a parasitic element happens to be longer than the driver, it does not automatically become a reflector. Its function as a reflector or as a director depends upon the relative current magnitude and phase on the two elements, and those values change with each change in frequency for a fixed set of dimensions.

Maximum-gain 2-element Yagi designs have very limited SWR bandwidths, as demonstrated in **Table 2-8** and in **Fig. 2-7**.

Table 2-8. SWR from 28 to 30 MHz relative to the resonant impedance of the Yagi.

Spacing	SWR at	28	28.5	29	29.5	30 MHz
0.08 wl		39.8	16.1	1.02	7.03	14.43
0.12		15.1	5.22	1.01	3.00	5.37
0.16		7.09	2.84	1.01	2.07	3.21
0.20		4.24	2.03	1.00	1.65	2.28
0.24		2.97	1.67	1.01	1.43	1.83

Only at a spacing of 0.24 λ do we obtain any significant operating bandwidth, and by that spacing, gain and front-to-back ratio have fallen severely. In fact, gain has decreased to the levels of more closely spaced maximum front-to-back designs.

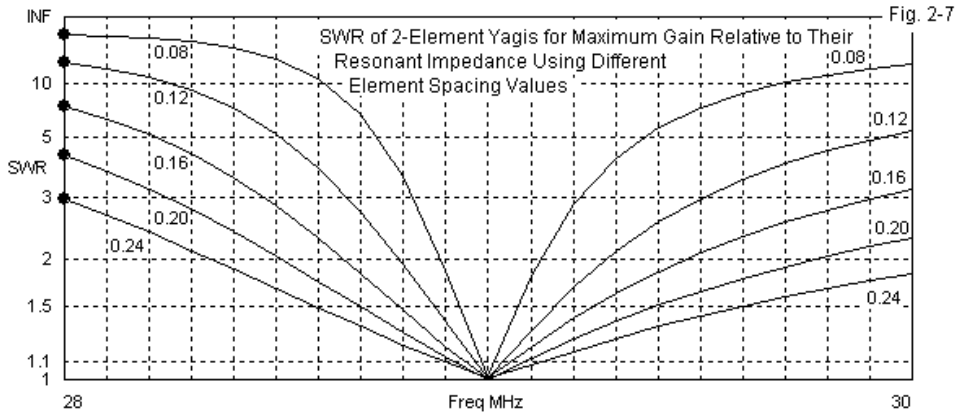

As if these factors were insufficient reasons for designers to move the operating point of the array toward the maximum front-to-back region, an additional problem emerges if one examines the beam's properties across a frequency span. **Table 2-9** provides a rough indication of the difficulty.

The entries labeled "R" indicate gain in the reverse direction from that of the remainder of the entries. The maximum gain point in the geometry of a 2-element Yagi occurs just above the frequency at which the parasitical element begins to function as a reflector. Below a certain critical frequency that varies with spacing, the parasitical element becomes a director, even though it is physically longer than the driven element. (It would be shorter if the driven element were lengthened to resonance.) **Fig. 2-8** shows the transition in graphical form using 3 of the sampled spacing values (0.08, 0.16, and 0.24 λ).

Table 2-9. Operating characteristics from 28 to 30 MHz of Yagis designed for maximum gain.

Frequency	28	28.5	29	29.5	30 MHz
0.08 wl spacing					
Gain (dBi)	7.14 R	6.08 R	7.02	6.60	6.04
Gain (dBdr)	5.01 R	3.95 R	4.89	4.47	3.91
F-B (dB)	10.44	0.86	6.16	10.54	10.57
0.12 wl spacing					
Gain (dBi)	6.92 R	6.23	6.99	6.67	6.21
Gain (dBdr)	4.79 R	4.10	4.86	4.54	4.08
F-B (dB)	4.49	1.31	6.38	9.97	10.87
0.16 wl spacing					
Gain (dBi)	6.30 R	6.37	6.88	6.63	6.23
Gain (dBdr)	4.17 R	4.24	4.75	4.50	4.10
F-B (dB)	2.21	1.96	5.95	9.09	10.51
0.20 wl spacing					
Gain (dBi)	5.52 R	6.37	6.69	6.45	6.06
Gain (dBdr)	3.39 R	4.24	4.56	4.32	3.93
F-B (dB)	0.50	2.65	5.85	8.50	9.91
0.24 wl spacing					
Gain (dBi)	5.41	6.26	6.43	6.17	5.78
Gain (dBdr)	3.29	4.13	4.30	4.04	3.65
F-B (dB)	0.63	3.07	5.65	7.87	9.17

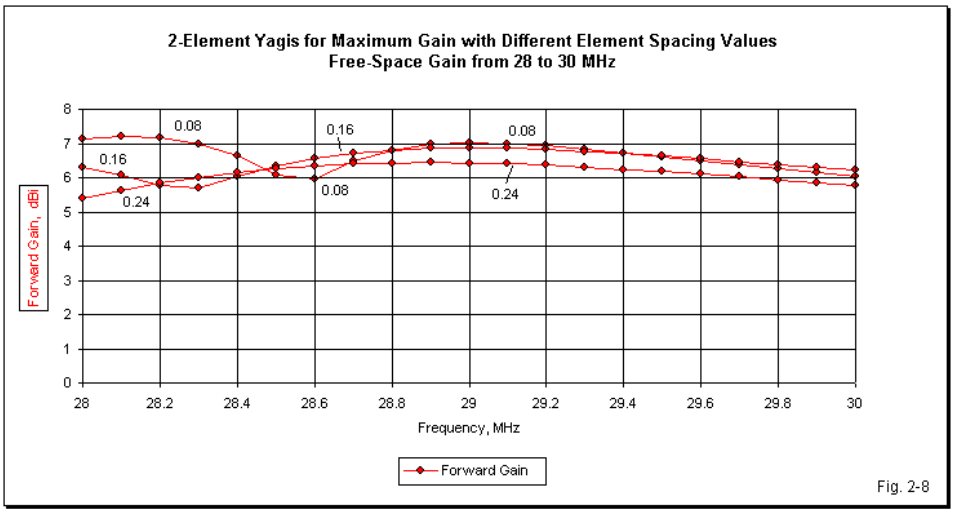

Fig. 2-8

The curve for a spacing of 0.24-λ does not undergo the reversal. However, the curves for the closer spacing values show a distinct minimum value, and below the frequency at which this occurs, the gain rises again, but in the reverse direction. Even though the graph uses 0.1-MHz increments, the minimum gain values do not approach zero. The actual transition occurs between sampled points and occurs over a very narrow frequency span. The frequency of transition, as a spread from the design frequency, is about 600 kHz for 0.16-λ spacing and only 400 kHz for 0.08-λ spacing. As spacing is increased, the frequency at which the beam flips directions grows more distant from the frequency of maximum gain. However, performance of the beam in the range between reversal and maximum gain is marginal at best.

The front-to-back curves, shown in **Fig. 2-9** for the same three samples, provide the same information relative to the frequencies at which the pattern reverses itself. The indicator is the minimum value of front-to-back ratio for each of the curves. From the rapidly declining value of front-to-back ratio, the 0.24-λ sample beam might reverse itself within 100-200 kHz below the limit of the sweep.

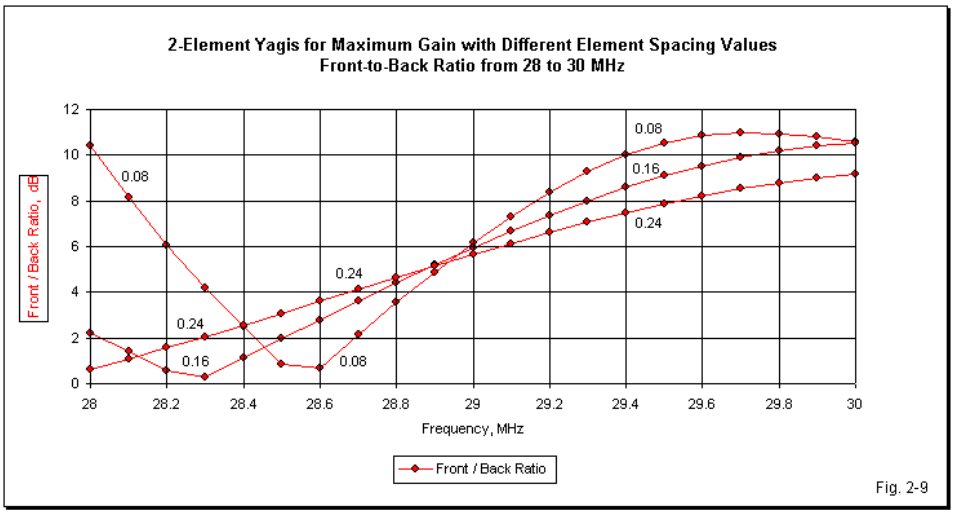

Fig. 2-9

We may note in passing, with an eye on the 0.08-λ spaced beam, that the driven-element-director configuration is capable of slightly higher gain than the driven-element-reflector arrangement.

The purpose of these latter tables and graphs is twofold. First, they demonstrate the maximum gain of which a full size 2-element driven-element-reflector Yagi is capable, and the conditions surrounding that achievement. Second, they also illustrate why designers tend to give up maximum gain in favor of maximum front-to-back ratio as the design focus: adequate gain, wider operating bandwidth, higher feedpoint impedances, and higher front-to-back ratios. We may reiterate that above the frequency of maximum front-to-back ratio, the feedpoint SWR (referenced to the impedance at the design center frequency) decreases more slowly than below the maximum F-B frequency, but both gain and F-B ratio decrease together. Hence, specifying the peak values of gain, front-to-back ratio, and operating bandwidth does not always give a fair indication of beam performance. That is why we need to view tables or graphs of performance over the entire operating passband. We may also note that in no case of normal directional operation does the driven-element-reflector free-space gain reach 5 dBd(r).

Height above Ground

The characteristics of a given 2-element Yagi design are not constant with height above ground until the beam is well above 1 λ high. **Table 2-10** provides data on gain, elevation angle, front-to-back ratio and feedpoint impedance for one of the 2-element Yagis that we have explored in free space. To maximize gain while having a workable feedpoint impedance, I have selected the version with a spacing of 0.12-λ between the driver and reflector. However, with suitable changes in the exact numbers, any of the beams in the free-space collection would show similar trends as we vary the height above ground. (See model 2-11.ez.)

29 MHz 2-Element Driver-Reflector Yagi with 0.12-Wavelength Element Spacing at Various Heights above Average Ground					
Height wl	Gain dBi	Gain dBd	F-B	Feed R	Feed X
0.0625	-0.24	-0.73	4.14	40.8	-7.57
0.125	5.1	0.46	6.18	25.44	-5.47
0.1875	7.44	1.66	7.92	24.73	0.4
0.25	8.57	2.84	9.79	27.5	3.86
0.3125	9.28	3.53	11.63	30.95	4.94
0.375	9.84	3.77	13.35	34.03	4.08
0.4375	10.35	3.73	14.29	35.94	1.7
0.5	10.8	3.57	13.36	35.78	-1.38
0.5625	11.1	3.44	11.52	33.47	-3.25
0.625	11.23	3.48	10.22	30.9	-2.78
0.6875	11.27	3.71	9.8	29.71	-0.98
0.75	11.27	3.99	10.09	29.98	0.8
0.8125	11.31	4.19	10.86	31.15	1.85
0.875	11.37	4.22	11.82	32.61	1.92
0.9375	11.48	4.14	12.55	33.75	1.03
1	11.6	3.97	12.55	34.1	-0.2
1.0625	11.69	3.84	11.69	33.13	-1.53
1.125	11.72	3.82	10.78	31.73	-1.63
1.1875	11.71	3.9	10.33	30.83	-0.78
1.25	11.7	4.07	10.4	30.78	0.31
					Table 2-10

To gather an appreciation of this data, you may wish to simultaneously view the data in Chapter 1 on the dipole at the same heights above average ground. Both the dipole and the Yagi use the same element material: 3/8" diameter aluminum. Therefore, we may make some fair comparisons between the two antennas.

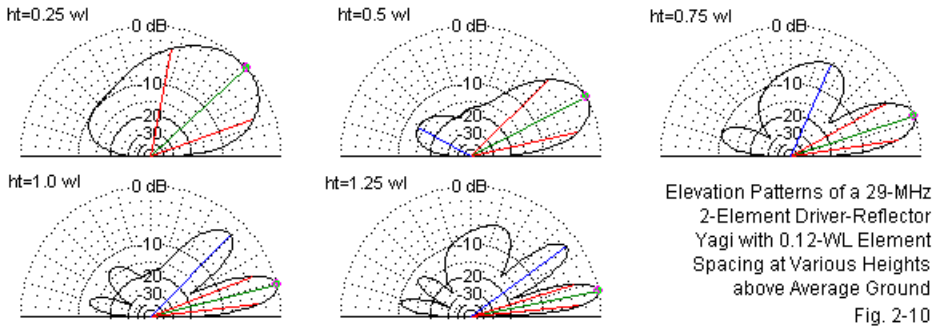

Elevation Patterns of a 29-MHz 2-Element Driver-Reflector Yagi with 0.12-WL Element Spacing at Various Heights above Average Ground
Fig. 2-10

Fig. 2-10 shows elevation patterns for the Yagi at increments of 1/4-λ in height. These patterns correspond to the dipole elevation patterns in Chapter 1's **Fig. 1-10**. For every dipole elevation lobe and null, there is a corresponding lobe and null in the Yagi patterns. However, we find two major differences between the patterns. The first difference is obvious: the lobes to the rear of the Yagi's forward direction are much weaker than the corresponding dipole lobes. We might easily overlook the second difference. Compare the emerging dipole and Yagi lobes at the highest elevation angles, especially at heights of 0.75 λ and 1.25 λ. The Yagi higher-angle lobes are always smaller than corresponding dipole lobes. In Chapter 1, we noted that beams obtain forward gain from several sources, one of which is a reduction in both the vertical and the horizontal beamwidth. The reduction in the strength of the Yagi upper-angle lobes is part of the reduction in the vertical beamwidth.

As we observed in the behavior of the dipole, the gain of the 2-element Yagi does not increase smoothly as we increase its height above ground. However, the Yagi gain curve (in dBi), shown in **Fig. 2-11**, is much smoother than the dipole curve in Chapter 1. In fact, the only section of **Table 2-10** that shows a very tiny decline in gain is between heights of 1.125 λ and 1.25 λ. That decline is only 0.02 dB.

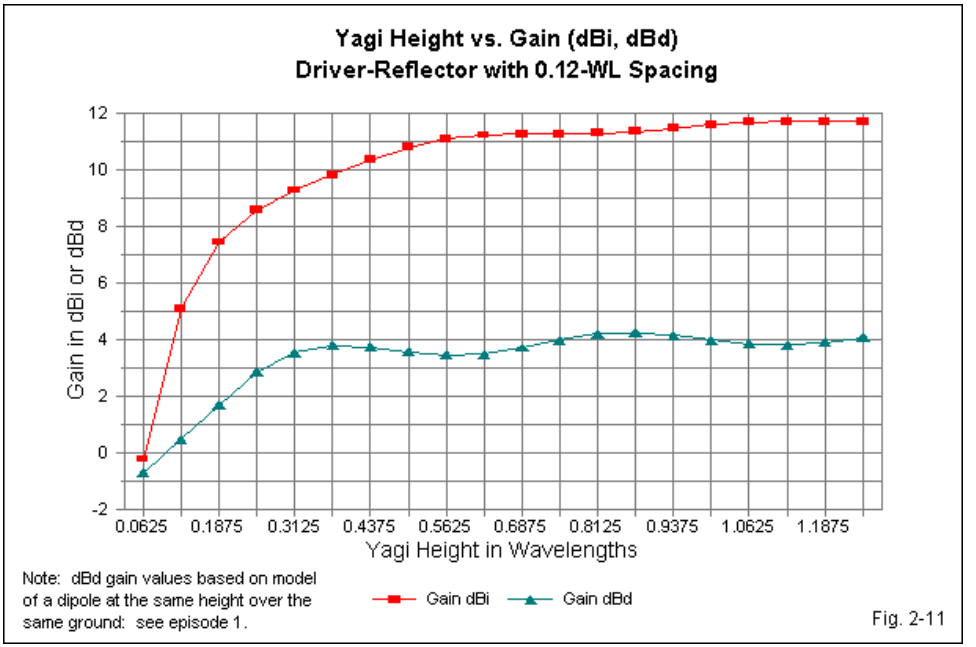

Fig. 2-11

The curve designated dBd shows a different curvature than the one marked dBi. The dBd gain is based on the difference in gain in dBi between the Yagi and the dipole in Chapter 1. Since the gain of the dipole varies over a greater range than does the Yagi gain, the Yagi gain in dBd shows higher peaks and deeper nulls. Now suppose that you were selling a 2-element that is for all practical purposes identical to the Yagi sold by a competitor. If you check the gain of your antenna at a height of 7/8-λ, you may claim a gain of 4.22 dBd. If you check your competitor's beam at 5/8-λ, then its gain is only 3.48 dBd. By "judiciously" omitting the details of how you obtained the figures, you might even claim in your sales literature that your Yagi has more than a half-dB higher gain than your competitor's. This small demonstration perhaps enlightens you as to why we shall focus upon dBi as the more useful unit of gain measurement.

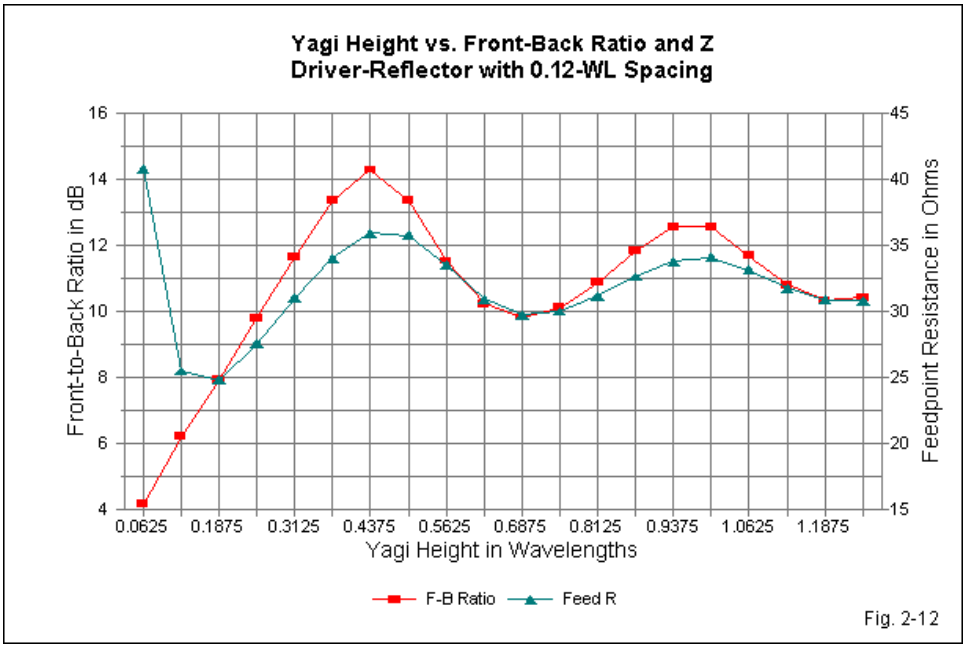

Fig. 2-12

The undulations in the front-to-back ratio with changing antenna height are much more pronounced than the small changes in forward gain. **Fig. 2-12** graphs the 180° front-to-back ratio of our sample Yagi. Using the right Y-axis, the graph also tracks the changes in the feedpoint resistance. The Yagi uses a single set of physical measurements, shown in **Table 2-1**. Hence, as **Table 2-10** makes clear, the reactance drifts slightly off resonance relative to the free-space value of the original design. However, the reactance drift is small and varies from being slightly capacitive to being slightly inductive, depending upon the exact height.

More significant than the reactance drift--especially for our understanding of 2-element Yagi behavior--is the fact that above a height of about 3/16-λ, the feedpoint resistance and the front-to-back ratio curves track each other very closely. In contrast, the gain curves--to the degree that one can detect peaks

and nulls--are offset from these two curves. In a 2-element driver-reflector Yagi, the feedpoint impedance and the front-to-back ratio are very closely related. This and related height phenomena were reported upon extensively in "The Effects of Antenna Height on Other Antenna Properties: A Computer Study," *Communications Quarterly*, 2 (Fall, 1992), 57-79.

Needless to say, when fine shades of performance comparison are at stake, mere numbers for gain, front-to-back ratio, and operating bandwidth are normally meaningless without a complete specification of their derivation. Even summaries of typical cases of derivation can make comparison elusive, since they often leave ambiguous which derivation was used for a particular antenna. Until buyers of amateur radio antennas are provided with the same detailed information that can be demanded by military, government, and private corporations for contract fulfillment, *caveat emptor* must still rule the marketplace.

With this caution, we may complete our sampling of 2-element driver-reflector behavior--at least so far as full-size Yagis are concerned. However, modern-day urban and suburban amateurs are cramped for antenna space. They wonder if they can effectively shrink an antenna and still derive adequate performance from it. Since the 2-element Yagi seems the simplest beam to shrink, we should explore the possibilities.

3. Shortened Dipoles and Capacity Hat Yagis

There are two very general ways in which we may shorten a linear element and maintain resonance or some other desired property. One method is to add in one form or another inductive reactance to the capacitively reactive shortened element. The two most popular positions for placing inductive reactances are at the element center and somewhere outward from the center position. We normally use a single inductive reactance when we center-load an element. However, mid-element-loading requires 2 equal reactances placed equally distant from the element center.

The second form of achieving shorter but still resonant elements is to add hats at the element ends. Although we shall examine only symmetrical hats, it is also possible to use non-symmetrical structures, including lengths of wire compressed into a solenoid configuration. Since there are more forms of center- and mid-element-loading than of hats, let's begin with the hat.

Shortened Yagis with Capacity Hats

No 2-element driven-element-reflector Yagi with shortened elements can achieve the gain of a full-size Yagi of the same configuration over an extended bandwidth. However, a shortened Yagi often achieves a significantly higher front-to-back ratio than its full-size counterpart.

There is one seeming exception to these principles: the shortened Yagi "loaded" at the element outer ends with so-called capacity hats. The exception is an illusion, because the hatted dipole is not loaded in the conventional sense. Rather, the main linear element section is shortened and the remaining length is composed of a symmetrical array of wires that is at right angles to the linear section and whose net radiation is at or near zero. **Fig. 3-1** illustrates the hat-loaded dipole, and shows several configurations of hats.

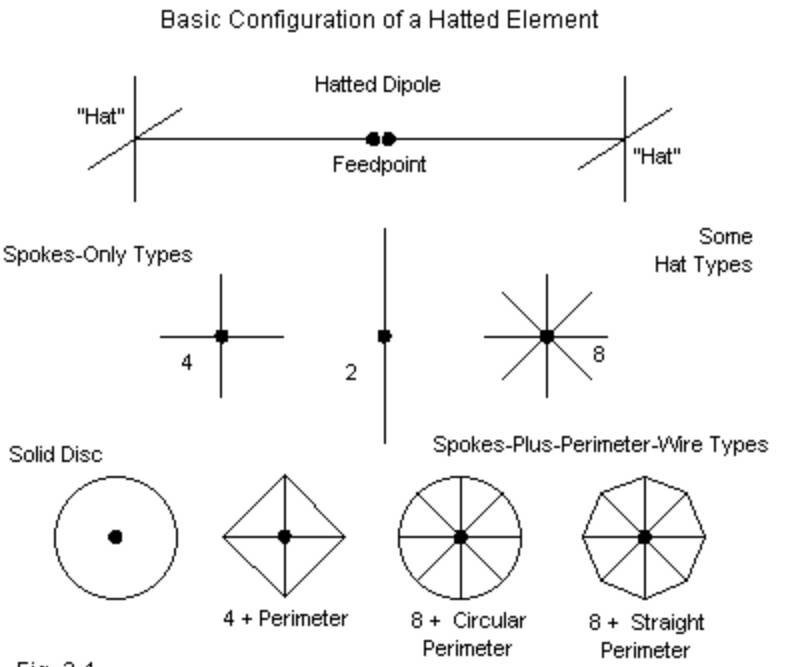

Fig. 3-1

Hats that use spokes alone require a larger radius than when the same number of spokes are terminated by a perimeter wire. Essentially, the perimeter wire continues each spoke in two directions, so that the zero-current point is midway between two spoke tips. With or without a perimeter wire, we require shorter spokes as we increase their number. Once we reach about 60 spokes, the length decrease ends, since the structure effectively simulates a solid disc.

Fig. 3-2 compares the current distribution along a standard full-size dipole and a hatted dipole that is about 70% full-size. Both antennas use 3/8" diameter aluminum elements throughout. Current along the linear section of the hatted dipole at the point where the hat begins is the same as it would be on a full-size linear element at the same distance from the feedpoint. The current divides

among the wires of the hat array, and the hat array must be large enough to permit the element to reach resonance at the same frequency as the full-size element. The two assemblies in **Fig. 3-2** are 16.24' and 11.33' long, respectively for the full-size and the shortened antennas. The 4 spokes on the two ends of the hatted dipole are each 12" long. (See model 3-1.ez.)

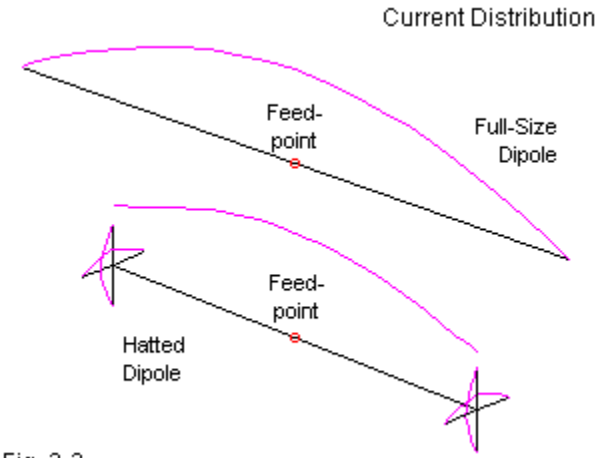

Fig. 3-2

Under these conditions, the performance of a full-size dipole and a shortened, hatted version will be very similar, at least with shortening no greater than to about 70% of full size. Since the distribution of current along the dipole element is roughly (but not perfectly) sinusoidal, most of the current contributing to the antenna radiation pattern occurs along the linear section of the elements and very little in the hat arrays.

Modeling an element-end hat is not so problematical in NEC as modeling closely spaced wires of complex geometries. Because the net radiation from a hat is zero, interactions with the main element that might make results unreliable when adjacent segments differ in diameter are minimized. NEC hat models

correspond very closely with those created with MININEC. The potential slight differences are minimized in this exercise by making the hat wires of the same diameter as the main element: 0.375 inch. See **Table 3-1**.

Table 3-1. A comparison between a full-size and a 70%-hatted dipole

Antenna	Frequency MHz	F-S Gain dBi	Feedpoint Z Ohms	SWR
Full	28	2.09	64.82 – j35.98	1.700
Hat		2.00	52.77 – j33.78	1.833
Full	28.5	2.11	68.34 – j17.87	1.296
Hat		2.01	55.61 – j16.39	1.338
Full	29	2.12	72.04 + j 0.18	1.003
Hat		2.02	58.60 + j 0.95	1.018
Full	29.5	2.14	75.94 + j18.20	1.286
Hat		2.03	61.75 + j18.27	1.356
Full	30	2.16	80.05 + j36.19	1.622
Hat		2.04	65.06 + j35.58	1.776

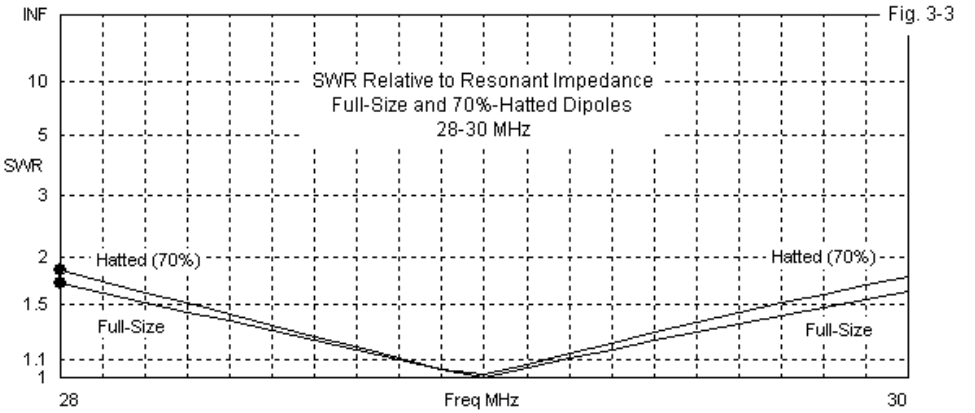

Although the hatted dipole at 70% of full size has a lower feedpoint impedance and a 0.1 dB lower gain, in practice, no difference in performance could be detected by any station using the two antennas side-by-side. If we plot the SWR performance of each type of dipole, as in **Fig. 3-3**, we discover that the hatted dipole has an SWR curve with nearly the same operating bandwidth as the curve for the full-size dipole. In fact, for any level of element shortening,

hatting provides a wider operating bandwidth than any method of inductive loading. Nonetheless, all forms of element shortening result in lower feedpoint resistive impedance values. With a length of 70% of full size, the shortened dipole has an impedance about 14 Ω less than the full-size antenna. For a fixed element length, all forms of inductive loading result in much lower impedance values.

A similar situation accrues to 2-element Yagis when we shorten each element to 70% full size and add hats. Let's compare the full-size Yagi from the last episode to a version that uses the 4-spoke hats of the dipole that we just created. **Fig. 3-4** shows the comparative sizes of each beam, using 0.12-λ (4.1') spacing. (See model 3-2.)

Fig. 3-4

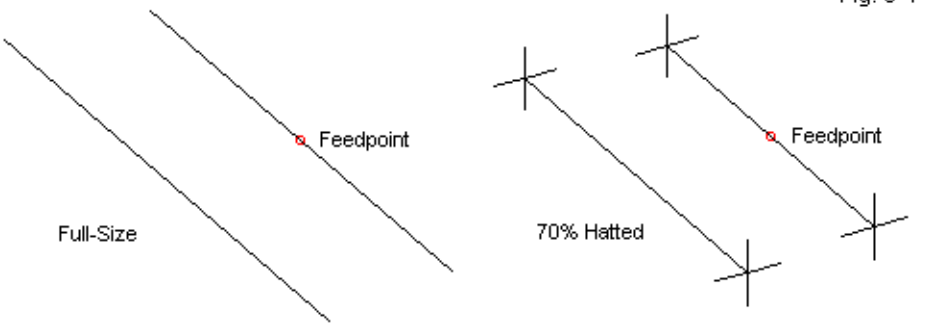

Comparative Sizes: Full-Size and 70% Hatted 2-element Yagis

Note an important aspect of Yagi design. Just because we may use various means to shorten the element lengths of a Yagi, we cannot significantly shorten the element spacing and hope for comparable performance. **Table 3-2** shows the dimensions of each array.

Table 3-2. Dimensions of full-size and 70% hatted Yagis. All elements 3/8" aluminum.

Spacing		Driver Length		Reflector Length		Hat-Spoke Length	
WL	Feet	WL	Feet	WL	Feet	WL	Feet
Full Size Yagi							
0.12	4.07	0.466	15.82	0.503	17.06	---	---
70% Hatted Yagi							
0.12	4.07	0.322	10.92	0.348	11.80	.0293	0.99

There are numerous ways in which to apply hats to elements. The technique used here, which has proven itself in prototypes, is to set a fixed size for the hats, regardless of whether they go on the driven element or on the reflector. As a result, the linear portions of the two elements have different lengths. This technique appears to yield somewhat better performance that using the same length for both linear element sections, with differences in the length of the spokes of the hat.

Table 3-3 provides a comparison between the performance of full-size and hatted Yagis.

Table 3-3. A comparison of the modeled performance of full-size and 70% hatted Yagis

Antenna	Frequency MHz	Gain dBi	F-B dB	Feedpoint Z Ohms	SWR
Full	28	6.98	5.43	15.49 – j48.55	7.34
Hat		6.53	2.47	10.39 – j48.51	11.29
Full	28.5	6.74	9.79	23.05 – j22.49	2.37
Hat		6.94	9.28	16.99 – j21.54	2.88
Full	29	6.25	11.20	32.14 – j 0.00	1.00
Hat		6.35	13.85	26.74 + j 0.77	1.03
Full	29.5	5.82	10.37	40.83 + j20.05	1.82
Hat		5.78	12.41	36.03 + j19.22	1.95
Full	30	5.48	9.17	48.75 + j38.76	2.78
Hat		5.34	10.15	43.81 + j35.77	2.99

The designer may select almost any proportion to use in dividing the element lengths between the linear section and the hat spokes. The combination used here actually gives the hatted Yagi a slight performance improvement at the design frequency. As is clearly visible in **Fig. 3-5**, the chief advantage occurs with respect to the hatted Yagi's front-to-back ratio.

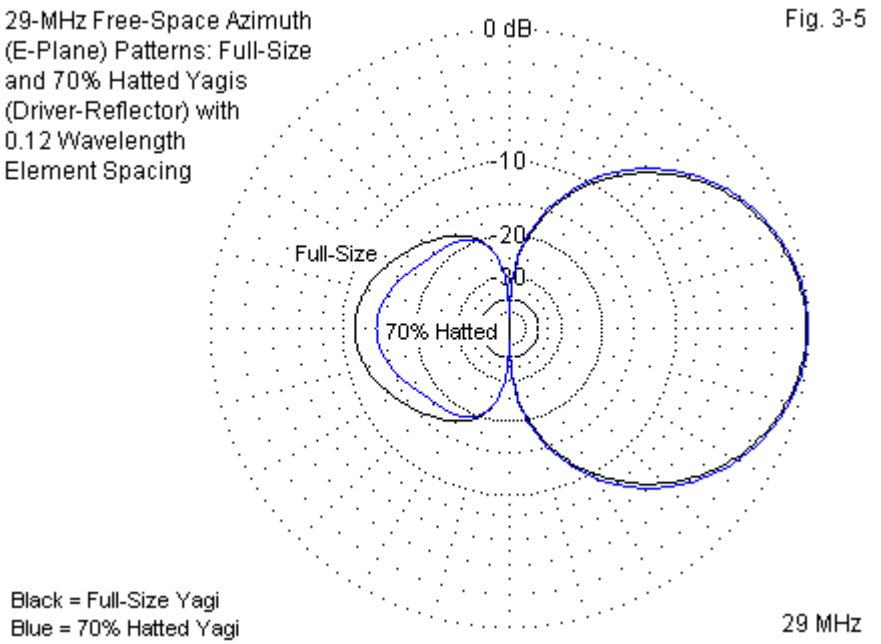

If we only view the data and patterns for the design frequency, we might go away with a misimpression about the seeming superiority of the hatted Yagi. However, a careful check of the tabular data across the 28-30-MHz sweep suggests that the hatted Yagi has a somewhat narrower operating bandwidth in every category. For example, as shown in **Fig. 3-6**, the hatted Yagi's gain curve is somewhat steeper than the curve for the full-size version, especially at the low end of the sweep. The hatted Yagi is on its way toward the point of pattern reversal, just where the full-size Yagi is reaching maximum gain.

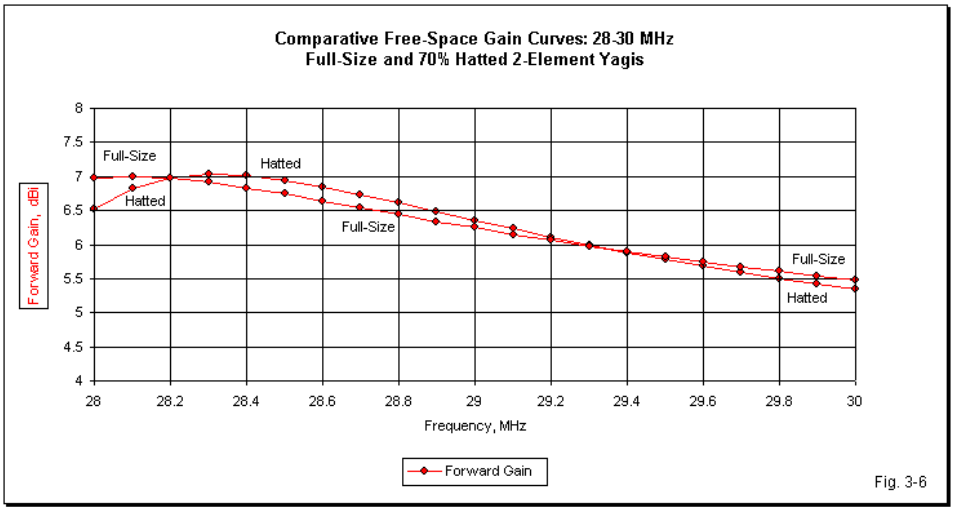

Fig. 3-6

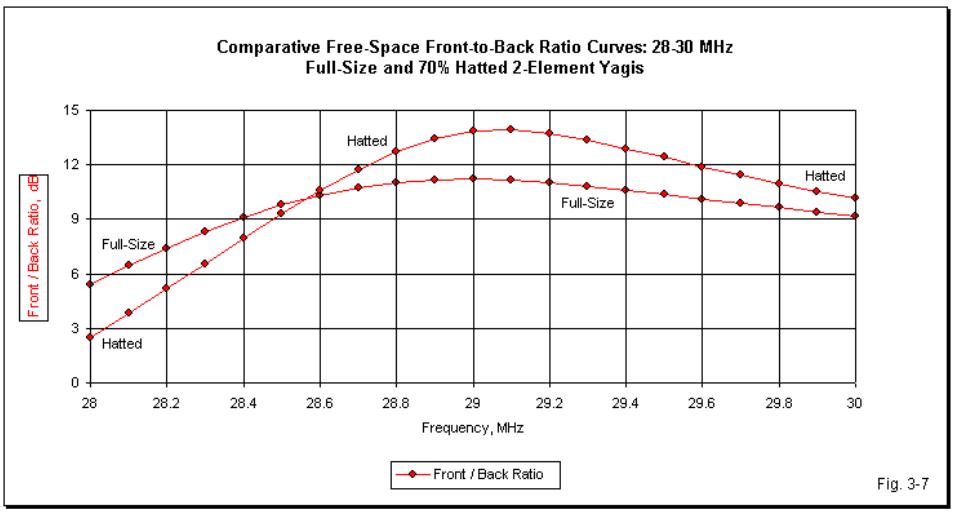

Fig. 3-7

The same general phenomenon appears in the curves for the front-to-back

ratio, shown in **Fig. 3-7**. The hatted curve is steeper, and the increased rate of fall-off is especially apparent at the low end of the sweep. In both cases, one might juggle the reflector length slightly so that the curves have equal front-to-back ratios at both ends of the sweep span, although the change might move the frequency at which the ratio reaches its peak value.

Because we have shortened the elements in the hatted Yagi, the design-frequency resonant impedance will be lower than for the full-size Yagi. In addition, as shown in **Fig. 3-8**, the SWR curves relative to the resonant impedance is steeper, resulting in a reduced operating bandwidth using the 2:1 SWR value as the bandwidth marker. Nevertheless, as we examine other forms of loaded Yagis in the next episode, it will be useful to keep these curves and the data in **Table 3-3** at hand for comparisons. In general, hatting elements of a set length yields the widest operating bandwidth of any form of element shortening.

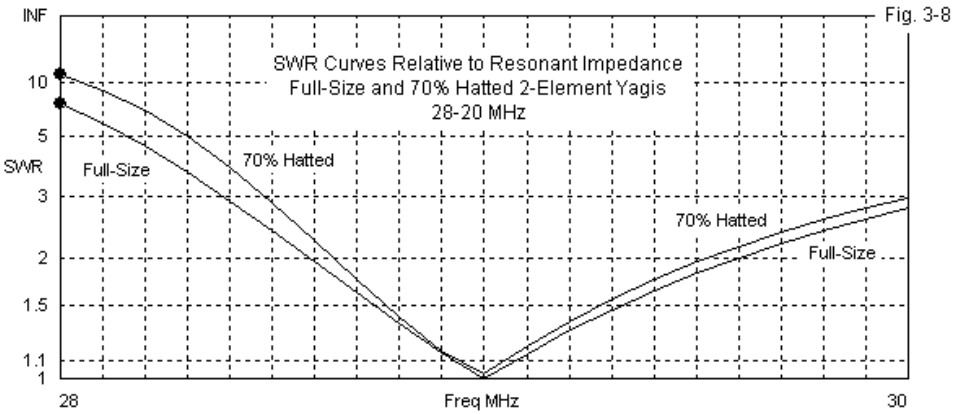

As will be evident later, hatted Yagis perform like what they are: almost full size beams. The slight performance differences are due to two variables: the shorter elements and the revised geometric relationships offered by those shorter elements.

Loaded Dipoles

A truly shortened element is one that terminates at its linear end. Such elements are not inherently resonant, but show significant capacitive reactance. To achieve resonance requires the insertion of a largely non-radiating inductive reactance. The form of the inductive reactance can be either a solenoid inductor or a shorted transmission line length: the latter are usually called linear loads. Linear loads are placed at the feedpoint (even when they may appear to have been placed elsewhere). Solenoid inductors are placed either at the feedpoint (center-loading) or somewhere farther out along the element as a pair of solenoids, one on each side of the feedpoint (mid-element loading).

Wherever an inductive load is placed, there is a current gradient representing the missing linear length for which the loading element substitutes. Compare the current distribution curves in **Fig. 9** for a full-size and a loaded dipole. Note the sharper step in current at the loading coil positions. Because such loads are only effective where antenna current is relatively high, the missing lengths of linear element represent radiation that for all practical purposes does not occur. Moreover, inductive loads, whatever their form, have losses associated with their resistance. Even high Q inductors introduce losses into the antenna element.

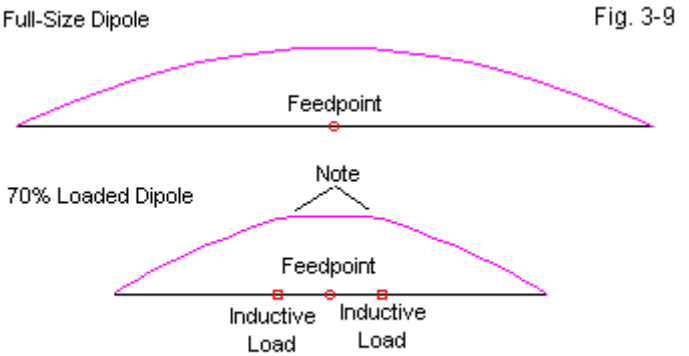

Current Distribution on Full-Size and 70% Loaded Dipoles

Both of these phenomena may be demonstrated by reference to shortened dipoles relative to full-size counterparts. Some loads are more difficult to model than others, but simple solenoid inductors may be modeled well within the limits of variables affecting any model's transfer to fabricated reality. NEC models treat solenoid inductances as wholly non-radiating elements, which is largely but not absolutely true in reality. Physical coils do radiate a bit as a function of the fact that the current magnitude at each end of the coil is not equal, a necessary condition for a solenoid being a "pure" inductance. However, the model also assigns the coil an effective zero space by distributing its loss along the element segment to which it assigned. That segment functions like a linear element, which in a real antenna is missing and replaced by the coil. The results remain as accurate to real antennas as any other aspect of antenna modeling. The more significant keys to accurate modeling lie in the realm of using adequate load values, placing them precisely, and using the proper technique of load assignment for the modeling task at hand.

To see effects of shortening antenna lengths alone, however, requires no load, but only an examination of short dipoles. For any model, the capacitive reactance at the feedpoint can be canceled by a lossless center inductance without any change of antenna radiating characteristics. Notice in **Table 3-4** the reduction of gain of the following antennas gradually shortened from full size to 40% of full size. All antennas are at 29 MHz in free space, with the same 0.375" diameter aluminum element.

Table 3-4. The effects of simply shortening the length of a dipole.

% of Full	Gain	Feed R	Feed Xc
100	2.13	72.04	0.79
90	2.05	52.41	102.3
80	1.98	37.76	205.0
70	1.92	26.71	312.5
60	1.87	18.33	430.8
50	1.83	12.01	568.6
40	1.79	7.31	741.6

These gain reductions are equivalent to using lossless center inductors as loading elements, each sized exactly to compensate for the capacitive reactance remaining at the feedpoint. Although the loss of gain is modest per step, it adds

up quickly as we shorten the antenna. Missing gain in the individual dipoles of a 2-element Yagi cannot be restored for any given design. Notice also the reduction of resonant feedpoint impedance down to values where basic efficiency may become a concern.

If we use real inductors having a finite Q, the losses grow even faster with element shortening. **Table 3-5** gives free space gain figures for coil Qs ranging from 300 to 50. Although higher values of Q are possible using coils with a high radius-to-length ratio, a Q of 300 may be about the best obtainable in a practical coil before weathering effects reduce that value. A Q of 50 represents a worst-case scenario where maintenance is lax and acid rain is heavy.

Table 3-5. Some dipole gain values for center-loaded dipoles of various lengths with inductors having various values of Q.

% of full	Gain with Q =	300	200	100	50
90		2.02	2.00	1.96	1.88
80		1.90	1.86	1.75	1.53
70		1.75	1.67	1.44	1.01
60		1.54	1.39	0.95	0.20
50		1.19	0.90	0.14	-1.07
40		0.52	-0.01	-1.25	-3.03

A dipole 50% of full size with a loading coil Q of 300 has lost nearly a full dB of gain, while the loss at 70% of full length is less 0.4 dB. Obviously, the gain loss increases faster than the rate of shortening. The rate of loss for lower Qs increases proportionately. (See and modify model 3-3.ez.)

A center-loaded dipole can present the user with an illusion of well-being. The feedpoint impedance at resonance will be roughly the sum of the feedpoint impedance with no losses plus the resistive component of the coil's Q. With time, weathering, and lowering Q, a short, loaded dipole may seem to show an improvement in SWR relative to a 50-Ω feedline. In actuality, it is more likely that coil losses are increasing, and the additional resistance is simply converting power to heat.

An alternative to center loading is mid-element loading, that is, the placement of loading inductors somewhere along each element away from the feedpoint. **Fig. 3-10** shows the physical difference between the two methods of

applying inductive element loading. Claims for significantly increased efficiency unfortunately do not materialize from this arrangement, although the arrangement does show a slightly lower rate of gain decline.

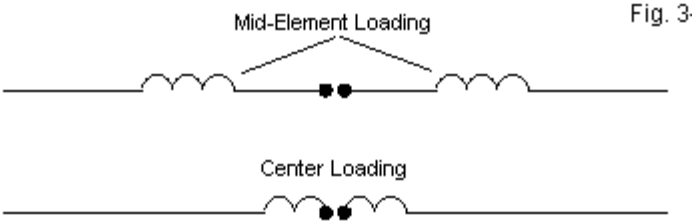

Fig. 3-10

Mid-Element vs. Center Loading

As the loading coil is split and moved outward from the antenna center, the required value of inductive reactance necessary to achieve resonance increases. By the time the coils are midway between the element center and the element ends, each coil must have an inductive reactance of about 93% of what a single center-loading inductor would require. For equivalent coil Q, the nearly doubled series resistance of mid-element loading coils tends to wash out most of the gain increase occasioned by letting full current exist at and near the feedpoint. (See ands revise model 3-4.ez.)

Table 3-6. Dipole Performance with mid-element loading coils of various values of Q. Coils are located at the mid-point of each element half.

% full	Load coil reactance per coil	Feed R Ohms	Gain (dBi) for Q = inf.	300	200	100	50
90	93.0	63.16	2.06	2.03	2.02	1.98	1.90
80	188.0	53.66	2.00	1.93	1.89	1.78	1.57
70	288.0	43.86	1.94	1.80	1.71	1.50	1.09
60	399.0	34.20	1.89	1.59	1.45	1.05	0.35
50	528.0	25.02	1.84	1.27	1.01	0.32	−0.8
40	690.0	16.78	1.80	0.68	0.21	−0.9	−2.6

As **Table 3-6** shows, gain improvements are marginal. The chief benefit of mid-element loading is that the feedpoint impedance remains higher than with center loading. As with the previous table, dipoles are 3/8" diameter aluminum

in free space.

Mid-element feedpoint impedance figures average about 10 Ω higher than center-loaded dipole feedpoint impedances for equivalent shortening. However, even with this improvement, illusions of well-being are possible. If one ends up with loading coils with a Q of 50 in a dipole only 40% of full size, the antenna will seem to match a coax cable very well--because the RF resistance in the coils will roughly add to the natural resonant impedance of the antenna. In that extreme case, the loss resistance would double the antenna resistance and occupy corresponding amounts of power.

In the end, there is little to choose between center and mid-element loading except feedpoint impedance and such mechanical considerations as may apply to the antenna structure. Center loads are more easily supported, but in some cases are a problem to feed. Mid-element loading coils often require one or two upward steps in element diameter to support the coil. Gains for the two systems, with coils of equivalent Q, would be indistinguishable in practice.

Linear-Loaded Dipoles

An alternative to either system of loading is the use of a linear load. Once veiled in mystery, linear loads turn out to be simplicity itself. In purest form, they are nothing more nor less than shorted series transmission line stubs used to provide the necessary inductive reactance for center loading. Each side of the feedline attaches to a section of line that runs parallel to the main element. The line continues back to the original center junction area and attaches to the main element. **Fig. 3-11** shows two popular ways to configure linear loads.

If both lines are equidistant from the main element, then straightforward, shorted transmission line stub calculations are sufficient to calculate the required length of each stub. Each stub will provide 1/2 of the reactance required for center loading. If the stub lines are not equidistant from the main element, unequal currents will be induced by the field from the main element, resulting in longer linear load lines for the same degree of loading. (For more on this subject, see "Modeling and Understanding Small Beams: Part 4: Linear-Loaded

Yagis." *Communications Quarterly*, Summer, 1996, pp. 85-106.)

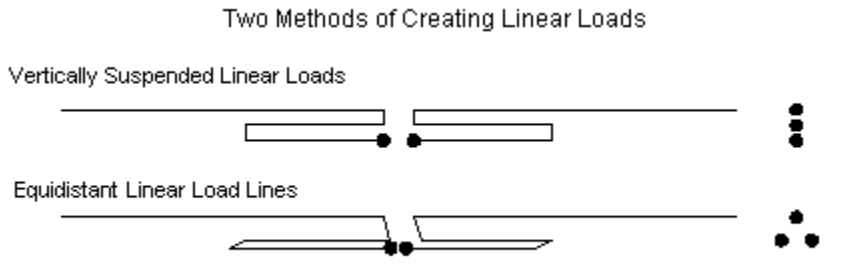

Fig. 3-11

In some commercial beams, the linear load is made to appear to be placed farther out along the element. The main (large-diameter) element is fed and, on each side, breaks at some distance from center. Smaller lines are run back toward the feedpoint, make a turn and return to the break, to be connected beyond the break point. Despite appearances, these antennas have center-loading linear loads composed of one fat wire and one thin wire. The main antenna element is actually the return thin wire back to the break point where it attaches to the tubing used to finish the element. Although the system has much in the way of mechanical soundness to recommend it, and although the difficulty of calculating the precise length of needed linear load makes empirical experimentation more efficient in antenna development, the system is electrically quite normal.

To gain a sense of the advantages of linear loading, let's look at a dipole 70% of full length (11.8') and try to model linear loads of varying proportions upon it. For consistency and comparability of results, all models were done in NEC-4. Due to constraints within NEC, this procedure restricted the construction of linear loads using the same diameter material as the main element: 3/8" diameter aluminum. (See model 3-5.ez.)

Two types of linear loads were modeled: those placing both load lines

equidistant from the main element and those lining up the lines vertically beneath the element. For these rough samples, variations were limited to changing the spacing from the main element and from line to line. The spacing values were equalized; that is, if the space between lines was 3", then the space from the main element was also 3" for both types of loads. Where E = equidistant load lines and V = vertically suspended load lines, the sample models appear in **Table 3-7**:

Table 3-7. Sample linear load models used for comparisons

Antenna	Specification
E3	Equidistant lines 3" apart and 3" from the main element
E6	Equidistant lines 6" apart and 6" from the main element
V1	Vertically suspended lines with 1.5" spacing
V3	Vertically suspended lines with 3" spacing
V6	Vertically suspended lines with 6" spacing

In **Table 3-8**, the meaning of all values is obvious, except perhaps equivalent Q. Replacing the linear load with an inductor of sufficient size to resonate the antenna and then adding resistive losses until the element gain equals the gain of the linear-loaded element derives the value of equivalent Q. Although these values are useful markers with respect to gain, they will be less useful with respect to operating bandwidth. "Length" indicates the total length of the linear load from outer tip to outer tip.

Table 3-8. Modeled performance of the sample linear-loaded dipoles

Antenna	Length	Gain dBi	Feed Z (R +/- jX Ohms)	Equiv. Q
E3	4.46'	1.88	24.1 + j0.12	1150
E6	3.14'	1.89	21.3 + j0.32	1400
V1	7.50'	1.71	25.7 - j0.37	230
V3	5.36'	1.83	22.9 + j0.16	500
V6	3.64'	1.90	20.2 + j0.31	2000

For each type of linear load (equidistant and vertically spaced), wider spacing results in a shorter load length. The inductive reactance of a shorted transmission line is the characteristic impedance of the line times the tangent of the line's electrical length. Since we need the same reactance in each case, as the characteristic impedance of the lines goes up the length comes down. As we

increase the spacing between the lines, the characteristic impedance goes up. Even though vertically spaced linear loads do not adhere strictly to the general equations due to variable coupling on the two lines of the load, they do follow the trends very well. From these few samples, some other trends (verified by a large number of file samples) are also evident:

1. The wider the spacing among elements, the higher the element gain and equivalent Q at the design frequency.

2. Vertically suspended linear loads vary more widely in length, gain, and equivalent Q than equidistant linear loads.

3. The wider the spacing (between lines and from the antenna to the lines), the lower the feedpoint impedance of the resonant element.

Most notable is the lack of significant variation in the gain of the two equidistant linear load models. The spacing is doubled between the two, but the gain varies by almost nothing. These models correspond most closely to a pair of series connected shorted transmission line stubs. Independent calculation of required stub lengths produces values for each side of center that are longer than the modeled stubs by about the length of the vertical connectors. The connecting lines are not the entire story here, since stub line calculations presume that the shorting connection at the stub end is insignificant. However, 3" and 6" connecting rods are likely of some significance at 29 MHz.

Vertically suspended linear loads vary more widely, in part due to the unequal induced currents from the nearby main element. For these loads, the designer is faced with a trade-off: load spacing and element gain on the one hand and feedpoint impedance on the other. Equidistant load lines may be placed close to the main element to increase the feedpoint impedance without significant loss of element gain.

For a final comparison, we may look at the operating bandwidths of all the loaded elements, including those with a center-loading inductor, mid-element-loading inductors, and linear loads. As before, the table will show calculated

SWR values for 28 through 30 MHz at 0.5 MHz intervals. Linear loaded antennas will be designated as given in this section. Center-loaded and mid-element-loaded antennas will be called CL and ML, respectively, and followed by a number representing a value of Q used in earlier comparisons. The inductor-loaded antennas will be restricted to those 70% of full size to correspond to the linear loaded models. A full-size dipole and a 70% hatted dipole for 29 MHz are included for comparison. See **Table 3-9**.

Table 3-9. SWR performance of all of the types of dipoles in this episode
Note: all shortened dipoles are 70% of full size.

Antenna SWR at	28	28.5	29	29.5	30 MHz
Full size dipole	1.71	1.30	1.00	1.28	1.62
70% hatted dipole	1.83	1.34	1.02	1.36	1.78
CL-300	4.06	2.06	1.00	1.99	3.57
CL-200	3.96	2.03	1.00	1.96	3.50
CL-100	3.72	1.96	1.00	1.90	3.31
CL-50	3.32	1.84	1.00	1.79	3.00
ML-300	3.77	2.00	1.02	1.89	3.32
ML-200	3.70	1.98	1.02	1.86	3.28
ML-100	3.51	1.92	1.02	1.81	3.11
ML-50	3.20	1.83	1.02	1.71	2.82
E3	4.35	2.14	1.01	2.08	3.87
E6	4.34	2.12	1.02	2.10	3.88
V1	4.53	2.22	1.01	2.10	4.03
V3	4.30	2.12	1.01	2.08	3.85
V6	4.35	2.12	1.02	2.10	3.88

Figures for inductor-loaded models were developed by introducing the model load(s) as inductors (values of inductance in μH) with the requisite reactance for resonance at the design center frequency. Since reactance varies with frequency, using a constant reactance in the load model would have produced too optimistic a set of SWR figures. All models retain the 3/8" diameter aluminum construction, and figures are for free space.

Carrying out SWR to 2 decimal figures is largely spurious in terms of practical operation. However, adding the final decimal place makes the trends

clearer and also clarifies the lowest SWR on which the other figures are based.

All forms of element loading narrow the operating bandwidth and are roughly related to the Q of the loading element(s). For inductor loading, the 2:1 SWR bandwidth increases as Q decreases, but the differences are small. The differences between comparable Q-values for center and mid-element loading are smaller yet.

The operating bandwidth for a linear loaded element shows the inherently higher Q of the system, but the actual SWR figures are not directly related to an assignable value of Q. Among the vertically suspended linear loads, V1 had the lowest assignable Q in terms of gain equivalence, but also displays the narrowest bandwidth of the entire group. Once a certain lower limit of element spacing is exceeded, operating bandwidth tends to be the same for all practical purposes.

In the end, the use of linear loading trades higher gain for a narrower operating bandwidth than inductor loading. Mid-element loading provides a higher feedpoint impedance than either form of center-loading. (However, the hat-method of shortening elements yields the broadest bandwidth and the highest feedpoint impedance of all of these 70%-length elements.)

We have summarized the electrical details of the methods by which we may shorten an element and then restore its electrical length. Let's pause a moment to create an equal summery for the mechanical aspects of the loading issue.

1. Although the hatted element is the most efficient of the shortened elements, it may also be the least mechanically solid. A hat structure at the end of an element places an assembly at right angles to the element and the assembly has some wind resistance. If we construct the assembly to be light enough for a normal linear element to support at its end, the assembly itself may be too fragile to sustain strong winds. If we make the assembly strong enough to withstand the winds, then we may require a more massive linear element to support it.

2. Mid-element loading provides higher feedpoint impedance values than elements of the same length that use center loading. However, if we wish to obtain the highest Q from the inductive loads, we must increase their diameter. That increase also raises the load's wind resistance. If we make the load with a smaller diameter, then we shall likely be limited in the Q that we can obtain. Shielded loads may slip wind better, but often become the home of flying "things" and may also collect moisture. Open coils are invitations for "things" that nest.

3. Center-loading coils are perhaps the least efficient and yield the lowest feedpoint impedance values for any given element length. However, by using a fiberglass rod or an equally strong substitute, we can support the coil more easily, since the weighty structure is at the element center.

The next question is how the characteristics of inductively loaded elements will show up in 2-element Yagis.

4. Loaded Yagi Elements

One poorly appreciated fact about shortened Yagis is to what degree the antenna geometry plays a role in optimizing performance. When looking at shortened Yagis with hatted elements, we found a set of dimensions for the driven element and the reflector, which provided close to the best obtainable performance for a 2-element beam designed to maximize front-to-back ratio and to resonate the beam. Interestingly, if we retain a driven element that is about 70% full size, we may use virtually the same main element dimensions with all forms of loading and achieve close to the best performance obtainable.

Inductively Loaded Yagis

In essence, all methods of loading (center inductor, mid-element inductors, or linear loading) are doing the same job in the same manner: replacing a linear section of antenna element with inductive reactance. A beam with elements about 70% of full size will have the same optimal geometry, whichever loading method is used.

Because maximum gain at the design center frequency results in poor, if not unusable, performance below the center frequency, the models we shall examine will by optimized for maximum front-to-back ratio and resonance. For some models, the maximum gain frequency will lie very close to (and below) the front-to-back peak frequency, and the beam reversal point for a few samples will fall inside the 2 MHz 10-meter span we have chosen as our test bed. In fact, for loaded Yagis, the performance below the center frequency drops off much more rapidly than performance above the center frequency, especially when compared to the rates of degradation for a full size beam.

We may begin with 3 models: 1 each of the center inductor, mid-element inductors, and linear loaded variety. Each antenna will be spaced 0.12 λ (4.1' at 29 MHz). The elements will be close to 70% of full size. The driven element will be 11.48' long, with a reflector 11.95' long. Elements, as in all the models in this

refresher, will be 3/8" diameter aluminum.

The center-inductor loaded model called for an inductive reactance for each element of 288 Ω. This translates into a solenoid with an inductance of 1.5806 μH to achieve resonance and very close to peak front-to-back ratio.

The mid-element loading coils that we needed to yield the same result had 281-Ω reactance or an inductance for each of the 4 coils of 1.5422 μH. **Fig. 4-1** shows the outlines of the two types of inductively loaded Yagis.

Fig. 4-1

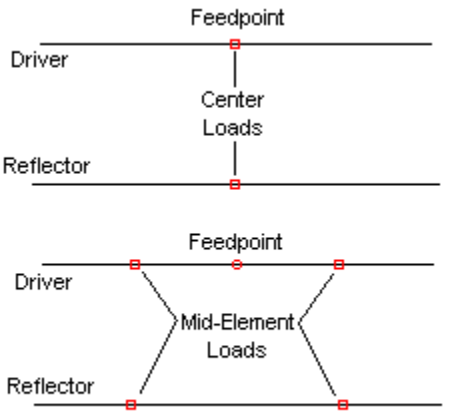

Two Types of Inductively Loaded 2-Element Yagis

Table 4-1 lists the gain, front-to-back ratio, and feedpoint impedance of these two initial antennas. The table also shows a series load resistance that is necessary to produce coil Qs of 300, 200, and 100, in order to investigate the effects of Q on performance. (See and revise as necessary models 4-1.ez and 4-2.ez.) Models are in free space for this initial design test. The table includes a full-size Yagi of the same (0.12 λ) spacing for comparison.

Table 4-1. Modeled performance of inductively loaded 2-element Yagis

Antenna	Resistance	Gain (dBi)	F-B (dB)	Feed Z (R +/- jX)
Full-size	--	6.25	11.20	32.14 - j0.00
Center-load				
Infinite Q	0	6.20	20.04	17.07 - j0.00
Q=300	0.96	5.79	18.31	18.14 - j0.68
Q=200	1.44	5.59	17.57	18.67 - j1.00
Q=100	2.88	5.03	15.71	20.28 - j1.92
Mid-element-load				
Infinite Q	0	6.29	16.84	24.14 + j0.41
Q=300	0.93	5.87	15.66	25.76 - j0.53
Q=200	1.40	5.67	15.14	26.58 - j0.98
Q=100	2.80	5.09	13.75	29.03 - j2.30

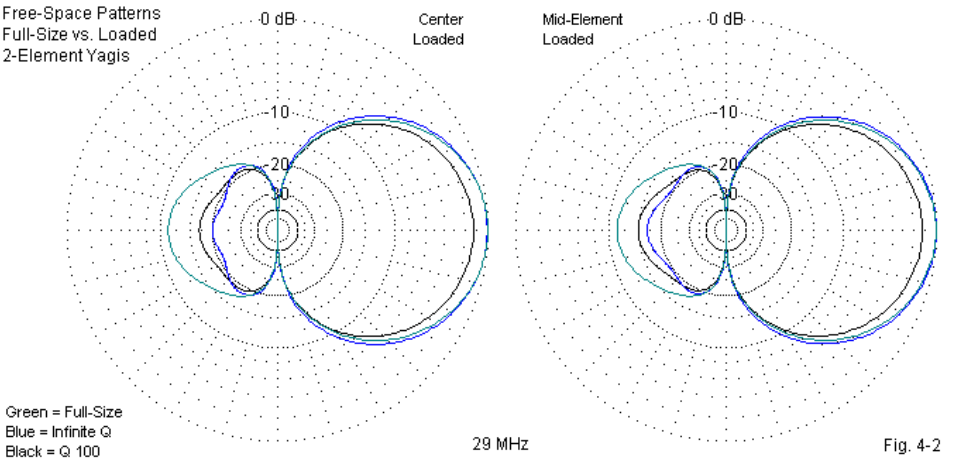

Fig. 4-2

Let's first look at the patterns, shown in **Fig. 4-2**. Each patterns set includes the full size Yagi for comparison. The other plots show (for effective contrast) the patterns for an infinite Q and a low Q of 100. In both cases, the patterns show that loaded elements often do better at improving the front-to-back ratio at the design frequency than they do with respect to gain. Only with infinite Q does the loaded Yagi gain equal the full size Yagi gain. But, of course, all loading

inductors have a finite Q.

Gain: Once we introduce a finite Q, the gain drops rapidly, as is evident if **Fig. 4-3**, which tracks the gain over the levels of Q in **Table 4-1**. Note that the X-axis is not a linear scale. With an optimistic Q of 300, the gain of either load model approaches a half dB less than a full size Yagi with the same design goals. Another 3/4 dB disappears in the transition from a Q of 300 to a Q of 100. Most coils cited in commercial designs have had values below 300 and above 100, so the actual gain of such antennas will be between 5 and 5.75 dBi (or around 3 to 3.5 dB better than a dipole in free space). Gain expectations for a beam 70% full size and spaced 0.12 λ that are higher than this value are unwarranted.

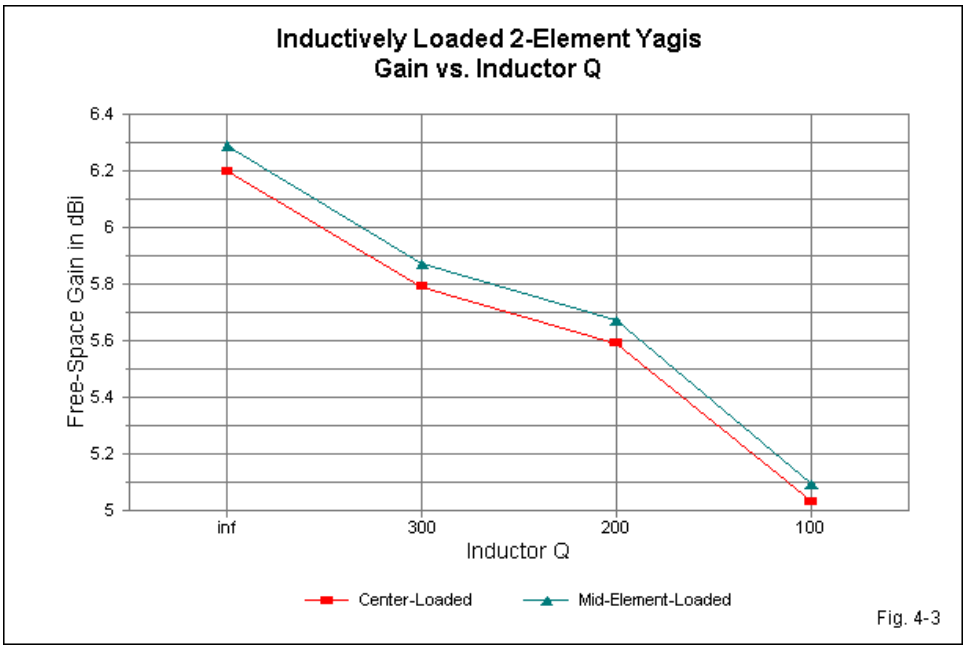

Fig. 4-3

Front-to-back ratio: Shortened Yagis are capable of much higher front-to-

back ratios than full size 2-element Yagis, as is clear in **Fig. 4-2**. As shown in **Fig. 4-4**, the front-to-back ratio does decrease as the Q decreases. The center-loaded model has a theoretic 3 dB advantage over the mid-element model, although that advantage begins to evaporate with finite Qs. Nonetheless, one true advantage of a loaded Yagi over a full-size model is the superior front-to-back ratio.

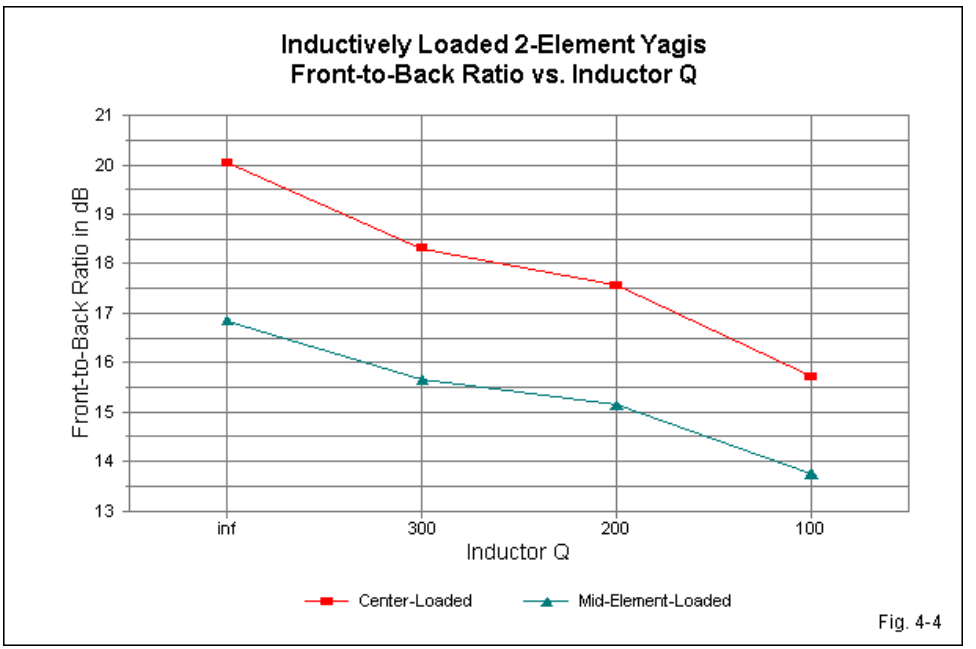

Fig. 4-4

Feedpoint impedance: **Fig. 4-5** tracks the feedpoint resistance for both forms of loading as we change the load Q. The resistance increases in step with the series resistance of the loading inductors. The center-loaded model exhibits the lowest feedpoint impedance of any of the loaded 2-element Yagis. Although it can be used with coax and a beta match, the low impedance raises questions of basic efficiency in terms of power consumed by resistive losses throughout any practical assembly. Note that as Q decreases, the feedpoint impedance

increases proportionally to the total series resistance in the driven element.

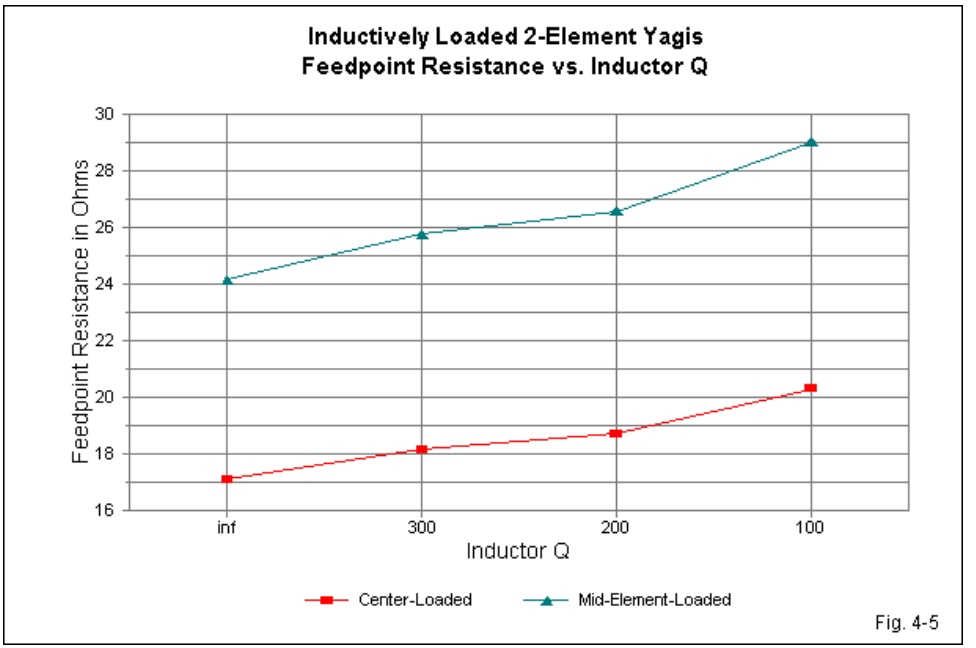

Fig. 4-5

It is also significant to examine the operating bandwidth of loaded 2-element Yagis. We would expect something narrower than a full-size Yagi, and figures do not disappoint us. Models for obtaining operating bandwidth and other figures across a span of frequencies must enter the resistance and inductance of the loading coils (rather than resistance and reactance) and allow NEC to calculate the reactances for each frequency selected. Again, the full-size Yagi is presented in **Fig. 4-6** and in **Table 2** for comparison with only the Q=200 models of loaded Yagis. (The use of a Q of 200 corresponds closely to the Qs of coils used in trapped and loaded commercial beams.)

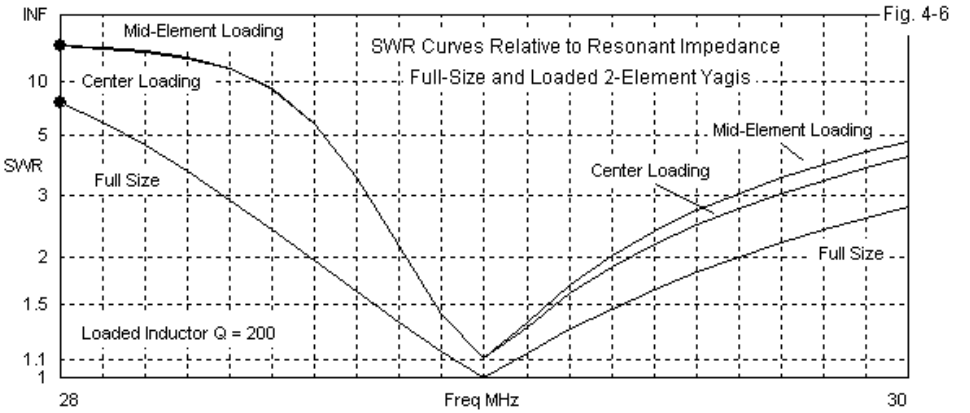

Table 4-2. A comparison of SWR values relative to driver resonance
Note: All antennas spaced 0.12-wavelength

Antenna SWR at	28	28.5	29	29.5	30 MHz
Full-size	7.34	2.37	1.00	1.82	2.78
Center-ld, Q=200	22.85	8.96	1.11	2.45	4.12
Mid-el-ld, Q=200	21.90	8.77	1.12	2.71	4.75

The operating bandwidth of the loaded Yagis is so narrow that the 2 MHz spread is too wide to be informative. It is clear that the SWR climbs very much more slowly above the design center frequency than below it. Whether the antenna has worthwhile characteristics in that region requires that we look at most of the antenna's properties over a narrower spread of frequencies--perhaps a half MHz either side of center. Therefore, **Table 4-3** provides data for 28.5 to 29.5 MHz in 0.25-MHz increments.

Table 4-3. Detailed performance from 28.5 to 29.5 MHz

Frequency	28.5	28.75	29	29.25	29.5 MHz
Full size Yagi					
Gain (dBi)	6.74	6.49	6.25	6.02	5.82
F-B (dB)	9.79	10.91	11.20	10.41	10.37
SWR	2.37	1.48	1.00	1.39	1.82
Center-loaded Yagi, Q=200					
Gain (dBi)	4.87	5.92	5.61	5.08	4.64
F-B (dB)	2.24	9.90	17.63	13.16	9.69
SWR	8.96	2.70	1.11	1.75	2.45
Mid-element-loaded Yagi, Q=200					
Gain (dBi)	4.86	5.93	5.67	5.17	4.74
F-B (dB)	1.98	9.01	15.14	12.74	9.75
SWR	8.77	2.70	1.12	1.85	2.71

If the design center frequency is shifted downward by about 150 kHz, the full size Yagi would provide a 2:1 SWR operating bandwidth over the full 1 MHz spread. Gain and front-to-back ratio would be respectable throughout the range (for an antenna of this type).

The operating bandwidth for the loaded Yagis is less than 700 kHz. The maximum gain frequency occurs within this spread and marks the limit of the lower frequency excursion for a 2:1 SWR. Above the design center frequency, the SWR climbs at half the rate as below it. Gain and front-to-back ratio fall off much more rapidly than with a full size model. **Fig. 4-7** shows the gain from 28 to 30 MHz for the 3 antennas using an increment of 0.1-MHz to reveal the finer detail. Note the gain dip at or very near to 28.4 MHz, indicating the frequency at which the forward pattern reverses direction. The reversal point for the full-size Yagi occurs below the limit of the sweep.

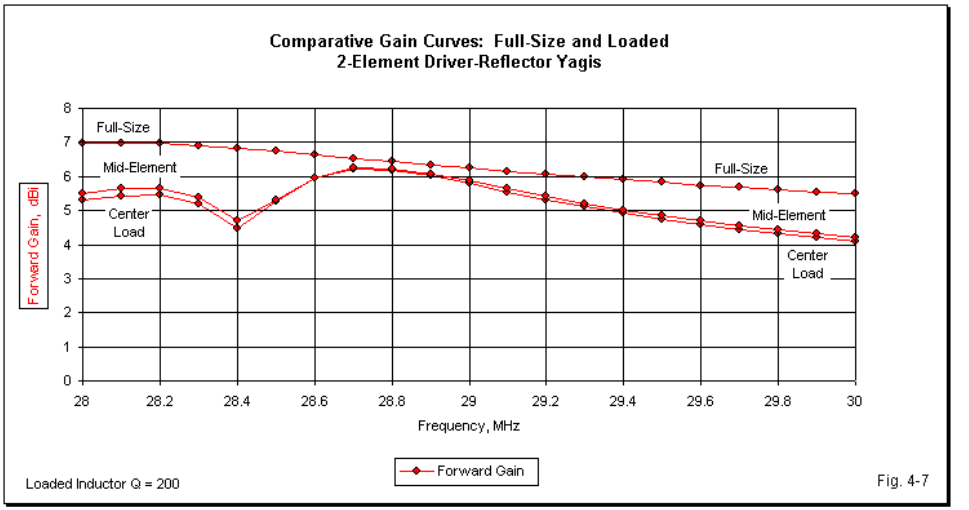

Fig. 4-7

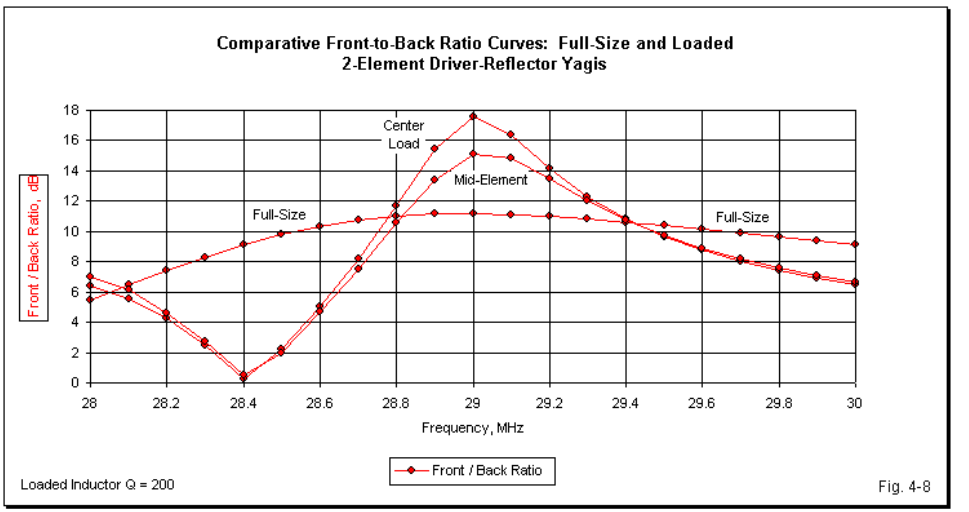

Fig. 4-8

Indeed, the higher front-to-back ratio obtainable with shortened and loaded

elements now shows itself for what it is: a fairly narrow peak with extended values closer to those of the full size antenna. At the upper frequency limit, gain is less than 3 dB better than a dipole. **Fig 4-8** gives us a wider view that once more shows the pattern-reversal frequency to be near to 28.4 MHz.

The performance of the two inductively loaded Yagis parallels to a very high degree the performance of the full-size Yagi as we vary the height of the antenna above average ground. **Table 4-4** provides data from 0.0625 λ to 1.0 λ above ground for the loaded Yagis with inductor Q values of 200--with the full-size Yagi for comparison. The table lists only one column for the elevation angle of maximum radiation, since that value is the same within +/-1° at the very low heights and is exactly the same above a height of 3/8 λ. (See and revise as necessary models 4-3.ez and 4-4.ez.)

29 MHz 2-Element Driver-Reflector Yagis with 0.12-Wavelength Element Spacing at Various Heights above Average Ground — Table 4-4

	Full-Size Yagi				Center-Loaded with Q=200				Mid-Element-Loaded with Q=200				
Height wl	Gain dBi	F-B Ratio	Feed R	Feed X	Gain dBi	F-B Ratio	Feed R	Feed X	Gain dBi	F-B Ratio	Feed R	Feed X	El Angle
0.0625	-0.24	4.14	40.8	-7.57	-0.84	3.89	24.52	-0.12	-0.87	4.13	35.53	-0.48	62
0.125	5.1	6.18	25.44	-5.47	4.49	7.04	15.97	-4.1	4.45	7.29	22.58	-5.17	54
0.1875	7.44	7.92	24.73	0.4	6.74	9.76	15.08	-1.74	6.74	9.59	21.4	-1.65	49
0.25	8.57	9.79	27.5	3.86	7.85	12.87	15.99	0.1	7.88	12.14	22.88	0.91	43
0.3125	9.28	11.63	30.95	4.94	8.56	16.26	17.38	0.99	8.62	14.69	25	2.03	38
0.375	9.84	13.35	34.03	4.08	9.15	19.99	18.79	1.04	9.21	17.38	27.05	1.94	33
0.4375	10.35	14.29	35.94	1.7	9.69	23.56	19.95	0.42	9.76	20.06	28.62	0.83	29
0.5	10.8	13.36	35.78	-1.38	10.17	22.36	20.49	-0.85	10.24	19.83	29.17	-1.06	27
0.5625	11.1	11.52	33.47	-3.25	10.51	18.34	19.94	-2.14	10.57	16.75	28.18	-2.79	24
0.625	11.23	10.22	30.9	-2.78	10.64	15.94	18.69	-2.51	10.7	14.42	26.37	-3.1	21
0.6875	11.27	9.8	29.71	-0.98	10.64	15.04	17.76	-1.92	10.69	13.39	25.17	-2.14	20
0.75	11.27	10.09	29.98	0.8	10.6	15.19	17.54	-1.05	10.67	13.39	25	-0.89	18
0.8125	11.31	10.86	31.15	1.85	10.62	16.17	17.88	-0.36	10.69	14.12	25.57	0.02	17
0.875	11.37	11.82	32.61	1.92	10.69	17.8	18.52	-0.07	10.77	15.37	26.5	0.35	16
0.9375	11.48	12.55	33.75	1.03	10.82	19.75	19.18	-0.23	10.89	16.8	27.4	0.01	15
1	11.6	12.55	34.1	-0.2	10.97	20.7	19.59	-0.74	11.04	17.55	27.9	-0.74	14

Fig. 4-9 provides some insight into the variations of gain and front-to-back ratio for the antennas by overlaying elevation and azimuth patterns at heights of 7/16 λ, 11/16 λ, and 1 λ. The elevation patterns show the decreasing elevation angle of the main lobe as the height increases, along with the development of higher angle lobes. As well, note the varying strength of the rearward lobe in the elevation patterns.

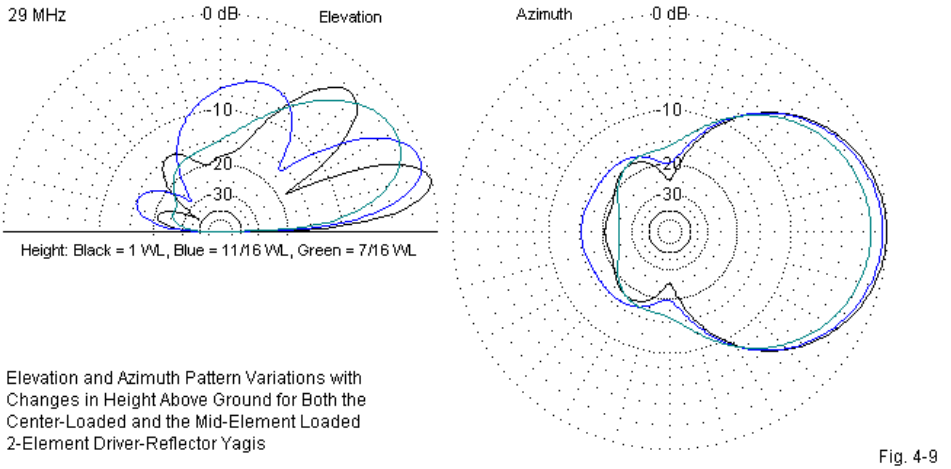

Elevation and Azimuth Pattern Variations with Changes in Height Above Ground for Both the Center-Loaded and the Mid-Element Loaded 2-Element Driver-Reflector Yagis

Fig. 4-9

The azimuth patterns show the growth of forward gain with increasing antenna height. However, a more significant feature is the evolution of the rearward lobe or lobes as the height varies. Although these patterns derive from the center-loaded model, they also apply with only very small modification to the mid-element-loaded and the full-size Yagis.

In general, the overlapping gain lines for the two inductively loaded Yagis track very well with the gain of the full-size Yagi, as is evident in **Fig. 4-10**. However, both loaded Yagis show greater sensitivity than the full size Yagi in the height region around 7/8-λ. Note the visible decrease in gain (that is nonetheless operationally insignificant) in that height region.

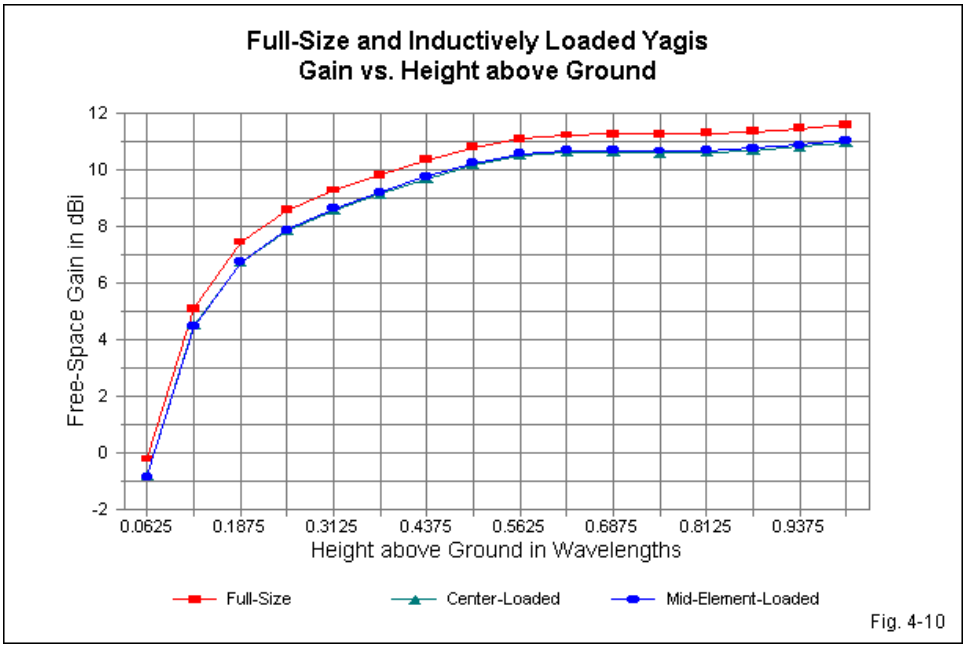

Fig. 4-10

The front-to-back curves are more distinct for the three antennas, as shown in **Fig. 4-11**. At the design frequency, 29 MHz, the full-size Yagi shows the lowest front-to-back ratio. However, the full-size antenna curve is also the shallowest in terms of its peaks and valleys. In contrast, the difference between a peak value and the adjacent low value is considerably greater for the loaded Yagis.

In the preceding episode, we determined that recording gain values in dBd could be both misleading and a source of mischief. Simply subtracting 2.15 from the gain in dBi is a fairly useless exercise. Comparing the antenna gain over ground with a dipole at the same height yields curves of dubious utility. Therefore, these exercises have omitted that data. However, the dipole information is available in past episodes for anyone who wishes to perform the simple calculations.

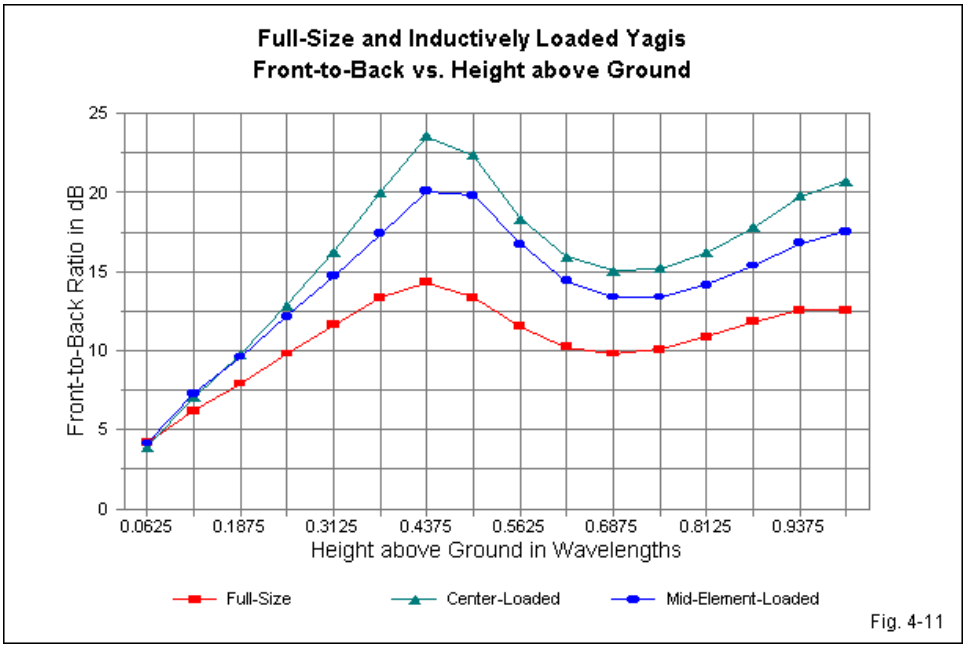

Fig. 4-11

Between the two types of inductively loaded Yagis, the center-loaded model yields higher peak front-to-back ratios, while the mid-element-loaded model has higher feedpoint impedances for lower losses for loss sources other than the loading coils. The final decision on which type of loaded Yagi to build is an individual option that may depend upon construction and matching variables as well as basic performance. Both loaded Yagis use elements that are 70% of full size, which is about the recommend limit to shortening. If the element lengths decrease any further, the gain would fall rapidly as a function of both the short elements and the higher losses in practical loading inductors. As well, the operating bandwidth would also decrease, limiting the utility of the antenna on all but the smallest amateur bands (such as 30, 17, and 12 meters).

Linearly Loaded Yagis

I have purposely excluded the linear-loaded 2-element Yagi of 70% full size from the comparison so far because it has some interesting properties. Linear-loading, especially when executed using loading elements the same size as the main element, is inherently high Q, with all the advantages and disadvantages. Let's scan one of the linear-loaded models, choosing the one with load lines equidistant form the main element by 3" and 3" apart. With the 3/8" diameter aluminum elements 11.48' and 11.95' for the driven element and reflector, respectively, the load lines were 2.37' either side of center (4.75' overall) for resonance and maximum front-to-back ratio. Because the linear-loading elements are directly modeled as physical entities, there are no mathematical loads in the model. **Fig. 4-12** provides the general outline of the beam.

Fig. 4-12

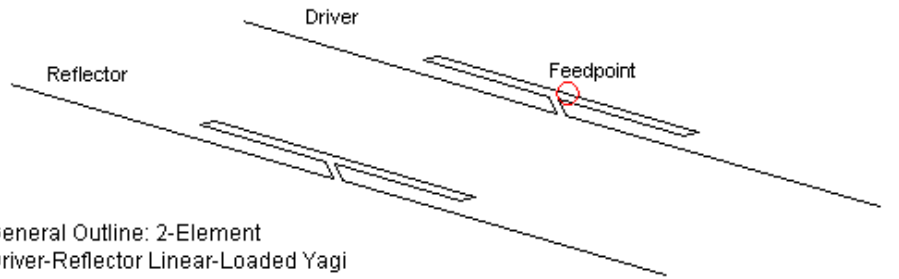

General Outline: 2-Element
Driver-Reflector Linear-Loaded Yagi
with 0.12-Wavelength Element Spacing

If we use the restricted passband (28.5 to 29.5 MHz) that we used for the inductively loaded beams, we can sample the performance of the antenna at 0.25-MHz intervals. See **Table4-5**.

Table 4-5. Performance of a 70% linear-loaded Yagi from 28.5 to 29.5 MHz

Frequency	28.5	28.75	29	29.25	29.5 MHz
Gain (dB	4.78	6.26	5.95	5.15	4.50
F-B (dB)	0.86	6.05	16.31	16.81	11.19
R +/- jX	6.36-j34.83	8.08-j16.56	14.54+j0.03	22.35+j12.14	28.35+j21.34
SWR	15.82	4.47	1.00	2.14	3.27

The SWR-based operating bandwidth for this high-Q model is under 400 kHz at 29 MHz (and proportionately less for lower band models). Peak values are comparable to those obtainable from inductor loading, but very short-lived as one changes frequency. In fact, within even this restricted passband, the pattern reversal occurs, as indicated by the dips in both the forward gain and the front-to-back values, shown in **Fig. 4-13**. (See model 4-5.ez.)

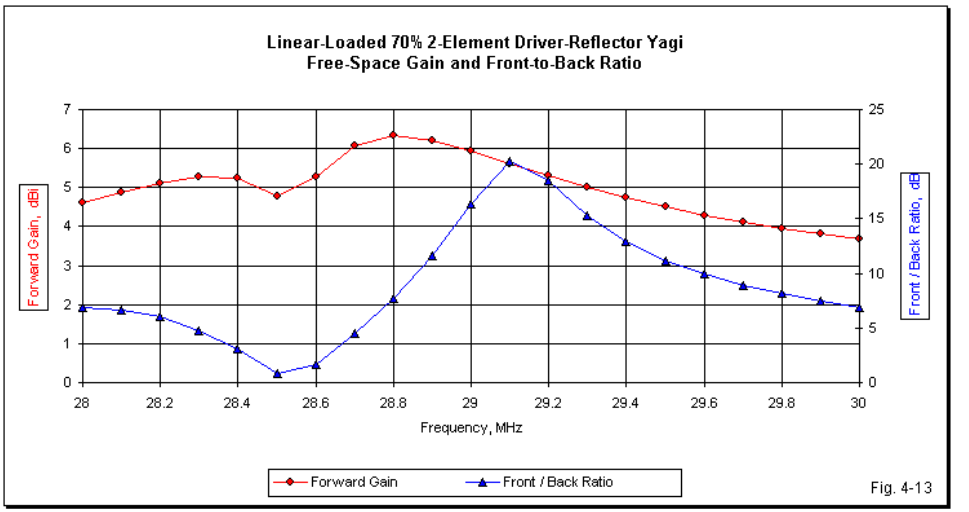

Fig. 4-13

The graph uses a swept increment of 0.1-MHz, and the lowest values occur at 28.5 MHz. However, the reversal occurs slightly above this frequency, but below 28.6 MHz. To illustrate how sudden and complete the pattern reversal is below the frequency of maximum gain, **Fig. 4-14** shows free-space patterns for the linear loaded Yagi at half-MHz intervals.

Although the front-to-back ratio at 28.5 MHz is negligible, the forward lobe has definitely change direction. With its inherently high-Q linear loading system, the sample Yagi is useful only over a very narrow bandwidth. Indeed, for most purposes, the lower Q of the sample inductively loaded versions may be more useful. Nevertheless, they do not have very wide bandwidths, just slightly larger

spreads than the linear-loaded version.

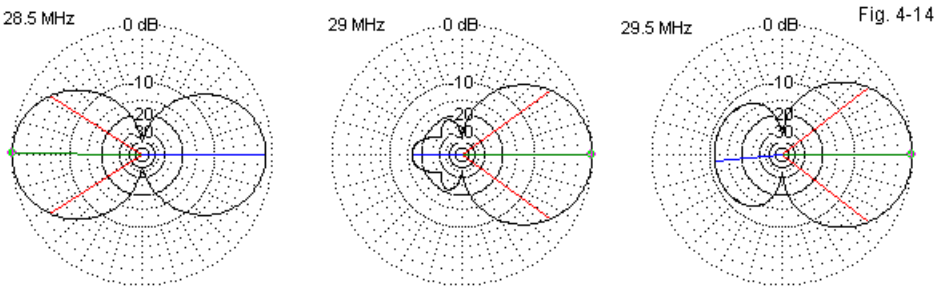

Fig. 4-14

Selected Free-Space Azimuth (E-Plane) Patterns: Linear-Loaded Yagi

Strategies for Increasing the Bandwidth of Loaded Yagis

Can anything be done to increase the operating bandwidth of this antenna? One strategy that is open to all three forms of loading is to increase the spacing between elements. If we select 0.16 λ (5.4' at 29 MHz), we can expect not only a wider operating bandwidth, but also somewhat higher feedpoint impedances, along with reductions in gain and front-to-back ratio.

Table 4-6 presents the results of this design experiment. A full-size version of the antenna appears as a comparator for the 3 loaded Yagis. At a spacing of 0.16 λ, a full-size 2-element Yagi is a good match (with a 1:1 balun or choke) for 50-Ω coaxial cable. The other beams require a beta match (or similar). However, note the table carefully: the center-loaded models--both inductor and linear--improved their operating bandwidths and increased their feedpoint impedances by a greater amount than the mid-element-loaded model. At the closer (0.12 λ) spacing, the center and mid-element inductor loaded models were very similar in operating bandwidth, with the linear-loaded version much narrower. With the wider (0.16 λ) spacing, the mid-element and linear loaded models are on a par with each other (with the linear-loaded model showing a slightly narrower bandwidth), while the center-loaded model shows at least 100 kHz wider operating bandwidth.

Table 4-6. Performance of full-size and loaded Yagis with 0.16-wavelength spacing

Frequency	28.5	28.75	29	29.25	29.5 MHz
Full size Yagi					
Gain (dBi)	6.56	6.34	6.12	5.92	5.74
F-B (dB)	9.79	10.60	10.84	10.68	10.29
R +/- jX	36.9-j19.8	41.9-j9.5	46.9-j0.0	51.5+j9.1	55.8+j17.9
SWR	1.70	1.27	1.00	1.22	1.47
Center-loaded Yagi, Q=200					
Gain (dBi)	6.29	6.15	5.75	5.34	4.98
F-B (dB)	6.78	11.35	13.98	12.86	10.87
R +/- jX	13.5-19	17.9-9	22.4-1	26.0+5	28.7+11
SWR	3.12	1.66	1.06	1.28	1.62
Mid-element-loaded Yagi, Q=200					
Gain (dBi)	6.17	6.11	5.72	5.32	4.97
F-B (dB)	6.97	13.05	15.84	13.12	10.62
R +/- jX	14.3-30	20.5-14	27.7-.4	34.1+10	39.4+20
SWR	4.51	1.89	1.02	1.50	2.02
Linear-loaded Yagi					
Gain (dBi)	6.62	6.59	5.91	5.28	4.79
F-B (dB)	4.30	10.84	14.87	11.95	9.26
R +/- jX	9.3-22	14.3-9	20.1+.4	24.3+8	26.9+15
SWR	4.96	1.85	1.02	1.49	2.08

At the same time, the wider mid-element-loaded model has lost less of its gain and front-to-back ratio relative to the closer-spaced model than either of the other two antennas. The advantage of one method of loading over another is marginal and may be secondary to structural and other design concerns. The general effect of wider spacing to increase the operating passband of a 2-element Yagi is most effective on the center-loaded models and least effective on the mid-element-loaded model.

Pint-Sized Loaded Yagis

Before drawing this refresher to a close, let's briefly look at a pair of beams with elements that have been shortened even further: to 50% of full size point. At 29 MHz, the driven element would be about 4' long, with the reflector 4.095' long with a spacing of 0.12 λ. We shall compare a center inductor with mid-element inductors as loads with a Q of 300. By now, we know not to expect wide differences between the two types of loading. More interesting are expectations of operating bandwidth, gain, and front-to-back ratio. As always, the elements are 3/8" diameter aluminum, and these models are once more in free space.

Table 4-7 provides the modeled data for free-space. A linear-loaded model does not appear due to the very large size of the loading transmission-line stubs. In the gain column, R means that the pattern shows gain in the reverse direction. To maximize the potential of these beams, I have raised the inductor Q to 300.

Table 4-7. Performance of half-length Yagis using inductive loading with 0.12-wavelength element spacing

Frequency	28.5	28.75	29	29.25	29.5 MHz
Center-loaded Yagi, Q=300					
Gain (dBi)	2.06 R	3.73	4.46	3.97	3.46
F-B (dB)	1.09	6.07	27.15	11.07	7.11
R +/- jX	5.5-j27	6.6-j14	12.8-j3	19.2+j2	20.7+j5
SWR	12.7	4.56	1.23	1.52	1.76
Mid-element-loaded Yagi, Q=300					
Gain (dBi)	6.32 R	4.16	4.59	4.07	3.57
F-B (dB)	0.98	7.18	31.15	11.04	7.27
R +/- jX	10.6-47	13.4-j24	25.0-j.4	35.3+j6	38.9+j15
SWR	11.1	3.79	1.16	1.50	1.90

At the design frequency, gain has dropped to about 2.5-dB higher than a dipole, and the rate of change is higher than for the 70% models with which we have experimented. However, as elements are radically shortened, it is possible to achieve for very narrow frequency limits indeed exceptional front-to-back ratios with a 2-element Yagi. Of course, the front-to-back ratio quickly diminishes off the design frequency to ordinary levels associated with an antenna with a very narrow operating bandwidth.

Newer operators, especially those whose prior antenna experience has been limited to verticals or simple wire dipoles, often make an error when they use their first beam. Received stations in the forward direction seem to be clearer and stand out above the background noise, whether atmospheric or from other stations. The new beam user tends to assume that the increased signal-to-noise ratio is a function of gain. As a result, many a mediocre beam has enjoyed an unwarranted reputation for its forward gain.

The attribution of clarity to gain is very often an illusion. For very small beams--like the 2-element Yagis with which we have experimented--the improvement in received signals may be largely due to the antenna's front-to-

back ratio. More correctly, it is due to the general reduction of gain to the rear quadrants. Even a 10-dB front-to-back ratio tend to indicate an average gain level to the rear that is 15 or more dB lower than in the forward direction. (Remember that for almost all of our designs, the 180° front-to-back ratio is also the worst-case front-to-back ratio.) For reception, the front-to-back ratio is as important--and often more important--than forward gain in allowing us to hear well in the favored direction.

The actual forward gain plays its most important role with the transmitted signal. Whether the station on the other end can hear us is a joint function of our forward gain and the conditions between us. (In many instances, the outgoing and the incoming conditions may not be the same, and so what we receive may not indicate correctly what is happening in the ionosphere to the signal that we transmit.) Since we lack means to separate and measure the two factors, we tend to over-estimate the gain of our 2-element antenna. The illusion may create a happy feeling, but it is often just an illusion.

There is one more design illusion we can create with this half-size beam. Note that the SWR increases above the design frequency at a slow rate. The antenna is capable, in strictly SWR terms, of an operating bandwidth of over 0.5 MHz. However, in the upper half of the range, gain exceeds a dipole only by about 1.5 dB or so, and the front-to-back ratio is on a constantly descending curve. Citing the design frequency performance figures and then, without further explanation, providing a figure for operating bandwidth, might easily mislead a potential builder with respect to performance anticipation.

It would be interesting to see to what degree the problems associated with half-size 2-element Yagis might be overcome by increasing the spacing. Therefore, let's look at these same antennas re-optimized for front-to-back ratio and resonance with a spacing of 0.16 λ (5.4' at 29 MHz). **Table 4-8** supplies the modeling data.

Table 4-8. Performance of half-length Yagis using inductive loading with 0.16-wavelength element spacing

Frequency	28.5	28.75	29	29.25	29.5 MHz
Center-loaded Yagi, Q=300					
Gain (dBi)	2.75	4.83	4.61	3.92	3.40
F-B (dB)	0.34	8.56	17.16	9.99	7.90
R +/- jX	6.7-j22	9.1-j11	14.2-j3	16.6+j2	17.2+j8
SWR	7.78	2.72	1.22	1.25	1.71
Mid-element-loaded Yagi, Q=300					
Gain (dBi)	2.89	4.95	4.78	4.13	3.61
F-B (dB)	0.15	7.78	15.94	10.55	7.40
R +/- jX	13.3-j41	17.7-j19	27.2-j2	33.1+j8	35.3+j20
SWR	7.00	2.50	1.10	1.40	1.96

Interestingly, the wider spaced versions of the half-size Yagi achieve marginally more gain than the closer spaced versions, although the front-to-back ratio peak is much smaller for these Q=300 models. As a reminder, the fact that the SWR does not go to 1.0 is due to the modeling process used: the antennas were resonated with lossless coils and then losses were added to achieve the desired Q.

Clearly, the SWR curve is also flatter for these antennas than for the closer models, and operation over a 600 kHz span of 10 meters should be possible (with proportionately smaller bandwidths on lower bands to which the antennas might be scaled). Although the resistive component of the feedpoint impedance of the center-loaded model is low enough to cause concern, the impedance of the mid-element model is high enough for an efficient beta match to coaxial cable.

As a parting shot, let's place the mid-element-loaded version of the half-size 2-element Yagi, with its 3/8" diameter aluminum elements, over real ground and see what we get. **Table 4-9** tells the story.

Table 4-9. Mid-element-loaded Yagi, Q=300, at various heights above average ground

Height	TO Angle	Gain dBi	F-B dB	Feed Z Ohms
FS	--	4.78	15.94	27.23 - j2.46
1/8 wl	58	3.92	5.82	22.13 - j4.73
1/4	45	7.17	11.40	23.94 + j0.08
3/8	34	8.46	17.41	28.24 + j0.36
1/2	26	9.47	19.13	29.74 - j3.01
5/8	21	9.89	14.38	26.65 - j4.49
3/4	18	9.81	13.85	25.69 - j2.09
7/8	16	9.91	16.20	27.41 - j1.13
1	14	10.19	18.14	28.49 - j2.58

Compared to a dipole, the half-size Yagi suffers at low heights (below 3/8 λ) due to its high elevation (or take-off) angle of maximum radiation angle. Above that height, it provides a consistent gain over a dipole in the 2.5 dB ballpark. Front-to-back ratio and feedpoint impedance are stable with height increases, making the antenna quite predictable. The one limiting factor in these figures is that they are peak figures. Performance in one or another way will be less as we move off the design frequency.

This and the other models should make usable antennas, especially when scaled for lower frequencies--so long as we do not expect of them or claim for them more than they can do.

Conclusion to Notes on Driver-Reflector Yagis

We have just about exhausted the potential for the 2-element driver-reflector Yagi, at least in broad outline. Or goal has been to develop an understanding of the performance patterns and limitations of these antennas, not only at their design frequency, but also across a reasonable operating passband. Some of the designs are subject to refinement, and some we should likely not waste our time on in trying to achieve better performance from them.

A word about the models: although every effort has been made to optimize them in accord with the expressed design goals of maximum front-to-back ratio at antenna resonance, there is no guarantee that another few hundredths or

even a tenth of a dB might not be garnered by even more painstaking modeling. However, do not expect NEC or MININEC to yield much more than these models. If a model seems to deliver a lot more than the ones in this refresher, it is likely that the model has a problem or in some way presses one or more of the limits of the modeling program.

Two-element driver-reflector Yagis, in either full-size or shortened versions, have an important place in amateur radio. Understanding what they can and cannot do is critical to station and operation planning. I hope this refresher on 2-element performance contributes something to that cause. However, we have wholly neglected the driver-director 2-element Yagi. Therefore, let's spend one more episode on this type of Yagi and other methods of increasing 2-element Yagi performance.

5. Strategies for Improving Forward and Rearward Performance

There are strategies to improve the gain and/or the front-to-back ratio of a 2-element array. The gain and front-to-back performance given in earlier sections are the best obtainable within the design goals (maximum front-to-back ratio and resonance) for a 29 MHz Yagi model using 3/8" aluminum elements in a reflector-driven element arrangement. As noted, these elements scale to reasonable values for lower HF bands, but are not the final word on desirable element sizes. Limitations of both the antenna type and the method of study have been noted throughout.

Let's look at some of the strategies for improvement and divide the work into 2 parts: strategies that can improve front-to-back ratio and strategies that may improve both the gain and the front-to-back ratio. Additionally, we shall look at only some samples of strategies, because the total number of ways to go about the process is limited only by the antenna designer's imagination. However, we shall be able to note some very interesting general trends.

Improving Rearward Performance

There are two chief ways to improve front-to-back performance of a 2-element array: phasing the two elements and altering standard 2-element geometry.

The 2-Element Phased Array: I have done an extensive study of the ZL Special, in "Understanding and Modeling Small Beams: Part 5: The ZL Special," *Communications Quarterly*, (Winter, 1997), 72-90. The ZL Special became popular in the 50s after a series of articles by ZL3MH/ZL2QQ, George Prichard, with some quick test work by G2BCX. Claims of 7 dBd gain and 40 dB front-to-back ratios were common, mostly because the antenna outperformed many of the ill-designed 3-element Yagis of the period. It remained almost a

constant claim that the antenna was a phased array 1/8 λ separated and using a twisted 45° phase-line to give 135° phasing. It was Roy Lewallen who pointed out in the 1980s that is was not the impedance at the rear element that was critical, but the current, and this changed the analysis ball game, although it appears few have taken up the challenge.

Fig. 5-1

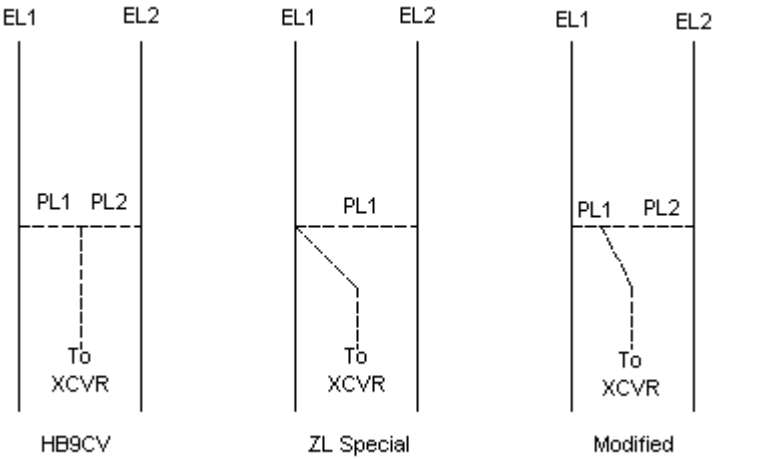

3 Ways to Phase-Feed a 2-Element Array

The ZL-Special is only one of several types of the 2-element horizontal phased arrays, and **Fig. 5-1** does not show all of the possibilities. While the ZL-Special, with a single phase-line, is popular in the U.S and in the British Commonwealth, the HB9CV, with 2 phase lines fed at the center point between elements is popular in the rest of Europe. Due to the impedances of the lines and the elements, it usually requires a gamma match at each element. A much simpler double phase-line arrangement appears under the title "modified." The two lines have unequal lengths, with the feedpoint at the junction of the two lines. It achieves the same goal as the other two designs, but allows the use of common transmission lines, such as coaxial cable, as the phase line. The

variety of phasing techniques led to Volume 1 of this set. Note that in **Fig. 5-1**, we do not refer to the elements as a driver and reflector, since we are driving both elements. In fact, both elements receive energy via direct feed and by coupled energy from the other element. Generally, we call the element in the direction of the forward lobe element 1 and the rearward wire element 2.

Since current goes through a 360° cycle, not a 180° cycle like impedance along a transmission line, the proper analysis of a one-line ZL-Special must treat it as a -45° phased array. The minus sign is the product of the phase line twist. Once we make this shift in perspective, we can analyze the relationships of the current magnitudes and phases along the line such that they yield correct values for the spacing used and wind up with identical voltage magnitudes and phases at the junction with the feedline. For a given situation, line length, characteristic impedance, and velocity factor combine so that few values will satisfy the requirements, and fewer still if we stick to available commercial lines.

The spacing need not be precisely 1/8 λ, since every spacing between a very small one and something just under 1/4 λ has a current magnitude and phase requirement for the rear element that will yield maximum front-to-back ratio. In fact, for 1/8-λ spacing, the current phasing must be about -43° to -44°, at 0.1-λ spacing, the current phasing must be about -34°, and at 0.15-λ spacing, the current phase must be about -53°. A similar analysis applies to other types of phased arrays. Indeed, the goal of the phase lines, if we have more than one of them, is to establish the relative current magnitude and phase relationship required for a desired pattern based on the length of the two elements and on the spacing between them. The element diameter will have a small but noticeable effect on the process, since it also affects the mutual coupling between elements.

In general, a pair of phased horizontal elements is not capable of a maximum forward gain in excess of about 7.1 dBi in free space. That gain level is approximately the peak gain of the 2-element parasitic Yagi when set for maximum gain. Like the maximum-gain Yagi, the phased array--when set for maximum gain--has a very poor front-to-back ratio, usually well below 10 dB. The phased element pair, however, can achieve a much higher front-to-back

ratio than the parasitic driver-reflector Yagi. Because we can control the current magnitude and phase-angle relationship between the two elements, we can reach front-to-back levels as high as 50 dB at a design frequency. The high front-to-back ratio has several limitations. First, it occurs at a specific frequency and decreases immediately as we move above or below that frequency. Second, the gain that accompanies the maximum front-to-back ratio is slightly less than we can get from driver-reflector Yagis with element spacing values between 0.12 λ and 0.16 λ.

For these reasons, most serious phased-array designer aim for a middle ground between maximum gain and maximum front-to-back ratio. There is a middle ground that shows a small gain improvement but a considerable (8 to 10 dB) front-to-back ratio improvement over the driver-reflector Yagi. The benefit of designing in this region is that one can usually spread the benefits over a sizable operating bandwidth.

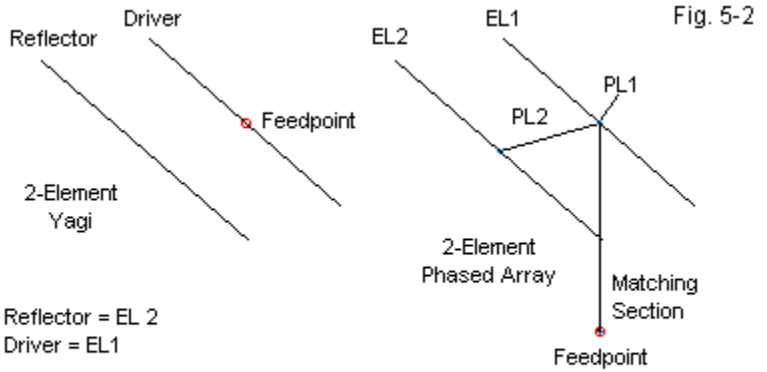

Fig. 5-2

Converting a 2-Element Yagi into
a 2-Element Phased Array

As a sample phased array, let's look at a design that I published several years ago using different element structures than the 3/8" aluminum elements

used throughout this series of notes. One interesting feature of this design is that we can use the beam as a reflector-driver Yagi or as a phased array with a variety of phase-line arrangements. **Fig. 5-2** shows the basic outline of the array. (see models 5-1.ez and 5-2.ez.)

Element 1 or the driver is 16.13' long, while the reflector or element 2 is 17.41' long. The spacing between elements is 4.8' or 0.139-λ. This spacing is at the edge of the Yagi broadband spacing range and allows a direct 50-Ω feedpoint when we use the antenna in this mode.

When we wish to convert the antenna into a phased array, we have at least 2 choices. We can use a single 35-Ω cable (RG-83) in ZL-Special style. The line length will be 4.83' for a cable with 0.66-velocity factor (VF). The resulting feedpoint impedance at the junction of the phase line with the forward element is close to 25 Ω. So we need a roughly quarter-wavelength matching section (5.69') of 35-37-Ω, 0.66-VF line. We can make up such a line with parallel sections of RG-59 cable. If we cannot obtain 35-Ω cable for the phase line, we can use 50-Ω RG-8X with a velocity factor of 0.78. However, we need two sections. A 6" section goes from the feedpoint junction to the forward element, while a 64" (5.33') section goes from the junction to the rear element. The impedance at the junction will not be identical to what we obtain from the 35-Ω phase line, but a 34" (3') matching section of paralleled RG-59 will yield a 50-Ω match.

The performance difference between the Yagi and phased modes of operation shows up in the overlaid patterns in **Fig. 5-3** at the design frequency of 28.5 MHz for this antenna. The phased version has about 1/3-dB higher gain, but the main benefit occurs in the rearward direction. The phased version has double the front-to-back ratio of the Yagi version. For a broader view of the antenna's performance, **Table 5-1** presents modeled free-space values at 28 and 29 MHz as well as at the design frequency.

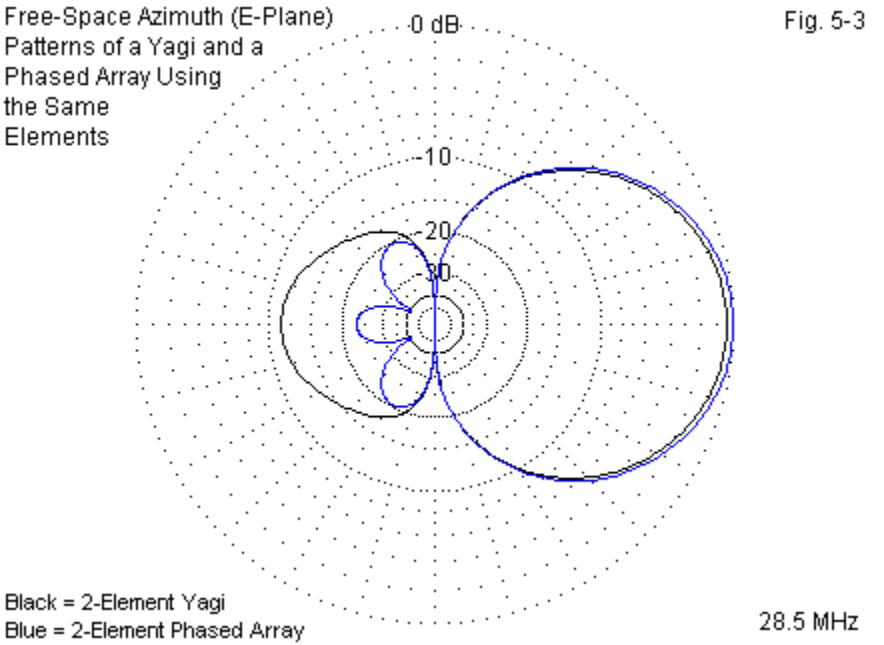

Table 5-1. Performance of a two element array as a Yagi and as a phased-array

Antenna	Frequency (MHz)		
	28	28.5	29
Yagi			
Gain (dBi)	6.61	6.14	5.74
F-B (dB)	10.06	11.01	10.21
Feed Z	30.6 - j17.1	40.5 + j4.4	49.4 + j23.7
50-Ohm SWR	1.91	1.26	1.61
Phased Array			
Gain (dBi)	6.00	6.50	6.99
F-B (dB)	21.02	22.91	12.51
Feed Z	75.9 - j12.5	51.4 - j9.3	32.7 + j5.5
50-Ohm SWR	1.59	1.20	1.56

Both versions of the antenna offer very good SWR curves for a 50-Ω cable across the entire first MHz of 10 meters. **Fig. 5-4** provides the modeled SWR

values in 0.1-MHz increments. Note that the Yagi version requires no matching section, but the phased array version requires both a phase line and a matching section. The fact that the phased array version shows a descending feedpoint resistance as the frequency increases results from the impedance transformation within the matching section.

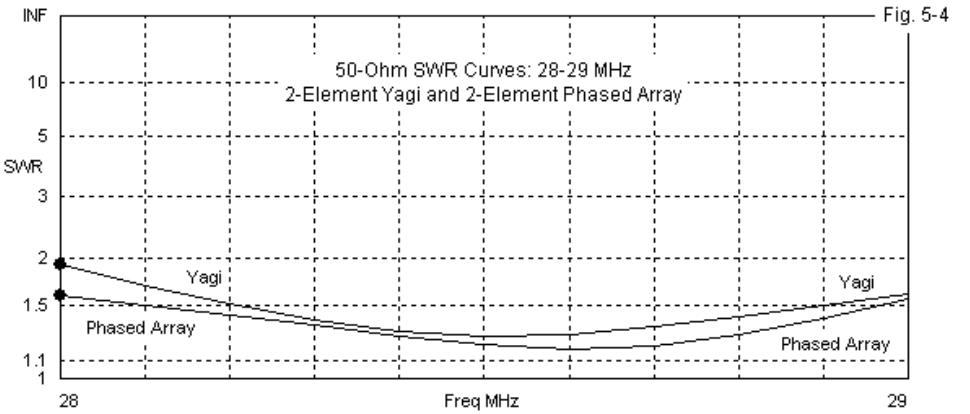

The gain curves for the two antenna show opposite trends, as is evident in **Fig. 5-5**. The Yagi shows the typical driver-reflector trend of decreasing gain with increasing frequency. In contrast, the phased array shows increasing gain with frequency, a trend that is more typical of parasitic Yagis with one or more directors.

Fig. 5-6 shows the two front-to-back curves for the Yagi and the phased array. The Yagi curve is very flat across the entire passband for the antenna. In contrast, the phased array shows a definite peak. Because the phased array is an adapted use of a Yagi design, the peak does not occur at the design frequency, but about 200 kHz lower. Still, the front-to-back ratio remains higher than the value for the Yagi throughout the operating passband. However, we note in passing that as the gain approaches the 7-dBi mark, the front-to-back ratio is in serious decline.

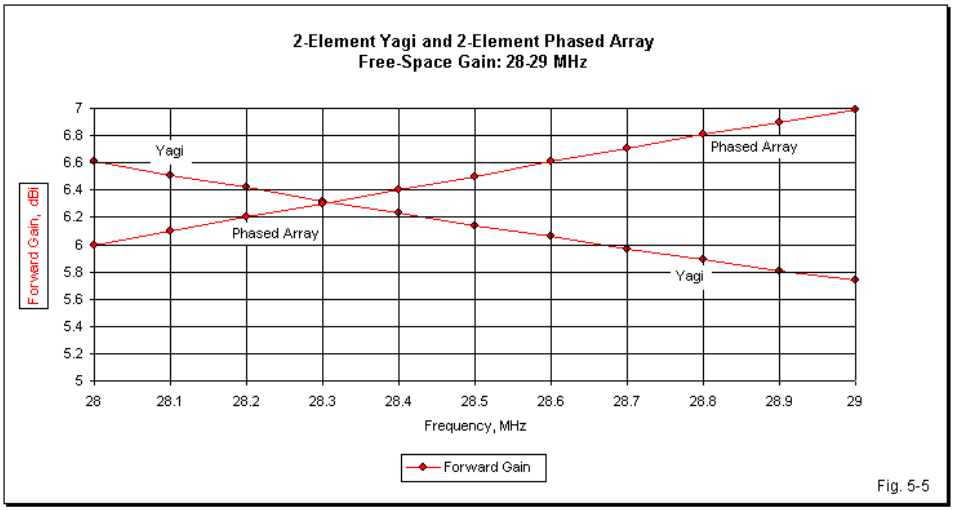

Fig. 5-5

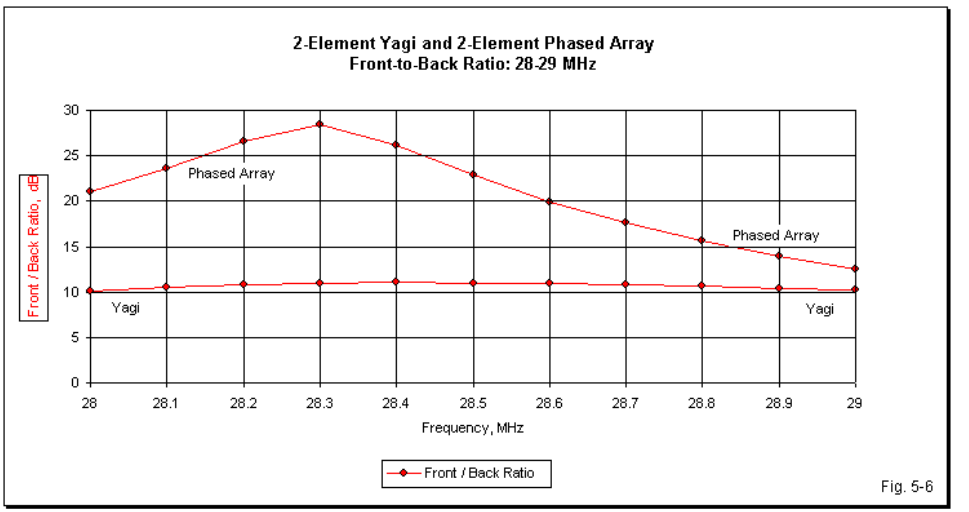

Fig. 5-6

The sample phased array has provided us with a good example of typical

performance as well as a good comparison with a comparable driver-reflector Yagi. Since there are so many ways to handle the phasing and matching requirements of phased arrays, other sampled arrays will yield other results. However, all will fall within the limits of what is possible for phasing with 2 elements.

The Moxon Rectangle: What the phased array does with phasing lines, the Moxon rectangle does with geometry, that is, establish the correct rear element current magnitude and phasing for maximum front-to-back ratio. Derived from the VK2ABQ square, which is actually a rather poor performer, but with a germinal insight, the G6XN rectangular modification arose from practical considerations rather than a through understanding of what was going on. In fact, Moxon himself used the antenna with remotely tuned elements in order to flip the direction, and did not provide any solid basic information on its design. That led me to a considerable study of the antenna. See "Modeling and Understanding Small Beams: Part 2: VK2ABQ Squares and Moxon Rectangles," *Communications Quarterly*, (Spring, 1995), 55-70. Since that time, the Moxon rectangle has evolved steadily as a 50-Ω 2-element beam. There are numerous articles at the web site on various aspects of Moxon rectangle design, assembly, and application. See the general listing called "Moxon Rectangle" for a list of available articles.

The Moxon rectangle bends the forward and rear elements of a Yagi toward each other, with a small but critical space between the ends. The precise dimensions are a matter of design goal choice. Broader bandwidth of the front-to-back ratio occurs with squarer versions, but at a higher feedpoint impedance (80 Ω or so). One can also build versions that are narrow from front to back, and hence a bit wider from side to side, and achieve a 50-Ω feedpoint impedance, although the front-to-back ratio goes down toward the edges of a frequency sweep. Models can be built with anything from wire to aluminum tubing. I have also developed a set of algorithms for designing Moxon rectangles from uniform-diameter elements from wire-size to fat tubing that covers the HF, VHF, and UHF ranges.

Fig. 5-7

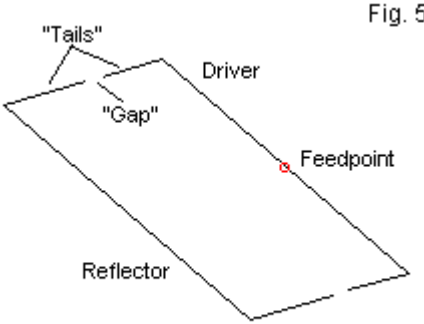

General Outline: Moxon Rectangle

Fig. 5-7 shows the outline of a Moxon rectangle for a direct 50-Ω coaxial-cable connection. Because we have bent the elements, the side-to-side dimension is only about 70% of the length of comparable Yagi elements. For an element diameter of 3/8", the dimension for 28.5 MHz model is 150.3" or 12.54'. The spacing between the driver and the reflector is 55.5" or 4.63'. The driver tails are 21.0". Hence, the total driver length is 192.3" or 16.03'. The reflector tails are 28.6" long, for a total reflector length of 207.5" or 17.29'. Note that the overall element lengths are not far distant from lengths that we meet with driver-reflector Yagis with linear elements. However, the operation of the Moxon depends on the element bends and the second form of coupling formed by the gap between the tails. The gap distance depends on the element diameter. Our 3/8" elements require a 5.9" gap at 28.5 MHz. (See model 5-3.ez.)

In one sense, the Moxon has slightly less forward gain than a 2-element Yagi or a phased array, about 0.3-0.5-dB down on average. However, that gain applies over a much wider beamwidth. A typical 2-element Yagi has a beamwidth between half-power (-3dB) points of about 70◦. Moxon half-power points are typically 80◦ or more apart, and the pattern circle extends beyond the 90◦ side direction. Hence, the proper application of a Moxon is where one wishes a broad forward hearing area and silence from the rear. It is ideal in the US for stations on the coast wanting to work the US without QRM from DX--or to

work the DX across the water with silence from the US. **Fig. 5-8** shows the patterns from the sample Moxon rectangle across the first MHz of 10 meters.

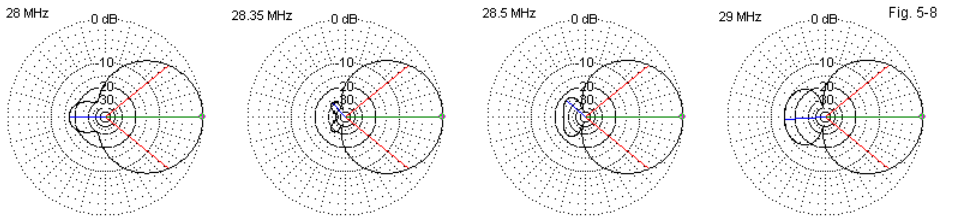

Free-Space Azimuth (E-Plane) Patterns: Moxon Rectangle from 28 to 29 MHz

The figure presents 4 patterns rather than the usual 3 for an interesting reason. Both the front-to-back ratio and the SWR grow worse than ideal at a slower rate above the actual design frequency than below it. Hence, to obtain roughly equal front-to-back and SWR values at both the upper and lower operating frequency limits, the best design frequency is between 0.35 and 0.4 of the passband width above the lower end. For the sample model, I chose 28.35 MHz, the frequency that yields the best SWR and the best front-to-back ratio. As **Table 2** shows, I came close to but did not hit the precise frequency that would yield equal performance values at both 28 and 29 MHz.

Table 5-2. Modeled free-space performance of a Moxon rectangle

Frequency	28	28.5	29
Gain (dBi)	6.43	5.87	5.39
F-B (dB)	16.96	26.21	14.88
Feed Z	38.2 - j16.3	56.3 + j1.1	69.8 + j12.6
50-Ohm SWR	1.58	1.13	1.48

Fig. 5-9 translates the data into graphical form for the forward gain and the front-to-back ratio. The gain curve shows the typical trend of a parasitic driver-reflector array. The front-to-back curve does not show the peak value because that value occurs between sampling points. However, the curve amply illustrates the more rapid decline in the front-to-back ratio below the design

frequency than above it.

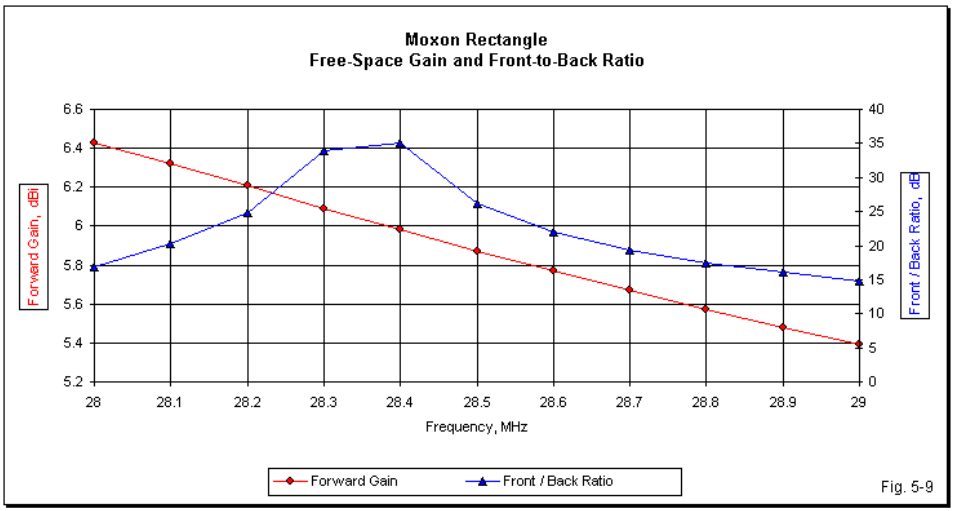

Fig. 5-9

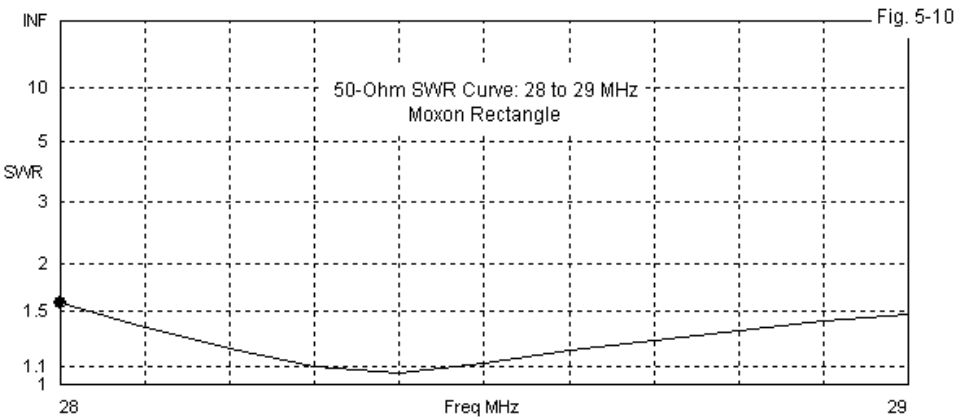

Fig. 5-10

The 50-Ω SWR curve in **Fig. 5-10** mirrors the front-to-back curve. The

Moxon rectangle has a broad SWR curve that makes the beam fairly easy to replicate successfully in a home workshop. Of course, the SWR passband will vary with the element diameter used, with wire showing a steeper curve and fatter elements (such a 1") showing a flatter curve across the first MHz of 10 meters.

The dual coupling between element ends and between the parallel portions of the elements does with antenna geometry much of what a phasing line does in a phased array. That is, it sets (on the design frequency) nearly ideal current magnitude and phase angle relationships that yield a very high front-to-back ratio. Because the geometry that yields the correct current magnitude and phase on the rear element to maximize front-to-back and front-to-rear ratio is frequency specific, the ratio falls off more rapidly than with the phased array sampled earlier--which was purposely not designed for absolutely maximum front-to-back ratio. However, the Moxon rectangle remains superior to a standard 2-element Yagi driver-reflector array across the entire frequency sweep. It does all this from an antenna about 3/4ths the size of a standard Yagi.

Other designs have also been used to increase the front-to-back performance of the 2-element Yagi, but these two designs reveal what is at stake in making them work.

Improving Forward Performance: The Driver-Director Yagi

To improve the forward performance of 2-element parasitical beams, one can always use longer, higher gain elements. Or one may add an element. However, for the standard reflector-driven element Yagi using half-wavelength dipoles, there are only a few routes to slightly increasing forward gain. Up to a certain point, one can improve the performance of a 2-element Yagi by increasing the size of the elements. **Table 5-3** illustrates both the gains and the limits on this tactic.

Table 5-3. The effect of element diameter on 2-element driver-reflector Yagi performance

Element inches	Gain dBi	F-B ratio dB	Feed Z R +/- jX Ohms
Full size; 0.16 wl spacing			
0.375	6.12	10.86	46.67 – j0.35
0.75	6.15	10.89	46.01 – j0.31
1.50	6.15	10.92	45.34 – j0.64
3.00	6.15	10.95	44.62 – j0.39
Fill size; 0.12 wl			
0.375	6.25	11.19	32.47 + j0.23
0.75	6.31	11.23	31.33 – j0.98
1.50	6.31	11.27	31.08 – j0.52
3.00	6.30	11.31	30.74 – j0.99

Clearly, elements with diameters larger than 3/4" add virtually nothing more to the gain of the antenna. In each case, the beams in question used re-sized element lengths to achieve the best combination of gain and front-to-back ratio. As the element diameter grows, the required length decreases. As we learned early on with respect to dipole, shortening the dipole reduces its gain. At a certain point, the gain increase resulting from increasing element diameter crosses the gain decrease resulting from reduced length. Hence, the tactic becomes self-defeating beyond a certain point.

An alternative is to give up operating bandwidth and front-to-back ratio in favor of higher gain over a narrower passband. In our exploration of full-size reflector-driven element Yagis, we saw that the closer the elements, the higher the gain of the antenna. We need only review the antennas when the elements are spaced 0.08 λ (2.8') and 0.12 λ (4.1'): see **Table 5-4**.

Table 5-4. Relative performance of driver-reflector Yagis with closely spaced and moderately spaced elements

Frequency	28	28.5	29	29.5	30 MHz
Maximum front-to-back-ratio designs					
0.08 wl spacing					
Gain (dBi)	6.37	6.92	6.32	5.77	5.37
F-B (dB)	1.82	8.65	11.38	10.12	8.57
SWR	31.2	5.88	1.04	2.91	5.52
0.12 wl spacing					
Gain (dBi)	6.98	6.74	6.25	5.82	5.48
F-B (dB)	5.46	9.79	11.19	10.37	9.18
SWR	7.12	2.33	1.01	1.81	2.76
Maximum gain designs					
Frequency	28	28.5	29	29.5	30 MHz
0.08 wl spacing					
Gain (dBi)	7.15 R	6.01 R	7.02	6.59	6.02
F-B (dB)	10.29	0.72	6.29	10.61	10.54
SWR	40.6	16.4	1.01	6.87	14.2
0.12 wl spacing					
Gain (dBi)	6.94 R	6.13	6.99	6.70	6.24
F-B (dB)	4.74	1.05	6.12	9.80	10.87
SWR	14.7	5.20	1.01	3.03	5.43

If a higher gain is desired and the conditions of obtaining it are acceptable, then a 2-element driver-director Yagi may serve the purposes at hand. Due to its narrow operating passband, the driver-director 2-element Yagi has restricted use. It is most apt for covering one of the narrow amateur bands, such as 30, 17, or 12 meters. In addition, amateurs who wish specialized antennas to cover only the CW-digital part or the SSB part of a wider amateur band may sometimes find the 2-element driver-director Yagi suitable.

The Driver-Director 2-Element Yagi: A director plus driven element is capable of higher gain at close spacing values than a reflector plus driven element. The general outline of this Yagi type appears in **Fig. 5-11**.

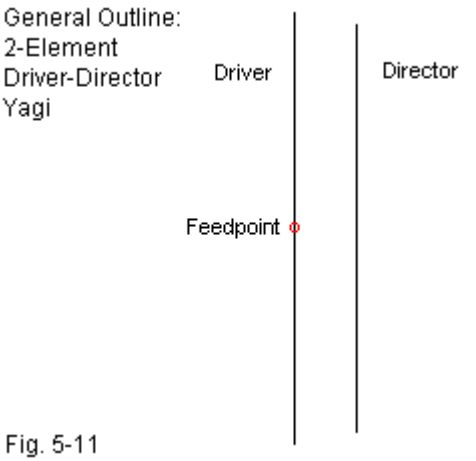

Fig. 5-11

If we use 3/8" aluminum elements (to be consistent with all of the other beam designs in these notes), we can optimize a series of 2-element driver-director Yagis at 29 MHz using different values of element spacing from 0.06-λ (2.03') up to 0.14-λ (4.75') at 0.02-λ intervals. The results of our first step appear in **Table 5-5**. (See models 5-4.ez through 5-8.ez.) Each version has been optimized for maximum front-to-back ratio at the design frequency.

Table 5-5. Dimensions and 29-MHz performance of 2-element driver-director Yagis in free space

El. Spacing (WL/feet)	0.06 / 2.03	0.08 / 2.71	0.10 / 3.39	0.12 / 4.07	0.14 / 4.75
Driver Length (WL/feet)	0.474 / 16.07	0.467 / 15.85	0.462 / 15.66	0.457 / 15.50	0.452 / 15.34
Director Length (WL/feet)	0.499 / 16.92	0.497 / 16.85	0.494 / 16.74	0.490 / 16.62	0.487 / 16.52
Gain dBi	6.51	6.50	6.42	6.32	6.12
Front-to-Back Ratio dB	45.18	20.95	14.83	11.33	8.91
Feed Z (R +/- jX)	14.82 - j0.11	22.98 + j0.06	29.69 + j0.16	34.53 - j0.05	38.94 + j0.20

As we increase the spacing between the elements, the lengths of both the driver and the director decrease. In addition, the gain also decreases as we increase the spacing between elements. The gain values at 0.12-λ and at 0.14-λ closely resemble the values that we might obtain from a driver-reflector Yagi.

Perhaps the most notable feature of the driver-director Yagi is the front-to-back ratio. If we use a close spacing value that is less than 0.10-λ, we can

exceed the front-to-back ratio that we can obtain from the most common designs of the driver-reflector version of the Yagi. However, we pay a price: the resonant feedpoint impedance decreases to levels that we may find more difficult to match without also incurring losses.

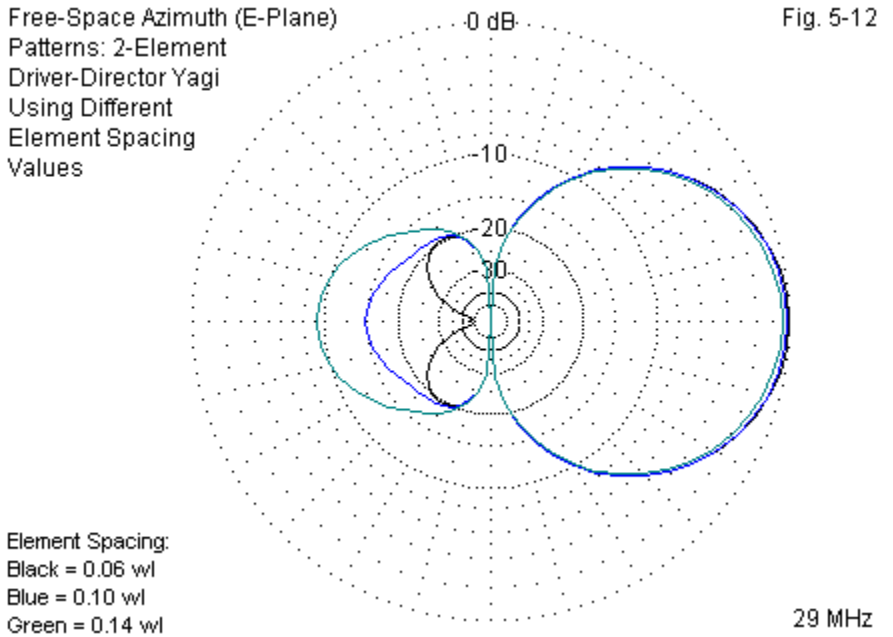

Fig. 5-12 overlays sample patterns from the 0.06-λ, 0.10-λ, and 0.14-λ versions of the antenna. The overlay shows the development of the rearward radiation pattern, and you may easily interpolate the patterns for the missing plots (that would have made the overall graphic difficult to read). Note especially the rearward pattern for the smallest element spacing. Although the 180° front-to-back ratio is about 45 dB, the worst-case value at the center of each rearward lobe would be closer to 20 dB. The radiation in these directions does not change in strength as we increase the spacing. As a consequence, the

best compromise design spacing might be in the vicinity of 0.08-λ, a value that yields a 21-dB 180° front-to-back ratio. This value would also approximate the worst-case value and the average values of front-to-back ratio over the entirety of the rearward quadrants. At the same time, the feedpoint impedance is about 23 Ω, a value that is well within the ability of either a gamma or a beta match to provide a relatively low-loss matching system for a 50-Ω feedline. Finally, the 0.08-λ spacing also provides a bit of added forward gain relative to common driver-reflector Yagi designs.

So far, we have examined the driver-director Yagi at its design frequency. We should reserve final evaluations of any of the design versions until we examine the patterns of performance behavior over an operating passband. For the sample values in **Table 5-6**, we have returned to the wide passband that runs from 28 to 30 MHz. Using this passband will facilitate comparisons with full-size driver-reflector Yagis. The SWR values in the following table are relative to the resonant feedpoint impedance at 29 MHz.

Table 5-6. Performance of driver-director Yagis from 28 to 30 MHz

Frequency	28	28.5	29	29.5	30 MHz
0.06 wl spacing					
Gain (dBi)	4.69	5.46	6.51	7.21	6.46R
F-B (dB)	7.36	10.51	45.18	6.90	2.12
Feed Z	39.5 - j 42.0	27.4 - j24.8	14.8 - j0.1	6.89 + j31.1	5.9 + j64.3
SWR	5.82	3.59	1.01	11.90	49.57
0.08 wl spacing					
Gain (dBi)	4.86	5.58	6.50	7.26	6.02
F-B (dB)	7.98	12.13	20.95	8.79	0.57
Feed Z	44.4 - j 37.9	34.9 - j21.9	23.0 + j0.1	13.1 + j29.5	9.6 + j63.8
SWR	3.57	2.35	1.00	5.05	21.15
0.10 wl spacing					
Gain (dBi)	4.95	5.61	6.42	7.14	6.61
F-B (dB)	8.06	11.29	14.83	9.05	2.15
Feed Z	46.5 - j 36.2	39.5 - j20.1	26.7 + j0.2	19.8 + j27.2	14.8 + j60.6
SWR	2.78	1.89	1.01	3.10	10.72
0.12 wl spacing					
Gain (dBi)	4.99	5.60	6.32	6.94	6.71
F-B (dB)	7.69	9.90	11.33	8.12	2.83
Feed Z	47.1 - j 36.6	42.1 - j19.8	34.5 + j0.1	26.1 + j25.2	20.7 + j56.9
SWR	2.50	1.72	1.01	2.36	6.59
0.14 wl spacing					
Gain (dBi)	4.59	5.50	6.12	6.67	6.64
F-B (dB)	6.91	8.28	8.91	7.06	3.24
Feed Z	47.8 - j 36.9	44.4 - j19.4	38.9 + j0.2	32.3 + j24.0	27.3 + j53.6
SWR	2.34	1.62	1.01	1.99	4.60

The feedpoint impedance and the SWR figures make clear that the driver-director 2-element Yagi is not inherently a wide-band antenna. Only with the widest spacing do we achieve an operating passband that is 1-MHz wide at 10 meters, but by the time we reach 0.14-wavlength spacing, the front-to-back ratio has fallen below the levels that we might expect from a driver-reflector Yagi with similar element spacing. **Fig. 5-13** overlays 3 of the SWR curves to provide a more visual idea of the shrinkage of the operating passband as we tighten the spacing and improve the performance at the design frequency.

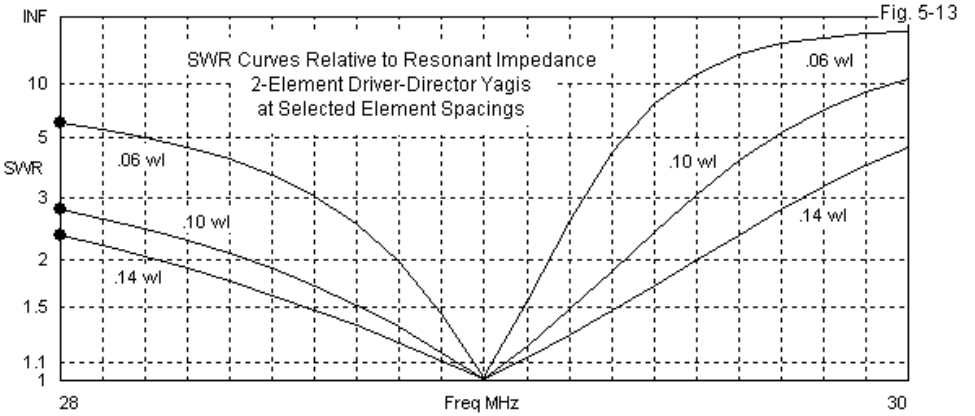

Nevertheless, the sample Yagis have something to teach us about their basic behavior. In a driver-reflector array, we expect the feedpoint resistance to increase as we raise the operating frequency. The driver-director Yagi has the opposite tendency. The feedpoint resistance decreases with rising frequency. The feedpoint resistance trend parallels the trend in forward gain as we increase the frequency. As shown in **Fig. 5-14**, the forward gain of the driver-director Yagi increases as the operating frequency rises. This characteristic holds true of larger Yagis of standard design, a fact that gives us some idea of the relatively greater control exerted by directors relative to reflectors in general Yagi theory.

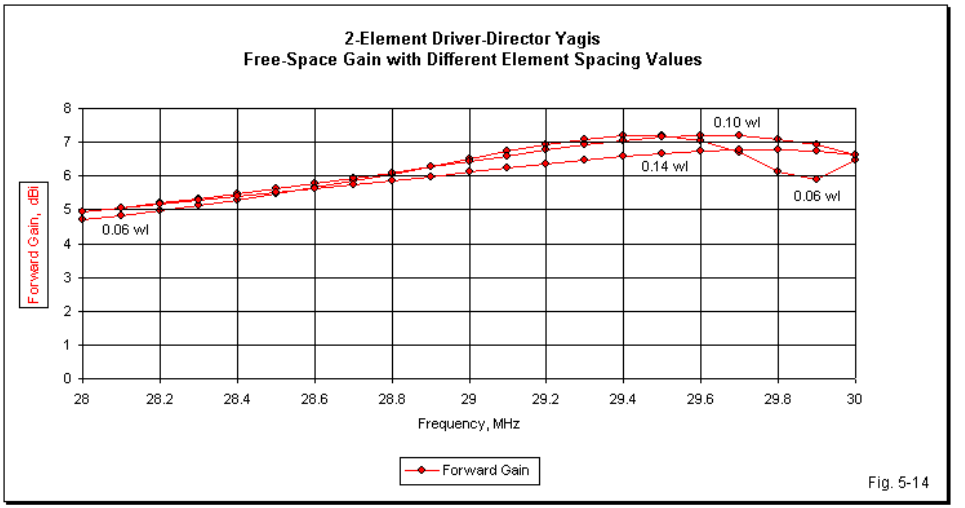

Fig. 5-14

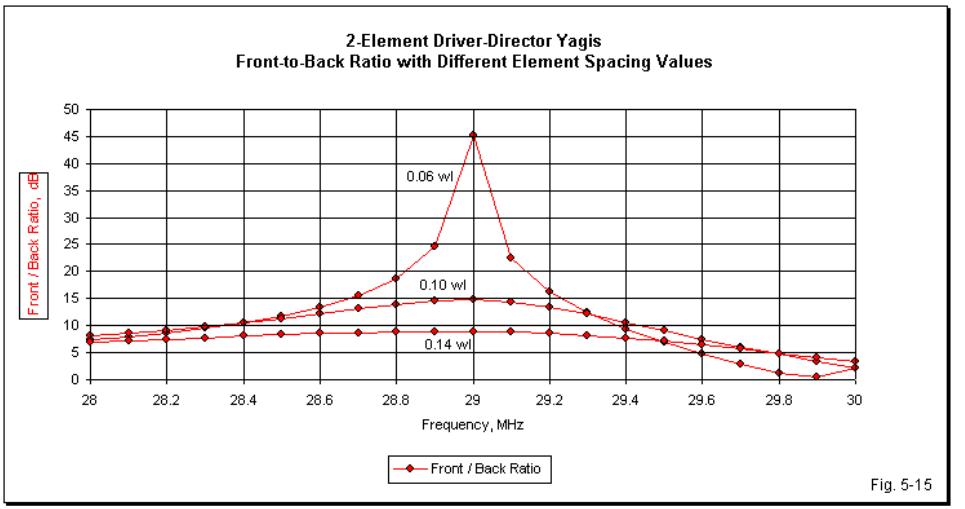

Fig. 5-15

The reversal in the gain trend for the driver-director array holds true of some

other characteristics of this Yagi form. Note that the gain decreases more slowly from its peak as we lower the operating frequency than when we raise it. In fact, the forward lobe direction reversal that occurs within the sweep range for the narrowest element spacing occurs at the upper end of the sweep range. For driver-reflector Yagis, the reversal occurred at the lower end (or outside the lower limit) of the sweep. We also find the same trend when we examine the impedance and the SWR values. For a driver-director Yagi, the SWR increases more rapidly above the design frequency than below it.

The selected front-to-back curves in **Fig. 5-15** confirm that the trends also apply to the front-to-back ratio. The high peak front-to-back value for the array with the closest element spacing may obscure some of the fine detail. However, the front-to-back ratios at the high limit of the sweep are universally lower than the values for the low end of the sweep range.

The sweep data tends to confirm our initial evaluation. The driver-director 2-element Yagi is a relatively narrow-band array for performance values that exceed what we may obtain from a driver-reflector Yagi. The best compromise among all of the values for a practical version of the antenna might use element spacing in the vicinity of 0.08-λ. At this spacing and over a confined operating bandwidth, we can achieve a bit more gain and a lot more front-to-back ratio relative to driver-reflector Yagis. These notes do not include an examination of driver-director arrays with shortened elements. As we saw in connection with shrunken driver reflector arrays, element loading reduces the operating passband. For high performance driver-director designs, the passband is already very small, and further reductions would almost defy replication of the beam in a home workshop.

Conclusion

In the end, the pursuit of gain with a 2-element Yagi is always at the expense of something else: either or both operating bandwidth and front-to-back ratio. More gain with respectable operating bandwidths and front-to-back ratios requires more elements, longer elements, or other antenna configurations, such as a stacked parasitical collinear extended double Zepp array or a long-boom

Yagi with many elements.

This survey of strategies for improved forward and rearward 2-element performance is necessarily incomplete. But hopefully, it will alert you to both the opportunities and the pitfalls of the search.

Part II: Beam-Matching

6. Series Matching Systems

The subject of impedance matching, even when restricted to the idea of matching an antenna to a feedline, is far too wide for this volume. For example, it covers topics as widely separated as the use of parallel transmission lines and antenna tuners, on one side, to simple baluns, on the other. Since our overall subject for these volumes is the 2-element horizontal array, we can prune the subject to a scope that we might be able to handle.

Virtually all of the beams that we have observed in these two volumes have exhibit typical feedpoint characteristics for arrays. In general, the impedances are low to moderate, that is, have resistive values less than 100 Ω. Although I have striven to use samples that are resonant, some of the beams have shown some reactance, either capacitive or inductive. Therefore, the scope of our coverage will focus on these feedpoint properties, thus reducing the number of matching arrangements to three: the series system, the beta system, and the gamma system. We shall examine each of these systems in a separate chapter so that we do not grow confused as to which components, ideas, and calculations belong to which system. In this chapter, we shall work exclusively with series matching systems.

Some Basics and Preliminaries

Over the years, I have received a number of seemingly strange inquiries about beam designs that show a 50-Ω feedpoint impedance. The question generally has this form: What sort of matching system should I use with this beam? The obvious answer is “None,” but the fact that the question perennially arises deserves some comment.

From 1950 to about the turn of the century, almost all beam designs had low impedance feedpoints—some as low as 9 or 10 Ω. Many current designs have 20-25-Ω impedances. Amateurs working in the HF range almost (but not quite) universally use 50-Ω coaxial cable as the feedline for beam antennas.

Therefore, almost every new design that appeared in amateur journals contained a section on adjusting the matching system. Matching systems seemed to newcomers to be a necessary part of the beam itself. The tightness of the connection appears in another often-asked question: What affect does the matching system have on the performance of the antenna?

These renewable questions give us good reason to start at the beginning and set the stage for our examination of matching systems. We might achieve this goal with a set of basic propositions.

1. *A matching system is an adjunct to the antenna and hence does not materially affect basic antenna performance.* The forward gain, beamwidth, and front-to-back ratio of a beam do not change when we place a matching system between the antenna and the feedline. This statement is true of well-designed matching systems that do not add material bulk to the antenna's geometry. Some matching systems require the addition of significant bulk—for example, the gamma match. However, even this bulk will not change the basic performance ratings by any amount that an operator might detect in operation. (There are mal-designed gamma matching systems that have succeeded in offsetting radiation patterns, but these are more the exception than the rule, especially in the HF range.)

Our first proposition is not without some exceptions. Perhaps the most notable one is the beta match, which uses the intentional detuning of the driver element to create a capacitive reactance at the feedpoint. This reactance becomes part of the matching network. Nevertheless, the detuning does not change basic beam performance.

2. *A 50-Ω feedpoint impedance requires no matching system when the feedline is a 50-Ω cable*. If the feedpoint impedance and the transmission line match closely, then we may connect the feedline directly to the antenna terminals and be assured of a good match, that is, an efficient transfer of energy from the feedline to the antenna—or from the antenna to the transmission line when receiving. However, this situation carries with it some other considerations.

A beam's feedpoint is normally balanced, since we are feeding the center of a horizontal element that is approximately ½-λ long. We call coaxial cable "unbalanced" for a variety of reasons. At the transceiver end of the cable, we connect the line to single-ended circuits, with the braid connected to the system ground buss. We often think of the antenna end of the line as also grounded. Although the line may serve as an effective path to discharge static charges from the element, the upper end of the coax may not be at ground potential for the RF energy that is our primary interest. At the feedpoint, some energy may travel down the outer side of the braid. Although the radiation from the braid is usually not significant, we do not require much energy back at the equipment to create problems. To prevent common-mode currents from extending past the antenna feedpoint, we usually install a balun or a choke to attenuate them. For a 50-Ω antenna and a 50-Ω feedline, we use a 1:1 balun, since we do not require any adjustment to the impedance.

A 50-Ω feedpoint impedance naturally requires that we insulate and isolate the driver element from a conductive boom structure. This natural condition for beams of any design has exceptions. At one time the exceptions were the rule in amateur beam construction. We wanted to use what became the "plumber's delight" method of construction in which every element made a solid mechanical and electrical connection to a metallic boom. For some, the construction offered mechanical simplicity. For others, it offered a static discharge path for every element. However, mechanically connecting a beam element to the boom is not necessary for proper beam operation. As well, the connection requires element length adjustments relative to the same designs when the elements are insulated and isolated from the boom. Throughout this volume, all of the sample beams presume that the elements have no connection—or even excessively close proximity—to a conductive boom. (NEC cannot model boom effects.) Only one of our three matching systems will accommodate a driver element that makes a direct connection to a boom. All of the others (including the "no-matching-system" 50-Ω to 50-Ω situation) require that the driver elements use some effective form of insulation.

3. *Well-designed matching systems, whatever their type, are about equally efficient*. If the impedance ratio involved in the match is fairly low (say 2:1), then

most matching systems will dissipate less than about 2% of the power, an insignificant amount if we convert the figure to dB or if we compare the figure to other losses in the overall antenna system from the transmitter to the antenna. Losses rise as the impedance ratio rises, or as we fail to make good and durable electrical connections that will stand up to weather without increasing the junction resistance.

Efficient rudimentary matching circuits, such as those used to match beams to feedlines, do not improve the inherent operating passband of the antenna. If we use the resonant impedance of the pre-matched driver and the driver with the matching circuit installed, we shall find virtually the same SWR curve. However, the pre-matched driver SWR curve may not be directly usable with the intended feedline.

With these preliminaries out of the way, let's look at series matching systems. In each case, we shall look at the equations used to calculate the matching system—or at least at one set that will do the job. We shall also see the practical applications and consequences of each matching system. As an aid to those who dislike hand calculators, I have appended with the models for the volume a spreadsheet that allows you to calculate each type of matching system. I wrote the spreadsheet in Quattro-Pro (.qpw), but have also saved it in the Excel format (.xls). I have used no error-blocking techniques, so it is possible to press them beyond their limits. As well, I have not locked any cells, so you may wish to preserve an archival version in a safe directory in case you accidentally change something critical to one or more of the progressions.

The ¼-λ Transformer

Perhaps the most fundamental impedance transformation system that is useful with beams consists of a ¼-λ transmission-line transformer. Since the basis of the transformer is accurate measurement of ¼-λ, you must know (from references or from measurements) the line's velocity factor (VF). The velocity factor varies from about 0.66 to 0.8 for common (RG-series) coaxial cables and from about 0.8 to 0.95 or so for parallel transmission lines. Multiplying this number times the true quarter-wavelength provides the physical length that a

given line must be to be an electrical quarter-wavelength. The following equations may prove convenient in finding the line length.

$$1/4\lambda = VF\frac{299.7925}{4\,F_{MHz}}(meters)$$
$$= VF\frac{983.57}{4\,F_{MHz}}(feet)$$
$$= VF\frac{11802.85}{4\,F_{MHz}}(inches)$$

Very simple relationships govern the use of a quarter-wavelength impedance transformer. There are three impedance values of interest: the antenna-end impedance (Zload), the source or line-end impedance (Zsource), and the characteristic impedance of the line (Z_0).

$$Z_O = \sqrt{Z_{load}\,Z_{source}} \qquad Z_{source} = \frac{Z_O^2}{Z_{load}}$$

To use a ¼-λ transformer, the driver element must be insulated from the boom. **Fig. 6-1** shows the outlines of two common ways of implementing a transmission line transformer. For matching Yagis to coaxial cable, the sketch on the right is what we normally see and use. However, the scheme on the left may prove useful for matching other types of arrays to a main coaxial feedline.

In both installations, the use of a common-mode current suppressor (or, more correctly, attenuator) is as advisable as with a directly driven element. The attenuator will likely be either a 1:1 balun (transmission-line) transformer or a ferrite bead choke. The most common forms for these devices use a 50-Ω design impedance. Therefore, both become part of the main feedline cable. The proper installation point for such devices is at the junction of the impedance transformer and the main cable.

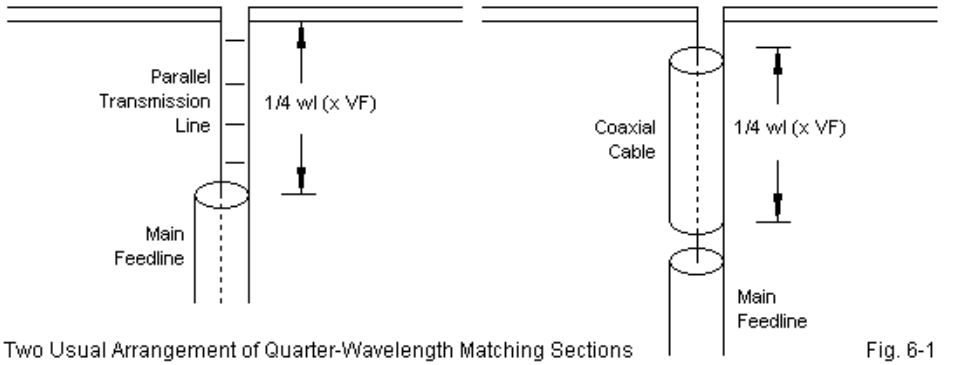

Two Usual Arrangement of Quarter-Wavelength Matching Sections Fig. 6-1

As well, the input and output impedance values must match up with the characteristic impedance of a line that is either available or buildable. For situations that allow the use of a ¼-λ section of parallel transmission line with an impedance of about 200 Ω or more, shop construction is very feasible. However, the majority of beam-matching applications call for a coaxial cable. **Table 6-1** lists some coaxial cables and a few of their matching possibilities possible applications. In some cases, we may construct a cable using parallel sections of a higher-impedance line. For example, the entry for RG-83 is almost gratuitous, since the cable is not easy to obtain. However, we can construct a 35-Ω cable by using parallel sections of RG-11 or RG-59, both of which are 70-Ω cables. Other combinations are also possible.

Table 6-1. Some impedance transformations possible with common coaxial cables

Cable Designations RG-Series	Cable Zo Ohms	Z at One End Ohms	Z at Other End Ohms
83 (or parallel 70-Ω)	35	24.5-50	50-24.5
174, 58, 8X, 8, 213	50	25-100	100-25
59, 6, 11, 216	75	25-225	225-25
62	93	35-250	250-35

Transmission-line transformer matching is amenable to NEC modeling, since we may simulate (lossless) transmission lines. We can insert one between the regular element feedpoint and a short, thin wire that we model as the line termination segment. **Fig. 6-2** outlines the model.

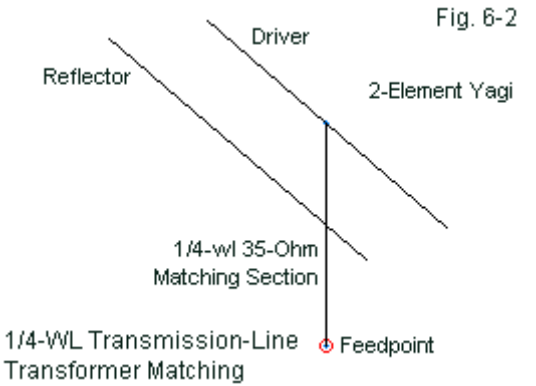

The model uses 3/8"-diameter aluminum elements, and is similar to driver-reflector models in preceding chapters. At 29 MHz, the model uses a 0.502-λ reflector, with a 0.468-λ resonant driver. The free-space gain is 6.28 dBi, with a 11.31-dB front-to-back ratio. The driver feedpoint impedance is 24.8 Ω. See model 6-1.ez.)

Let's add a ¼-λ 35-Ω transformer to the model. The impedance at the source end of the line is now 49.5-Ω. (See model 9-2.ez.) **Fig. 6-3** tracks the resistance and reactance of the sample beam at the element feedpoint (prior to matching) and at the source end of the transformer.

With no matching transformer (NM), both the resistance and the reactance at the feedpoint climb upward in a nearly linear fashion. Since we have a driver-reflector Yagi, resistance increases with frequency and reactance becomes more inductive with frequency.

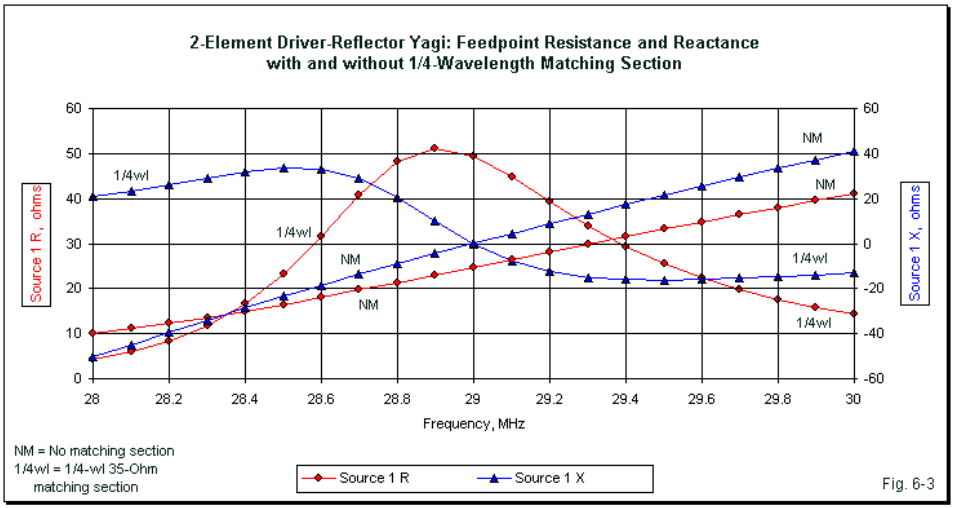

However, with the transformer in place, the curves are no longer linear. As we move off of the design frequency, the line length is no longer exactly ¼-λ. Below the design frequency the line is short, while above the design frequency the line is long. In addition, the feedpoint is no longer resonant above and below the design frequency. As a consequence, the impedance transformation that occurs along the line does not answer precisely to the simplified equations shown earlier. The more complex transformations result in "waves" along both curves.

In the immediate region of resonance, the transformed input impedance shows trends that reverse the expectations that we have of impedances at the element feedpoint. Many basic texts note that in simple dipoles and in the driver of our 2-element beam, an inductive reactance indicates a driver that is too long, while a capacitive reactance suggests a driver that is too short. These rules of thumb apply only to beams without matching networks. In many cases, like the present ¼-λ transformer matching system, the source end of the system may show exactly the reverse trend.

Despite the undulations in the curves for resistance and reactance at the matching transformer feedpoint, the use of a lossless matching transformer does not alter the SWR curve when we adjust the SWR readings for the resonant impedance. **Fig. 6-4** overlays the curves for the pre-matched and post-matched beams. Relative to the reference impedance in each case, there is simply no difference between the operating bandwidths as measured by SWR values.

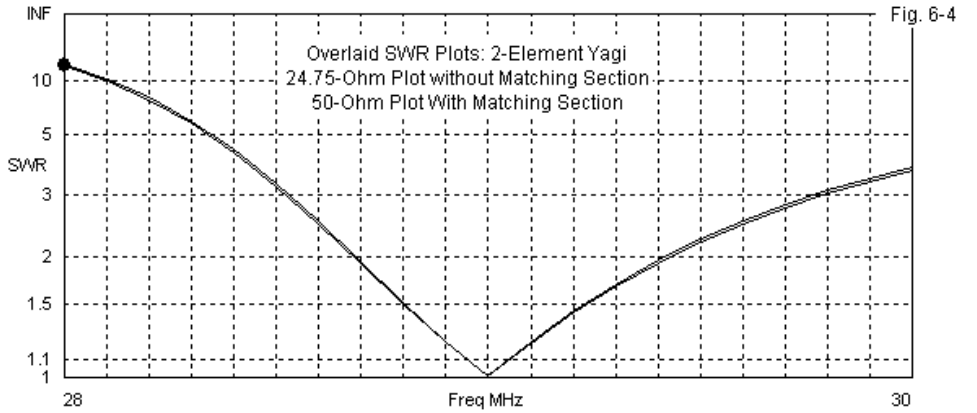

The sheer simplicity of the equations for ¼-λ transmission-line transformers has fostered a number of misconceptions. Among the most limiting false idea is that the transformer must be exactly ¼-λ long at a design frequency. Let's re-consider this idea for a moment. Our goal is to provide a usable operating bandwidth in terms of SWR for a given beam design. In many cases, we may set 2:1 50-Ω SWR limits to define the operating bandwidth (assuming that other beam properties do not change unacceptably over this span of frequencies). In **Fig. 6-4**, the operating bandwidth extends from about 28.7 to 29.4 MHz.

Next, let's remember that whenever a transmission line Zo does not match the impedance at the load (the driver element in this case), the transmission line will transform the impedance continuously along its length (with repetitions every ½-λ). Therefore, we may alter the transformer line length and arrive at

impedance values that might turn out to be useful in terms of our goal.

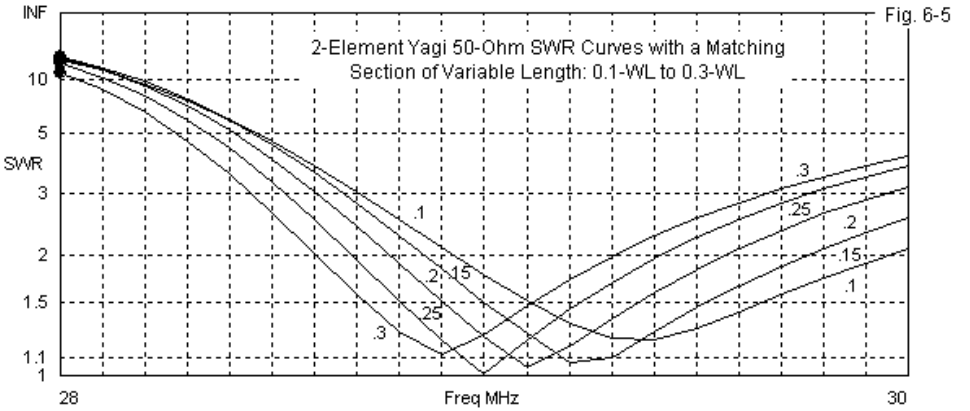

If we use our test model, we can simply vary the transformer line length over a range of lengths and see what happens. **Fig. 6-5** records the 50-Ω SWR curves for the 35-Ω transformer line using lengths from 0.1-λ up to 0.3-λ in 0.05-λ increments. In each case, we find a range of impedance that has SWR values less than 2:1 relative to 50 Ω. Longer lines provide an SWR bandwidth that is about 0.7-MHz wide. However, as we reduce the transformer line length, the operating bandwidth increases gradually to about 0.9 MHz. For some operations, the increase may be significant—at least significant enough to keep the technique in mind.

Similarly, if an element feedpoint impedance has some reactance but also has a resistive value near to the desired level for transformation, the transmission-line transformer may still work. We simply must search for a line length that produces the best SWR curve for not only the design frequency, but for the desired operating bandwidth. Antenna model software, such as NEC provides a relatively easy way of testing various line lengths to arrive at the optimal value for a given antenna design.

The Bramham Limited Series Matching Solution

The ¼-λ transmission-line transformer is perhaps the simplest implementation of a more general matching system. We may label the general collection “series matching,” since each element in any system consists of one or more sections of transmission line installed serially between the driven element and the main feedline. The advantages of using a series matching system are many. First, for almost any set of conditions, one can find commercially made transmission lines to serve as the elements of the system. Second, losses are generally low because the required lengths for lines are short. Third, connections between the line lengths can be made with standard commercial connectors. We can weatherproof these connectors by standard means. The result is that we can avoid using fixed and variable lumped components (coils and capacitors) to create the impedance transformation, components which are often more difficult to weatherproof.

The key limitation to all series section matching systems is that they are frequency specific. Since all are composed of lengths of transmission line that will be specified in electrical degrees, the physical length of the lines will vary with frequency. In most cases, the effective operating bandwidth of these systems will be quite sufficient to cover any of the ham bands (at least above 80 meters). However, they are not broad-banded systems in the sense that a well-designed impedance-transforming balun or unun is broad-banded.

One way to get a handle on series matching systems and their utility is to do a little history, but only as far back as 1961. Depending on the age of the reader, those 37 years may seem like a very long time or only yesterday. In *Electronic Engineering* for January, 1961 (pp. 42-44), B. Bramham published a paper on "A Convenient Transformer for Matching Coaxial Lines," based on work he had done for a CERN report in 1959. His problem and his solution are sketched in **Fig. 6-6**. Essentially, he wanted to match two coaxial transmission lines having different characteristic impedances, and he wanted to use only the materials at hand, namely, the two types of line to be joined.

Bramham recognized that other matching systems, some of them falling into

the series category, were available, such as impedance tapering line sections, single and multiple quarter-wavelength transformer sections, and slug and stub matching techniques. (Balun and unun techniques were not well-developed in 1961, although--as Sevick has shown in his several books and many articles--the principles were available.) However, all of these methods required special materials besides the two line types to be joined.

Fig. 6-6

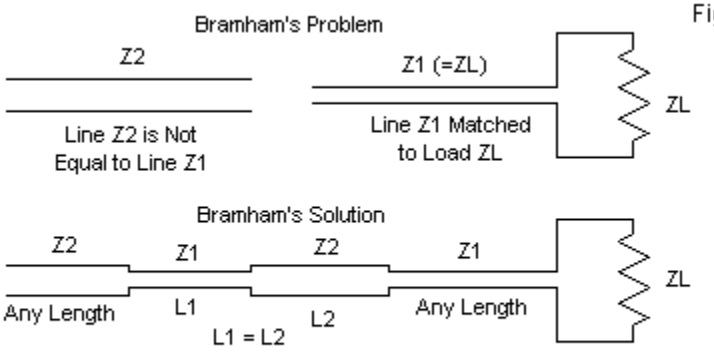

Bramham's Limited Series Matching Problem and Solution

Note the special conditions that apply to Bramham's problem. The connection is between two types of transmission line. The system presumes that the initial line is matched to the load so that the VSWR is 1:1. Hence, the impedances in question are resistive, with no significant reactive component.

Bramham's solution was to develop a means for calculating equal lengths of the two lines, Z1 and Z2, which would effect the impedance transformation for a given frequency. The solution is elegantly simple. First, let's define a special term, M:

$$M = \left(\frac{Z_2}{Z_1} + 1 + \frac{Z_1}{Z_2} \right)$$

Z1 and Z2 are the values of the two lines to be joined in the scheme shown

in **Fig. 6-6**.

The only question is how long to make the two equal section of line inserted between the line to the load and the line to the source. The answer is available on a calculator (or in the attached spreadsheet).

$$L_1 = L_2 = \arctan \frac{1}{\sqrt{M}}$$

L1 is the length of the matching line Z1 and L2 is the length of the matching line Z2. I have transposed Bramham's equation to the "tan" form useful with calculators, although his original was expressed as a "cot" equation.

The answers will be given in either degrees or radians, depending on how you set your calculator. If you wish the answer as a fraction of a wavelength, divide the answer in degrees by 360 and the answer in radians by 2π. Multiply that figure by a wavelength at the frequency of interest, and you have the required line lengths with a velocity factor of 1.0. You can then multiply each line length by the relevant velocity factor for that line to reach the final line lengths to be used.

The line lengths will never exceed 30° (1/12-λ) each, a condition that represents the limiting case of the two lines approaching the same impedance. The operating bandwidth of the system is almost equal to that of a single quarter wavelength matching system and is widest where the two lines are closest in characteristic impedance. However, unlike the quarter wavelength system, which often cannot be implemented because a suitable intermediate impedance line does not exist, the Bramham system can always be implemented where the load matches the initial line. Moreover, it can be implemented at any convenient point down the initial line and need not be placed at the terminals of the load.

The applications are obvious. For example, one might run surplus 75-Ω hard line from the shack to a tower. At a convenient point at either end, one may use a Bramham series section transformer to effect a match to 50-Ω cable to be run at one end into the shack and at the other up the tower or around the rotator to the antenna. However, this technique would apply only to a monoband

installation.

We may test this matching system with a simple model. Consider a 2-element driver-reflector Yagi for 29 MHz with 0.169-λ spacing. The driver is 0.464-λ long, and the reflector length is 0.503-λ. With 3/8"-diameter aluminum elements, the beam's free-space gain is 6.08 dBi with a 10.75-dB front-to-back ratio. The feedpoint impedance of the basic beam is 50.2 Ω. (See model 9-3.ez.)

Fig. 6-7

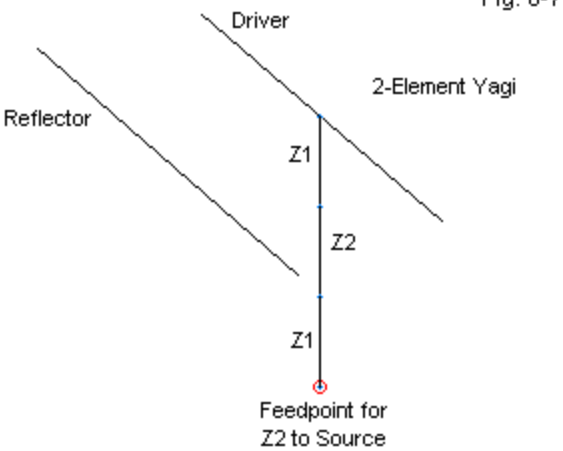

Model to Test Bramham Series-Matching Solution

Suppose that we wish to use a 70-Ω cable as the main feedline. **Fig. 6-7** shows how we may modify the beam to install a Bramham matching system. The line section marked Z1 nearest the driver element is a 50-Ω line with an arbitrary length to establish the claim that we may insert the matching system anywhere along the line. The next two lines toward the ultimate feedpoint (Z2 and Z1) are alternating sections of 70-Ω and 50-Ω line. Bramham's equations require a length of 0.0821-λ for each line. (See model 6-3a.ez.) With this set-up, the new feedpoint impedance is 69.8 Ω.

Although the solution to the equations is frequency specific, the series-matching sections do not restrict the operating bandwidth of the antenna. **Fig. 6-7** overlays the new 70-Ω SWR curve and the 50-Ω curve that would be applicable to the same beam without the matching system in place. The curves are virtually indistinguishable.

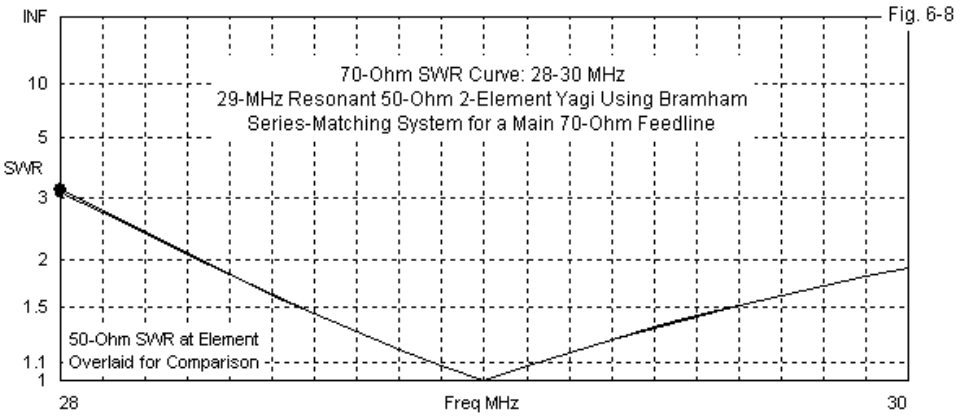

As is often the case, someone can come along and show a given matching technique to be a special case of a more general solution. Such was the fate of the Bramham series transformer section.

Regier's Series-Section Transformer

Between 1971 and 1978, Frank A. Regier, OD5CG, presented at least three papers on a general solution to the series-matching question. **Fig. 6-9** sketches the general conditions of the overall problem. Taking any load that is not matched to a desired feed line, we may attach a specific length of the desired feedline. That specific length will transform the impedance to another value. That value will, in turn, be transformed by the second line of certain characteristic impedance to a value that is a match with the desired system feedline. The two lengths of line for the series matching sections depend on

frequency, and the solution is frequency specific with a certain operating bandwidth. The lengths are also dependent on the characteristic impedance selected for the special section of line.

Fig. 6-9

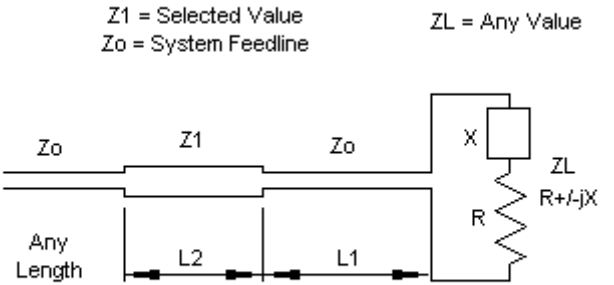

Regier's Series-Section Matching System

The details of Regier's solution can be found in the following references:
"Impedance Matching with a Series Transmission Line Section," *Proceedings of the IEEE* (July, 1971), 1133-1134
"The Series-Section Transformer," *Electronic Engineering* (August, 1973), 33-34
"Series-Section Transmission-Line Impedance Matching," *QST* (July, 1978), 14-16.

I list these important references in the text rather than in a footnote because experience has taught me that most folks simply pass over footnotes. These items are too important to the subject to ignore. A summary of Regier's work is available in almost any edition of *The ARRL Antenna Book*. In the 18th Edition, the basic information appears on pages 26-4 ff. Those interested in designing series section transformers with the aid of Smith Charts should see pages 28-12 ff or the *QST* article.

Regier's solution is best used in "normalized" form, where the ratios of one

impedance to another are first reduced to single values. Otherwise, the calculation equations tend to look terribly opaque. So let's define a few quantities.

$$n = \frac{Z_1}{Z_O} \qquad r = \frac{R_L}{Z_O} \qquad x = \frac{X_L}{Z_O}$$

The load impedance is specified as RL +/- jXL and Z1 is the selected impedance of the special matching section. Note that we shall let L1 be the electrical length in degrees of the line Zo between the load and the special matching section, while L2 is the electrical length in degrees of the special matching section.

Now we can calculate the two lengths, starting with L2, since it plays a role in calculating L1.

$$L_2 = \arctan \pm \sqrt{\frac{(r-1)^2 + x^2}{r\left(n - \frac{1}{n}\right)^2 - (r-1)^2 - x^2}}$$

Although this equation looks a bit forbidding, it can be handled on a calculator (or with the attached spreadsheet). The equation produces two good results, plus and minus. The positive result gives a shorter length for L1 and hence is preferred. If the result is an imaginary number, then the value of n must be changed. You can do this by increasing the value of Z1, the characteristic impedance of the special matching section. Remember that the series matching technique can use parallel transmission line sections as well as coaxial cables, so using a length of 300-Ω or 450-Ω line as the special matching section is perfectly appropriate.

Now let's turn to L1.

$$L_1 = \arctan \frac{\tan L_2 \left(n - \frac{r}{n}\right) + x}{r + x\, n \tan L_2 - 1}$$

In some cases, a calculator will return a negative value for the electrical

length of L1. To arrive at the correct positive value, simply add 180° to the calculated result. For example, should L2 return a value of -62 degrees, the correct result will be 118°.

Since the lengths L1 and L2 are in electrical degrees, divide them by 360 to arrive at a fraction of a wavelength. Then, for the frequency of interest, multiply the fraction times a wavelength for a set of physical lengths with a velocity factor of 1.0. Finally, for the lines actually to be used, multiply each length by the velocity factor of actual line, and arrive at the actual line lengths.

For those who shy away from math, Regier's equations appear to be too complex for the average ham to use. Taking this viewpoint leads the builder often to miss a simple and useful load-to-line matching procedure for monoband antennas. To make the Regier series-section equations more accessible to every ham, they are available as one of the utility programs available in the HAMCALC collection as well as in the attached spreadsheet.

To test the Regier series-matching system, let's use a model that yields a complex impedance at the element feedpoint. Consider a 2-element reflector-driver beam for 29 MHz with a 0.458-λ driver and a 0.502-λ reflector. We shall set the spacing at 0.1-λ. With 3/8"-diameter aluminum elements, the free-space gain of the beam is 6.25 dBi, with a 11.49-dB front-to-back ratio. At the driver, we find a feedpoint impedance of 23.5 – 22.1 Ω. (See model 9-4.ez.) We wish to use a 50-Ω main feedline.

Fig. 6-10 shows the outline of the model once we add the two lines required by the Regier solution. L1 uses 50-Ω transmission line and is 0.4003-λ. L2 requires 0.796-λ of 125-Ω transmission line (RG-63). (See model 6-4a.ez.) If you calculate L2 on the basis of 75-Ω transmission line, the spreadsheet version of the program will return errors everywhere. The impedance is too low to work with the element and main feedline values. 93-Ω line (RG-62) will work and calls for 0.1377-λ of the line as L2. (See model 6-4b.ez.) The 50-Ω length decreases to 0.3778-λ. However, the total series-section length for RG-63 grows to 0.5155-λ, while the RG-63 solution uses a total section length of 0.4799-λ. The two solutions are theoretically equivalent. However, practical considerations

may govern the final selection. Among the factors to consider are line availability, losses at the operating frequency, and available space for the line sections.

Fig. 6-10

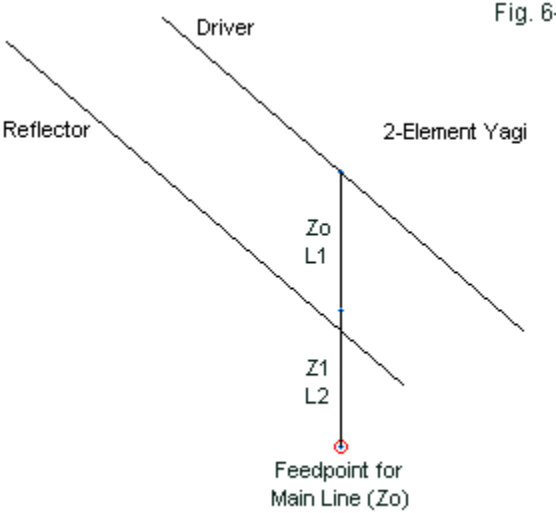

Model to Test Regier Series-Matching Solution

The solution that uses the 125-Ω line and the solution that uses 93-Ω line both show a final feedpoint impedance of 50.0 Ω. **Fig. 6-11** presents the 50-Ω SWR curve for the array plus matching section from 28 to 30 MHz. Compare the graph to the curves in **Fig. 6-4**, the SWR values for the beam using a ¼-λ series-matching transformer. The two beams are identical with respect to the element spacing (0.1-λ) and reflector length (0.502-λ). The only physical difference between the element structures of the two models is the length of the driver. The resonant version of the antenna uses a driver length of 0.468-λ. In contrast, the version that shows a capacitive reactance (before matching) decreases the driver length to 0.458-λ. Although there are some very small numerical differences in the reported free-space performance, they are too small ever to show up in operation.

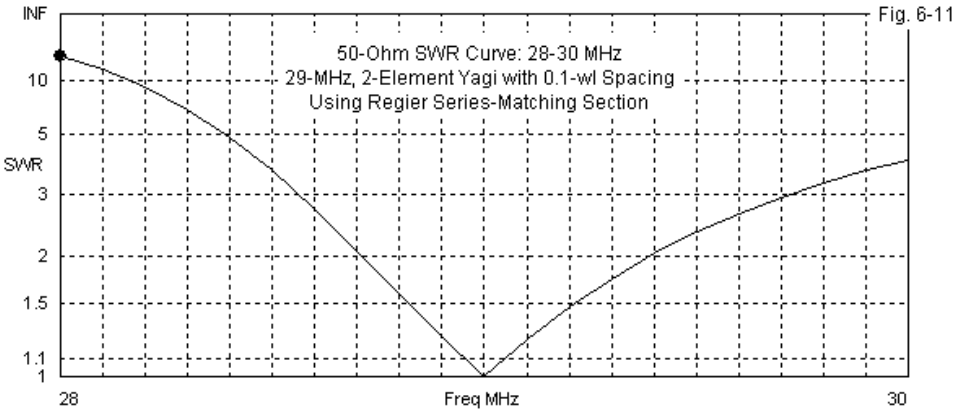

Since we may change the beam's driver slightly without altering its performance, the ¼-λ transformer and the Regier series-matching section become equivalent routes to the same goal: a 50-Ω match to the main feedline. The decision on which solution to use may rest on the availability of cables to use in the series matching section.

Notes and Applications

The common quarter wavelength matching section is actually a special case of Regier's general solution. For the required intermediate value of characteristic impedance of the special matching section, Z1, the length goes to 90◦, while the require length of system feedline between the load and the special section (L1) goes to zero.

Likewise, the Bramham alternating section system is also a special case of the Regier solution. If you examine the equations, you may first let x go to zero, since the Bramham system presumes a matched load with no reactance. Then n and r become equal, since the load or the line to the load has the same impedance value as the characteristic impedance of the special matching section.

Unlike the Bramham system, the Regier series matching system permits matching to many types of loads, with or without a reactive component. Let's take a look at a few sample cases, as sketched in **Fig. 6-12**.

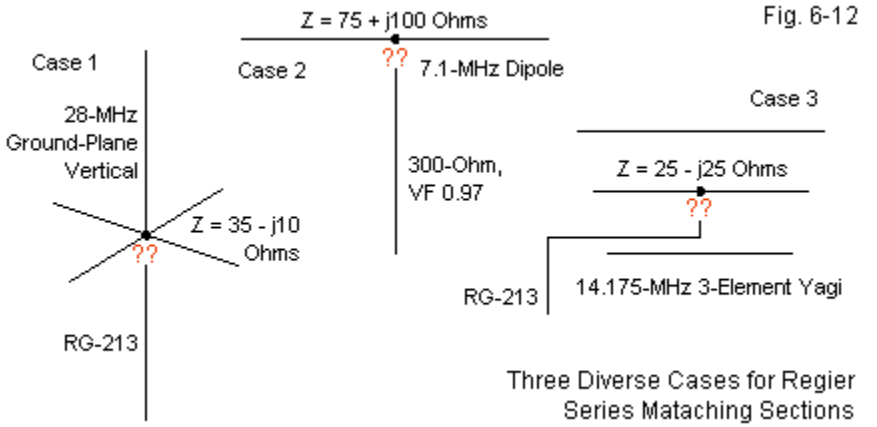

Fig. 6-12

Three Diverse Cases for Regier Series Matching Sections

Our first antenna (Case 1) is a ground plane antenna cut for 28 MHz and fed with 50-Ω RG-213 coaxial cable. The antenna presents a source impedance of 35 - j10 Ω. Although we might live with the natural VSWR of the antenna, we are artificially reducing the 2:1 VSWR bandwidth, because the lowest value is nearly 1.5:1. To achieve a lower minimum SWR value, we can introduce a series matching system consisting of a 138.6° length of our main cable (13.52') connected to the antenna. Follow this with a 31.1° length of 75-Ω RG-11 (3.04). Finally, return to the main RG-213 cable to the shack. The main cable sees, at the design frequency, a 50-Ω resistive impedance. Of course, adjust the physical lengths for the velocity factors of the lines actually used.

Case 2 consists of a wire dipole cut for 7.1 MHz and presenting a feedpoint impedance of 75 + j100 Ω. The 300-Ω feedline presents a very high value of VSWR. We can overcome this high SWR, if we use a 2.57° length of the 300-Ω line (0.96' at a velocity factor of 0.97) from the antenna, followed by a 25.97°

length of 75-Ωm cable (9.99'), and return to our 300-Ω line, the line to the shack sees a 1:1 SWR at the design frequency.

All of these Regier calculations can not only be verified by measurements of actual antenna-cable systems, they can also be modeled on NEC using the TL facility as a pre-construction crosscheck on the initial calculations. Because these samples fall outside the range of 2-element beams, I have not included models.

Our final example is a 14.175 MHz Yagi that presents a source impedance of 25 - j25 Ω. Such antennas often use beta-match systems to arrive at a match with a 50-Ω feedline. As an alternative, we can also use a Regier series matching system consisting of a 153.1° length (29.5') of 50-Ω cable from the antenna, followed by a 6.5° length of 450-Ω parallel line (1.2' at if VF = 0.97), before returning to the 50-Ω line that to the shack. The line to the shack sees a 50-Ω load at the junction with the parallel section. This case uses the high-impedance line for the special section because the minimum characteristic impedance that would satisfy the calculations is 80 Ω for higher Zo matching sections. Although there are 93-Ω coaxial cables, the 450-Ω line is easily made from shop scrap and works just as well with a shorter length. Once more, adjust the coax lengths by the velocity factor of the actual line used.

For almost all cases, there are multiple solutions, which fact allows you to select from a reasonable range of lines to achieve the electrical and mechanical goals of your matching challenge. If you use a choke balun to block common-mode currents from the main feedline, install it on the shack side of the special section. The higher SWR and mismatch along the first two sections of cable may not be suitable for some types of choke balun designs.

These additional sample cases of Regier series matching systems provide you with a feel for the variety of materials that you may bring to bear on a matching problem without using any discrete components.

7. Beta/Hairpin Matching Systems

The hairpin or beta match is a useful and effective system for matching the lower impedance values of many Yagi designs to the standard 50-Ω coaxial cable used by most beam users. However, to the uninitiated, the visible portion of the matching system—a rather short U-shaped heavy wire piece—looks very much like a short circuit across the antenna terminals. Viewers do not recognize the so-called hairpin for what it really is: a shorted transmission-line stub.

The beta match is over a half-century old. Gooch, Gardiner, and Roberts explained the basic concepts underlying the match system in the *QST* article, "The Hairpin Match," in April 1962 (pages 11-14, 146, 156). The *ARRL Antenna Book* has had a basic account in the chapter on coupling the line to the antenna for a very long time. Nevertheless, the basic concepts of the beta match still elude many antenna enthusiasts. Therefore, we shall take a somewhat longer than average look at the system. Everything necessary to calculate a beta match appears in the spreadsheet page devoted to the system.

Beta-Match Fundamentals

The use of a beta match requires three conditions. First, the driven element must be insulated and isolated from any conductive boom. Second, the impedance of the driven element must be lower than the impedance of the main transmission line. For most Yagi designs, fulfilling this condition is often automatic. Third, the driven element must be shorter than resonant so that the impedance at the feedpoint shows capacitive reactance. The amount of capacitive reactance will vary with the resistive impedance, and we shall eventually calculate the ideal value for any given matching situation that meets the other criteria for using a beta match.

The beta match is essentially an L-network that down-converts impedance from the source to the load. How we arrive at an L-network with only one visible

component appears in **Fig. 7-1**. We begin with a resonant dipole (that is, the driver element of a beam), which shows a purely resistive impedance. We then shorten the element to obtain a series combination of resistance and capacitive reactance at the antenna terminals.

Fig. 7-1

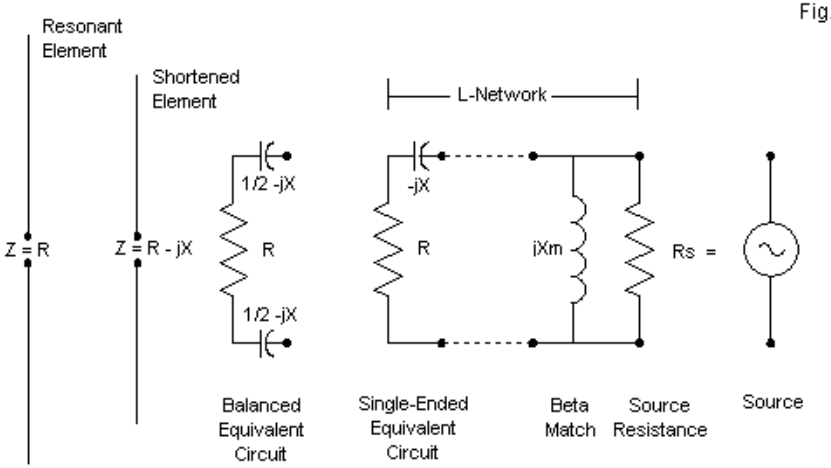

Basic Elements of the Most Common Form of a Beta-Match

As the figure shows, we may view the reactance in two ways: as equally split on each side of the antenna element or as a single lumped value. Either view amounts to the same thing, since the component values are in series.

The series values at the antenna terminals form the resistive load and the series reactance required by a down-converting L-network. To complete the network, we only need to add a parallel or shunt component and a source resistance. The source resistance is the characteristic impedance of the feedline arriving from the ultimate energy source. The parallel reactive component appears on the source side of the network and is the opposite type of reactance relative to the antenna series reactance. Since we have shortened the driven

element to create a capacitive reactance in the figure, the required shunt reactance will be inductive. That reactance will be the beta component that we place across the feedpoint terminals.

Despite its appearance of deceptive simplicity, the beta match is an electrically sound matching system. Since it rests on a very old and solid foundation of electronic theory, we may with relative ease uncover the required reactance values. For any frequency and for any values of load and source resistance values, we may calculate the required values of reactance.

Let's begin our treatment of the L-network with the designation, δ (delta, lower case). The designation appears in Terman's 1943 classic, *Radio Engineers Handbook* (page 213 and elsewhere), but a number of more recent publications have come to use terms such as "working Q," "network Q," or "loaded Q (Q_L) (in contrast to the "unloaded Q or Q_U) in preference to the older term. However, δ will do nicely for our work.

In an L-network, we may express the relationships that define δ in two ways:

$$\delta = \sqrt{\frac{R_{in}}{R_{out}} - 1} \qquad \frac{R_{in}}{R_{out}} = \delta^2 + 1$$

The ratio of the input or source resistance (Rin) to the output or load resistance (Rout) defines the value of δ. I have chosen this starting point for our treatment as a tribute to George Grammer, whose classic volume *A Course in Radio Fundamental* makes use of the concept (pages 69-70). The fact that this starting point simplifies the calculation of the reactance components of the network adds some substance to the reference. In fact, the calculation of the reactive components is very easy.

$$X_s = \delta R_{out} \qquad X_p = \frac{R_{in}}{\delta}$$

For our down-converting version of the L-network, the series component is simply the product of δ and the load resistance. The parallel or shunt reactance is the ratio of the source or input resistance to δ. Both results are in Ω, but—as

noted earlier, the reactances are of opposite type.

Fig. 7-2

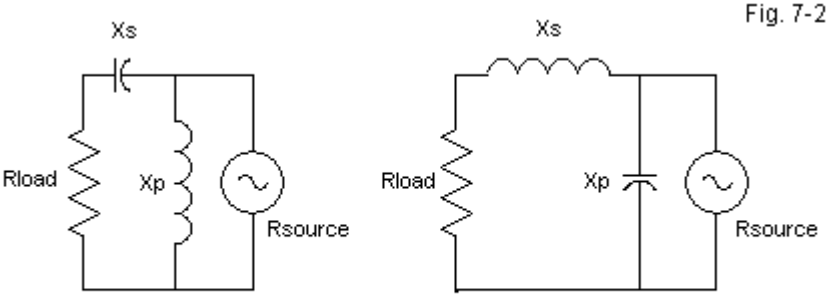

Alternative Equivalent L-Networks Where Rsource > Rload

Notice that nothing in the calculations specifies which reactance must be capacitive and which must be inductive. Beam builders tend to prefer lighter elements and therefore usually shorten the driven element. Hence, the series reactance becomes capacitive, requiring the shunt reactance to be inductive. However, in principle, we might as easily lengthen the driven element to yield an inductive reactance at the element feedpoint. Then, as shown in **Fig. 7-2**, we would need a shunt capacitive reactance. Although we shall not give the alternative beta match configuration much initial attention, before we conclude this chapter, we shall return to it in order to assess its strengths and weaknesses relative to the more usual form.

For the moment, we shall confine ourselves to the more conventional implementation of the L-network matching system, that is, the beta match. As well, we may also confine our attention to a 50-Ω value for Rin or the source resistance. Since the 50-Ω coaxial cable is the most common amateur-service feedline for beam antennas. Using the attached spreadsheet or simply a handy calculator, we may pre-figure the reactance components for various load value, given the single source resistance. **Table 7-1** provides a sample table, and you may embellish it to any degree you find convenient. However, even with only a few entries, the trends are clear enough to permit you to interpolate missing

values within normal construction variables.

Beta-Match Values for Rin = 50 Ohms					Table 7-1
Rload	35	25	15	10	5
Ratio Rin/Rload	1.43	2.00	3.33	5.00	10.00
Delta	0.65	1.00	1.53	2.00	3.00
Xload = Xs	22.91	25.00	22.91	20.00	15.00
Xp	76.38	50.00	32.73	25.00	16.67
Delta = working or network Q.					
Rload = antenna feedpoint resistance in Ohms.					
Rin = feedline characteristic impedance in Ohms.					
Xs = required feedpoint reactance in Ohms.					
Xp = beta component reactance in Ohms; in parallel across feedpoint.					
If Xs is positive, then Xp is negative; if Xs is negative, then Xp is positive.					

Note that as we lower the load resistance, the reactance of the shunt component also decreases. However, the series reactance reaches a peak when the ratio of Rin to Rout is 2.0, yielding a δ of 1.0. Hence, for any beta match to a 50-Ω cable, we never require more than 25 Ω of series reactance. If we use a series capacitive reactance, then the amount by which we must shorten the driven element of a beam has a very limited range.

With a series capacitive reactance, the shunt component is a form of inductive reactance. **Fig. 7-3** shows the most common forms of inductive reactance used in beta matches. From the center form, we derive the name "hairpin," since the shorted parallel transmission-line stub resembles that common device. In fact, many builders round the end short to increase the resemblance to a hairpin. The shorted coaxial stub on the right is exactly equivalent to the parallel hairpin. However, since the coaxial cable stub will have a lower characteristic impedance, it will be longer than the high impedance parallel line stub for any given reactance.

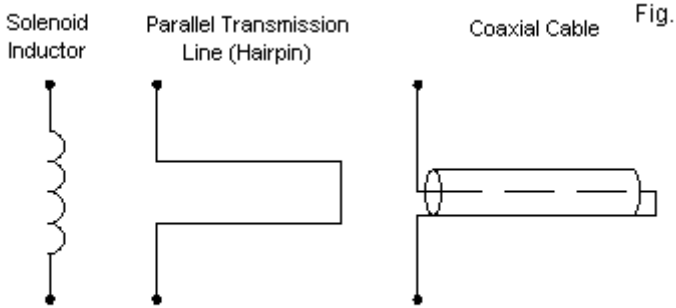

Fig. 7-3

Alternative Beta-Match Inductive Reactances

The calculation of the length of stub for a given inductive reactance requires only that we know the characteristic impedance of the transmission line from which we construct the device. The initial result will be in electrical degrees (or radians, depending on how we set our calculators). That value in degrees divided by 360 gives us the fraction of a wavelength occupied by the stub. If we know the length of a wave at the design frequency, we can translate the intermediate result into a physical length using whatever structural units are most convenient.

$$X_L = Z_O \tan\theta \qquad \theta = \arctan \frac{X_L}{Z_O}$$

If we happen to be using a series inductive reactance and require an open or capacitive stub, then we use different equations.

$$X_C = \frac{Z_O}{\tan\theta} = Z_O \cot\theta \qquad \theta = \arctan \frac{Z_O}{X_C}$$

Since the result is once more in electrical degrees, we go through the same process to arrive at a physical length for the stub.

The use of a solenoid inductor or coil as the beta shunt element involves a different calculation and some supplemental considerations. From the parallel

reactance, we may calculate the value of a coil or a capacitor by resorting to very basic equations.

$$L_{\mu H} = \frac{X_L}{2\pi F_{MHz}} \qquad C_{pF} = \frac{1000000}{2\pi F_{MHz} X_C}$$

The equations use the frequency as given in MHz. Hence, the results will be either in μH or in pF. We can use any convenient nomographs or calculation programs to develop the dimensions of a solenoid inductor. However, we must also consider the coil's Q (that is the unloaded or Q_U of the coil) in estimating matching circuit losses. Beta stubs generally have very low losses. However, most beta coils will be limit to values of Q at 300 or below. Hence, the beta coil may show slightly higher losses than a stub, but will slightly increase the operating bandwidth of the antenna.

For many years, rumors abounded that the beta match was for some unknown reason lossier than other matching circuits. Basic L-network theory should lay such beliefs to rest, since the δ of an L-network is as low or lower than for any other impedance matching network. We may define the loss factor this way:

$$\frac{\delta}{Q_u} = \frac{Power\ lost\ in\ network}{Power\ delived\ by\ network}$$

The efficiency of the network as a ratio of power supplied to power delivered is essentially the value of Q_U divided by the sum of Q_U and δ (multiplied by 100 to arrive at a percentage). If we do not try to match extremely low element impedances (say, below 10 Ω, relative to a 50-Ω line) and if a beta inductor has a Q of at least 200 Ω, then we may easily obtain 99% efficiency, less any additional losses created by physical connections between the shunt component and the element.

One reason that many antenna makers prefer shorted parallel line beta stubs is that the construction can use large diameter (between 1/8" and ¼") lines that form a single U-shaped assembly with only two connection points. Since the center of the shorting part of the U is electrically neutral, some builders connect the point to the boom, thereby grounding the driven element on both

sides with respect to static charges that might accumulate. When properly constructed, the ground does not affect the RF performance of the assembly.

Beta Samples

Let's examine a practical beta-matched 2-element driver-reflector Yagi, using our standard test frequency of 29 MHz with 3/8"-diameter aluminum elements. To establish a driver with capacitive reactance, we shall set the element length at 0.458-λ. The reflector is 0.502-λ and is 0.1-λ behind the driver. (See model 7-1.ez.) The initial model is identical to one that we used to create a Regier series match in the preceding chapter. Prior to adding any matching components, the free-space gain is 6.25 dBi with an 11.49-dB front-to-back ratio. The initial feedpoint impedance is 23.5 – j22.1 Ω. Even before we calculate the required reactive components for a beta match, interpolating from **Table 7-1** tells us that we have plausible starting values for matching the beam to a 50-Ω cable.

The standard calculations inform us that the transformation of a 23.5-Ω load to a 50-Ω source calls for a series reactance of -j24.96 Ω, in this case, capacitive. Our modeled value is about 10% off the mark. Rather than make changes at this point, we shall proceed as if the model's series capacitive reactance were correct and see what happens.

The standard calculations call for a parallel reactance of j47.1 Ω, in this case, inductive. We can model the reactance in two ways. The simplest technique is to use a shorted transmission-line stub created by NEC-s TL facility. EZNEC even allows us to use a physical length supplemented by a value for the velocity factor. Let's start with RG-8X as our transmission line. The cable is rated as 50 Ω with a VF of 0.78. These values, plus the required inductive reactance yield 0.0938-λ, which translates into about 3.18' at 29 MHz. (See model 7-2.ez.) Alternatively, we might use 450-Ω parallel line with a VF of 1.0. The alternate line requires a length of 0.166-λ or about 0.56' at 29 MHz. (See model 7-2a.ez.) Even if we adjust for the different velocity factors, the ratio of length values does not match the ratio of impedance values. However, note that the determination of line length is a tan (tangent) function on the ratio of

reactance to the line's characteristic impedance. Nevertheless, both models return a new feedpoint impedance of 44.2 + j0 Ω. The 50-Ω SWR at the resonant impedance is 1.13:1.

Creating a model with a solenoid inductor or coil as the beta component presents a special challenge within NEC software. If we simply add an inductance at the model's feedpoint segment, it will show up as a series reactance, which is not what we need. One way to install a parallel component is to create a small square that includes the feedpoint segment with 3 other wires. **Fig. 7-4** shows the general outline.

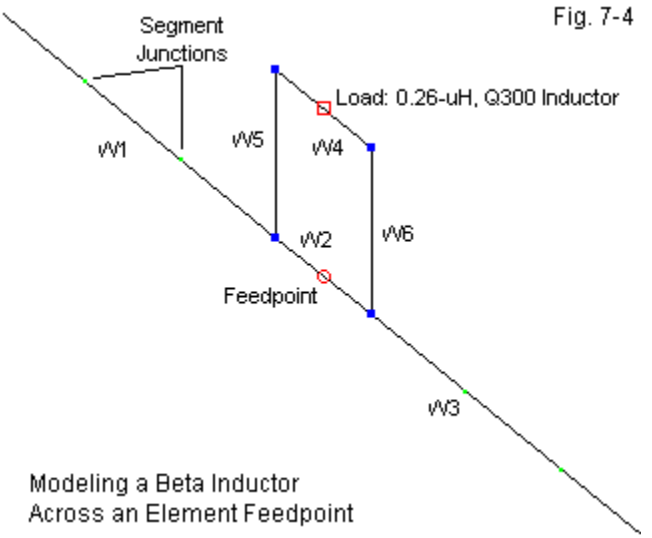

Modeling the wires requires considerable care. First, all wires must use the same diameter. With 3/8" diameter wires, we are limited in how short we can make the wires of the box. All of the models in this chapter use 101 segments per element as a preparation for just this model. This allows us to shrink the box to sides that are close to 2" long. Even though this construction minimizes any effects from the wires, the required structure will yield a slight modification of the

antenna's performance, but only at the level of numerical precision.

To the wire in the box that opposes the feedpoint, we add our inductor. Let's set the Q at 300 for this experiment. The required inductance for an inductive reactance of j47.1 Ω at 29 MHz is 0.26 μH. The reactance of this coil sets the series resistance at 0.158 Ω. (See model 7-3.ez.) With these values, we obtain 6.19 dBi free-space gain with a 11.5-dB front-to-back ratio. The new feedpoint impedance is 52.0 – j2.3 Ω. The 50-Ω SWR value, 1.06:1, gives us the impression that the inductor is providing a slightly better match than the shorted stubs. However, the impression is illusory and rests on two factors. First, the specification of the coil inductance is not as precise as the specification of the stub lengths. Hence, the rounded inductance value—about as precise as coil construction usually allows—yields a very small difference from the calculated inductive reactance value. Second, physical box structure adds a bit of complexity to the reactance situation. A real coil installation will have leads that approximate a box, but their diameter and length would be considerable smaller than the required box dimensions.

Essentially, the beta coil and the beta stub provide the same performance across the passband. At a Q of 300, the test coil does not reduce the efficiency or broaden the operating bandwidth to any noticeable degree. **Fig. 7-5** traces the feedpoint resistance and reactance for both types of beta matches from 28 to 30 MHz. This pass band is considerably wider than one would normally use with the subject antenna. In fact, the beam is likely to de designed for an 800 to 1000 kHz spread over 10 meters. The largest differences between the curves for each parameter between beta parallel components occur below 28.5 MHz. Within the center 1-MHz section of the frequency sweep, the curves coincide quite closely. Above the center section the graph lines nearly overlap. Below the center section, the coil shows higher peaks (or higher inductive values for the reactance curve). Very slight differences in component values will shift the curve peaks and may even reverse which method yields the higher low-frequency peak values. Thus, we may consider these patterns to be too similar to be called different.

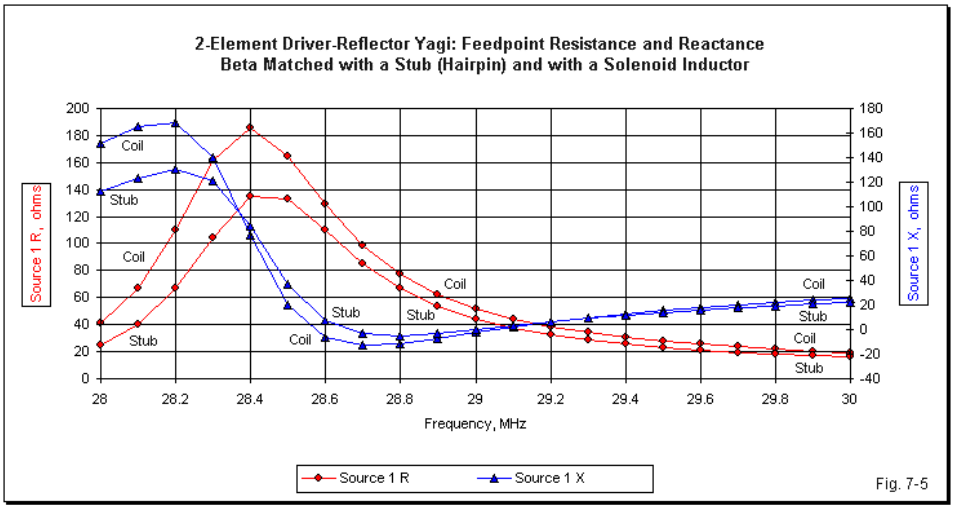

Fig. 7-5

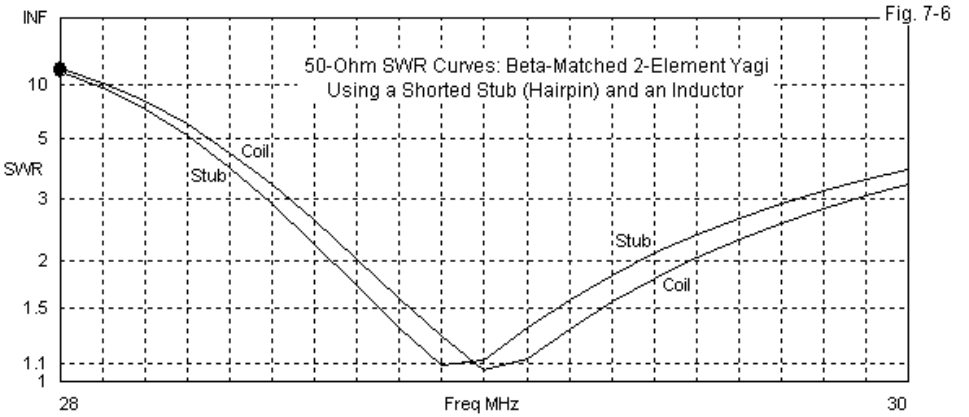

Fig. 7-6

The comparative 50-Ω SWR curves in **Fig. 7-6** tell a similar story. The slightly different design-frequency impedance values forewarned us that the two curves would be offset from each other by a small amount. The degree of offset

is about 100 kHz. Equally significant is the 2:1 SWR passband, which is nearly the same for both beta-matching methods. The coil exhibits a slightly greater passband width, but the amount would not be noticeable in practice, especially if we conduct SWR measurements from the far or rig end of the main 50-Ω feedline.

We noticed at the beginning of our work in designing a beta match for the test antenna model that the initial capacitive reactance was slightly low. If we wish to adjust the antenna system (that is, antenna elements plus matching network) for a perfect impedance at the design frequency, adjusting the element length is the best route to arriving at a refined resistance value. Changing the length of the beta stub has a more pronounced effect on the reactance than on the resistance. The equivalent process for a beta coil is squeezing or separating the turns of the coil slightly for the same change in design-frequency reactance.

Theoretically, we may set up a beam so that the driven element exhibits an inductive reactance. In that case, we would need a parallel beta component that shows capacitive reactance. To illustrate that this method works in principle, let's reformulate the initial beam prior to adding the matching system. We may retain the same element diameter (3/8"), element spacing (0.1-λ), and reflector length (0.502-λ). We need only change the driver length. In model 7-1, we used a length of 0.458-λ to obtain the necessary capacitive reactance for a beta coil or shorted stub. In the preceding chapter, the same model equipped with a 0.468-λ driver proved to be resonant. If we increase the driver length to 0.478-λ, the feedpoint impedance models at 26.1 + j22.6 Ω. In the process, we again change the reported performance figures slightly. The free-space gain is now 6.31 dBi, with an 11.13-dB front-to-back ratio. These changes would not be detectable in operation. (See model 7-4.ez.)

Calculations call for a series capacitive reactance of 25.0 Ω, slightly higher than the inherent 22.6 Ω shown by the driver. The required parallel capacitive reactance is -j52.2 Ω. We may create the parallel reactance using either a capacitor or an open stub. At 29 MHz, the capacitance is 105.2 pF. The required length of an open stub will vary with the characteristic impedance and the velocity factor of the transmission line that we use. A 50-Ω line such as RG-

8X with a velocity factor of 0.78 would need 0.0928-λ or about 3.22' at 29 MHz. (See model 7-5.ez.) If we use 450-Ω parallel line with a VF of 1.0, the required line length is 0.2316-λ or 7.86' at 29 MHz.

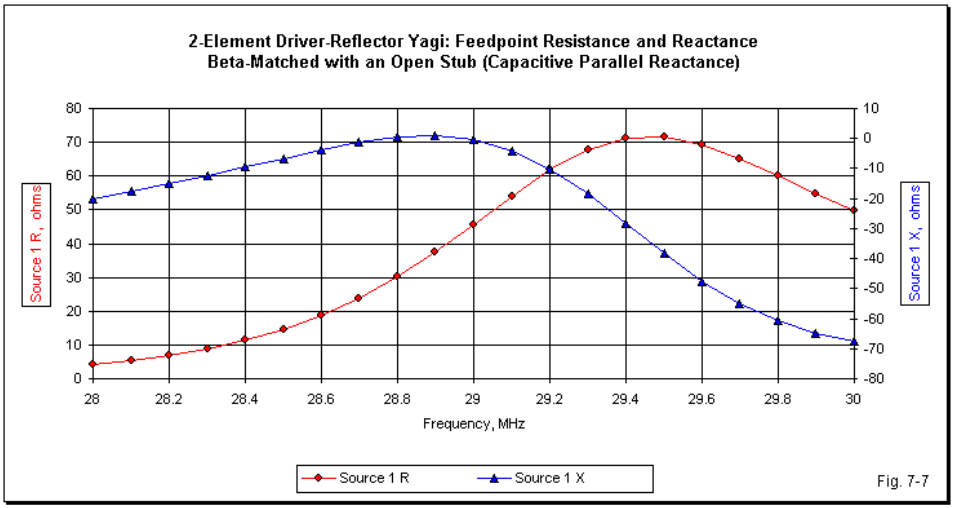

Fig. 7-7 shows the resistance and reactance curves from 28 to 30 MHz for the 50-Ω open stub. Compare these curves to the ones for a shorted stub with inductive reactance in **Fig. 7-5**. The reactance curves for the two cases are roughly similar in shape, but the values for the open stub are almost exclusively capacitively reactive. (The values for the shorted stub were almost wholly inductively reactive.) The resistance trends for the open stub reverse the trends shown by the shorted stub. The open stub shows a rising resistance with increasing frequency.

Despite the seeming differences in the patterns of resistance and reactance with change in frequency, the resulting 50-Ω SWR curves are almost identical, as shown in **Fig. 7-8**. Because the antenna-element reactance values are slightly shy of perfect, the curves for shorted and for open stubs are offset from the design frequencies in opposite frequency directions. Yet, the operating

passband—limited here by a 2:1 50-Ω SWR—is the same for both types of beta matches. In short, fundamental performance considerations do not give one type of beta match priority over the other.

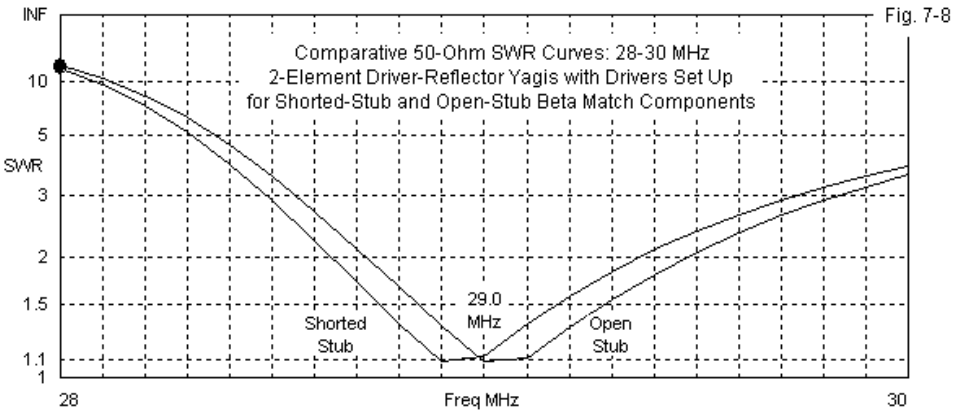

There are a number of considerations that tend to favor the shortened element with an inductively reactive parallel component. First, let's compare open stubs with shorted stubs for size. With a 50-Ω line, we have little to choose between if we are matching 25-Ω element impedances to a 50-Ω main feedline. In our samples, the shorted stub was about 3.18' long, while the open-stub line was 3.22' long. However, when we used a 450-Ω stub, the required length for the shorted version shrank to 0.56'. In contrast, the open-stub grew to 7.86'. Note the reverse relationship of reactance to the line characteristic impedance in the equations governing shorted and open transmission line stubs. In addition, open stubs offer no electrical neutral point that we may attach to a boom for static discharge.

In most cases, we also find limits to the use of capacitors. Variable capacitors do not weather well in antenna applications. As well, we must find a capacitor (or a combination that will together make up the required value) with construction that is able to handle both the voltages and the currents that will

occur in an antenna application. Wherever we can overcome these limitations, a capacitive parallel component in an L-network will provide essentially the same performance as an antenna element and L-network set up for a parallel inductive component.

Although the beta match requires that the source impedance be higher than the load impedance, a 50-Ω source impedance is not a requirement for their use. Rather, it is simply the most common use for them. In Volume 1, where we examine phased arrays, we saw multiple uses of beta matches in a single array. Chapter 7 gave attention to the N7CL 2-element phased array, the outline for which appears in **Fig. 7-9**.

Fig. 7-9

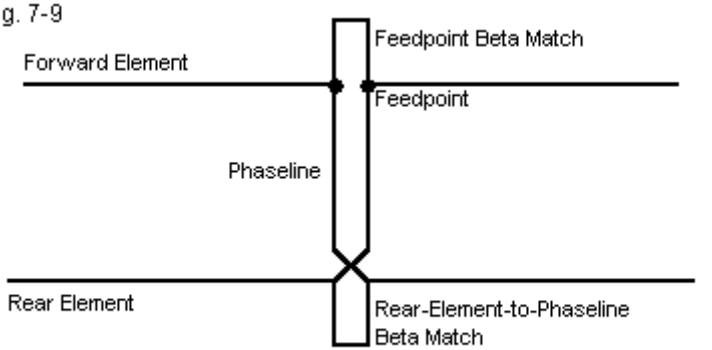

Beta Matches in the N7CL Phased Array

One use for a beta match appears at the feedpoint for the entire array to raise the impedance to the 50-Ω level. However, N7CL also used a beta match with the rear element in order to transform its impedance upward to a level that optimized the current magnitude and phase angle at the far end of a phaseline extending from the fed forward element. In both cases, the designer used 50-Ω transmission line and tucked the beta-match shorted stubs inside the element support boom.

Despite its initial odd appearance, the beta match is a sound means to effect

a match between the lower impedance of the average beam driven element and the higher impedance of the usual main feedlines used with beam antennas. In some ways, it provides an electrically simpler and mechanically sounder installation than almost any other matching system. As well, it is no less efficient than other matching schemes when freshly installed, and it may turn out to be more efficient as weather takes its toll on the multiple connections required by some other matching systems.

Like the series match system—in any version—the beta match requires that the driven element be electrically insulated and isolated from the support boom. In fact, there is only one common beam matching system that allows a direct connection between the boom and the driven element. We shall make our last beam-matching stop in gamma country.

8. Gamma Matching Systems

In Chapters 6 and 7, we examined various forms of series matching systems and the beta match. These two types of matching systems represent alternatives to the gamma match, especially when the task is to transform the generally low impedance of a Yagi array up to the value of 50 Ω, as required by the most common feedlines used in amateur and other services.

Compared to a gamma match, series and beta matching systems are both simple and precise. Both systems make no alteration to the driven element, but add networks composed of transmission lines (usually) to the element feedpoint. The beta match does require that we initially set the driven element length to arrive at an optimal value of reactance relative to the feedpoint resistance, but the beta component is or is equivalent to adding a simple reactance across the feedpoint. The matching systems do not affect the radiation properties of the element.

As a consequence of these conditions, we may calculate the required values for series-matching or beta-matching components very precisely. In practice, the key factor affecting field adjustment of the systems is the accuracy of the velocity factor that we use in the calculations relative to the value that actually applies to the line used. If we know the velocity factor with measured accuracy (in contrast to the values we find in lists and specification sheets), we can often obtain the desired result with no need for further adjustment.

These fundamental matching systems are therefore amenable to automated formulation, that is, a utility program or a spreadsheet page that will tell us the required values if we input the feedpoint conditions and other values related to the components. The attached spreadsheet contains calculations for 1/4-λ matching sections, Bramham transformations, and Regier series matching calculations. In addition, it allows beta-match calculations and returns results for using either a shorted transmission-line stub or a solenoid inductor as the most common beta components. However, it also yields open lines and capacitance

values should one choose to lengthen the driven element rather than shortening it. I wrote the pages in Quattro Pro (.qpw), but have also saved them in Excel (.xls).

The Gamma Difference

The gamma match differs fundamentally from the other matching systems because it alters the physical properties of the driven element in ways indicated by **Fig. 8-1**. First, it adds new wires to the element, giving the element a more complex shape. Second, it changes the element feedpoint relative to the original element. The simple element uses a feedpoint position that normally is at the center of the element. The gamma-matched element places the feedpoint on a wire that joins the gamma rod to the main element.

Fig. 8-1

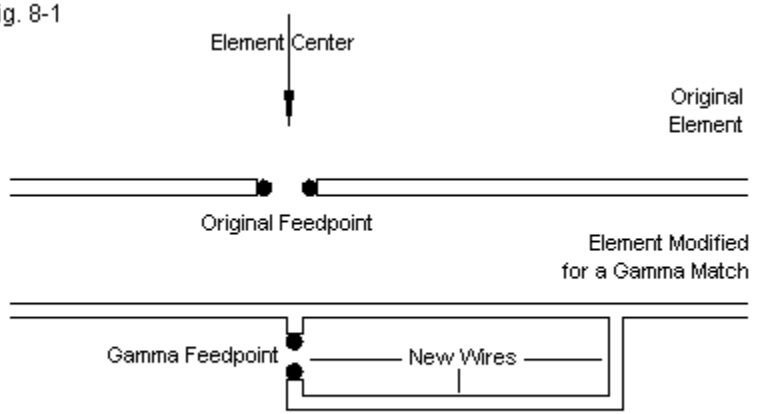

Why the Gamma Match Requires Special Attention

One gamma-match advantage to many builders is the fact that the element may now connect directly to the boom. Both series and beta matching systems require driven elements that are insulated and isolated from any conductive support boom. In the era in which so-called "plumber's delight" construction

methods ruled amateur Yagi construction, the gamma match equally ruled impedance transformation for coaxial feedlines. However, connecting the element to the boom changes its electrical length and therefore the feedpoint impedance prior to effective a gamma match. Therefore, most gamma match users began their calculations or experiments with only an estimated feedpoint impedance for the pre-matched element. NEC and MININEC antenna-modeling software offered no assistance here, since these programs only model axial currents (that is, along the element) and thus could not account directly for boom effects. Some builders have come to believe that a gamma match requires a direct connection between the boom and the element center. However, the connection is only an option, not a mandatory condition for the matching system.

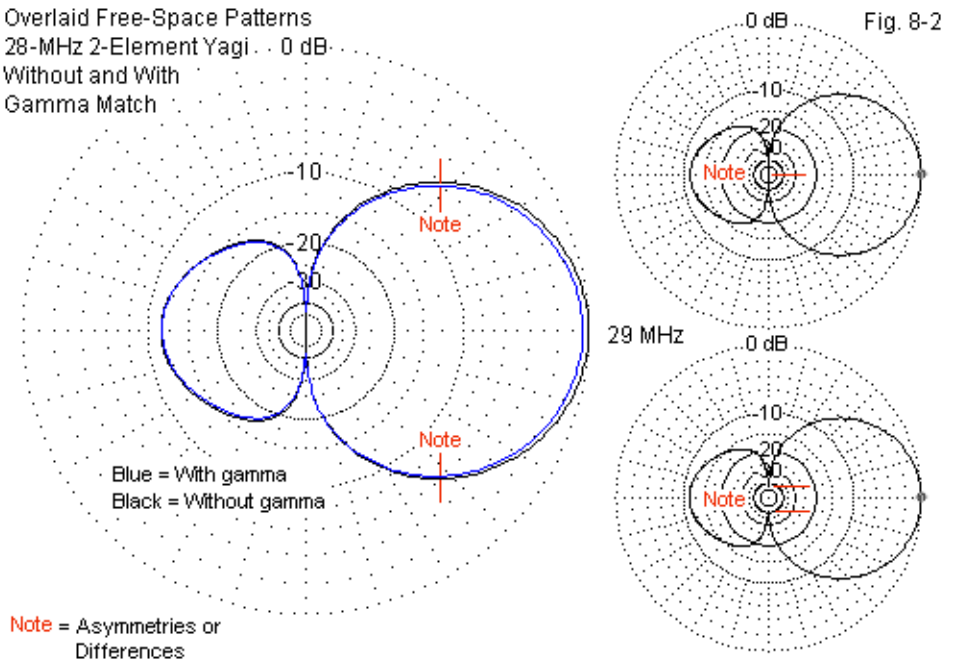

One criticism of the gamma match accuses it of displacing the pattern in the

direction of the match due to the size of the assembly. Effectively, as some believe, the assembly increases the diameter of the gamma side of the element, and this asymmetry of the driven element results in the main lobe's re-aiming. To test this notion, I constructed models of 28-MHz beams with identical reflectors and element spacing. One beam uses a simple driven element. The other uses a driver with the same overall length, but with a gamma match assembly (of course, with no boom). The gamma assembly is in the plane of the two elements and projects forward of the driver. The results of the test appear in **Fig. 8-2**.

The slightly lower forward gain of the gamma-matched version of the beam is an artifact of certain limitations of NEC (which we shall review shortly). The key factor in the overlaid patterns is the degree of lobe displacement, indicated by the lines that I added to the sides of the lobe. Displacement does indeed occur, but at a level too small for any user ever to notice in operation. The two patterns to the right show that the gamma match also has an effect on the free-space side nulls for the array. The simple beam has side nulls that show no limit. However, the gamma-matched beam has limited side nulls that are a mere 40-dB down from the level of maximum gain. I am unaware of any operational use of a beam in which one might be able to detect the difference.

The modeled test case assumes by its mathematical basis relatively perfect construction of the gamma-match driven element. I have in past years seen range-generated patterns for gamma-matched beams with a significant displacement of the main forward lobe. It would not be possible to perform a full analysis of such patterns without being able to model currents within the driven element and along the boom--if the elements makes a direct connection to the boom. However, in principle and assuming careful construction, pattern displacement is not a hindrance to the use of a gamma match.

Calculating the Gamma Match

H. H. Washburn, W3MTE, introduced the amateur community to the gamma match in his September, 1949, *QST* article, "The Gamma Match" (pp. 20-21, 102). D. J. Healey, W3PG, provided the first mathematical analysis of the

match in "An Examination of the Gamma Match," *QST*, April, 1969 (pp.11-15, 57). Healy's treatment, however, required the use of nomographs and a Smith chart.

Since these seminal articles, several alternative analyses have appeared in amateur journals. H. F. Tolles, W7ITB, presented a purely mathematical analysis in "How to Design Gamma Matching Networks" in *Ham Radio* for May, 1973 (pp. 46-55). Because the Tolles equations proved tedious to many gamma designers, R. A. Nelson, WB0IKN, set them into a Basic program in "Basic Gamma Matching," *Ham Radio*, January, 1985 (pp. 29-33). ARRL converted Nelson's Apple-Basic program into a version suitable for IBM computers, and a listing appears in *The ARRL Antenna Book*, 16th Ed. (p. 26-20). In 2000, Dave Leeson, W6NL, corrected portions of the program so that it is perhaps the most accurate of the available means to calculate gamma matches. This program is also available within the HamCalc collection of Basic utilities edited by George Murphy, VE3ERP. **Fig. 8-3a** and **Fig. 8-3b** show the GW Basic listing for the version of the program distributed by ARRL.

Since the work of Tolles and Nelson, two alternative mathematical analyses have appeared. Ron Barker, G4JNH, presented "A New Look at the Gamma Match" in *QEX*, May/June, 1999 (pp. 23-31). Barker changes some of the fundamental assumptions about the key factors in a gamma match to arrive at his results. Unfortunately, his work is less amenable to easy placement in a Basic utility or a spreadsheet, since the calculations require the solution to simultaneous equations. In contrast, Roger Wheeler, G3MGW, returned to the Healey analysis and converted the graphical techniques back into mathematical methods that allow a straightforward spreadsheet set of calculations. His work appeared first in *RadCom* and later in *antenneX* (October and November, 2006).

Both of these later analyses rely on something that was unavailable to earlier gamma calculations. In most cases, the determination of the initial or pre-match driver feedpoint impedance rested on assumption, guesswork, or rudimentary measurement. Measurement became difficult if the builder connected the driver to the boom and did not allow for a feedpoint gap, even if it would later be closed. Both Barker and Wheeler require the use of antenna

modeling software to determine the pre-match driver impedance. Other methods exist, for example, the Brian Beezley, K6STI, module in the overall program YO. However, Beazley has never published his procedures.

Fig. 8-3a

Program Listing for GAMMA.BAS

```
10 CLS
12 REM Removed corrections RA/2 and XA/2 per W6NL, Apr 1, 2000
15 REM Corrected error in wavelength conversion, Mar 1997
20 PRINT "           Gamma Match Design"
25 PRINT
30 PRINT "    Using W7ITB, WB0IKN, W6NL Equations"
35 PRINT "         Version 2.0, April 2000"
40 PRINT
45 PRINT
50 DEF FNCSH (X) = LOG(X + SQR(X * X - 1))
60 PI = 3.14159
120 INPUT "Frequency, MHz"; F
130 INPUT "Feed point resistance, ohms"; RA
140 INPUT "Feed point reactance, ohms"; XA
170 INPUT "Feed line impedance, ohms"; RO
180 PRINT : INPUT "Driven element diameter, inches"; DE
190 INPUT "Gamma rod diameter, inches"; DR
200 INPUT "Gamma rod spacing, inches"; S
210 HZ = (1 + ((FNCSH((4 * S * S - DE * DE + DR * DR) / (4 * S * DR))) /
      (FNCSH((4 * S * S + DE * DE - DR * DR) / (4 * S * DE))))) ^ 2
220 ZO = 60 * FNCSH((4 * S * S - DE * DE - DR * DR) / (2 * DE * DR))
230 T = HZ / ZO
240 A = ((RO * XA) / (HZ * RA - RO))
250 B = (RO * (RA ^ 2 + XA ^ 2)) / (HZ * RA - RO)
260 Q = A + SQR(A * A + B)
270 XS = HZ * ((RO * XA + SQR((RO * XA) ^ 2 + RO * (HZ * RA - RO) *
      (RA ^ 2 + XA ^ 2))) / (HZ * RA - RO))
280 LDRA = ATN(Q * T)
290 LDR = LDRA * 180 / PI
300 E = (RO / RA) * ((RA ^ 2 + XA ^ 2) / Q)
310 G = (RO / RA) * XA
320 CR = 1000000! / (2 * PI * (E + G) * F)
```

Program Listing for GAMMA.BAS (continued) Fig. 8-3b

```
330 CLS
360 PRINT
380 PRINT
390 PRINT "Frequency, MHz: "; F
400 PRINT "Driven element diam: "; DE
410 PRINT "Gamma rod diam: "; DR
420 PRINT "Gamma rod spacing: "; S
430 PRINT "Feed point resistance: "; RA
440 PRINT "Feed point reactance: "; XA
450 PRINT "Feed line impedance: "; RO
460 PRINT
470 PRINT "Gamma length (degrees): "; LDR
480 FT = (984 / F) * (LDR / 360): PRINT "Gamma length (feet): "; FT
490 IN = FT * 12: PRINT "Gamma length (inches): "; IN
'print "HZ = ";HZ;
'print "  ZO = ";ZO
500 PRINT "Gamma capacitor (pF): "; CR
510 PRINT : INPUT "Do another (Y/N)"; T$
520 IF T$ = "y" OR T$ = "Y" THEN GOTO 10 ELSE SYSTEM
```

Note: lines 210 and 270 are folded for this presentation. Convert lines to a single continuous line in each case before attempting to use the program.

The attached spreadsheet (in Quattro-Pro and Excel formats) contains pages for the Healey-Wheeler (HW) and the Tolles-Nelson-Leeson (TNL) methods of calculating gamma match rods and series capacitors. Every gamma-match calculating system tries to yield a physical value for the length of the gamma rod and a series capacitance value at the feedpoint to leave a pure resistive impedance. The required inputs appear in **Fig. 8-4**. We need to know the diameters of the main element in the region of the gamma assembly and of the proposed gamma rod, tube, or wire. As well, we must input the center-to-center spacing between the main element and the gamma rod. Ordinarily, the physical dimensions for the inputs and the outputs are in the same units of measure. Like the Basic program shown in **Fig. 8-3**, the spreadsheets use inches.

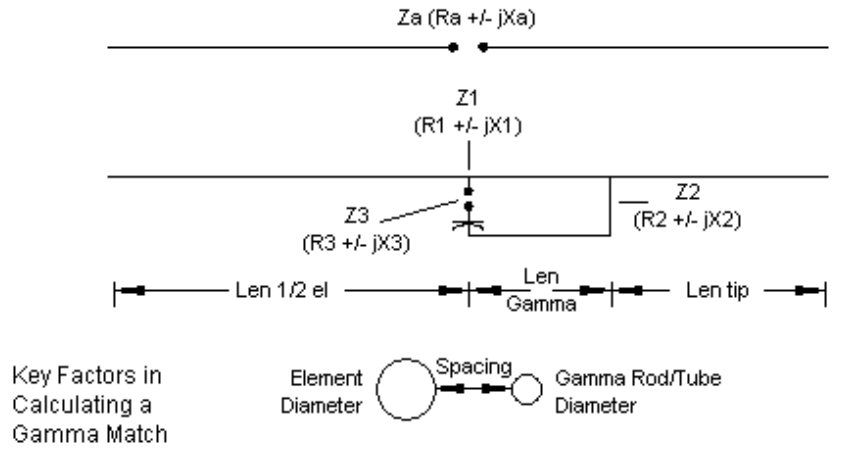

Fig. 8-4

In addition, we require two impedance values. One value is for the simple driven element, designated Ra and jXa in **Fig. 8-4**. We also need to specify a desired feedpoint impedance, Rf, which is the target resistive impedance that matches the main feedline. For our samples, we shall use 50 Ω, since it is the most common value that we encounter in amateur radio applications. However, we may apply the gamma match for virtually any reasonable line impedance.

Fig. 8-4 also shows some of the points in the gamma assembly that exhibit derived impedances calculated somewhere within the system. Z1 is the transformed impedance based on the fact that the gamma assembly forms a shorted transmission line stub. (One misguided criticism of the Healey system was that it treats the gamma assembly as a folded dipole. Every folded dipole exhibits both radiation and transmission-line currents. In the calculation of the gamma line, we are concerned with the transmission-line performance of the assembly.) We can derive the characteristic impedance (Zo) of the stub using conventional equations that involve only the physical dimensions of the line. S is the center-to-center line spacing, and d1 and d2 are the diameters of the gamma rod and the main element, respectively.

$$Z_0 = 276 \log\left(\frac{2S}{\sqrt{d_1 d_2}}\right)$$

The TNL system uses more fundamental equations involving havercosines. However, in the typical range of Zo (perhaps 200 to 600 Ω), the differential in results between equations is less than 1% and normally only about 0.1%.

While we are using only the physical dimensions that we input to the calculation system, we can also calculate a step-up ratio between the original simple-driver impedance and the value shown as Z1 in **Fig. 8-4**. The most usually form of the equation again employs the three input physical values, S, d1, and d2.

$$r = \left(1 + \frac{\log\left(\frac{2S}{d_1}\right)}{\log\left(\frac{2S}{d_2}\right)}\right)^2$$

Once more, the TNL system uses more fundamental equations, but the differential in result, compared to the more usual engineering formulation is well under 1%. Both the HW and TNL systems use this equation to calculate the value of Z1 (R1 +/- jX1) simply by multiplying Ra and jXa by the value of r. If the diameters of the main element and the gamma rod are the same, then r = 4. If the gamma rod is thinner than the main element, then r > 4. If the gamma rod is thicker than the main element (an unusual but possible situation), then r < 4 but r > 1.

We may add two side notes here. First, the Barker calculation system does not use the step-up ratio derived from the usual equation. Barker uses the impedance ratio between a simple driver element in isolation (essentially a dipole) to the impedance of the simple driver in service within the beam antenna. Second, at least the HW system does not account for the fact that the impedance undergoes not only a step-up in value, but also a shift in phase angle

when we move from the driver without the gamma assembly to the driver with the assembly. If we model a gamma system and place the feedpoint at the position it would occupy on the pre-gamma driver element, we can observe the phase-angle shift in the impedance.

The HW system calculates the value of Z2, the impedance presumed to exist at the far end of the gamma assembly. If we assume that the current distribution is sinusoidal--which is close to correct but not precise--then we may use a standard equation to determine the values of R2 and X2.

$$R2 = \frac{R1}{\cos^2\theta} \qquad jX2 = \frac{jX2}{\cos^2\theta}$$

Theta is the electrical length of a gamma assembly either in degrees or in radians at the design frequency. Since we cannot determine the value of theta without a physical gamma rod, the HW system calls for a trial length. In concert with the remaining calculations, we simply adjust the trial length until the value of Rf becomes 50 Ω, if that is the target feedpoint impedance.

The TNL system operates differently. By addressing the required impedance and phase angle at the feedpoint, it calculates the required rod length using the factors already derived plus some ratios that appear in the listing in **Fig. 8-3**. The original Tolles article in *Ham Radio* provides the source of these ratios as they are applicable to the calculations. The Barker system uses neither of these methods, but creates an assumption of what must be the relative impedance at the gamma junction with the main element. He then calculates actual values from the initial driver impedance in a set of simultaneous equations.

The HW system derives the feedpoint impedance from two values in parallel. One value is the impedance of the gamma assembly as a shorted transmission-line stub having the length, theta, and the characteristic impedance Zo.

$$jXg = jZ_o \tan\theta$$

The other values are Z2 as transformed by the same length of transmission

line back to the new feedpoint. Wheeler follows Healey in using the following equation for this part of the impedance combination.

$$Z_3 = \left(\frac{Z_2 + jZ_O \tan\theta}{1 + \frac{jZ_2}{Z_O} \tan\theta} \right)$$

To resolve the equation, of course, one must break it into real and imaginary parts and then recombine them to arrive at the final value of Z3. (The TNL system essentially reverses the procedures and calculates the rod length from the required transformation.) We combine the parallel combination to arrive at an impedance that is the desired Rf in series with a value of Xf that is inductive. From this inductive reactance and the design frequency, we may determine the required series capacitance to leave us with a purely resistive feedpoint impedance.

I have tracked some of the rudimentary elements of gamma calculating systems to show what sort of thinking goes into them. However, the treatment is in no way complete, nor does it touch a number of the dimensions of the TNL and Barker systems. Instead, it is simply complete enough to allow one to track through the attached spreadsheet formulations of the HW and the TNL systems, in case one wishes to calculate a few typical gamma assemblies.

Testing the Gamma-Calculating Systems

Virtually all published gamma-calculating systems use one or two examples of the system's application and then declare the system adequate. Wheeler applied his formulation to gamma assemblies on quad loops. Tolles preferred VHF Yagis using gamma rods considerably thinner than the main element. Barker uses a single 20-meter beam as his test case. Of course, trying to develop a systematic set of test cases would be nearly impossible if we were restricted to constructing physical antennas having an interesting range of feedpoint impedance values for transformation.

It is possible to construct a series of antenna models to serve as a surrogate for the physical antennas. However, we cannot do the job in NEC-2 or even NEC-4. As suggested in **Fig. 8-5**, the gamma assembly presents NEC with two problems. First, unless the gamma and main elements are the same diameter, we encounter angular junctions of wires with dissimilar diameters. Although NEC-4 improves on the performance of NEC-2 under these circumstances, the results are insufficiently accurate for use as a comparator to the calculated values. In addition, gamma spacing is rather narrow for most beams that use relatively fat element diameters. Under these conditions, NEC tends to yield less than precise results. The relative unreliability appears in the average gain test (AGT) scores, which generally are no better than 0.92 when a perfect score would be 1.00. Since arriving at a feedpoint impedance of 50 Ω is critical to the comparisons, AGT values in the range of 0.92 are too far from ideal to be useful. Values of 0.98 to about 1.02 are more valuable to the task of comparison.

Fig. 8-5

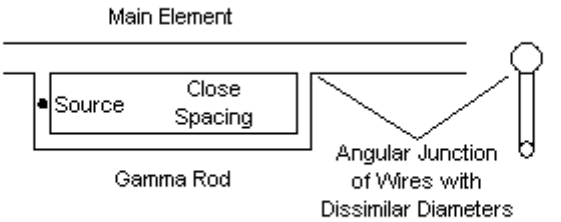

Why a NEC (-2 or -4) Model is Inadequate

Fortunately, MININEC is not sensitive to angular junctions of wires with differing diameters. However, in its raw form, it is subject to limitations related to close wire spacing and to angular junctions in general. One version of MININEC, Antenna Model, has introduced correctives that make it suitable for some first-order comparisons with the calculation systems. Note that I do not call the models "standards" against which we test the calculation systems. At best, the models are comparators so that we may observe some general trends as well as similarities and differences in outcomes.

Fig. 8-6 shows the general set-up for the modeling process. Although unnecessary for the pre-match model, I have assigned to each element the same number of segments used in the gamma model. The number of segments for each element derives from the test values of gamma spacing. All test models will use 28 MHz as the design frequency. The gamma spacing will use 4" as a center value and require 2 segments in the feedpoint wire to place the feedpoint at that wire's center. Hence, a 2" segment length becomes the standard. For some tests, we shall use gamma spacing values of 2" and 6", but the segment length differential will not prove too detrimental to the AGT scores. In fact, in the accumulated data, I shall show not only the modeled gamma rod length and the indicated series capacitor, but as well the AGT score to permit you to reach your own conclusion about the model's reliability.

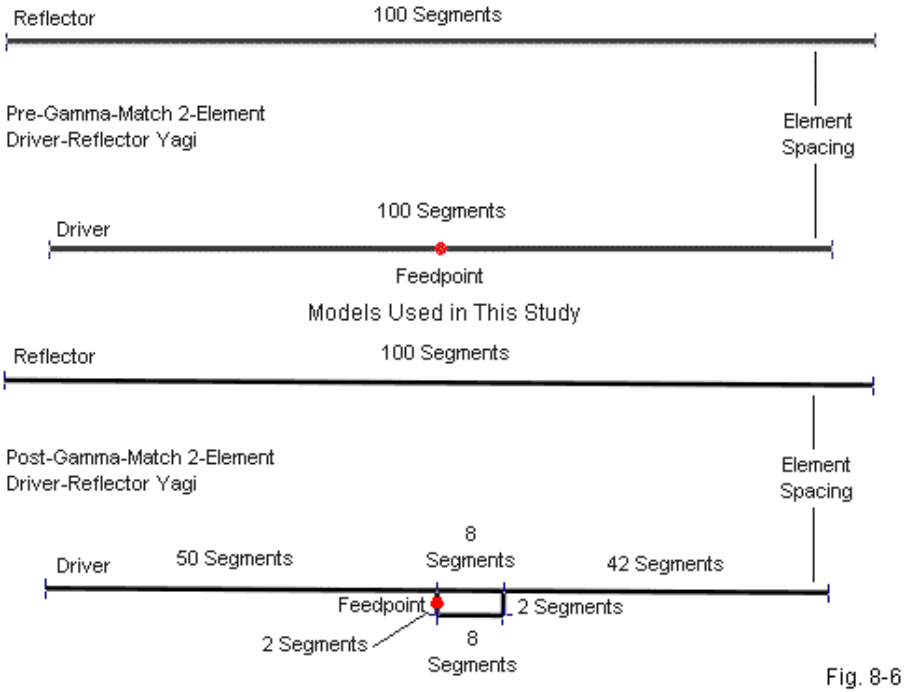

Fig. 8-6

From the very start, we recognize some important differences between the models and the calculation systems. Foremost among the differences is the fact that the models contain actual physical structures for the gamma far end shorting bar and for the feedpoint connecting assembly. In all models, I shall use end wires that have the same diameter as the main element, since in gamma assemblies applied to Yagis, the shorting bar and the coax connector plate tend to be substantial. Neither the HW not the TNL calculation system includes any allowance for such structures. Barker does add some fudge factors to his system, and the HW spreadsheet page includes an optional fudge-factor section at the end. The reason for the fudge factors is that calculations tend to call for capacitance values that are too high, and the models will reflect this fact by requiring lower capacitance values than the calculations indicate.

Test 1: A Simple Scaling Project

As an initial test, let's compare 3 perfectly scaled antennas with gamma matches. The test frequencies are 7, 14, and 28 MHz. For each frequency, I created a basic 2-element driver-reflector Yagi with a feedpoint impedance of 29.84 - j25.73 Ω (typical of 0.12-λ element spacing). To ensure perfect scaling, the elements are lossless. (The calculation systems do not take material losses into account, and given the small size and generally large element surface areas used in beams, the losses would indeed by small.) The 10-meter antenna uses a 0.5" main element diameter, with a 0.375" gamma rod. The element-to-rod spacing is 4". All of these dimensions also scale upward as we lower the test frequency. Therefore, the 7-MHz version of the antenna uses a 2" main element, a 1.5" gamma rod, and 16" spacing. Even though the 40-meter dimensions may be somewhat larger than realistic, they will serve well in this test. The top section of **Table 8-1** provides a more detailed run-down of the beam dimensions.

The lower portion of the table shows the calculated length of the gamma rod and the calculated series capacitance using the Healey-Wheeler and the Tolles-Nelson-Leeson system. It also shows the modeled values in the AM MININEC program. Because all dimensions are perfectly proportional, the calculated values of the gamma-line characteristic impedance, Zo, and the step-up-ratio, r,

are the same for all three antennas. A review of the basic equations shown earlier will confirm this result.

As a consequence, we find that the two calculation systems also produce scaled values for both the gamma rod length and the required series capacitance. Likewise, the modeled gamma rod and series capacitance also internally scale within the limits that I set for modeling precision. I adjusted the rod length and the series capacitance until the feedpoint impedance reached 50 Ω resistive, +/-0.1-Ω, and j0 Ω reactive, +/-j0.1 Ω.

Scaled Beams and Gamma-Match Assemblies								Table 1
Freq MHz	Dr. Len	Ref Len	El Space	El Dia	Rod Dia	G-Space	Pre-R	Pre-jX
7	762.802	847.444	202.335	2	1.5	16	29.84	-25.73
14	381.400	423.722	101.167	1	0.75	8	29.84	-25.73
28	190.700	211.862	50.584	0.5	0.375	4	29.84	-25.73

Gamma Length and Series-C Results for a 50-Ohm Match							
	Healey-Wheeler		Tolles-Nelson-Leeson			Antenna Model	
Freq MHz	Length	Cap pF	Length	Cap pF		Length	Cap pF
7	62.08	335.59	62.82	239.57		74.37	153.50
14	31.04	167.79	31.41	119.78		37.18	76.70
28	15.52	83.90	15.71	59.89		18.58	38.50
	Zo	r	Zo	r			
	349.58	4.43	349.60	4.42			
Notes:	All calculations and models assume lossless conductors and a free-space environment.						
	All lengths are in inches.						
	Pre-R and Pre-jX = modeled feedpoint impedance of the beam before matching.						
	Zo = Characteristic impedance of gamma line						
	r = impedance step-up ratio						
	Zo and r apply at all 3 test frequencies.						

For this test case, the two calculating systems yield quite similar values for the gamma rod length. However, both values are 16-17% shy of the modeled value. One reason that I selected this initial test case was the fact that the calculation systems yield values smaller than the model. Theoretically, if we simply assume that the calculation system does not take the shorting bar into account, we would expect the calculated lengths to be slightly long. Hence, the

systems and the model must have other differences.

As we expected from general gamma-match experience, both calculation systems over-estimate the required amount of series capacitance needed to bring the feedpoint impedance to a resistive 50-Ω value. In this early test, we may also note that the two systems yield very different series capacitance values. Therefore, a single method of adding fudge factors into the determination of the final series capacitance value will not work for both systems.

However, I have to insert a reminder here. The modeled gamma match is only a comparator in this test (and in those yet to appear). It is not a standard against which to measure the adequacy of the two calculating systems. With the exception of the gamma-rod length, the 3 systems of determining the required gamma-rod length and the series capacitance merely yield different results.

Test 2: Changing the Ratios among Element Diameter, Rod Diameter, and Spacing

For a second test, let's modify the initial beam so that it is very close to resonant, with a feedpoint impedance of 32.07 - j0.05 Ω. For this test, we may use a 28-MHz beam. Like the beam in the first test, the element spacing is 0.12-λ, so the only change is to the driver length. The main element diameters are 0.5". Once more, we shall explore the HW and TNL calculating system results and compare them with AM MININEC modeling results.

This test will be somewhat more complex. We shall explore 3 element-to-rod spacing values: 2", 4", and 6". As well, we shall look at gamma-rod diameters from 0.125" to 0.625" in 1/8" increments. A gamma rod that is fatter than the main element is unusual in reality, but certainly possible. Because we are changing both the diameter ratio between linear parts of the gamma assembly and the spacing between those parts, the values of both Zo and r will change with each sample case. The value of Zo will range from about 233 Ω (for the 0.625" rod at a 2" spacing) to nearly 465 Ω (for the 0.125" rod with a 6" spacing). The versions using 2" spacing will show the widest range of step-up

ratio (r) values, running from about 3.6 for the fattest rod to 7.1 for the thinnest.

Test Series at 28 MHz: Changing Gamma Spacing and Gamma Rod Diameter for a 50-Ohm Match												Table 2
Dimensions		Dr. Len	Ref Len	El Space	El Dia	Pre-R	Pre-jX					
Resonant		195.64	211.862	50.584	0.5	32.07	-0.05					
Gamma Match		Healey-Wheeler		Tolles-Nelson-Leesor		Antenna Model			Length Differences		Cap. Differences	
Spacing	Rod Dia	Length	Cap pF	Length	Cap pF	Length	Cap pF	AGT	AM-HW	AM-TNL	AM-HW	AM-TNL
2	0.125	27.15	51.67	23.38	60.44	20.50	55.00	0.9836	-6.65	-2.88	3.33	-5.44
	0.25	30.41	56.94	24.10	72.24	20.52	62.90	0.9843	-9.89	-3.58	5.96	-9.34
	0.375	33.10	59.82	25.35	81.94	20.52	68.60	0.9854	-12.58	-4.83	8.78	-13.34
	0.5	35.41	61.72	26.31	90.86	20.51	73.40	0.9871	-14.90	-5.80	11.68	-17.46
	0.625	37.42	63.12	27.31	99.52	20.49	77.60	0.9892	-16.93	-6.82	14.48	-21.92
4	0.125	25.45	50.65	18.17	65.59	15.49	54.40	0.9996	-9.96	-2.68	3.75	-11.19
	0.25	29.12	52.19	18.89	75.89	15.45	59.90	0.9998	-13.67	-3.44	7.71	-15.99
	0.375	31.84	52.58	19.49	83.38	15.45	63.70	1.0000	-16.39	-4.04	11.12	-19.68
	0.5	34.01	52.67	20.06	90.86	15.45	66.60	1.0003	-18.56	-4.61	13.93	-24.26
	0.625	35.80	52.67	20.60	97.32	15.45	69.00	1.0007	-20.35	-5.15	16.33	-28.32
6	0.125	24.93	48.98	16.08	67.88	13.43	51.70	0.9968	-11.50	-2.65	2.72	-16.18
	0.25	28.73	49.04	16.68	77.45	13.43	56.00	0.9969	-15.30	-3.25	6.96	-21.45
	0.375	31.40	48.65	17.17	84.68	13.43	58.80	0.9972	-17.97	-3.74	10.15	-25.88
	0.5	33.47	48.25	17.61	90.86	13.43	60.90	0.9974	-20.04	-4.18	12.65	-29.96
	0.625	35.13	47.95	18.02	96.46	13.43	62.70	0.9976	-21.70	-4.59	14.75	-33.76
Miscellaneous Derived Data												
Length change as rod diameter increases from 0.125" to 0.625"												
Spacing	Length Range											
2		10.27		3.93		-0.01						
4		10.35		2.43		-0.04						
6		10.20		1.94		0.00						
Series capacitance change as rod diameter increases from 0.125" to 0.625"												
2			11.45		39.08		22.60					
4			2.02		31.73		14.60					
6			-1.03		28.58		11.00					
Notes:	HW = Healey-Wheeler calculation method; TNL = Tolles-Nelson-Leeson method; AM = Antenna Model software											
	AGT = average gain test as a measure of model adequacy											
	All physical dimensions are in inches.											
	Pre-R and Pre-jX = modeled feedpoint impedance of the beam before matching.											

Table 8-2 catalogs the data for the series of tests. The top part of the table provides the initial antenna dimensions, along with the near-resonant pre-match feedpoint impedance. The next part of the table provides results for the three methods of determining the required gamma parameters. The AM section provides an additional column that lists the AGT score for each model in the set. The models using a 2" spacing are the farthest from ideal. It is not wholly clear that MININEC follows the same general AGT rules as does NEC. Hence, we cannot claim with assurance that the 50-Ω impedance derived from the models (within the limits used in the first test) is off by no more than about 1.25 Ω. However, the parallels among values for all three spacing values suggest that

the models are generally reliable within the limits of the average gain test.

The three methods of finding gamma parameters differ in almost every category. The HW and TNL systems show various degrees of gamma-rod length increase as we increase the rod diameter, regardless of the spacing. The models show virtually no change in length within each of the spacing groups. The HW system shows a considerable increase in length as the rod diameter increases, while the increase is fairly modest for the TNL system. In all cases, the calculating methods show longer rods than the models. However, we cannot draw conclusions until we review the second part of this test series, using a different initial or pre-match feedpoint impedance.

The series capacitance values produced by each method present an equally befuddling array of differences within each method and between any two methods. The HW system produces only small changes in value across the span of rod diameters for wide-spacing values, but larger changes for narrow spacing values. The HW changes within spacing groups are in all cases smaller than for the TNL intra-group changes. The modeled values partially parallel the HW values in terms of the amount of change within each spacing group. However, the trends are not consistent between the calculating systems and the modeling system.

Before we rush to conclusions, we should repeat the very same tests using a different pre-match impedance. We shall retain every other beam detail, except that we shall use the version of the beam that shows a pre-match impedance of 29.84 - j25.73 Ω. The results of this second survey appear in **Table 8-3**.

With respect to gamma rod length, within each group, the HW system shows an increasing length as we increase the rod diameter. Both the TNL system and the AM models show a decreasing rod length as we increase its diameter. Despite the different trends for the initial impedance of the antenna, the HW and TNL lengths are not very different from each other for any given element-to-rod spacing. However, the rod lengths required by the models are systematically longer. (This fact is exactly the reverse of what we saw when the beam's pre-match impedance was nearly resonant.)

With the high capacitive reactance of the pre-match impedance, the gamma-rod lengths remain relatively stable for all 3 methods within each increment of element-to-rod spacing. However, the series capacitance is another matter. The HW system shows the greatest rate of increase with increasing rod diameter, while the AM models show the smallest rate of increase. Both calculating systems produce much higher series capacitance values than the models, with the HW system showing values that are 100-150% too high. The TNL and AM series capacitance values are more closely--but not too closely--aligned

Test Series at 28 MHz: Changing Gamma Spacing and Gamma Rod Diameter for a 50-Ohm Match — Table 3

Dimensions		Dr. Len	Ref Len	El Space	El Dia	Pre-R	Pre-jX					
Non-Resonant		190.7	211.862	50.584	0.5	29.84	-25.73					
Gamma Match		Healey-Wheeler		Tolles-Nelson-Leeson		Antenna Model			Length Differences		Cap. Differences	
Spacing	Rod Dia	Length	Cap pF	Length	Cap pF	Length	Cap pF	AGT	AM-HW	AM-TNL	AM-HW	AM-TNL
2	0.125	18.62	56.14	21.26	45.07	24.45	34.30	0.9759	5.83	3.19	-21.84	-10.77
	0.25	18.85	68.78	20.93	52.77	24.30	38.10	0.9768	5.45	3.37	-30.68	-14.67
	0.375	19.27	79.81	20.76	58.57	24.17	40.85	0.9782	4.90	3.41	-38.96	-17.72
	0.5	19.88	90.63	20.67	63.93	24.05	43.00	0.9800	4.17	3.38	-47.63	-20.93
	0.625	20.73	101.92	20.65	68.68	23.91	44.90	0.9823	3.18	3.26	-57.02	-23.78
4	0.125	14.71	62.62	16.04	48.49	18.73	33.90	0.9908	4.02	2.69	-28.72	-14.59
	0.25	15.06	74.30	15.83	55.06	18.65	36.60	0.9912	3.59	2.82	-37.70	-18.46
	0.375	15.52	83.90	15.71	59.89	18.58	38.50	0.9915	3.06	2.87	-45.40	-21.39
	0.5	16.12	92.77	15.63	63.93	18.53	39.80	0.9919	2.41	2.90	-52.97	-24.13
	0.625	16.91	101.42	15.57	67.50	18.47	41.00	0.9925	1.56	2.90	-60.42	-26.50
6	0.125	13.10	65.54	14.01	49.98	16.35	32.75	0.9968	3.25	2.34	-32.79	-17.23
	0.25	13.48	76.64	13.84	56.02	16.30	34.90	0.9969	2.82	2.46	-41.74	-21.12
	0.375	13.93	85.54	13.75	60.37	16.26	36.30	0.9972	2.33	2.51	-49.24	-24.07
	0.5	14.50	93.55	13.68	63.93	16.22	37.40	0.9974	1.72	2.54	-56.15	-26.53
	0.625	15.25	101.13	13.63	67.03	16.18	38.27	0.9976	0.93	2.55	-62.86	-28.76
Miscellaneous Derived Data												
Length change as rod diameter increases from 0.125" to 0.625"												
Spacing	Length Range											
2		2.11		-0.61		-0.54						
4		2.20		-0.47		-0.26						
6		2.15		-0.38		-0.17						
Series capacitance change as rod diameter increases from 0.125" to 0.625"												
2			45.78		23.61		10.60					
4			38.80		19.01		7.10					
6			35.59		17.05		5.52					
Notes:	HW = Healey-Wheeler calculation method; TNL = Tolles-Nelson-Leeson method; AM = Antenna Model software											
	AGT = average gain test as a measure of model adequacy											
	All physical dimensions are in inches.											
	Pre-R and Pre-jX = modeled feedpoint impedance of the beam before matching.											

The trends shown within each of the two test situations generally failed to parallel each other, despite the fact that the only difference between system

inputs is the initial or pre-match impedance values. It would appear that we need a further type of test situation.

Test 3: Varying the Input Impedance

The goal of this test sequence is to determine--at least in a preliminary way--the effects of varying the pre-match feedpoint impedance, with special reference to the reactance. We already have sample of resonant and highly capacitively reactive impedances. We may use the same basic model of a 28-MHz 2-element Yagi and vary the driver length to create a reasonably fair sequence of reactance values. We need a positive limiting reactance value that is close to the negative limiting value. As well we need reactance values close to +/-13 Ω as intermediate values between resonance and the limits.

We can arrive at these values just by varying the length of the initial beam driver, as shown in the top section of **Table 8-4**. The resistive component of the pre-match feedpoint impedance will increase as the driver grows longer. However, the amount of increase should not be enough to invalidate this highly preliminary test sequence. We shall survey two gamma-rod diameters in order to assure ourselves that any trends are not mere quirks. The lower portion of **Table 8-4** shows the results of calculating the gamma parameters and of modeling them. Let's examine the results, separating the gamma length from the series capacitance, and also separating the two different gamma-rod diameters. **Fig. 8-7** graphs the gamma-rod lengths for the 0.125" diameter gamma rod.

Both the HW and the TNL calculating systems show roughly equal rod lengths at the extremes of the test series, with the inductively reactive initial driver requiring a considerably longer length than the capacitively reactive driver by a factor of about 2:1. However, between these extremes, the two systems show curves with almost exactly opposite tendencies. Moreover, when we examine the modeled gamma-rod lengths, we find a quite different curve. The rod is shortest when the pre-match impedance is closest to resonance, with increases in length as the impedance becomes more reactive, regardless of the type of reactance.

Gamma Assembly Comparisons by Pre-Match Impedances								Table 4
Prematch Models								
Model	Dr Len	Ref Len	El Space	El Dia	Pre-R	Pre-jX		
1	190.70	211.86	50.58	0.50	29.84	-25.73		
2	193.16	211.86	50.58	0.50	30.93	-12.99		
3	195.64	211.86	50.58	0.50	32.07	-0.05		
4	198.12	211.86	50.58	0.50	33.24	12.97		
5	200.54	211.86	50.58	0.5	34.43	25.77		
Gamma Outputs		All gamma rods spaced 4" center-to-center from main element						
		Healey-Wheeler		Tolles-Nelson-Leesor		Antenna Model		
Gam Dia	Pre-jX	Length	Cap pF	Length	Cap pF	Length	Cap pF	AGT
0.125	-25.73	14.71	62.62	16.04	48.50	18.73	33.90	0.9908
	-12.99	18.10	66.38	15.64	60.39	16.14	43.90	0.9972
	-0.05	25.45	50.65	18.17	65.58	15.44	54.40	0.9996
	12.97	31.06	37.83	23.78	58.45	17.08	59.60	0.9960
	25.77	34.57	30.39	30.67	47.58	20.38	57.70	0.9896
0.375	-25.73	15.52	83.90	15.70	59.91	18.58	38.50	0.9915
	-12.99	23.65	76.78	15.87	76.31	16.09	50.10	0.9977
	-0.05	31.84	52.58	19.49	83.87	15.45	63.70	1.0000
	12.97	36.05	40.19	26.65	73.56	17.16	72.30	0.9961
	25.77	38.56	32.99	34.85	58.69	20.57	72.20	0.9896
Notes:	HW = Healey-Wheeler calculation method; TNL = Tolles-Nelson-Leeson method;							
		AM = Antenna Model software						
	AGT = average gain test as a measure of model adequacy							
	All physical dimensions are in inches.							
	Pre-R and Pre-jX = modeled feedpoint impedance of the beam before matching.							

When we increase rod diameter to 0.375", as shown in **Fig. 8-8**, the same tendencies repeat themselves, although the calculated lengths increase the ratio between the most inductive and the most capacitive reactance values. However, the modeled gamma-rod lengths show virtually the same values as shown in the curve for the 0.125" rod.

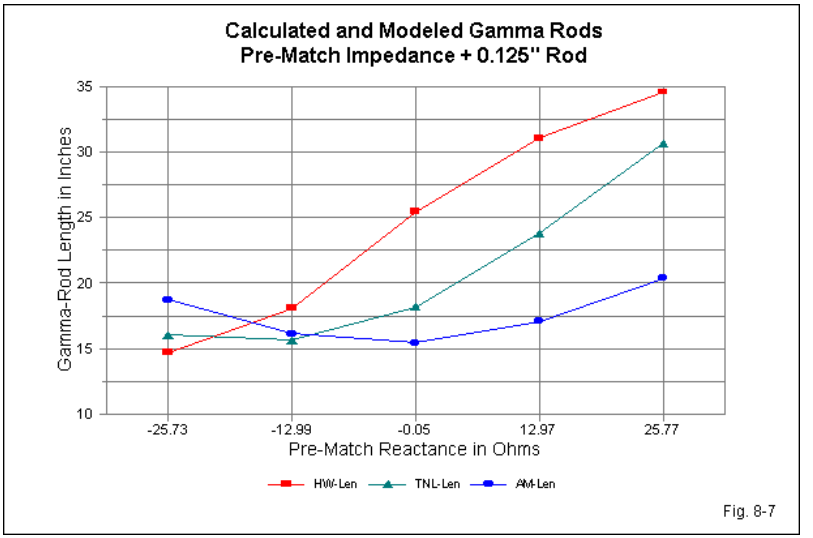
Calculated and Modeled Gamma Rods
Pre-Match Impedance + 0.125" Rod
Gamma-Rod Length in Inches
35
30
25
20
15
10
-25.73
-12.99
-0.05
12.97
25.77
Pre-Match Reactance in Ohms
HW-Len
TNL-Len
AM-Len

Fig. 8-7

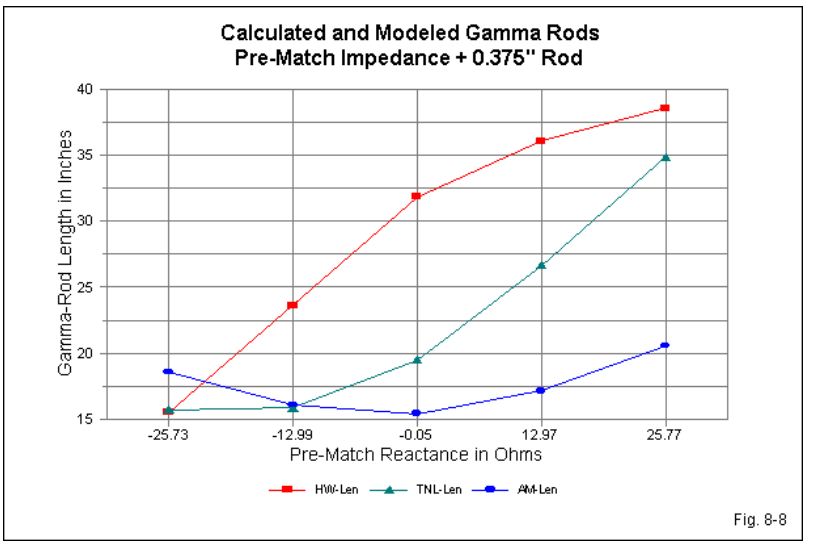
Calculated and Modeled Gamma Rods
Pre-Match Impedance + 0.375" Rod
Gamma-Rod Length in Inches
40
35
30
25
20
15
-25.73
-12.99
-0.05
12.97
25.77
Pre-Match Reactance in Ohms
HW-Len
TNL-Len
AM-Len

Fig. 8-8

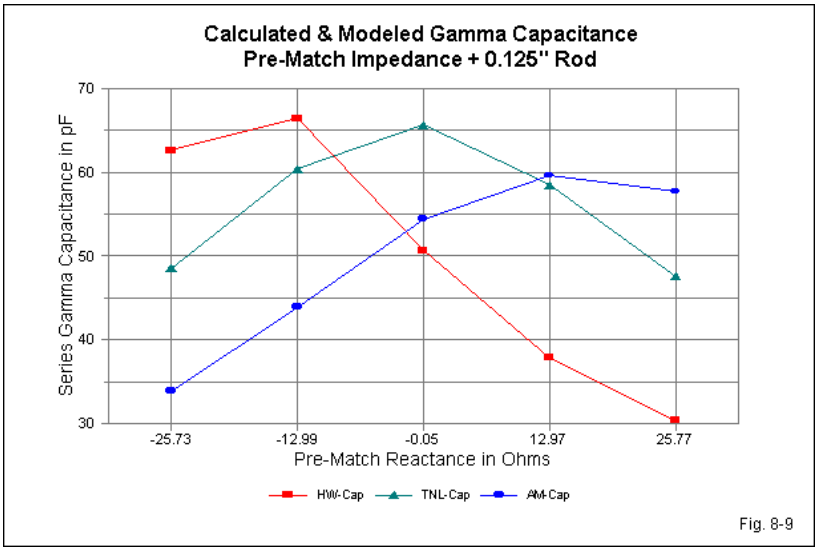

Fig. 8-9

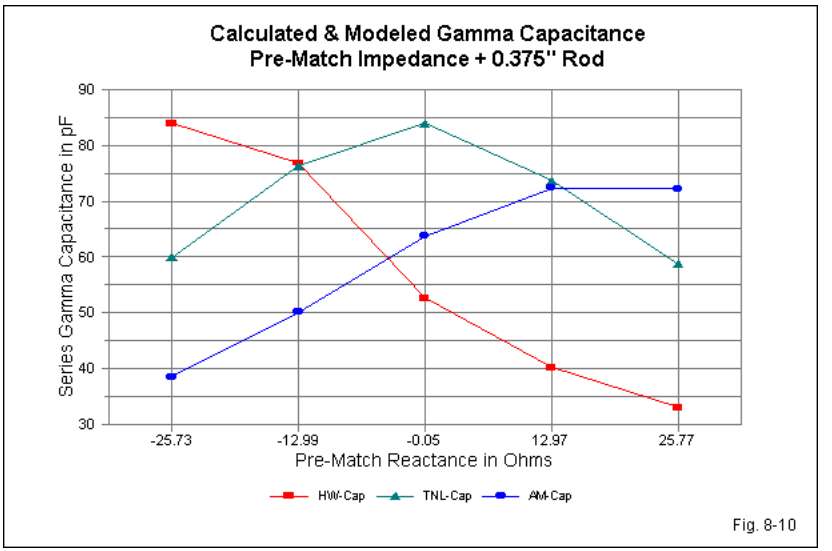

Fig. 8-10

If we graph the series capacitance values for the 0.125" rod across the spread of pre-match impedances, the curves become quite interesting, as suggested by **Fig. 8-9**. Each method of reaching a capacitance value shows a peak, and the peak occurs at a different impedance for each method. The HW system arrives at a peak capacitance value at the intermediate capacitive reactance value, while the TNL system peaks at (or close to) resonance. The modeling method shows its peak near the intermediate inductive reactance value. We should remember that the model contains gamma end wires that are not a part of the calculating systems.

The capacitance curves for the 0.375" rod diameter show similar traits to those for the 0.125" rod. See **Fig. 8-10**. The calculating systems appear to show peaks with higher levels of reactance than we found to be the case for the thinner gamma rod. Once more, the TNL gamma matches show peak series capacitance values close to an initial resonant impedance, with the HW peak in the capacitive reactance region and the modeled match's peak in the inductively reactive region, relative to the initial or pre-match driver impedance.

Perhaps more vividly than any other test, the final series of tests shows one of the chief sources of differences among the three systems. The two calculating systems respond to differences in the feedpoint reactance in similar ways, although the length curves show opposite tendencies as the pre-match impedance approaches and passes resonance. If the test is representative, then we have established that the two systems are the same in principle, although they differ in detail. However, for changes in the gamma-rod length, neither system correlates well with the modeling method of designing a gamma assembly. Otherwise expressed, the modeling system of design fails to correlate well with the methods of calculation.

Note that I have emphasized the conditional nature of the test series. We have examined only the impedances that tend to apply to Yagi beams, that is, impedance below the feedpoint impedance. Establishing that the results are in fact representative would require a very large series of test sequences involving many possible impedance combinations relative to the feedpoint target and the pre-match values. At most, this test has established the importance of the pre-

match impedance as a factor governing the results from each method.

Some Tentative Conclusions

I approached the gamma match out of curiosity. My inquisitiveness arose from the difference between series matching and beta matching calculation systems and the calculation of gamma matching systems. The first two methods produce precise results so that the most significant limitation when implementing one of them surrounds the physical properties of the components involved. For transmission line lengths, the accuracy of the velocity factor (or our ability to make linear measurements of the line) becomes the chief source of error.

The gamma matching system calculation methods show far less precise results. Some writers have ascribed most of the error to the lack of end wires in the calculated values. For many implementations, this convenient explanation seemed too weak to account for the differences. Therefore, I took two of the systems that are amenable to straightforward calculation progressions and compared their results to MININEC models using the most reliable version available of that software. The results of our preliminary series of tests--restricted to a 50-Ω target feedpoint and to pre-match impedance values typical of Yagi arrays--show something else entirely.

The two calculation systems--HW and TNL--produce seemingly divergent results, especially with respect to variations among the main element diameter, the gamma rod diameter, and the spacing. However, if we employ a range of pre-match impedance values that vary mostly with respect to reactance, we begin to see an emerging pattern in which the calculated gamma lengths converge at high pre-match reactance values and diverge when the pre-match impedance approaches resonance. (We may bypass capacitance calculations, since they depend on the calculated gamma rod length.)

Perhaps the most disturbing aspect of the test series is the fact that neither calculation method approaches--either in values or in trends--what we find when we model a gamma match using MININEC models with nearly ideal AGT scores. However, we cannot in this case give automatic priority to the modeled results

because they have not undergone confirming field tests. They simply serve here as a third method that differs in principle from the basic presumptions underlying the two calculation systems that we examined. Nevertheless, the differences in results among the methods strongly suggests that the present methods of calculating gamma match components fall seriously short of being precise.

We have had occasion to note that one point at which both the HW and TNL systems make a questionable assumption lies in the use of standard equations for calculating the transformed pre-match impedance to arrive at a value that we have called Z1. Remodeling the gamma to move the feedpoint to the main element at the junction of the gamma-half-element with the non-gamma-half-element suggests at least a phase shift and also significant variation from the calculated value of r that depends only on the physical properties of the assembly. The transformation also appears to relate to the pre-match impedance--especially the reactive component--although our test series is too small to reach two important conclusions. One conclusion would be the derivation of a revised step-up function, either as a correction factor on the usual calculation or as a substitute formulation. The other conclusion that we cannot draw is the adequacy of the modeled gammas to serve as source for such correctives.

Even if we could revise the available calculation systems, they would still fall short of the precision that we obtain from the calculations associated with series and beta matching systems. The methods by which we implement a gamma match include significant variables relative to even a precise calculation system. **Fig. 8-11** shows some of the factors involved.

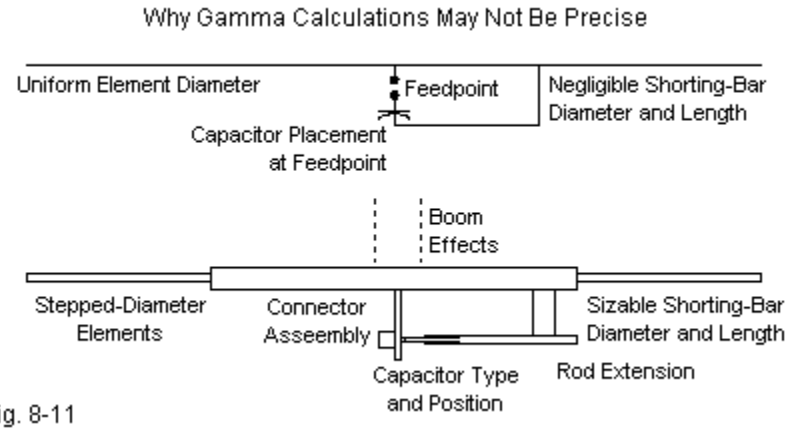

Fig. 8-11

The upper portion of the sketch shows the general situation presumed by all of the methods that we have examined. The elements have a uniform diameter and thus most closely approximate sinusoidal current distribution. The end wires at the gamma far end and at the feedpoint have no weight in the calculation--except as post-facto fudge factors. Third, the series capacitance is precisely at the feedpoint of the gamma system.

The lower portion of the sketch shows some typical variations in the theoretical arrangement used in calculations. The elements in the HF range may use stepped-diameter structures that may vary the usual expectations for current distribution. The gamma rod normally extends beyond the shorting bar, leaving a small but definite radiating structure. The shorting bar at the gamma far end and the plate holding the coaxial cable connector have significant proportions that will vary from one installation to another. The sketch also shows the use of a tubular capacitor, a common HF technique to provide the series capacitance without concern for the voltage and current levels on the component and without concern for the effects of weathering. Once set, we may effectively seal the capacitor so that it requires only long-term maintenance.

However, equally important to the type of capacitor used is its position.

Typically, without regard to the type of capacitor used, gamma-match builders install the component on the gamma rod rather than at the actual feedpoint. **Fig. 8-12** illustrates a sample of commercial gamma-match construction. By virtue of its position along the gamma line, the capacitor modifies both its influence on the feedpoint impedance and on the structure of the gamma line. For example, the gamma rod changes its diameter. In addition, we would be hard pressed to establish a precise location along the gamma rod for the capacitor, since we cannot see the termination of the smaller tubing inside the larger one. As well, the physical implementation of the gamma must take into account any affects of the boom, if one chooses to connect the driven main element to the boom.


Fig. 8-12

Despite all of these variations from the idealized version of the gamma-match used in calculations, the physical implementations work very well. The length of the gamma rod largely determines the feedpoint impedance's resistive component, while the capacitance adjustment reduces the feedpoint reactance at the design frequency. Of course, with a system like the one shown in the photograph, varying the capacitance requires that we loosen connections on the shorting bar to allow the inner gamma rod section to slide easily. As a consequence, the gamma-rod length changes with each adjustment of the capacitance. Hence, we must re-establish the shorting bar position for a 50-Ω feedpoint impedance. The process may require 3 or 4 iterations before we are satisfied with the physical positions of the components and lock the system in place.

In general terms, the practical gamma match system is designed for field adjustment to account for the variables that idealized calculations do not include. Therefore, even if we were to perfect gamma-matching system calculations, they would not yield the precision that we associate with other matching system calculations. Rather, they would serve only as a general guide to beginning a process that only field adjustment can perfect. Indeed, for any selection of main element diameter, gamma rod diameter, and spacing between the two, there is a gamma length and a series capacitance that will effect a usable match to a desired main feedline over a wide range of pre-match impedance values--although not a completely unlimited range. As well, the gamma match will work either with or without a direct connection of the driven element to the boom.

Whatever the complexity of the calculation system, its output is simply a starting point to the process. We might as easily replace it with a table encompassing all of the successful implementations of gamma-match systems arranged by frequency, main element diameter, gamma rod diameter, and element-to-rod spacing. We would also need annotations on the method of implementing the series capacitance. As well, the entries should include details related to the feedpoint connector plate and the shorting bar. In fact, the table should include detailed sketches of the assembly to guide builder who might wish to replicate a given assembly and to alert other builders to potential adjustment needs for variations on the basic scheme.

Such an archive--if it existed--would likely provide as much guidance to gamma-match dimensions as the current methods of calculating them.

Part III: Some Practical HF 2-Element Parasitic Beams

9. Beams for 20 through 10 Meters

For most home crafters, the upper HF region from 20 through 10 meters provides a fertile ground for successful antenna construction, especially if we limit our building to 2-element monoband Yagis, in keeping with the theme of this volume. Therefore, as a reference guide, let's examine some designs for each of the five upper-HF amateur bands.

The task is both simple and complex, all at once. The simple part stems from the fact that we may cull designs from any number of handbooks and journals, trying to replicate them. The complex part begins once we begin to tailor the designs for the particular properties of the individual bands. We tend to classify 20, 15, and 10 meters as wide bands, since coverage extends for 350 kHz on 20 up to a full MHz on the lower, more active end of 10 meters. In contrast, 17 and 12 meters are each only 100 kHz wide. We might wisely choose somewhat different designs for each type of band.

For 20, 15, and 10 meters, let's consider wide-band driver-reflector designs. We saw in previous chapters that if we increase the element spacing, something happens and something does not happen. What does not happen is that the performance does not degrade to any degree that we might notice in operation. What does happen is that the feedpoint impedance increases toward 50 Ω. Hence, we can design for these bands 2-element Yagis that allow a direct connection of the feedline to the driver feedpoint without needing a matching system. Of course, we may wish to insert a 1:1 balun or bead choke at the feedpoint to attenuate common-mode currents.

For 17 and 12 meters, a wide-band design may be a waste of boom length. For these bands, a driver-director Yagi will have sufficient bandwidth to cover each of these bands. Since the feedpoint impedance will be in the mid-20-Ω range, we can design the beams for use with a simple beta match. The result will be as compact a 2-element Yagi with linear elements as we can make. (See the next chapter for practical designs for the Moxon rectangle, which can

achieve even more compact dimensions due to the use of elements that fold toward each other.) Like the wide-band Yagis, the driver-director driven elements must be insulated from any conductive boom material. A common-mode current attenuator is also useful for these designs.

The designs that we shall present use elements that are well insulated and isolated from any conductive boom—or they use a non-conductive boom. A PVC or similar boom is especially useful on 12 and 10 meters. Below those bands, it may sag too much. Therefore, I recommend the use of polycarbonate plates and U-bolts as a convenient method of insulating the elements from the conductive aluminum boom while achieving a solid mechanical structure. At the end of this chapter and in the next chapter, you will find some construction notes, most of which are equally applicable to both linear-element Yagis and Moxon rectangles.

For HF beams, however simple or complex the design, I do not recommend the use of hardware-outlet tubing. Very often, we find the walls of this tubing to be thinner than standard hard aluminum tubing. So we cannot certify the element strength. As well, the fit from one size to the next may be loose. Even though we can create an initial tight fastening, we often cannot say if that connection will hold through several rounds of weather changes. The best material that is readily available from mail and on-line outlets is 6063-T832 aluminum. The tubing comes in sizes that change in 0.125” outer-diameter increments. The wall thickness is about 0.056”, which just allows smooth nesting of successive tubing sizes without binding, but also without any wobbling.

In the final chapter of Volume 1, we discussed a procedure to use in order to convert uniform diameter elements into elements with a stepped diameter. However, suppose that we wished to construct a 2-element Yagi with an adequate wind-load capability for most locations in the U.S. Simply converting the 3/8”-diameter elements used in all of our test Yagi models will not achieve our goal. We need to select an element taper schedule that will provide sufficient strength to withstand winds to perhaps 65-70 mph. Essentially, we have two choices. We can use a program such as YagiStress and design our own physical elements. Or else, we can use an element design that has already

been through that process. We shall need a different taper schedule on each of the upper HF bands to meet the wind load rating that we set.

If you prefer designs that have different dimensions or specifications from the ones that we shall show here, the best volume to consult may be the Yagi chapter of any recent edition of *The ARRL Antenna Book*. Editor Dean Straw, N6BV, has provided some very good designs (for large as well as for 2-element beams) that you may successfully copy. The designs that we shall provide are simply alternatives ways of achieving similar goals.

For each beam, we shall present a variety of information, with an emphasis on tabular and graphical data. Each design will include an element taper schedule and a list of element dimensions. We shall also tabulate free-space data on performance. The use of free-space data provides a fair comparison among designs. You may increase the rated gain values by 5 to 6 dB to account for ground reflections. The exact amount of reflection gain will vary with the height of the antenna above ground (as measured in wavelengths). Many commercially made antennas offer single values in each performance category, such as gain, front-to-back ratio, and feedpoint impedance. These numbers, however derived, do not give us an adequate picture of a beam's performance across a given passband. Therefore, we shall also provide graphs of key performance data. Finally, we shall present free-space E-plane (azimuth) patterns at the band edges and at the design frequency to let you see how the beam's pattern evolves as we change the operating frequency. Finally, the models for these antennas are attached to this volume. Therefore, you will be free to re-design any one of them to suit your needs.

A 20-Meter Wide-Band Driver-Reflector Yagi

The driver-reflector Yagi for 20 meters is the largest of our structures. Although it uses more tubing diameters to achieve the desired wind load, it shares a number of features with all of the other Yagis in the collection. The most notable feature is the doubling of the innermost tubing section by running the next size all the way to the element center. **Fig. 9-1** and **Table 9-1** both show the doubling. Normal element nesting requires a 2"-3" overlap. Longer

overlaps (when not doubling the wall thickness) are a waste of weight, while a shorter overlap may result in an insecure element section junction.

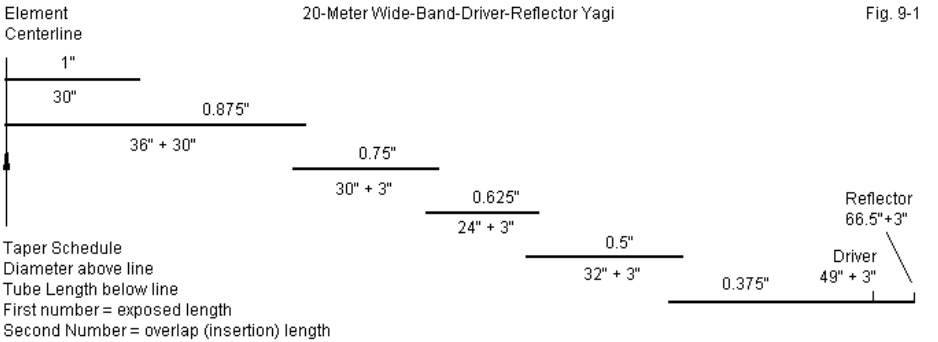

Table 9-1. 20-meter wide-band Yagi dimensions

a. Overall dimensions in inches

Driver	Reflector	Spacing
402”	437”	139”

b. Element taper schedule per half-element: all dimensions in inches

Segment Diameter		Exposed Length	Nesting Length	Segment Total	Cumulative Length
1.0		30	---	30	30
0.875		36	30	66	66
0.75		30	3	33	96
0.625		24	3	27	120
0.5		32	3	35	152
0.375	dr.	49	3	52	201
	ref.	66.5	3	69.5	218.5

Fig. 9-2 and **Fig. 9-3** provide graphs of the free-space gain, the 180◦ front-

to-back ratio, and feedpoint data. The feedpoint data include resistance, reactance, and the 50-Ω SWR across the 20-meter band.

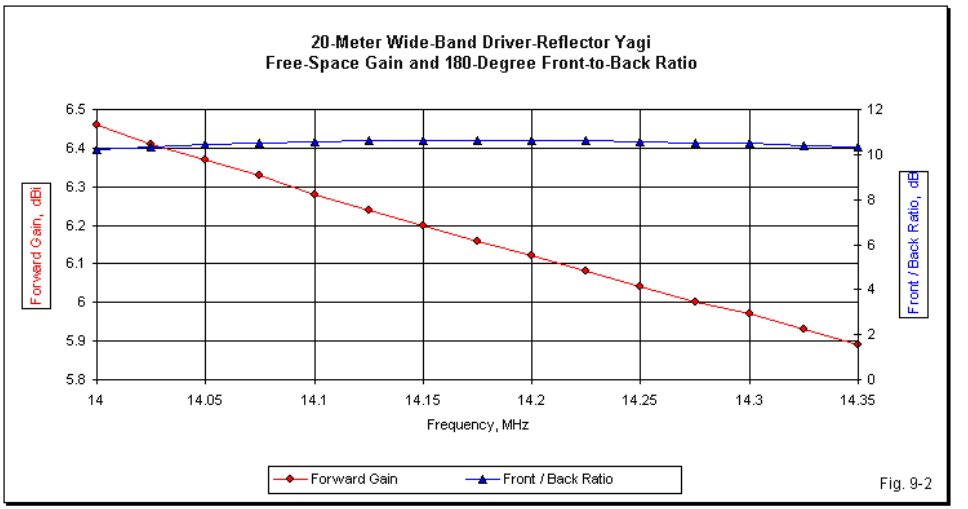

Fig. 9-2

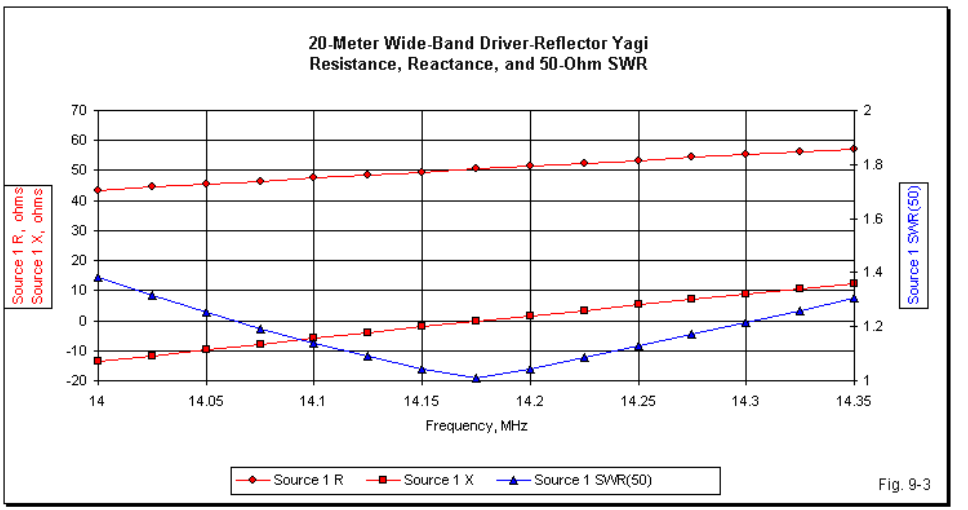

Fig. 9-3

The graphs show that the front-to-back ratio does not change significantly across the band. The gain curve shows the natural driver-reflector decrease with rising frequency. The resistance and reactance changes show why the SWR curve is so shallow as a natural function of the element spacing. The spot-frequency check of typical beam values in **Table 9-2** puts numbers with the curves.

Table 9-2. Modeled free-space performance: 20-meter wide-band Yagi

Frequency MHz	14.0	14.175	14.35
Gain dBi	6.46	6.16	5.89
180° front-back dB	10.23	10.64	10.35
Feedpoint R+/-jX Ω	43.3 – j13.7	50.5 – j0.2	57.1 + j12.4
50-Ω SWR	1.39	1.01	1.31

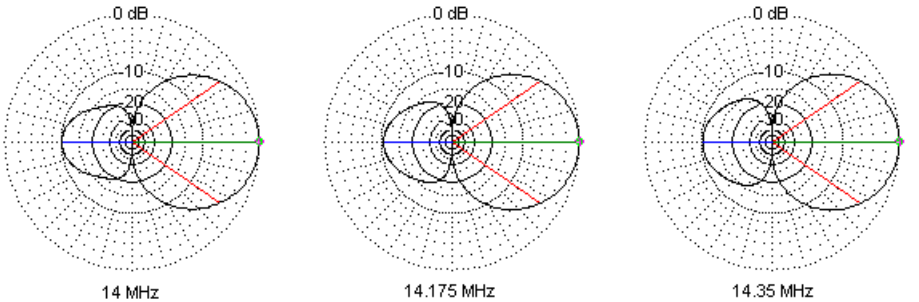

20-Meter Wide-Band 2-Element Yagi: Free-Space E-Plane Patterns

Fig. 9-4

Fig. 9-4 provides free-space E-plane (azimuth) patterns at the frequencies checked in **Table 9-2**. Note that the pattern does not change significantly across the band. You can obtain similar performance with a slightly shorter boom if you are willing to accept higher SWR values and lower resistance values, but still within a 1.5:1 SWR range.

The 20-meter beam illustrates a design that foregoes extreme compactness

in the interests of a direct 50-Ω feedpoint impedances and consistent performance from one band edge to the other. One further benefit accrues to this type of design, which originated in the 1980s from the work of Bill Orr, W6SAI. A very broadband antenna eases construction problems for the individual with only a modest shop and tool collection. Slight construction variations tend to have minimal performance effects, improving the odds of successful building for someone new to home-brew antennas.

A 15-Meter Wide-Band Driver-Reflector Yagi

The 15-meter wide-band driver-reflector Yagi is not merely a scaled version of the 20-meter antenna. Rather, it adjusts all dimensions to obtain essentially the same performance with elements that use 0.875" tubing as the largest size (rather than the 1.0" material used in the 20-meter beam). Nevertheless, the two largest sizes are doubled for increased element strengths. **Fig. 9-5** and **Table 9-3** provide the basic dimensions for the antenna.

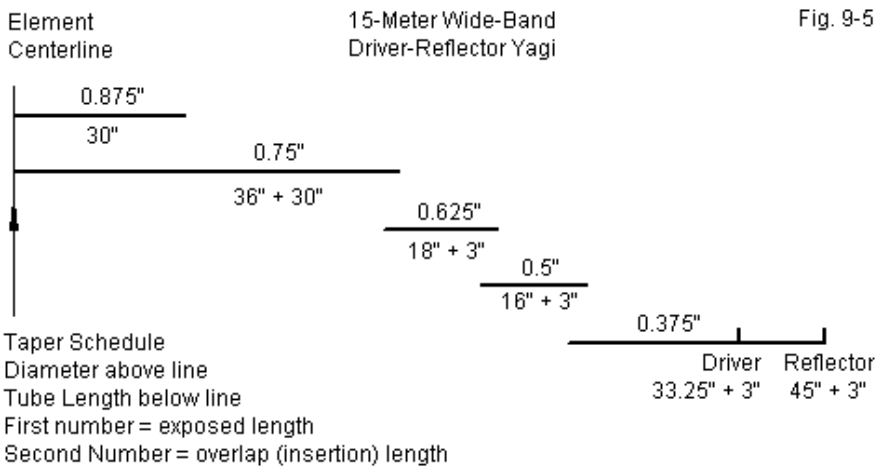

Table 9-3. 15-meter wide-band Yagi dimensions

a. Overall dimensions in inches

Driver	Reflector	Spacing
266.5”	290”	95”

b. Element taper schedule per half-element: all dimensions in inches

Segment Diameter		Exposed Length	Nesting Length	Segment Total	Cumulative Length
0.875		30	---	30	30
0.75		36	30	66	66
0.625		18	3	21	84
0.5		16	3	19	100
0.375	dr.	33.25	3	35.25	133.25
	ref.	45	3	48	145

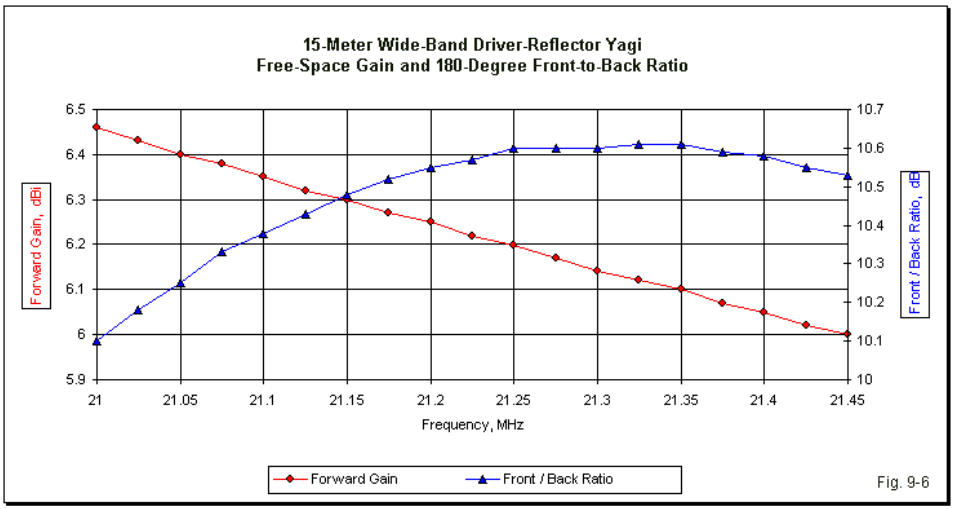

Fig. 9-6

Fig. 9-6 and **Fig. 9-7** provide the graphical data for the antenna's 15-meter performance. The higher minimum right-side Y-axis value shows the curve slope in more detail. However, the front-to-back value changes by less than 0.5-dB across the band. The peak value is not precisely centered in the passband because I limited the element-length change increment to about 0.25" per half element. **Table 9-4** provides numerical data to supplement the graphs.

Table 9-4. Modeled free-space performance: 15-meter wide-band Yagi

Frequency MHz	21.0	21.225	21.45
Gain dBi	6.46	6.22	6.00
180° front-back dB	10.10	10.57	10.53
Feedpoint R+/-jX Ω	44.3 – j10.3	50.3 + j0.5	56.0 + j10.8
50-Ω SWR	1.28	1.01	1.26

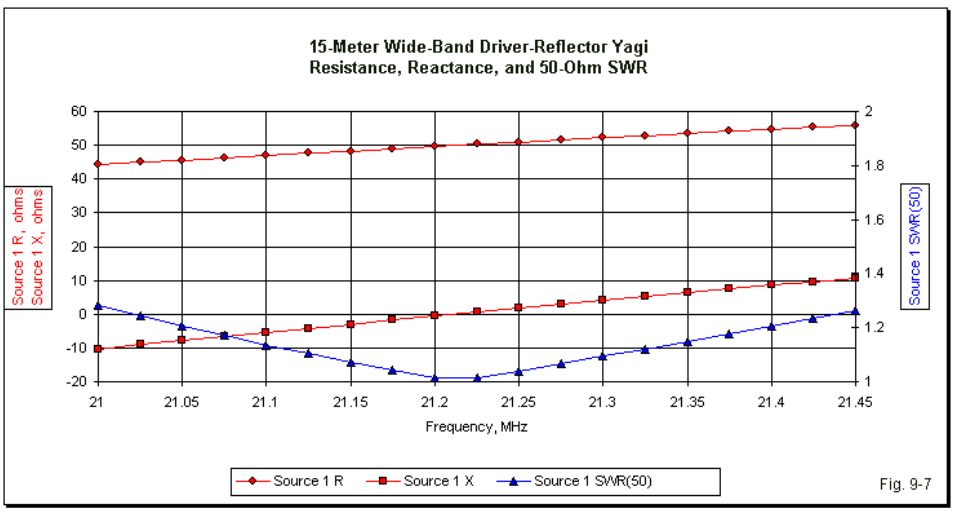

Fig. 9-7

The SWR curve for 15 meters is shallower than the corresponding 20-meter curve because 15-meters is a somewhat narrower band as a function of the bandwidth versus the center frequency. As shown in **Fig. 9-8**, the free-space E-

plane (azimuth) patterns do not show any significant variation across the band.

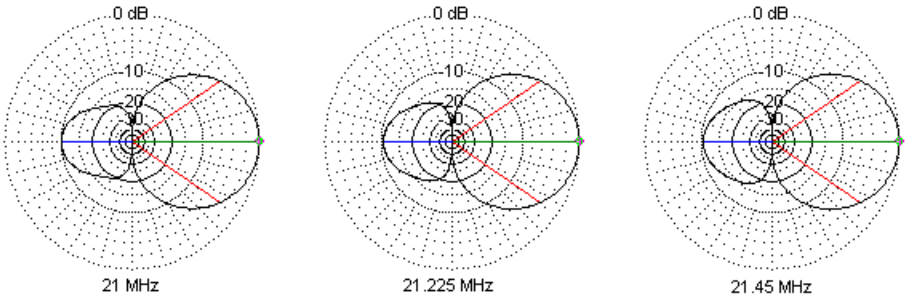

15-Meter Wide-Band 2-Element Yagi: Free-Space E-Plane Patterns

Fig. 9-8

A 10-Meter Wide-Band Driver-Reflector Yagi

The first MHz of 10 meters presents a band that is wider than either 20 or 15 when we measure the passband width against the center frequency. Consequently, the band presents more of a challenge to the basic wide-band driver-reflector design.

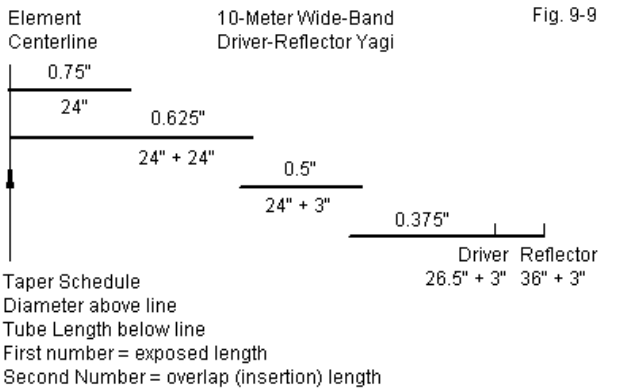

Fig. 9-9

Nevertheless, as shown in **Fig. 9-9** and in **Table 9-5**, the beam requires lighter construction for the same wind load strength. The largest tubing diameter is 0.75", doubled with the 0.625" second section.

Table 9-5. 10-meter wide-band Yagi dimensions

a. Overall dimensions in inches

Driver	Reflector	Spacing
197"	216"	70"

b. Element taper schedule per half-element: all dimensions in inches

Segment Diameter		Exposed Length	Nesting Length	Segment Total	Cumulative Length
0.75		24	---	24	24
0.625		24	24	48	48
0.5		24	3	27	72
0.375	dr.	26.5	3	29.5	98.5
	ref.	36	3	39	108

The performance of the 10-meter version of the wide-band design appears in **Fig. 9-10** and in **Fig. 9-11**, along with **Table 9-6**. The data show somewhat wider swings in the gain range and the band-edge SWR values. However, the beam is perfectly usable across the entire first MHz of 10 meters.

Table 9-6. Modeled free-space performance: 10-meter wide-band Yagi

Frequency MHz	28.0	28.5	29.0
Gain dBi	6.46	6.08	5.75
180° front-back dB	10.10	10.66	10.11
Feedpoint R+/-jX Ω	42.4 – j16.1	51.8 + j1.2	60.3 + j17.3
50-Ω SWR	1.47	1.04	1.44

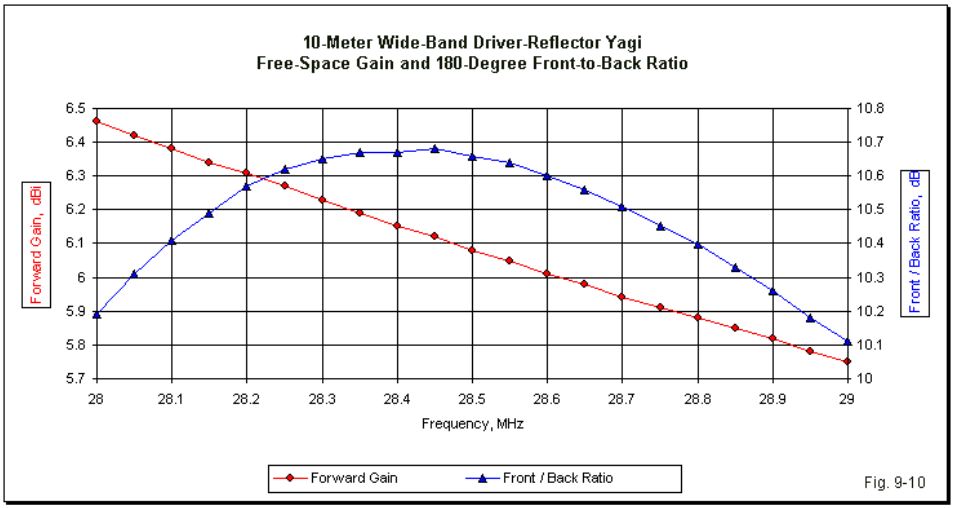

Fig. 9-10

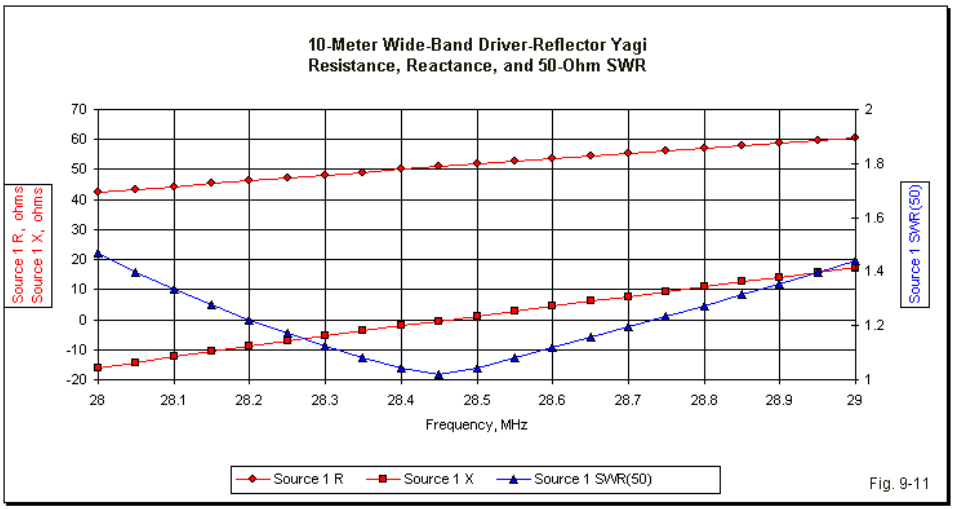

Fig. 9-11

Despite the wide operating bandwidth required of the 10-meter wide-band

Yagi, the pattern remains stable all across the band, as revealed by **Fig. 9-12**. In fact, if we were to set the design frequency at 28.85 MHz, we could use this design to cover the entire 1.7 MHz of the 10-meter band with less than 2:1 50-Ω SWR and with more than a 9 dB front-to-back ratio.

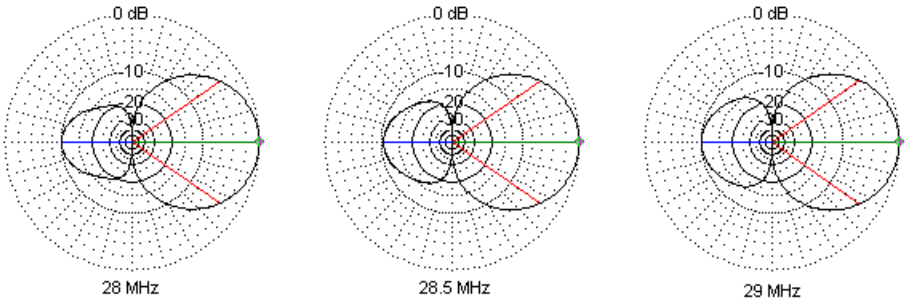

10-Meter Wide-Band 2-Element Yagi: Free-Space E-Plane Patterns Fig. 9-12

The 10-meter driver-reflector Yagi completes the trio of wide-band Yagis for the upper HF region. Compared to other driver-reflector designs, they use longer booms to achieve their goals. Shorter boom Yagis, as found in such sources as *The ARRL Antenna Book*, will also cover the bands adequately. As noted in earlier chapters, a space of about 0.125-λ provides the best combination of gain and front-to-back ratio that we can achieve in a driver-reflector design. However, the feedpoint impedance is lower and therefore requires a matching network or system to arrive at the usual 50-Ω cable impedance. As well, the bandwidth may be narrower so that the matched impedance provides higher band-edge values. The designs shown here increase the element spacing to about 0.17-λ. In the process, they lose no more than about 0.25-dB of gain and 0.5-dB of front-to-back ratio, but attain smoother performance—that is, with smaller changes—across the band, along with a direct 50-Ω match and somewhat less finicky construction.

Which design you select will result from your own operating and building circumstances. These designs offer alternatives, not claims of superiority.

A Driver-Director Yagi for 17 Meters

When we turn to the narrow upper-HF amateur bands, the long booms and wide operating bandwidths of the driver-reflector designs are largely wasted. For the 100-kHz bands, we may choose more compact 2-element driver-director designs. Instead of needing 0.17-λ booms, we shall need only about 0.9-λ for the 17- and 12-meter designs. In the design change, we shall gain additional front-to-back ratio—a noticeable 4+ dB improvement. However, we shall also pay a price in two departments. First, the inherent feedpoint impedance of each design will be about 25 Ω. If we shorten the driver, we can accommodate a very simple beta match with a shorted transmission-line stub. The data will list a length for a 50-Ω stub, but its velocity factor is 1.0 in the models. Multiply the length by the velocity factor of the line that you actually use. In fact, you can refigure the beta stubs for a higher impedance line, such as 450-Ω parallel feedline. However, adjustments will become more critical as you use a shorter, higher-impedance line.

Moreover, expect to make adjustments. Driver-director Yagis are inherently narrow-band antennas. Hence, tuning them to perfection is more time consuming than completing a wide-band driver-reflector design.

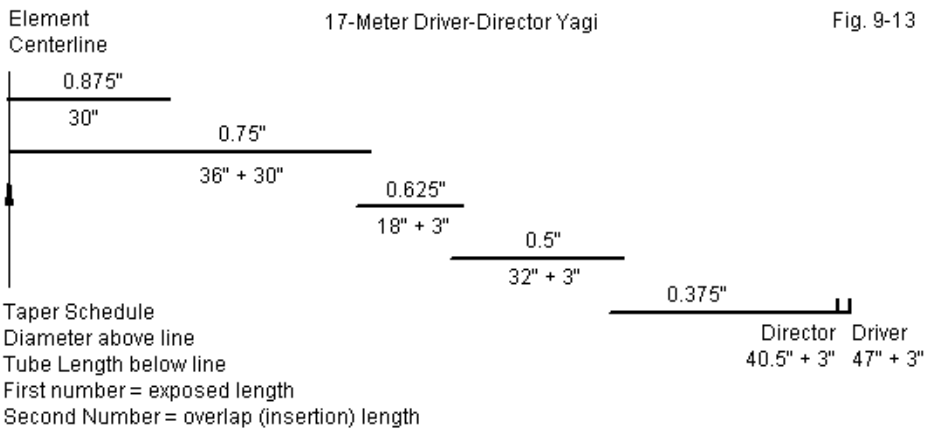

As shown in **Fig. 9-13** and in **Table 9-7**, the basic element structure does not change with the switch to a driver-director Yagi. We still double the innermost element sections and use section sizes and lengths that yield an adequate wind load. Because the design uses a beta match and a capacitively reactive driver, the maximum width of the beam is a few inches shorter than it would be with a resonant driver. You may use the model for this beam, delete the beta stub, and change the driver length to suit your own favorite method of impedance matching.

Table 9-7. 17-meter driver-director Yagi dimensions

a. Overall dimensions in inches

Driver	Director	Spacing
326”	313”	60”

Beta stub: 50-Ω, VF 1.0 transmission line, 80” long.

b. Element taper schedule per half-element: all dimensions in inches

Segment Diameter		Exposed Length	Nesting Length	Segment Total	Cumulative Length
0.875		30	---	30	30
0.75		36	30	66	66
0.625		18	3	21	84
0.5		32	3	35	116
0.375	dr.	47	3	50	163
	dir.	40.5	3	43.5	156.5

Fig. 9-14 shows the gain and front-to-back curves. See also the numerical data in **Table 9-8**. The improved front-to-back ratio is clear apparent, as is the fact that a driver-director design shows a rising gain value as we increase the operating frequency. Even though the gain at the low end of the band is similar to the low-end gain of the driver-reflector designs, the driver-director gain at the high end of the band is almost a dB higher than the gain of the designs with reflectors only.

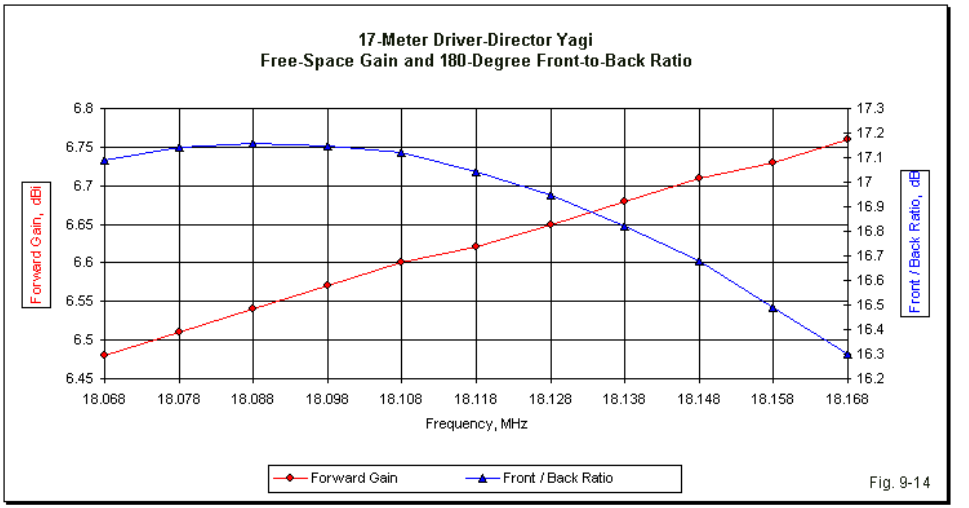

Table 9-8. Modeled free-space performance: 17-meter driver-director Yagi

Frequency MHz	18.068	18.118	18.168
Gain dBi	6.48	6.62	6.76
180◦ front-back dB	17.09	17.04	16.30
Feedpoint R+/-jX Ω	54.8 + j5.1	48.0 + j0.8	40.7 – j1.6
50-Ω SWR	1.14	1.05	1.23

The front-to-back curve reveals another feature of the driver-director design. By limiting the increments of change in element lengths, the curve fails to place the peak front-to-back value at the band center. Small changes in element length in these designs make larger changes in the performance. Hence, they require more patience to adjust.

The tabular data and the curves in **Fig. 9-15** show that the driver-director design yields a very low 50-Ω SWR value across the band once the beta match has reached its final pruned length. However, note that the matched reactance values within the passband show the opposite trend relative to their values

without the matching system in place. Reactance grows more inductive below the center frequency. Antenna adjustment must take this trend into account in the pruning process.

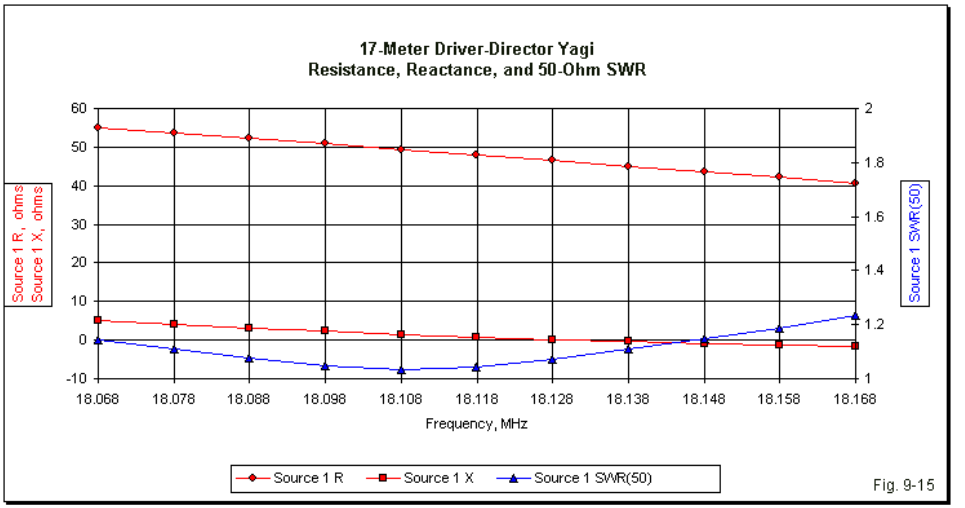

Fig. 9-15

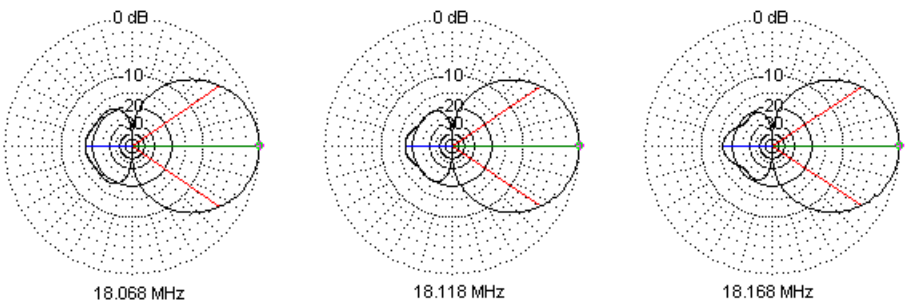

17-Meter Driver-Director 2-Element Yagi: Free-Space E-Plane Patterns

Fig. 9-16

Although the patterns in **Fig. 9-16** show good stability, we can note that even

across only 100 kHz, the rear lobes are changing shape in visually noticeable ways. If we were to try to use this type of beam across the entire span of 20 meters, we would see considerable degradation of the front-to-back ratio at the band edges, and we likely could not obtain acceptable matched SWR values at both band edges. Hence, the driver-director design is most suited to narrow bands—or to operations that use only a portion of the wider bands.

A Driver-Director Yagi for 12 Meters

Although the 12-meter band is also 100 kHz wide, it is narrower as a function of its operating frequency. Therefore, a driver-director 2-element Yagi is especially suited to this band, since it yields a compact array for the band. **Fig 9-17** and **Table 9-9** provide the physical dimensions for the 12-meter design. Essentially, the structure is similar to the 10-meter beam in terms of element tubing sizes. However, we retain the doubling of the inner tubing sections for strength. The outer or tip sections can be longer than the intermediate sections since they bear the least weight and can flex most readily.

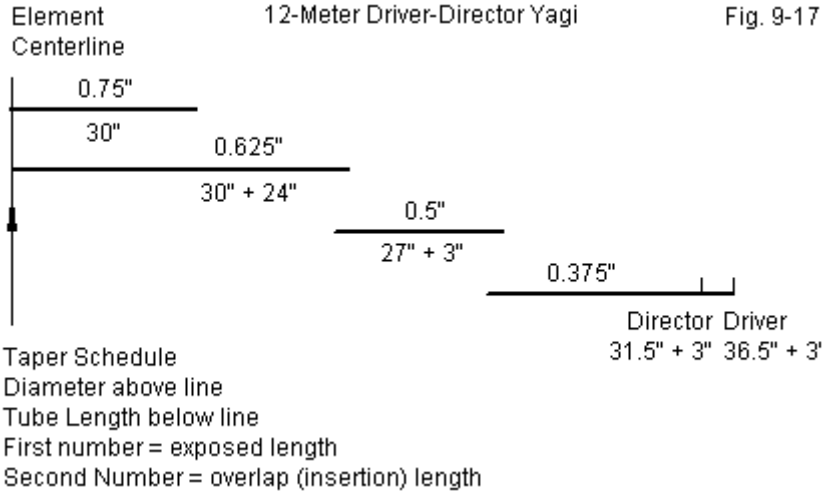

12-Meter Driver-Director Yagi Fig. 9-17

Table 9-9. 12-meter driver-director Yagi dimensions

a. Overall dimensions in inches

Driver	Director	Spacing
235”	225”	43.5”

Beta stub: 50-Ω, VF 1.0 transmission line, 62” long.

b. Element taper schedule per half-element: all dimensions in inches

Segment Diameter		Exposed Length	Nesting Length	Segment Total	Cumulative Length
0.75		30	---	30	30
0.625		24	30	54	54
0.5		27	3	30	81
0.375	dr.	36.5	3	39.5	117.5
	dir.	31.5	3	34.5	112.5

In general, the 12-meter driver-director Yagi is a smaller version of the 17-meter antenna, but with the necessary adjustments for the differences in the element taper schedule between the two antennas. **Table 9-10** reveals the similarities in performance between the beams for the two narrow amateur bands.

Table 9-10. Modeled free-space performance: 12-meter driver-director Yagi

Frequency MHz	24.89	24.948	24.99
Gain dBi	6.40	6.50	6.60
180° front-back dB	16.76	17.02	16.98
Feedpoint R+/-jX Ω	56.2 + j0.5	51.2 – j1.9	46.1 – j3.4
50-Ω SWR	1.13	1.05	1.11

The gain and feedpoint impedance change less across the band than we found on 17 meters as a function of the slightly narrower bandwidth. **Fig. 9-18** shows that the front-to-back curve is biased toward the upper end of the band,

again as a function of the limited increment used in changing dimensions.

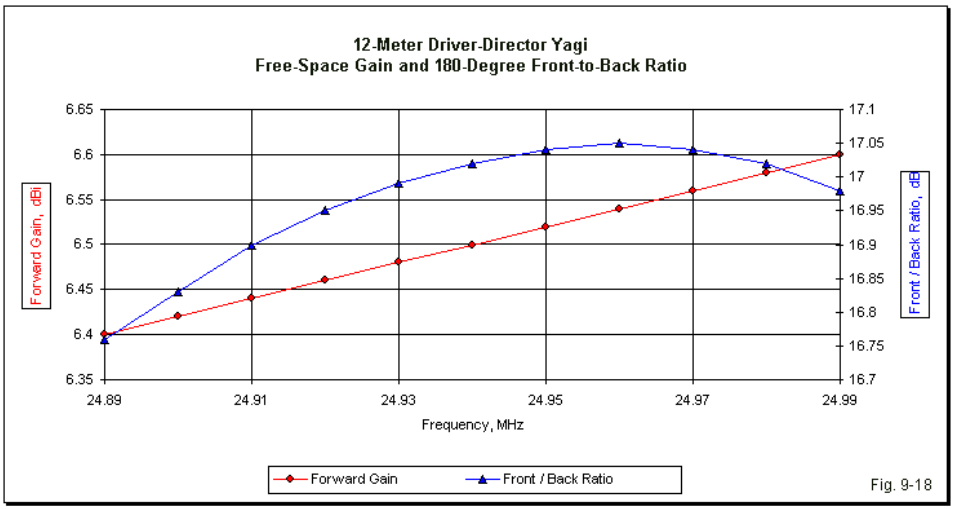

Fig. 9-18

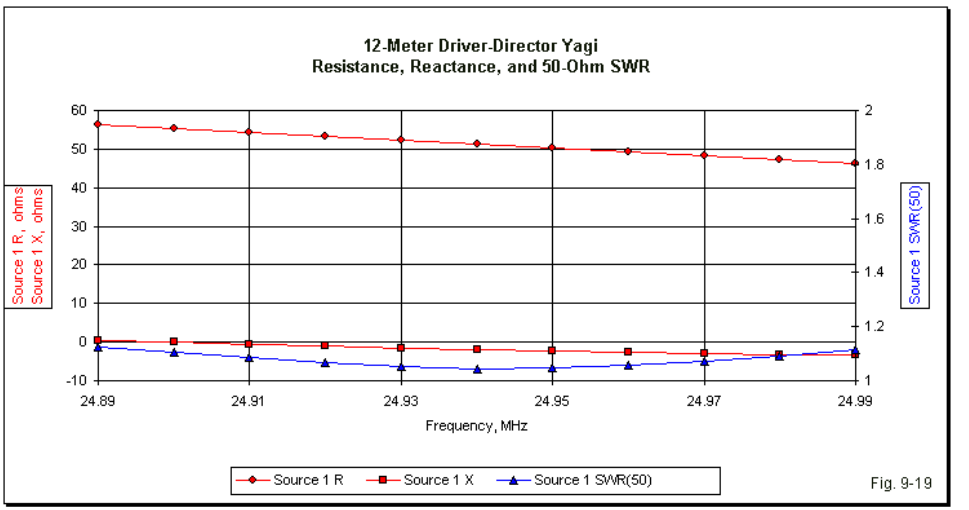

Fig. 9-19

The feedpoint data in **Fig. 9-19** show the typical matched patterns that we saw in the corresponding curves for the 17-meter version of the design. Likewise, the free-space E-plane (azimuth) patterns in **Fig. 9-20** also have a strong family resemblance to those we saw in **Fig. 9-16**.

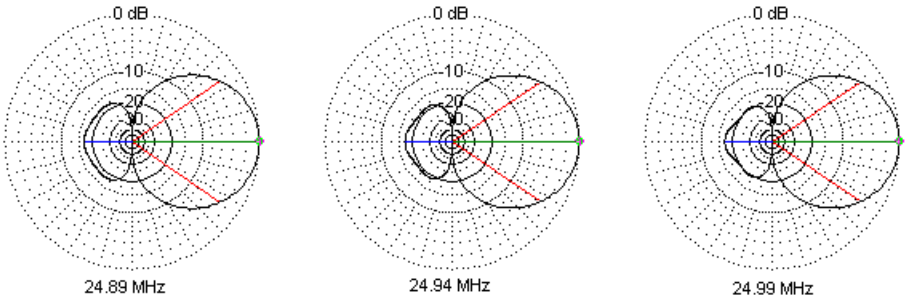

12-Meter Driver-Director 2-Element Yagi: Free-Space E-Plane Patterns Fig. 9-20

Like the driver-reflector designs for 20, 15, and 10 meters, these driver-director arrays for 17 and 12 meters are alternatives to other designs that you may find in handbooks of various sorts. They are not necessarily superior, although each design has a set of advantages and disadvantages when we make comparisons among designs. The one that is best for you is a function of many factors involving operating needs, building skills and tools, materials, and inclinations.

Some Construction Notes

Building durable antennas that will withstand many seasons of changing weather requires more than the usual array of junk-box parts and salvaged or adapted materials. Although we can certainly cobble together a semblance of any of the designs in this chapter for experimental or other short-term operation, I shall leave such ingenuity to each individual builder. In these notes, I shall note some proven techniques of construction that fit the designs and offer a good chance that the final beam will work as specified for many years.

The designs all call for elements that are insulated and isolated from a conductive boom. Connecting any of the elements to a boom will require that the length be adjusted to account for boom effects. The amount of adjustment will depend upon the boom diameter. Therefore, we shall employ a construction method that will provide sufficient electrical and spatial separation between the boom and the elements to assure that the arrays perform as modeled. The details appear in **Fig. 9-21** and **Fig. 9-22**. The individual parts of the assembly have letter keys. **Table 9-11** provides a list of the parts indicated by the letters for easy reference.

Table 9-11. Key to elements in the constructions sketches (**Fig. 9-21** and **9-22**)

A Polycarbonate element-to-boom mounting plate
B Boom
C Boom stainless-steel U-bolts and saddles
D Driven element tube
E Driven element gap insulating rod or tube
F Element stainless-steel U-bolts and saddles
G Stainless-steel nuts/bolts/washers/soldering lugs
H Reflector or director element tubes
I Inner linking conductive tube
J L-stock coax connector mounting plate
K Through-chassis coax connector
L Stainless-steel sheet-metal screws

The boom is likely to have a 1.25" outer diameter. Short booms—up to 6'—for 10- and 12-meter beams can use a single tube with a 1/16" thickness of 6063-T832 or 6061-T6 material. Longer booms for these 2-element beams should use a tube with a 1/8" thick wall or double the outer tubing with the next smaller size—for example, 1.125" tubing inside 1.25" tubing. If the tubes come in 6' lengths for transport by general carriers, you may stagger the doubling so that inner seams occur at the center of outer sections. Clean the mating inside and outside surfaces before nesting the tubes. In addition, if you warm the outer tube and cool the inner tube, the nesting will generally proceed more smoothly. Use sheet metal screws to lock the two tube sets together.

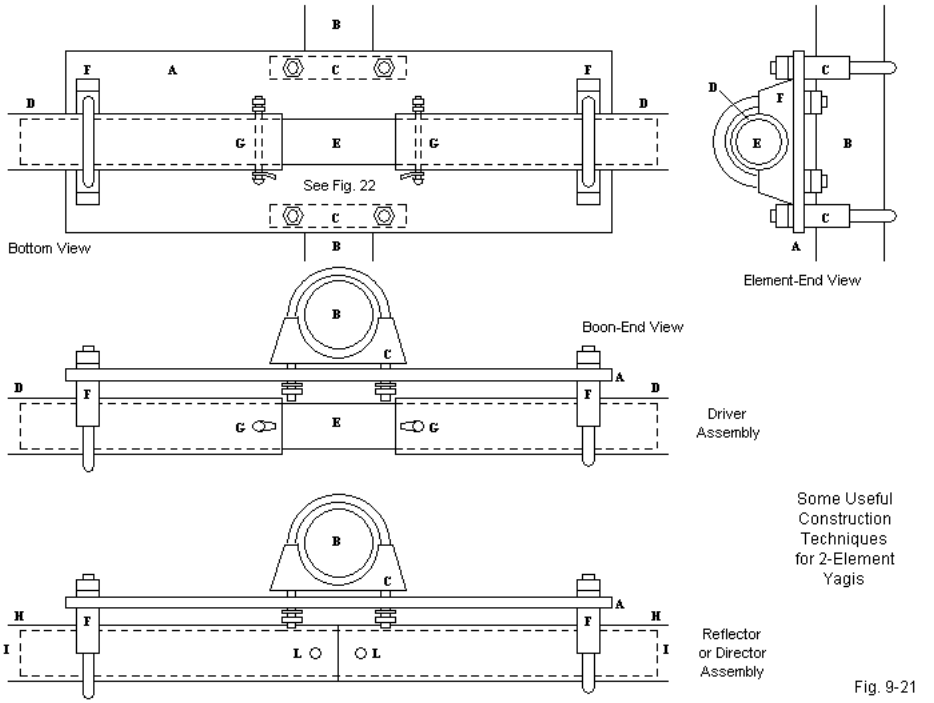

Fig. 9-21

The elements require a linking piece at the center. The parasitic elements (reflectors or directors) require a scrap of conductive tubing (I), while the driven element requires an insulating material, such a fiberglass rod (E). The sketch in **Fig. 9-21** does not show doubled tubes, but the linking pieces should be sized to fit inside the inner element tube. The linking pieces extend just beyond the outer U-bolts to allow element alignment with only two U-bolt fasteners. The driver gap size is not especially critical in the upper HF region, but should be as small as good electrical separation and easy connection assembly permit. The gap is a part of the overall element length, not an addition to it.

All hardware should be stainless steel. This requirement applies to U-bolts (C and F), nut-bolt-washer combinations (G), and sheet metal screws (L).

Stainless steel serves two purposes. First, it resists corrosion across the range of weather conditions we are likely to experience in the U.S. Second, it is not subject to electrolysis, which can occur when other dissimilar metals join. Therefore, use washers liberally at the connection of copper conductors to the aluminum driven element. The U-bolts show solid aluminum saddles, which are less subject to element compression than double-edge muffler-clamp types of saddles. I do not recommend U-bolts without saddles. I do recommend standard washers between U-bolt lock washers and the mounting plates to avoid gouging the plate and loosening the connection.

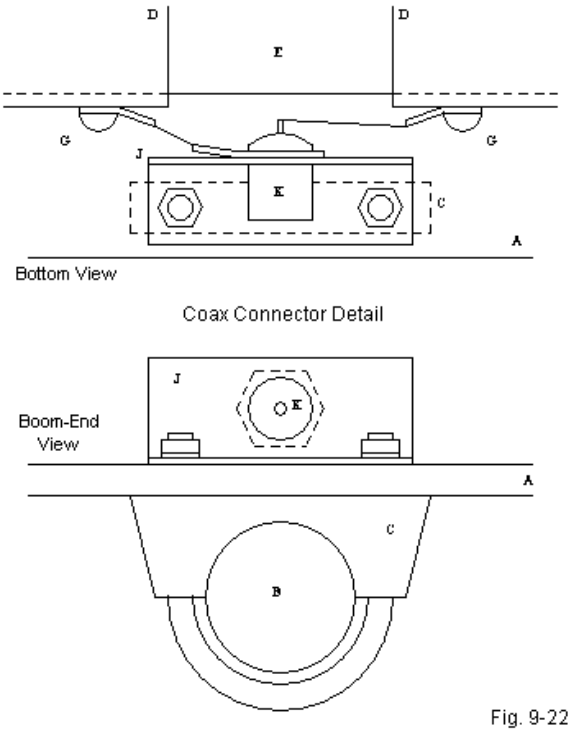

Fig. 9-22

Fig. 9-22 shows one way to install a coax connector (K) to the driven element. Through-chassis connector will fit neatly in the space provided by aluminum L-stock with 1" wide walls and 1/16" thickness. The mounting plate L-stock (J) can extend between two boom U-bolt ends for secure fastening. The connector end of the coax fixture should face the mast position along the boom.

The basic plates that I prefer are polycarbonate, sold under the trade name Lexan in some places. The plate size will vary with the amateur band, which generally determines element size and weight. ¼" thick material generally satisfies most upper HF requirements. The material should be UV-protected. It is available from various on-line sources. Like Plexiglas, it cuts and drills like wood, in contrast to the acrylic materials available in many home centers. In conjunction with the non-conductive polycarbonate plates, the U-bolt saddles insure satisfactory separation between the element and the boom to attenuate potential interactions to the negligible level. Although polycarbonate is satisfactory well into the lower UHF range, many VHF and UHF beam builders prefer Delrin and other later materials for insulating plates and shapes.

You will find other construction suggestions and hints in the next chapter in connection with a discussion of stepped-diameter designs for Moxon rectangles. However, you should also examine various antenna articles and handbooks for additional construction ideas. Antenna construction has a highly personal dimension that accounts for the individual builder's experience with materials, available tools and techniques, and any special skills that the builder brings to the task. As a result, there is no single best way to build a beam antenna. It should have a sound electrical basis. As well, combining low weight and strength reduce the strain on the beam's rotator. Commercial beam manufacture around the world tends to place the suggestions shown here between two extremes. Some (but not all) U.S. makers use a light but strong selection of tubing that follows the "willow" principle of allowing element flexing. Numerous European makers use elements with thicker walls to create sturdy "oaken" beams that show very little element flexing in the wind. Snow and ice loads sometimes call for this raw element strength, but rotators should be heavier to accommodate them. We might classify the designs and techniques in this chapter as simple "practical American home-builder" practice. The

techniques that we have surveyed are equally applicable and adaptable to some of the designs of phased arrays discussed in Volume 1 of this set.

Conclusion

Once more, I should stress that the beam designs that we have explored in this chapter make no claims of overall superiority relative to other designs found in various articles and handbooks. Rather, they offer alternatives that have certain advantages, but with disadvantages attached. The wide-band beams for 20, 15, and 10 meters allow a direct 50-Ω match to the main feedline cable at no significant loss of performance in the driver-reflector class. Their broadband characteristics give the newer builder greater promise of success on the first attempt to construct a monoband Yagi. The cost is the larger boom length relative to a number of other designs that require a matching network.

In contrast, the driver-director arrays for 17 and 12 meters provide more compact arrays. They show enough bandwidth to permit a simple beta match to cover the bands with a very low 50-Ω SWR. However, because the beams have a narrower performance bandwidth, they require more finicky field adjustment to derive the higher performance that we can obtain from the designs.

Other designs abound, and you should survey as many as possible before investing in tubing, hardware, and the other materials necessary to build your own 2-element Yagi. The designs in this chapter simply show that home construction of monoband 2-element Yagis is both feasible and practical.

10. Stepped-Diameter Moxon Rectangles

The Moxon rectangle has proven itself to be an effective 2-element parasitic beam of good performance and compact size. The forward gain is slightly lower (by about 0.2 dB) than a standard reflector-driver Yagi, but the beamwidth is wider (by about 10°) and the front-to-back ratio is very much improved (by an average of over 10 dB). The side-to-side dimension is about 70% of the comparable dimension in a Yagi, while the space between elements is between 0.13 λ and 0.14 λ.

We may design the Moxon rectangle for almost any feedpoint impedance from about 35 Ω to about 100 Ω. The lower the feedpoint impedance, the wider and narrower the beam becomes physically. Wider rectangles with lower feedpoint impedances tend to show slightly higher gain than higher impedance versions with squarer shapes.

The Moxon combines 2 forms of coupling to achieve its performance. First, we have the coupling between parallel elements, just as we find in a Yagi. However, Moxon beams bend the element ends toward each other, resulting in fairly close spacing of the tips. Hence, we have additional coupling. The gap between the element tips is fairly critical and varies depending upon the diameter of the element. Thinner elements require considerably closer spacing than thicker elements. Since there is some current in the side portions or tails of the elements, the beamwidth increases relative to a standard Yagi. As well, the side nulls move from the standard Yagi position of 90° away from the main forward heading to between 110° and 120° away from that heading.

Some years ago, I develop a set of algorithms for calculating the dimensions of any Moxon rectangle that uses a uniform-diameter element set. The initial algorithms focused on beams with a 50-Ω feedpoint impedance, although I later added a different set for feedpoint impedances closer to 100 Ω. The latter Moxon type has particular application in turnstile antennas used for fixed satellite operation. The main algorithms for 50-Ω arrays allow a direct feedpoint

connection with the usual coaxial cable, although a common-mode suppression (1:1) balun or ferrite-bead choke is a standard precaution at the feedpoint. **Fig. 10-1** shows the general outline of a Moxon rectangle, along with the conventional designations of the element dimensions used in design algorithms. A is the total side-to-side dimension of the antenna. B is the driver tail and D is the reflector tail. The most critical dimension is C, the gap between carefully aligned tails. E is the total front-to-back dimension of the beam and is the simple sum of B, C, and D.

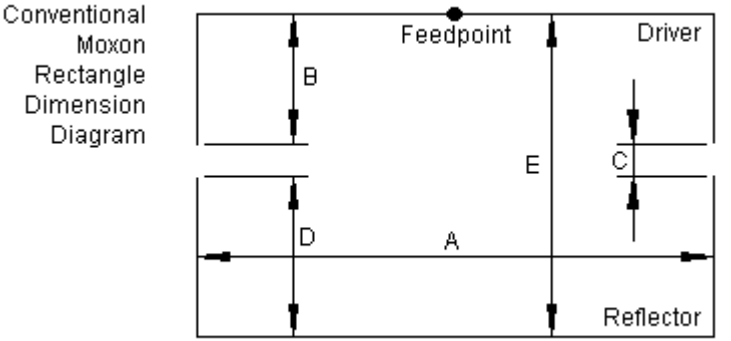

Fig. 10-1

The algorithms for uniform-diameter elements are highly useful at VHF and above, since virtually all arrays above the HF region use single tubes or rods for elements. However, over the years, I have received numerous requests to design for HF use some Moxons that use a tapered-diameter element schedule. The design of such Moxons has two challenges. First, an element with a stepped or tapered diameter that decreases as we move away from the element center will be physically longer than a comparable element with a uniform diameter. This fact changes the current distribution and results in a rectangle that is longer (side-to-side) and narrower (front-to-back) than an array that uses elements with a uniform diameter. Moreover, changing the diameter steps also changes the ultimate outer dimensions of the Moxon, including the required gap. The changes that may alter rectangle dimensions include not only the set of

element diameters used, but also the length of each section of tubing along the element. The result of the stepped-diameter effect is that we can no longer rely on the Moxon calculator as a guide to design, although it may still provide a starting point for the necessary re-design work. The remainder of the work proceeds on a case-by-case basis.

Second, we must find a set of tubing steps that can withstand significant wind loads. Therefore, not all stepped diameter progressions are usable. With linear elements, we may use a program such as YagiStress to calculate the wind load for a given element design. However, these programs are set for linear elements, and the Moxon rectangle has tails. The tails not only add weight to the end of the long portion of the element, but they introduce additional forms of loading. For example, the rectangle will show some stresses associated with wind-induced racking forces.

Despite the challenges, I have designed a series of HF Moxon rectangles using stepped-diameter element construction. The element structures should be able to withstand winds up to about 70-75 mph. U.S. antenna builders have an advantage due to the availability of 6063-T832 aluminum tubes. These tubes come in outside diameters that step in 1/8" increments from 3/8" upward. The wall thickness for readily available tubes (from sources such as Texas Towers) allows for close nesting of one tube size inside the next larger tube. The wall thickness is just under 1/16" (actually, 0.056") for a snug and strong fit with simple fasteners. For all of the designs in the set, the tailpieces use 3/8" tubes for their light weight. The center-most section of the 10-meter beam uses 3/4" stock. The diameter increases to 1" at 20 meters. For strength, the center-most element sections are doubled.

Each beam in the set of 5 is a separate design for the HF bands from 20 through 10 meters based on NEC-4 models. To provide nearly equal front-to-back and 50-Ω SWR values at the band edges, the design frequency for the wider amateur bands is about 1/3 the way up from the lowest frequency in the band. Since the gain of any 2-element parasitic array decreases with rising frequency across a defined passband, the designs tend to favor the lower end of the band with respect to gain. The amount of gain decrease depends upon the

overall width of the band as measured in percentage. (Dividing the total width of the band by the center frequency—using the same units for both—and multiplying by 100 determines the bandwidth of a passband as a percentage.) For the smaller WARC bands, designing for the band center works very well. Because the progression of tube sizes and lengths varies from one band to the next, the beams are not direct scalings of those for any other band. However, all will show the same narrowing and widening relative to calculated models using elements with a uniform diameter.

The design notes that follow consist of tables, sketches, and graphs to show the design details and the performance potential of the beam on each band. The tables will include a comparison of the dimensions (A through E) of a calculated rectangle using a 1/2" element and the dimensions of the present design using stepped-diameter elements. Figures and tabulated data will provide a more detailed look at the element construction for each band. The potential performance—as modeled in free space—will appear in graphs, with a table sampling the numerical values at the band edges and at the design frequency. Finally, a set of free-space E-plane (azimuth) patterns will conclude the data collection for each band. I use free-space data because the patterns will vary slightly depending upon the antenna mounting height. Free-space patterns are generally almost identical to those obtained at the take-off angle for any antenna mounted at least 1 λ above ground. Of course, to all free-space gain values, you must add the ground reflection component, which usually runs between 5 and 6 dB, depending upon mounting height.

20 Meters

The 20-meter Moxon rectangle is the largest and beefiest of the entire set. It uses tubing sizes from 1" down to 3/8". Note in **Fig. 10-2** that the 7/8" tube runs from its outer end back to the centerline, effectively doubling the tube wall thickness for the portion inside the 30" section of 1" diameter tube. **Table 10-20** compares the outer dimensions of the tapered model with a calculated 1/2" model. The side-to-side widening and front-to-back narrowing are evident. However, also note the reduction in the gap distance, which is a consequence of the other dimension changes based on the need to bring the array to its

performance curves and a 50-Ω feedpoint impedance.

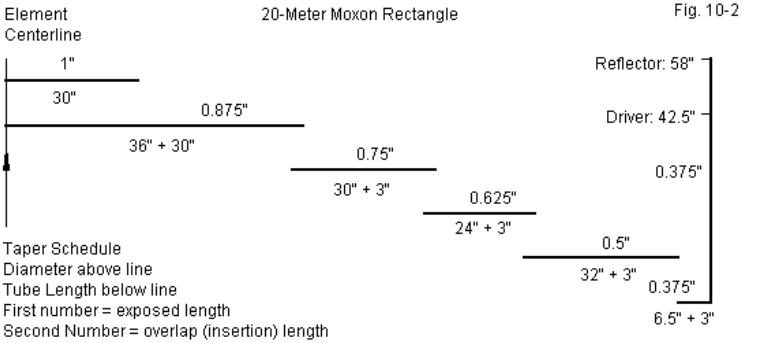

Table 10-20. A Comparison of the Dimensions of a Tapered Element Diameter Moxon and a Uniform-Diameter Moxon

20 Meters (14.15 MHz) See text for element diameter tapering schedule.
Uniform diameter = 0.5"

Dimension	Tapered Model	Uniform Model
A	317"	301.78"
B	42.5"	43.07"
C	7.5"	10.88"
D	58"	57.19"
E	108"	111.14"

Half-Element Diameter Taper Schedule

The difference between the exposed length and the total length is the amount of the smaller diameter tube inserted into the larger tube. Trim about 1/4" from the largest diameter tube at the centerline of the driver element for the gap required for feedline connections. All dimensions are in inches.

Diameter	Exposed Length	Total Length	Element Length
1"	30	30	30
0.875"	36	66	66
0.75"	30	33	96
0.625"	24	27	120
0.5"	32	35	152
0.375"	6.5 *	9.5 *	158.5 *

* Add length of either driver or reflector tail to the length of the 0.375" diameter tube.

The half-element table correlates directly with the sketch in **Fig. 10-2**. The second column lists the length of tube needed for both the exposed section and for insertion into the next larger tube size. Except for the doubled second section, the normal insertion length is about 3" as a compromise between strength and weight minimization. The 3/8" section length represents only the portions in the parallel element section. The tube will be bent at 90° so that it includes the driver or reflector tail length, as applicable.

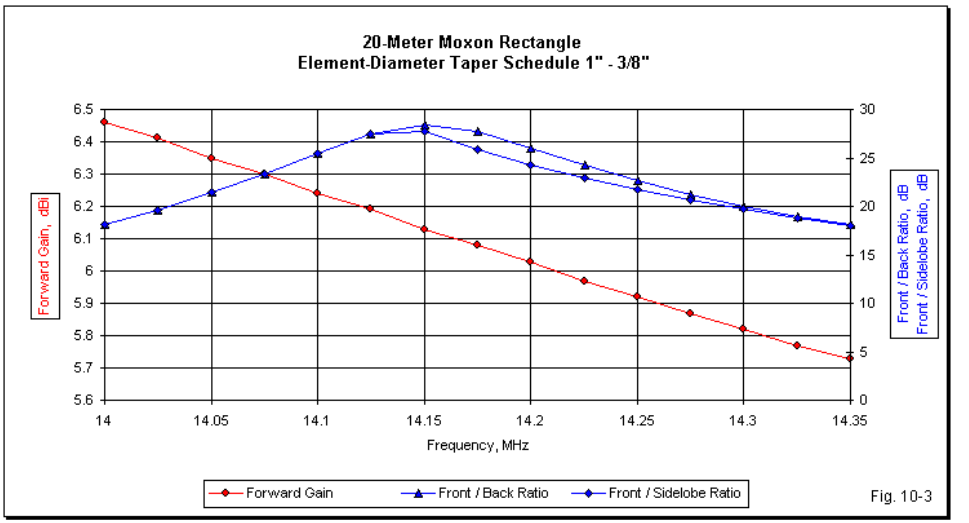

Fig. 10-3 graphs the free-space performance of the beam across 20 meters in terms of gain and front-to-back ratio. The front-to-back data includes the 180° ratio (labeled front-to-back) and the worst-case ratio (labeled front-to-side).

To translate the curves into representative numbers, the **Table 10-20a** samples the data at 14, 14.15, and 14.35 MHz. The design frequency is 14.15 MHz.

Table 10-20a. Moxon Rectangle 20-Meter Performance

Frequency MHz	Free-Space Gain dBi	Front-Back Ratio dB	Feedpoint Impedance R +/- jX Ohms	50-Ohm SWR
14.0	6.46	18.11	38.1 - j11.7	1.46
14.15	6.13	28.42	48.5 - j 0.2	1.03
14.35	5.73	18.09	60.6 + j11.6	1.33

The table shows a slightly higher SWR at 14 MHz than at 14.35 MHz, since the design frequency is slightly greater than 1/3 the way up the passband. **Fig. 10-4** shows the resistance, reactance, and 50-Ω SWR curves for the design across the entire band. It is possible to raise the impedance slightly at the design frequency and therefore to equalize the band-edge SWR values. However, for this exercise, I wanted to hold all dimension changes to increments of 1/2". As we move upward in frequency for the smaller Moxons in this series, it will be necessary to reduce the increment to 1/4". However, using standard dimension markers may ease the problem of replicating the design with physical element materials.

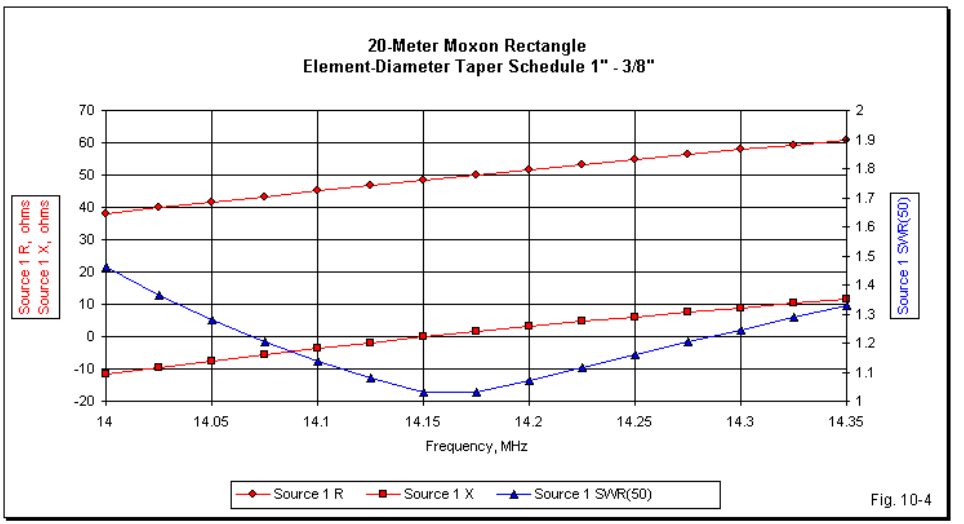

Fig. 10-4

The 20-meter band is fairly wide (about 2.5%), and so the patterns in **Fig. 10-5** show a fair amount of evolution. However, they are superior in front-to-back ratio and equal in gain to the patterns for any standard 2-element reflector-driver Yagi design. The blue line in the rear lobe shows the heading for the worst-case front-to-back reading that appears in the curve in **Fig. 10-3**. The red lines show the beamwidth of the forward lobe. As well, draw a virtual vertical line through the pattern rings to see how far the side nulls are from 90° relative to the forward lobe line.

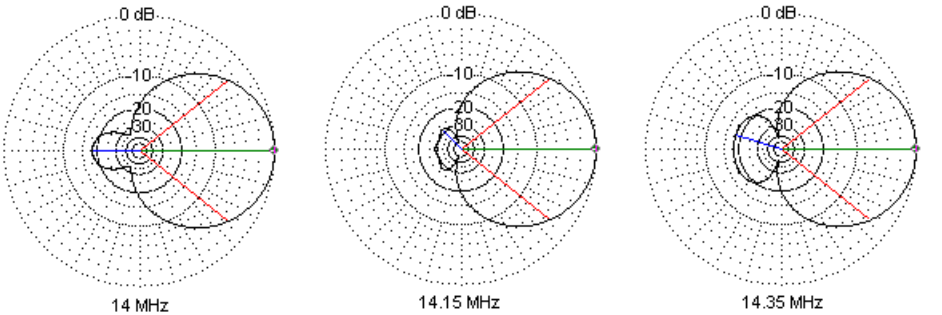

20-Meter Moxon Rectangle: Free-Space E-Plane Patterns Fig. 10-5

17 Meters

On 17 meters, we may design the Moxon rectangle for the center of the 100-kHz band, since the band is only about 0.5% wide. In terms of proportion, the dimension that differs most between the uniform-diameter and the tapered-diameter versions is the gap. **Fig.10- 6** and **Table 10-17** provide the dimensions for the array. Because the side-to-side dimension is about 70" shorter than the 20-meter Moxon, we may use 7/8" tubes at the center.

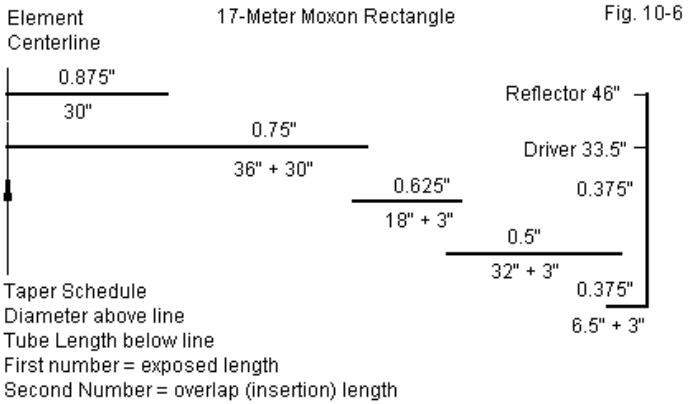

Table 10-17. A Comparison of the Dimensions of a Tapered Element Diameter Moxon and a Uniform-Diameter Moxon

17 Meters (18.118 MHz) See text for element diameter tapering schedule. Uniform diameter = 0.5"

Dimension	Tapered Model	Uniform Model
A	245"	235.40"
B	33.5"	33.16"
C	6.5"	8.94"
D	46"	44.73"
E	86"	86.89"

Half-Element Diameter Taper Schedule

The difference between the exposed length and the total length is the amount of the smaller diameter tube inserted into the larger tube. Trim about 1/4" from the largest diameter tube at the centerline of the driver element for the gap required for feedline connections. All dimensions are in inches.

Diameter	Exposed Length	Total Length	Element Length
0.875"	30	30	30
0.75"	36	66	66
0.625"	18	21	84
0.5"	32	35	116
0.375"	6.5 *	9.5 *	122.5 *

* Add length of either driver or reflector tail to the length of the 0.375" diameter tube.

As shown in **Fig. 10-7**, the gain and front-to-back ratio vary only a small amount across the 17-meter band. The gain curve is steep only because the total range is well under 0.2 dB. As well, the gain records only to 2 decimal places, giving the curve a somewhat stair-step quality. The actual change is smooth.

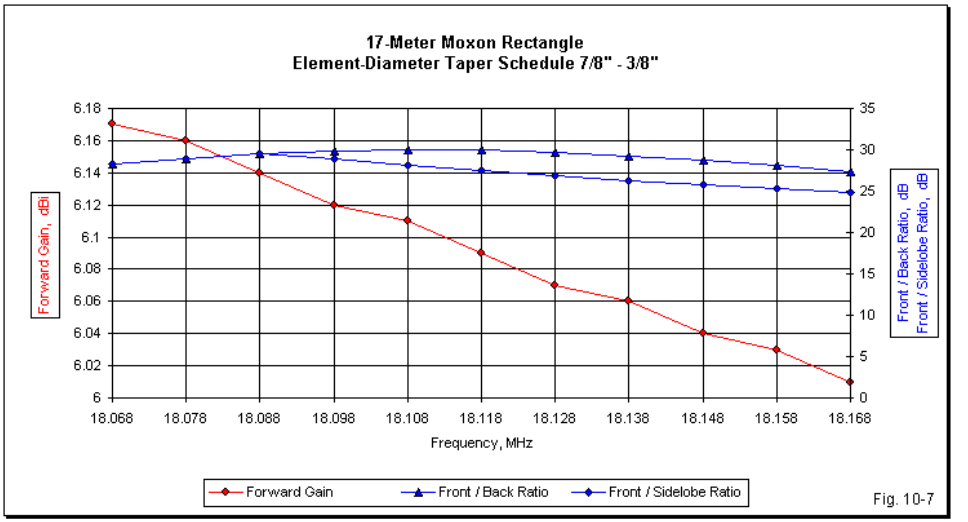

Fig. 10-7

Table 10-17A translates the curves into spot values at the band edges and center. **Fig. 10-8** provides a graphic view of the very small changes in resistance, reactance, and 50-Ω SWR.

Table 10-17a. Moxon Rectangle 17-Meter Performance

Frequency MHz	Free-Space Gain dBi	Front-Back Ratio dB	Feedpoint Impedance R +/- jX Ohms	50-Ohm SWR
18.068	6.17	28.24	48.0 - j 2.7	1.07
18.118	6.09	30.01	50.6 - j 0.2	1.01
18.168	6.01	27.40	53.1 + j 2.1	1.08

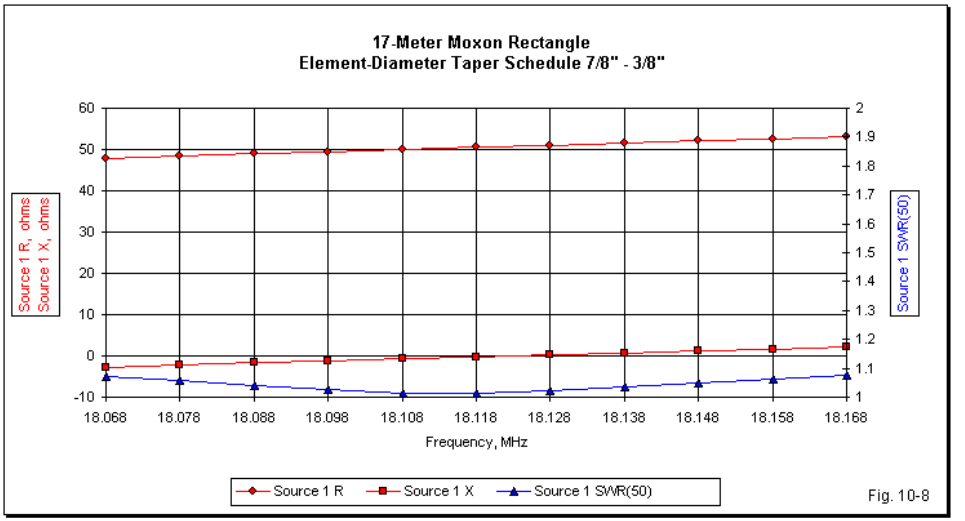

Fig. 10-8

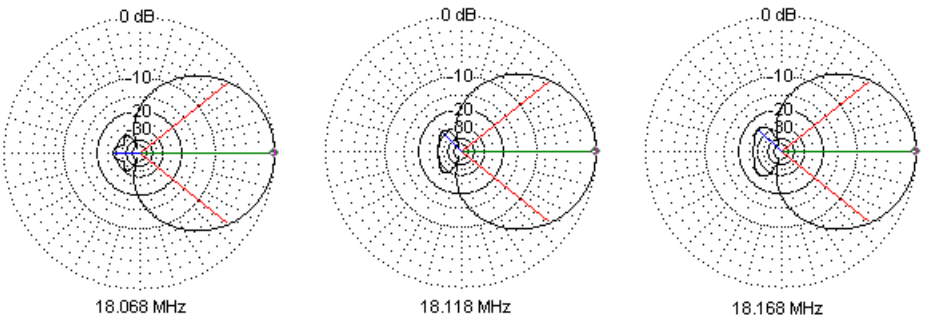

17-Meter Moxon Rectangle: Free-Space E-Plane Patterns

Fig. 10-9

Although the front-to-back curves in **Fig. 10-7** suggest a growing divergence between 180° and worst-case values, the patterns in **Fig. 10-9** show that the spreading curves are a function of the very small actual change in front-to-back values. Had the curves extended well above the upper end of the 17-meter

band, the 180° front-to-back ratio would decrease, while the worst case value would almost hold steady. The result would be a return to an overlapping curve, as shown in the comparable 20-meter curve.

15 Meters

15 Meters returns us to a fairly wide amateur band (2.1%). As a result, we may bring to the Moxon rectangle for this band similar expectations to those developed from the 20-meter results. The decreasing size of the Moxon rectangle, shown in the element taper sketch in **Fig. 10-10**, allows us to use the same center tube size that we used in the 17-meter array. In fact, the structure is the same until the beam nears the end of the rectangle's long dimension. The tabular dimensions appear in **Table 10-15**.

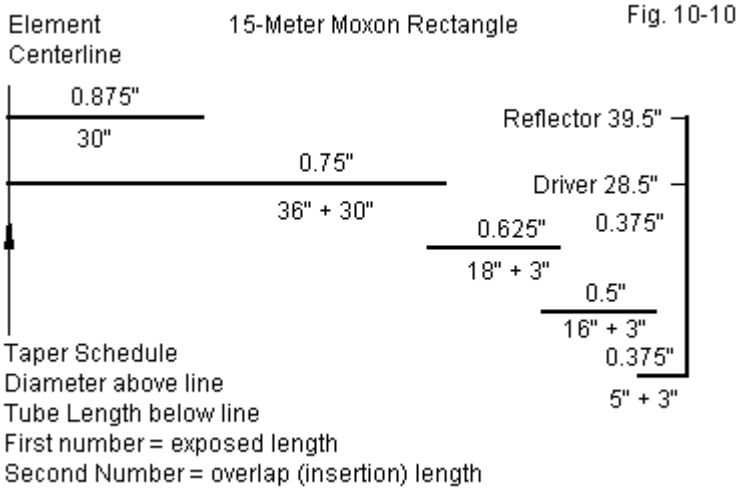

Table 10-15. A Comparison of the Dimensions of a Tapered Element Diameter Moxon and a Uniform-Diameter Moxon

15 Meters (21.15 MHz) See text for element diameter tapering schedule. Uniform diameter = 0.5"

Dimension	Tapered Model	Uniform Model
A	210.5"	201.49"
B	28.5"	28.14"
C	6"	7.91"
D	39.5"	38.36"
E	74"	74.41"

Half-Element Diameter Taper Schedule

The difference between the exposed length and the total length is the amount of the smaller diameter tube inserted into the larger tube. Trim about 1/4" from the largest diameter tube at the centerline of the driver element for the gap required for feedline connections. All dimensions are in inches.

Diameter	Exposed Length	Total Length	Element Length
0.875"	30	30	30
0.75"	36	66	66
0.625"	18	21	84
0.5"	16	19	100
0.375"	5 *	8 *	105 *

* Add length of either driver or reflector tail to the length of the 0.375" diameter tube.

Because the 15-meter band is slightly smaller than 20 meters in terms of bandwidth recorded as a percentage (2.1% vs. 2.5%), we can expect slightly shallower curves on 15 meters than on 20 meters. As shown in the gain and front-to-back curves in **Fig. 10-11**, the gain range is under 0.6 dB (compared to more than 0.7 dB on 20 meters). Both band-edge front-to-back ratio values are higher on 15 than on 20.

Table 10-15A provides selected performance values at the band edges and at the design frequency. 21.15 MHz is exactly 1/3 the way up the total passband for the array. **Fig. 10-12** converts the spot values for the feedpoint impedance components and the 50-Ω SWR into smooth curves across the band. A comparison of corresponding curves for 20 and 15 meters tells us that the Moxon rectangle performance is consistent from band to band once we find the

right dimensions for the selected element-diameter taper. The rates of gain decrease and of resistance and reactance increase across the band are very nearly linear.

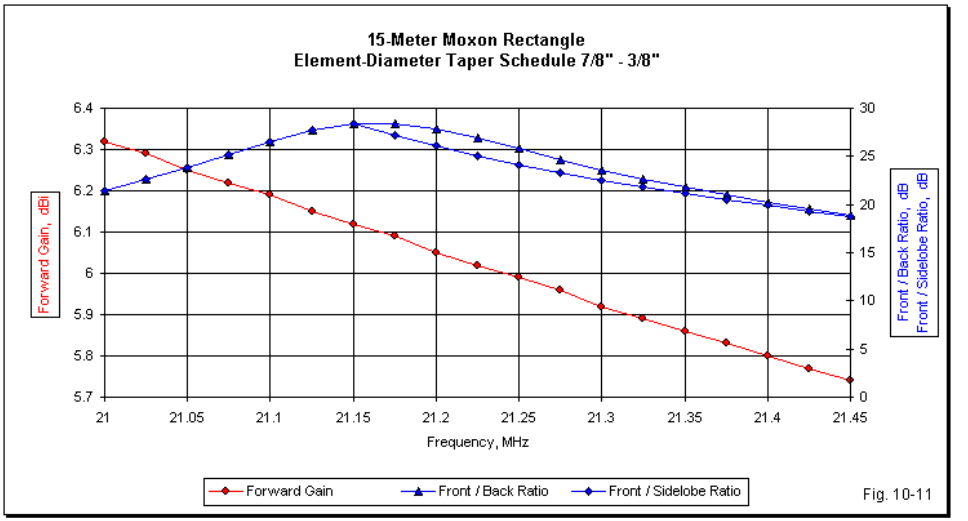

Fig. 10-11

Table 10-15a. Moxon Rectangle 15-Meter Performance

Frequency MHz	Free-Space Gain dBi	Front-Back Ratio dB	Feedpoint Impedance R +/- jX Ohms	50-Ohm SWR
21.0	6.32	21.41	42.9 - j 6.6	1.23
21.15	6.12	28.38	49.5 + j 0.1	1.01
21.45	5.74	18.93	61.0 + j10.9	1.32

Further evidence of band-to-band consistency of performance appears in the free-space E-plane (azimuth) patterns shown in **Fig. 10-13**. The patterns virtually replicate those for 20 meters. Note that we obtain this performance by re-optimizing the design for each band after selecting the desired element-diameter taper schedule.

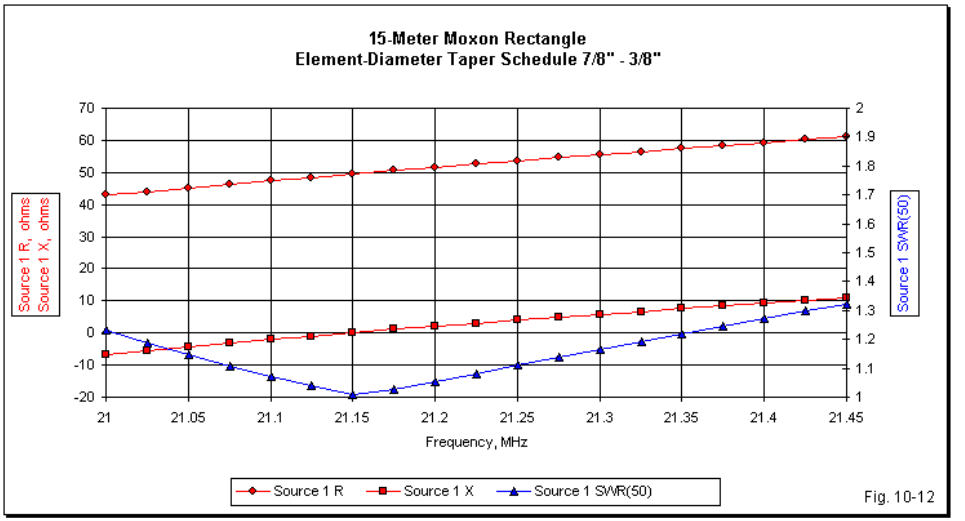

Fig. 10-12

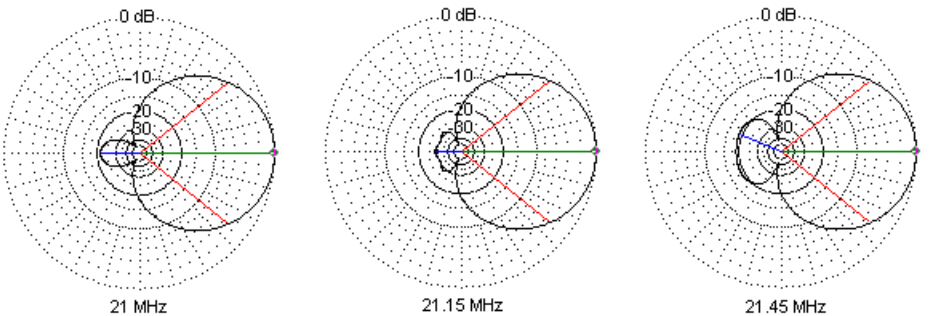

15-Meter Moxon Rectangle: Free-Space E-Plane Patterns

Fig. 10-13

12 Meters

12 meters returns us to a band only 100 kHz wide. However, as a percentage, the band has shrunk to only 0.4%. Hence, we should expect flatter curves than those we obtained for 17 meters. As well, the beam size has shrunk

so that we may use 3/4" tubes at the very center, as shown in **Table 10-12** and in **Fig. 10-14**. The total side-to-side dimension of a 12-meter Moxon rectangle is just over 14.5', with a width just over 5'.

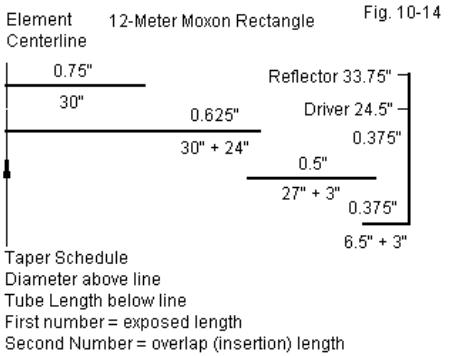

Table 10-12. A Comparison of the Dimensions of a Tapered Element Diameter Moxon and a Uniform-Diameter Moxon

12 Meters (24.94 MHz) See text for element diameter tapering schedule.
Uniform diameter = 0.5"

Dimension	Tapered Model	Uniform Model
A	175"	170.72"
B	24.5"	23.61"
C	4.25"	6.94"
D	33.75"	32.56"
E	62.5"	63.12"

Half-Element Diameter Taper Schedule

The difference between the exposed length and the total length is the amount of the smaller diameter tube inserted into the larger tube. Trim about 1/4" from the largest diameter tube at the centerline of the driver element for the gap required for feedline connections. All dimensions are in inches.

Diameter	Exposed Length	Total Length	Element Length
0.75"	30	30	30
0.625"	24	54	54
0.5"	27	30	81
0.375"	6.5 *	9.5 *	87.5 *

* Add length of either driver or reflector tail to the length of the 0.375" diameter tube.

The performance of the beam is almost invariant across the band with a 0.1-dB change in gain, as shown by the gain values in **Fig. 10-15**. Once more, the limitations in the decimal places of the gain reports provide the stair-steps in the graph. Because the worst-case front-to-back ratio remains almost constant across the band, it makes little difference that the peak 180◦ front-to-back ratio occurs at the upper band edge. To move that peak to the band's center frequency would have required a number of dimensions that used smaller fractions of an inch than the quarter-inch limit that I set.

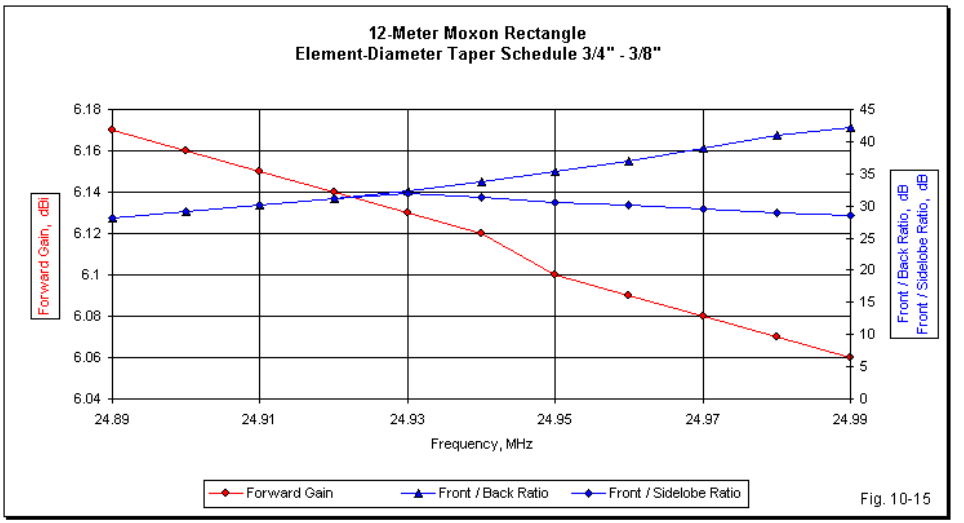

Fig. 10-15

Table 10-12a. Moxon Rectangle 12-Meter Performance

Frequency MHz	Free-Space Gain dBi	Front-Back Ratio dB	Feedpoint Impedance R +/- jX Ohms	50-Ohm SWR
24.89	6.17	28.17	48.5 - j 2.5	1.06
24.94	6.12	33.72	50.4 - j 0.7	1.02
24.99	6.06	42.14	52.4 + j 1.0	1.05

Table 10-12A supplies spot values across the band. I have included **Fig. 10-16** solely to make the record complete. All values of resistance, reactance,

and 50-Ω SWR are as close to flat lines as we are likely to find in such graphs.

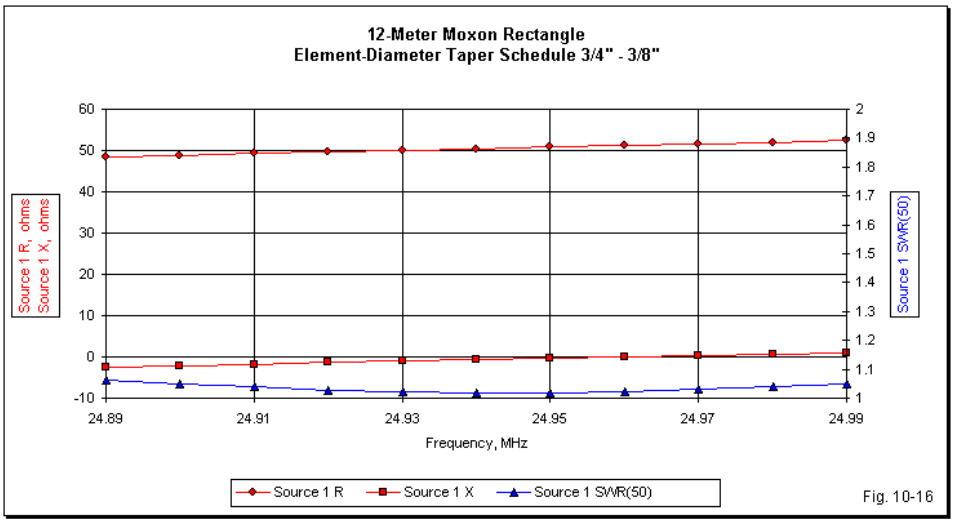

Fig. 10-16

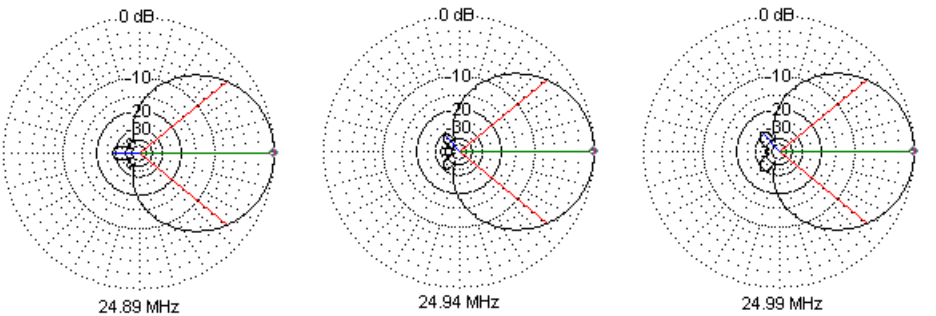

12-Meter Moxon Rectangle: Free-Space E-Plane Patterns

Fig. 10-17

The very small changes in the patterns in **Fig. 10-17** show how truly narrow the 12-meter band is. The rear lobe changes are visually noticeable, but operationally, it is unlikely that even the best ears could tell the difference in the

suppression of rearward QRM across the band. Indeed, normal construction variations are likely to move the peak front-to-back ratio to a slightly different frequency than the one shown in the graphs and tables.

10 Meters

If we define 10 meters in terms of the first MHz of the total band, we still obtain the widest of the upper HF amateur bands at 3.5%. Many Yagis (especially the 10-meter sections of tri-band designs) manage to cover only the first 800 kHz with under 2:1 50-Ω SWR. However, the Moxon rectangle easily covers the entire first MHz if we can accept the normal gain reduction across the passband. As the smallest of our rectangles (12.8' by 4.6'), the array has plenty of strength with 3/4" tubing at the center and 3/8" tail sections. **Fig. 10-18** shows the element taper schedule corresponding to the values in **Table 10-10**.

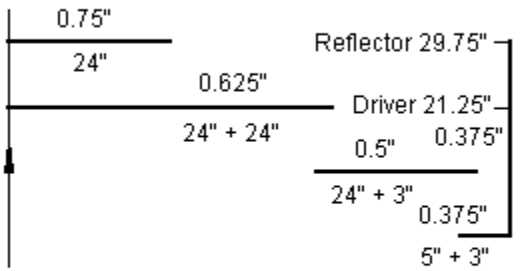

Table 10-10. A Comparison of the Dimensions of a Tapered Element Diameter Moxon and a Uniform-Diameter Moxon

10 Meters (28.35 MHz) See text for element diameter tapering schedule. Uniform diameter = 0.5"

Dimension	Tapered Model	Uniform Model
A	154"	150.08"
B	21.25"	20.59"
C	4"	6.27"
D	29.75"	28.67"
E	55"	55.53"

Half-Element Diameter Taper Schedule

The difference between the exposed length and the total length is the amount of the smaller diameter tube inserted into the larger tube. Trim about 1/4" from the largest diameter tube at the centerline of the driver element for the gap required for feedline connections. All dimensions are in inches.

Diameter	Exposed Length	Total Length	Element Length
0.75"	24	24	24
0.625"	24	28	48
0.5"	24	27	72
0.375"	5 *	8 *	77 *

* Add length of either driver or reflector tail to the length of the 0.375" diameter tube.

Because the 10-meter band is so wide, we cannot expect the design to show nearly equal gain across the entire passband. The gain decreases by about 0.9 dB from one end of the band to the other, as shown in **Fig. 10-19**. As well the front-to-back values at the band edges are between 16 and 17 dB. Still, these values are 5 to 6 dB higher than we might obtain with a wide-band 2-element reflector-driver Yagi, and a wide-band Yagi would have larger dimensions in both directions (side-to-side and front-to-back). See **Table 10-10A** to see numerical values at the band edges and center.

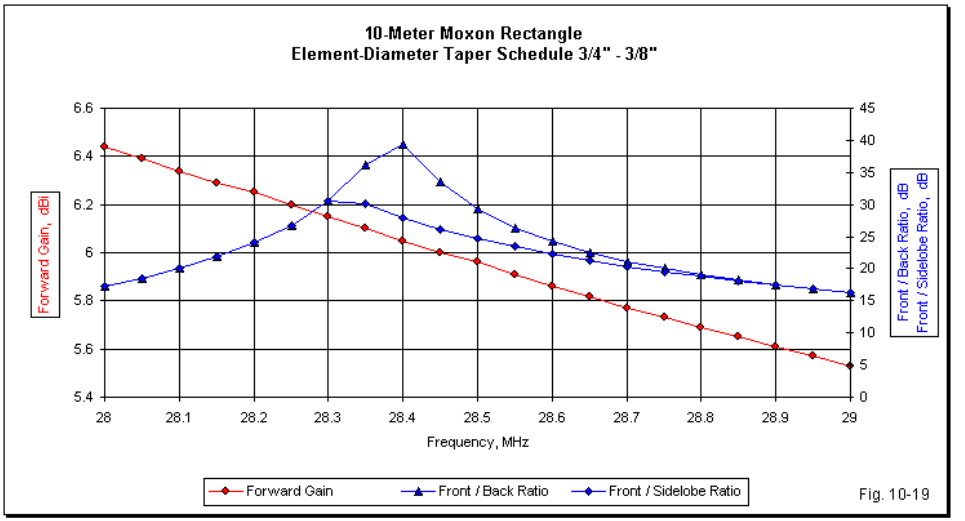

Fig. 10-19

Table 10-10a. Moxon Rectangle 10-Meter Performance

Frequency MHz	Free-Space Gain dBi	Front-Back Ratio dB	Feedpoint Impedance R +/- jX Ohms	50-Ohm SWR
28.0	6.44	17.18	38.6 - j13.6	1.49
28.35	6.10	36.07	50.6 + j 1.7	1.04
29.0	5.53	16.18	68.6 + j13.4	1.47

As shown by the performance table and the curve in **Fig. 10-20**, the Moxon rectangle with the selected element taper schedule still manages to show less than 1.5:1 50-Ω SWR across the band. Of course, cable losses at 10 meters begin to show themselves, so the SWR values recorded at the transmitter end of the feedline will be slightly less.

Even under wide-band conditions, such as those on 10 meters, the rearward lobes remain well behaved. Except for the peak value of 180° front-to-back ratio, where we find two lobes symmetrically arranged on each side of the centerline, the rearward radiation forms a single lobe. As shown in the patterns in **Fig. 10-21**, the rearward pattern is relatively straight-sided below the design

frequency. Above the design frequency, the pattern is a single bulbous lobe.

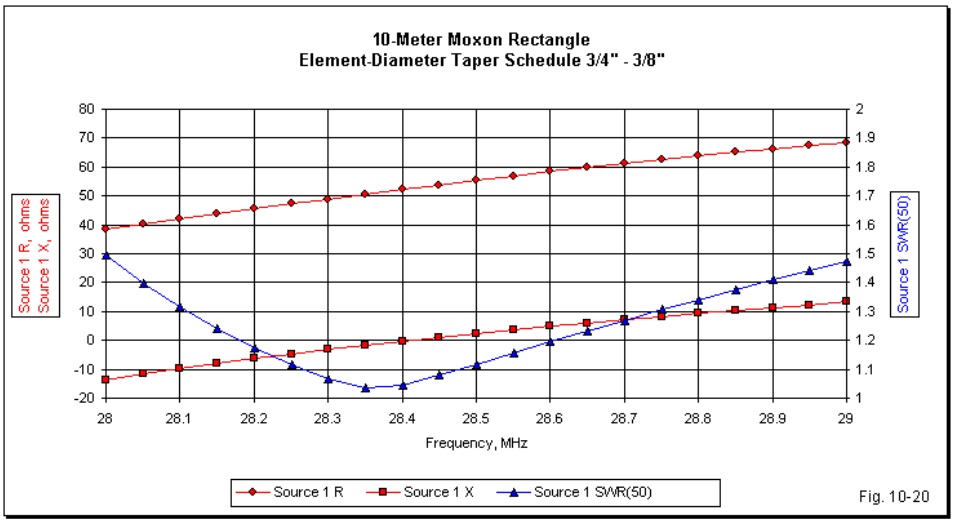

Fig. 10-20

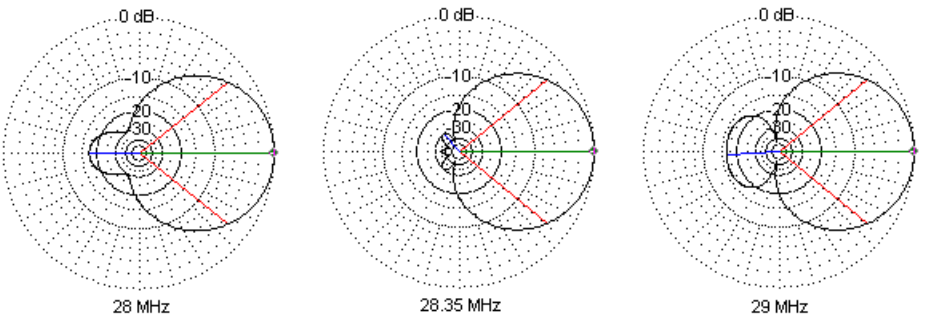

10-Meter Moxon Rectangle: Free-Space E-Plane Patterns

Fig. 10-21

I have provided complete design data and performance projections for each version of the Moxon rectangle. A complete record of design and performance data across each band of operation is perhaps the only fair way to allow a

potential builder or user to evaluate the design to determine if it is one to implement. I could have cited spot values only or, more extremely, peak values. Such data would have given a distorted picture of the true performance potential of the array. For example, citing the peak gain values for each band would have given the impression that performance changes from band to band. As well, citing only peak gain and peak front-to-back values would distort the portrait even further, since these values do not occur at the same frequency. With regard to feedpoint impedance issues, only the curves give the potential user a clear picture of the rates of change of SWR both above and below the design frequency. In these designs, I have no vested interest. Hence, I have no reason not to show all of the data for each band's design, including any performance facts that might count against the use of the Moxon rectangle. (For example, someone interested only in phone operation might wish to redesign one or more of the wide-band designs to favor that portion of the band.)

Since I brought attention to the Moxon rectangle back in the early 1990s, various enthusiasts have built numerous versions. The arrays range from fixed wire versions for the lower HF range to lightweight wire versions for upper HF to vertically and horizontally polarized versions for a variety of special VHF and UHF applications. More recently, commercially built stepped-diameter rectangles for the upper HF region have appeared. Aerial Acts of Silver Spring, MD (Craig Roberts, W3CRR) markets a series of Moxon rectangles (called the MaxiMoxon) that employ different taper schedules than the models shown here. The differences in the taper schedule result in a different set of overall dimensions, although they are likely not too far from the values shown in the tables. In addition, there are differences in the preferred construction methods. See http://www.aerialacts.com/index.htm.

Re-design of a Moxon rectangle that employs a stepped-diameter taper schedule is not a task for NEC-2. Because the stepped-diameter correction of NEC-2 implementations does not operate for non-linear elements, the program will not correctly handle the bent Moxon elements. Re-design should use either NEC-4 or a highly corrected version of MININEC 3.13, such as the one sold as Antenna Model. A MININEC implementation must have at least the frequency-drift correctives if it is to handle the 12- and 10- meter designs adequately.

A Few Construction Notes

Constructing a beam for long-term station use is not a casual task. Building a durable beam does not require a massive shop. Rather, it involves taking pains to ensure that the result is the best possible combination of strength and relatively low weight. Careful planning, careful measurement, and careful fabrication go hand-in-hand-in-hand. Indeed, having a third hand in the shop (in the form of someone willing to assist and equally committed to a quality finished product) is extremely helpful. If you work alone, take the trouble to construct jigs from scrap wood around the shop to aid in the drilling and other assembly processes.

The Moxon rectangle uses a direct 50-Ω feedpoint, which calls for a split driver to make connections at the element center. At HF, the size of the gap is generally not critical, although the actual gap is in principle simply the distance between the two conductors of the feedline cable. The leads from the cable or from the cable connector are part of the driven element. The element dimensions from end-to-end do not change, so we subtract half the gap size from each half-element in the driver.

Fig. 10-22

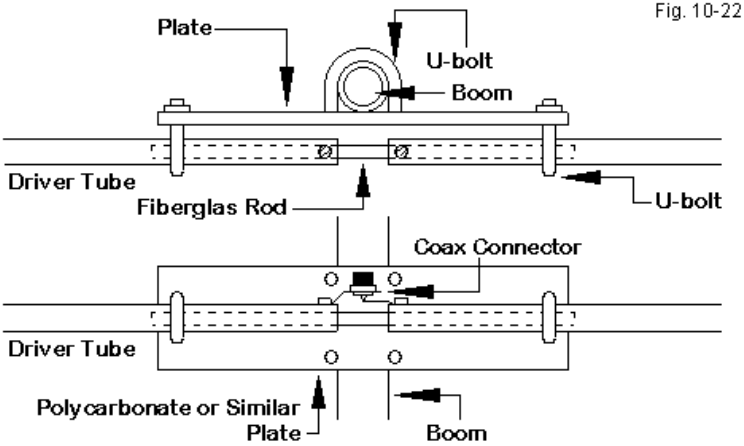

Driver Feedpoint and Element-to-Boom Assembly

Modeled designs also presume that all elements are well insulated and isolated from any conductive boom that might provide physical support. A section of 1.25" outside diameter aluminum tubing is probably the most common boom material. Although the assembly is fairly light, a 1/8" wall tube or a nest of 1.25" and 1.125" tubing is necessary to support the wind-induced twisting loads on the entire assembly. The double-tube boom is wise, even for the short 10-meter boom, since it will resist crushing at the boom-to-mast junction. **Fig. 10-22** shows one method (out of several) for constructing the feedpoint. A polycarbonate or similar plate provides the element isolation and supports the boom U-bolts. Size the plate according to the weight of the elements, using a larger plate for 20 meters and a smaller one for 10. UV protected polycarbonate sheets in 1/4" and 3/8" thicknesses are available from local plastic supply houses in medium to large cities and via the web (for example, McMasters-Carr). If we insert a non-conductive tube or rod into the ends of each element half, we assure element alignment with only 2 U-bolts and also establish an anchor point for the gap and the feedpoint connections. If we also run the inner tube to the gap, then it also provides support that will keep the aluminum elements from crushing as we tighten the U-bolts. The outside diameter of the gap-setting non-conductive tube should just fit inside the center tube section of the element. For the doubled Moxon element sections, the required rod or tube size would have an outside diameter 1/4" less than the outside diameter of the largest tube in the taper schedule. All hardware is stainless steel to prevent corrosion and to avoid bimetallic electrolysis.

As shown in **Fig. 10-23**, we may treat the reflector of any Moxon design in a similar manner. In this case, we bring the ends of the tubes together to form a continuous element or we use a single piece of tube to form the center element section. The advantage of using a split section at the reflector center is that we may use an interior piece of aluminum tubing to form the physical and electrical junction of the 2 element halves. Extending the inner tube to the center provides the same insurance against U-bolt crushing that we obtained from the non-conductive tube in the driver elements. The inner tubing should have the same diameter as the non-conductive tube in the driver. If we use a continuous center tube for the largest diameter in the reflector, we may also use separate tubes for the next size, bringing them together at the center of the largest tube. The

doubled section should provide sufficient strength to resist U-bolt crushing. U-bolts with solid aluminum saddles are available from sources such as DX Engineering. These U-bolts provide the most secure mounting and also resist element crushing better than U-bolts styled like muffler clamps.

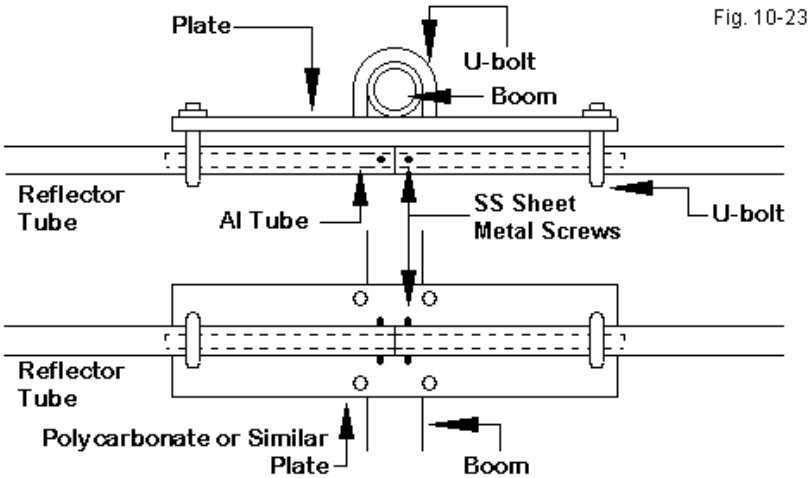

Reflector Element-to-Boom Assembly

The Moxon rectangle 3/8" tail sections must meet several criteria. First, they must turn a corner. Second, they must maintain the gap size, even in the face of winds. Third, they must keep the tail ends aligned. For 3/8" diameter tubing, turning a corner is not difficult. Starting with a tube section that is longer than needed, we can bend one end in the same tubing bender used for small copper tubing. Filling the tube with very fine play sand will further reduce the tendency for crushing during the bending operation, and many builders like to heat the tubing as a further precaution. We can insert the short end into the 0.5" diameter section with the standard 3" insertion overlap. The small curve at the corner will not alter the overall element length enough to cause any noticeable change of performance if we keep the total element length equal to the sum of

all of the exposed portions of the sections. **Fig. 10-24** shows the general scheme.

Fig. 10-24

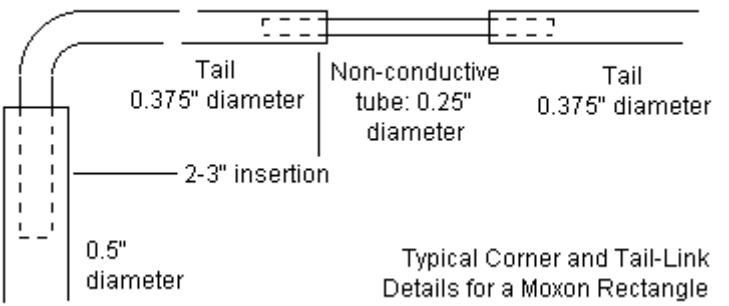

The figure also shows a simple way to maintain the gap and to keep the ends aligned. We simply insert a 1/4" non-conductive tube or rod into the tail ends and fasten it with stainless steel sheet metal screws. The tube or rod should be light and should also be UV protected. The result is a physically closed rectangle. Unlike beams with linear elements, the rectangle will not whistle, although you may wish to cap the boom ends. Because the Moxon rectangle in this configuration is subject to racking forces, we likely should reduce the wind load capacity of the elements by a small amount. The structures shown in the taper schedule sketches should handle winds up to about 70 mph.

There are as many variations on physical construction as there are potential element-diameter taper schedules. Therefore, consider these notes and the notes in Chapter 9 as simply a starting point for your own ingenuity.

Conclusion

These notes present usable designs for home built Moxon rectangles for the upper HF range. The Moxon rectangle is—for full performance—essentially a

monoband 2-element array with close to the gain of a full size 2-element Yagi but superior front-to-back performance. For wide-band use, the Moxon is shorter than most Yagis and offers a 50-Ω feedpoint impedance. The Moxon may also be used for yards that do not permit full-length linear elements that a standard Yagi requires.

The Moxon designs shown here employ element-diameter taper schedules that should suffice for winds up to about 70 mph, a condition for long-term home-station use. Due to the effects of the decreasing element diameter, the dimensions for each band differ from those for a uniform-diameter Moxon, and each design requires a custom fit to the selected taper schedule. Hence, each version in the series requires individual design optimizing and individual data graphs and tables. However, the construction of each version differs only in the size of the tubes and the boom-to-element plates. The construction techniques shown are but one set out of many that you might devise.

In the end, the exercise has satisfied my curiosity as to whether a complete line of Moxons might evolve, each with an element taper schedule suited to the beam size for the operating frequency. The answer is yes.

Other Publications

We hope you've enjoyed this Volume 2 of the **2-Element Horizontal Beams.** You'll find many other very fine books and publications by the author L.B. Cebik, W4RNL in the ***antenneX Online Magazine BookShelf*** at the web site shown below.

Published by
antenneX Online Magazine
http://www.antennex.com/
POB 271229
Corpus Christi, Texas 78427-1229
USA

ISBN: 1-877992-82-8
